Interpretation of Additives Effects in Enamine Catalysis and Application in Mechanistic Studies

A Thesis Submitted by

Matthew James Hughes

In partial fulfilment of the requirements for the degree of

DOCTOR OF PHILOSOPHY

Department of Chemistry

Imperial College London

South Kensington

London SW7 2AZ

United Kingdom

2013

I confirm that the material presented within this document is my own work. Where reference is made to the work of others, this is clearly acknowledged.

Abstract

Since 2000, a profusion of reaction types catalysed by functional organic molecules has steadily been discovered. Organocatalysis has thus become a major field of chemical research – but in spite of this, relatively few mechanistic studies have emerged. Additives can frequently alter reactivity in organocatalytic reactions, and can serve as powerful mechanistic probes. A holistic approach to understanding additives effects alongside other kinetic parameters has been shown to generate far deeper understanding of such processes. The research documented in this thesis strives towards the elucidation of the effects of additives in three important types of organocatalytic transformation.

An extraordinary reversal of enantioselectivity upon the application of basic additives to the proline-catalysed amination reaction has been investigated. By varying the additive loading, and through screening a range of different additives – including a bespoke set of isosteric guanidine bases – it was revealed that a positive relationship exists between additive basicity and enantioselectivity. Investigations were extended to the application of a range of preformed prolinate catalysts that were found to exhibit even higher selectivity, dependent on the nature of the counter cation. When focus then turned to the intermolecular aldol reaction, remarkably different reactivity was again observed on the switch from proline catalysis to prolinate catalysis. Surprisingly, the altered active species was found to be a retroaldol catalyst, which gives rise to reversible aldol processes and increased catalytic activity. The mechanism of the Hajos–Parrish–Eder–Sauer–Wiechert reaction was examined with the aid of additives effects and deuterium labelling. Protocols were developed for studying the reaction under completely homogeneous conditions to allow deconvolution of solubility effects from intrinsic mechanistic effects. It was found that while acidic and basic additives can accelerate the reaction, this is entirely due to catalyst solubilisation. The implications of these findings have answered key questions of mechanistic debate.

Contents

Acknowledgements 7

Abbreviations 8

1. Organocatalysis 12

1.1. Introduction 12

1.2. Covalent Catalysis – Enamines and Iminiums 13

1.3. Non-Covalent Catalysis – Ion-Pairs and Binders 20

1.4. Achievements and Challenges 24

2. Proline Catalysis 27

3. Mechanistic Debate 30

3.1. Mechanism of the HPESW Reaction 30

3.2. Houk–List Model 32

3.3. Seebach–Eschenmoser Model 36

3.4. Enamine Detection and Analysis 38

3.5. Additives Effects and Kinetic Investigations 41

3.5.1. Effect of Water on the Proline-Catalysed Aldol Reaction 41

3.5.2. Rising Rate in the Proline-Catalysed Amination Reaction 45

4. Amination 48

4.1. Introduction 48

4.2. DBU as an Additive 49

4.3. Implication of DBU Effect 52

4.4. Screen of Other Tertiary Amines 54

4.5. Phosphazene Bases 56

4.6. Guanidines – A Series of Isosteric Bases 58

4.7. Dependence on Basicity 70

4.8. Different Catalysts with DBU Additive 78
4.9. Secondary Amines as Additives 82
4.10. Preformed Prolinates 84
4.11. Preparation of Bulkier Prolinates 88
4.12. Prolinates of Other Metals 96
4.13. Steric Probe for Comparison of Prolinate Catalysts 98
4.14. Prolinate-Catalysed Amination Solvent Screen 101
4.15. Kinetics 103
4.16. Concluding Remarks 109
5. Aldol 111
5.1. Base Effect in the Aldol Reaction 111
5.2. Explanation for Selectivity Reversal 119
5.3. Retroaldol 121
5.4. Dicarboxylic Acid Catalyst 124
5.4.1. Synthesis of the Catalyst 125
5.4.2. Analysis of the Base Effect 127
5.5. Concluding Remarks 129
6. Hajos-Parrish-Eder-Sauer-Wiechert Reaction 130
6.1. Introduction 130
6.2. Model HPESW Reaction 131
6.3. Heterogeneous HPESW System 135
6.4. Proline Solutions 137
6.5. Soluble Proline Analogues 142
6.6. Basic Additives 148
6.7. NMR Experiments 153
6.8. Concluding Remarks 158
7. Summary of Novel Results 160

7.1. Amination Reaction 160
7.2. Aldol Reaction 161
7.3. HPESW Reaction 162
8. Experimental 163
8.1. General Comments 163
8.2. Amination 164
8.2.1. Amination Reactions 164
8.2.2. NMR Experiments 169
8.2.3. Synthesis of Required Materials 171
8.3. Aldol 184
8.3.1. Aldol Reactions 184
8.3.2. Synthesis of Required Materials 187
8.4. HPESW 193
8.4.1. HPESW Reactions 193
8.4.2. Deuterium Labelling Experiments 197
8.4.3. Synthesis of Required Materials 199
9. References 209

Acknowledgements

I am sincerely thankful to Prof. Alan Armstrong for giving me the opportunity to join his group. I cannot imagine a better environment in which to have worked, and learned. His constant enthusiasm and support have been instrumental to my development as a scientific researcher.

It has been extremely satisfying to work alongside collaborators who brought to projects a wide range of scientific expertise, and I would like to thank Prof. Donna Blackmond, Natalia Zotova, Antonio Moran, Jason Hein, and Jordi Bures for all of the stimulating and fruitful exchanges.

I am grateful to the NMR and mass spectrometry staff for their crucial support, in particular Pete Haycock who has always made himself available to offer advice and suggestions.

Thanks to everyone who I have shared the Heilbron lab with over the years. There has always been a very enjoyable working atmosphere and sense of community, even when old members departed and new faces appeared.

Thanks to my family, in particular my mum who has encouraged me in my academic pursuits throughout my life.

Lastly, I would like to dedicate this thesis to Lili, who is the constant good in my life and has been central to my reaching this point in more ways than she knows.

Abbreviations

Ac	acetyl
aq	aqueous
Ar	aryl
ArTMG	2-aryl-1,1,3,3-tetramethylguanidine
ATR	attenuated total reflectance
B:	generic base
BEMP	2-*tert*-butylimino-2-diethylamino-1,3-dimethyl-1,3,2-diazaphosphinane
Bn	benzyl
Boc	*tert*-butoxy carbonyl
br	broad
Bu	butyl
*t*Bu	*tert*-butyl
Calc.	calculated
Cbz	benzyloxy carbonyl
CI	chemical ionisation
config.	configuration
conv.	conversion
d	day(s)
DABCO	1,4-diazabicyclo[2.2.2]octane
DBN	1,5-diazabicyclo[4.3.0]non-5-ene
DBU	1,8-diazabicyclo[5.4.0]undec-7-ene
DEAD	diethyl azodicarboxylate
DFT	density functional theory
DIPEA	diisopropylethylamine
DMA	*N*,*N*-dimethylacetamide
DMAP	4-(dimethylamino)pyridine

DMF	*N*,*N*-dimethylformamide
DMSO	dimethylsulfoxide
E	generic element
$E^{\oplus}$	generic electrophile
EDG	electron-donating group
ee	enantiomeric excess
equiv.	equivalent(s)
E_{rel}	relative energy
ESI	electrospray ionisation
Et	ethyl
evap.	Evaporation
EWG	electron-withdrawing group
EXSY	exchange spectroscopy
FID	flame ionisation detector
GC	gas chromatography
h	hour(s)
HA	generic acid
HMDS	hexamethyldisilazane
HPESW	Hajos–Parrish–Eder–Sauer–Wiechert
HPLC	high performance liquid chromatography
HRMS	high resolution mass spectrometry
IR	infrared
I. S.	internal standard
L	ligand
LG	leaving group
m	minute(s)
M	metallic element

m. p.	melting point
maj.	major
Me	methyl
min.	minor
MS	mass spectrometry
MVK	methyl vinyl ketone
Nap	naphthyl
NMM	*N*-methylmorpholine
NMMO	*N*-methylmorpholine oxide
NMR	nuclear magnetic resonance
NOESY	nuclear Overhauser effect spectroscopy
$Nu^{\ominus}$	generic nucleophile
P_1-*t*Bu	*tert*-butylimino-tris(dimethylamino)phosphorane
P_2-*t*Bu	1-*tert*-butylimino-1,1,3,3,3-pentakis(dimethylamino)-1λ^5,3λ^5-catenadi(phosphazene)
P_4-*t*Bu	1-*tert*-butyl-4,4,4-tris(dimethylamino)-2,2-bis[tris(dimethylamino)-phosphoranylidenamino]-2 $\lambda^5$4 λ^5-catenadi(phosphazene)
PEA	1-(phenyl)ethylamine
PG	protecting group
Ph	phenyl
PhTEG	2-phenyl-1,1,3,3-tetraethylguanidine
PhTMG	2-phenyl-1,1,3,3-tetramethylguanidine
ppm	parts per million
*i*Pr	*iso*-propyl
q	heat flow
R	generic alkyl substituent
RC	reaction calorimetry
rac	racemic

rot.	rotamer
RPKA	reaction progress kinetic analysis
RSM	recovered starting material
rt	room temperature
sat.	saturated
t	time
TBA	tetrabutylammonium
TBS	*tert*-butyldimethylsilyl
TEMPO	2,2,6,6-tetramethylpiperidine-*N*-oxyl
Tf	trifluoromethanesulfonyl
TFAA	trifluoroacetic anhydride
TFE	1,1,1-trifluoroethanol
THF	tetrahydrofuran
TIPS	triisopropylsilyl
TMS	trimethylsilyl
TOF	turnover frequency
Tol	tolyl
T_R	retention time
Ts	4-toluenesulfonyl
TS	transition state
UV	ultra-violet
vis	visible light
vol%	percentage by volume
wt%	percentage by weight
X	generic atom or substituent

1. Organocatalysis

1.1. Introduction

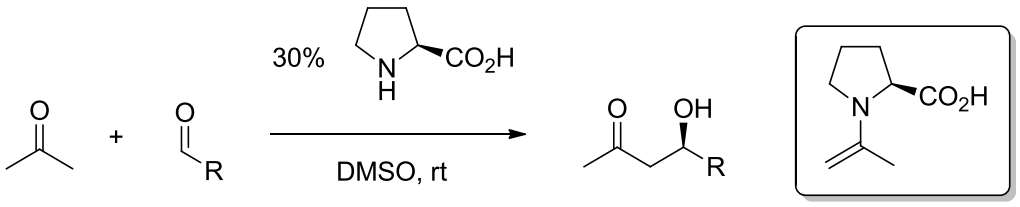
Organocatalysis is defined as catalysis performed by a small organic molecule. Simple compounds comprising carbon, hydrogen, oxygen, and nitrogen are usually chemically inert in comparison with species built from the full selection of elements. So, it may therefore seem surprising that such species are capable of activating and transforming other organic compounds that play the role of substrates. However, the concept is in essence the miniaturisation of biocatalysis, which could be described – in a parallel definition – as catalysis performed by a large organic molecule. In fact the most famous organocatalyst, the amino acid proline, has been dubbed "the simplest enzyme".[1] Like enzymes, organocatalysts generally rely upon the specific placement and orientation of a variety of functional groups with a structure activity relationship that prohibits large alterations.

This broad description encompasses a vast number of processes and catalyst types, and examples have been discovered throughout the history of synthetic organic chemistry that fit the definition: variants of the classical Knoevenagel and aldol reactions utilising simple amines as catalysts have long been known.[2] It is well established that nucleophilic catalysis, as seen in the activation of acylating agents and the Morita–Baylis–Hillman reaction, can also be performed with amines[3] – a particularly versatile example is DMAP.[4] The use of organic Brønsted acids and bases to achieve catalysis can clearly be included too. However, it is only recently that organocatalysis has been afforded its status as the third major branch of catalysis alongside the more established fields of transition metal and biocatalysis. This recognition is due to the significant advances and unprecedented interest in the field since the start of the 21st century, the intensity of which has been likened to the California gold rush.[5] In particular, considerable effort has been made towards the design of enantioselective variants of (often long-known) reactions through asymmetric organocatalysis. The remainder of this introduction will illustrate the major breakthroughs from this modern era of organocatalysis, in particular the

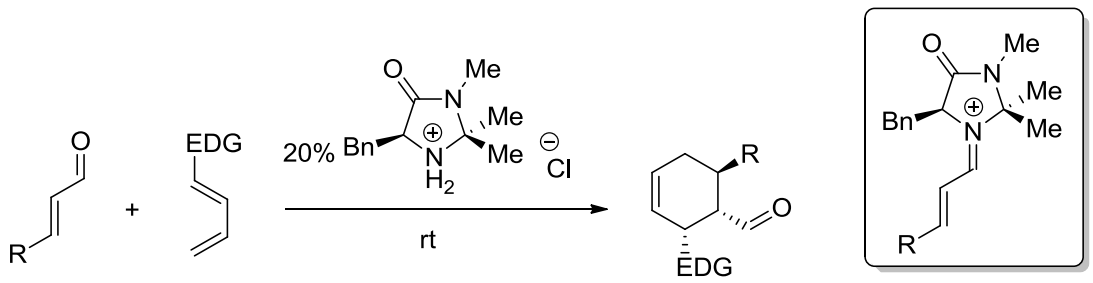
significant advances in enamine catalysis, which forms the focus for the research presented in this thesis.

1.2. Covalent Catalysis – Enamines and Iminiums

The simultaneous discovery and publication of two novel catalytic reactions in 2000 proved to be particularly portentous; it is now seen as the moment the new and sustained interest in organocatalysis began. The reports both utilised secondary amine catalysts to activate carbonyl compounds – a pairing of catalyst and substrate-type that is now so widespread that aminocatalysis is nearly synonymous with organocatalysis: List, Lerner, and Barbas reported a proline-catalysed asymmetric intermolecular aldol reaction (Scheme 1),[6] while MacMillan and co-workers presented an imidazolidinone-catalysed asymmetric Diels–Alder process (Scheme 2).[7]



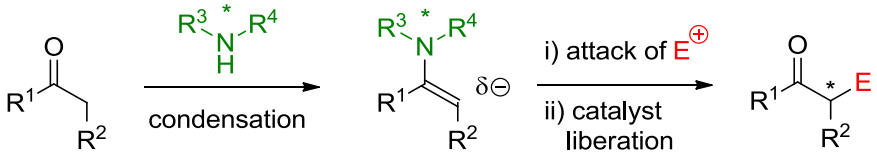
Scheme 1: The List–Lerner–Barbas proline-catalysed intermolecular aldol reaction; Key catalytic intermediate is displayed in the box; R = aryl group or branched alkyl group.



Scheme 2: The MacMillan imidazolidinone-catalysed Diels–Alder reaction; Key catalytic intermediate is displayed in the box; R = H, alkyl, aryl; EDG = electron-donating group.

The key catalytic intermediates are an enamine in the aldol reaction and an iminium ion in the Diels–Alder reaction, and these processes are for this reason classed as enamine and iminium catalysis.[i] Both of these classes can be further categorised as examples of covalent catalysis, since the catalyst forms new chemical bonds with the substrate to generate the active intermediate. This demonstrates how organocatalytic processes are usually divided, i.e. by their mechanism of action.

In asymmetric enamine catalysis, carbonyl compounds are converted to enamine intermediates with chiral amines, which can then react with electrophiles to give α-functionalised carbonyl compounds after catalyst liberation (Scheme 3).



Scheme 3: General mechanism of asymmetric enamine catalysis; $R_3R_4NH^*$ = chiral primary or secondary amine; $E^{\oplus}$ = electrophile.

Following on from the aldol reaction shown in Scheme 1, various new reaction types were established including the Mannich reaction,[8–10] hydrazination,[11,12] aminoxylation,[13–15] hydroxyamination,[16] hydroxylation,[17] fluorination,[18–21] chlorination,[22,23] bromination,[24] sulfenylation,[24] and selenenylation.[25] The types of enantioenriched products accessible through these transformations are shown below in Figure 1.

i) Technically, these terms are inexact because the catalyst itself is not an enamine or an iminium.

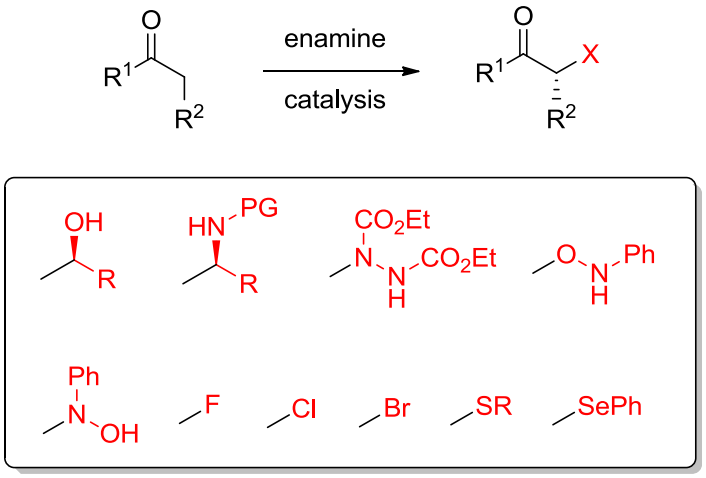
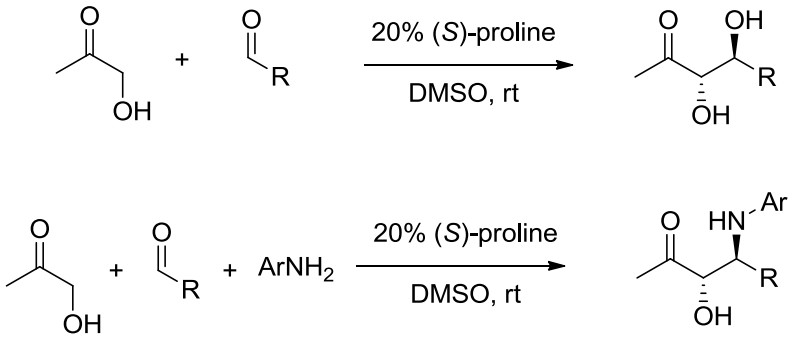


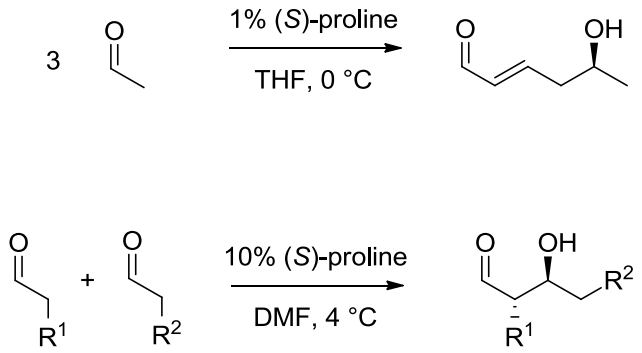
Figure 1: Enantioenriched products accessible through enamine catalysis.

A vast amount of research has since been performed to extend the substrate scope and improve aspects of the catalyst performance in these processes. Such augmentation, following initial discovery, is well-illustrated for the aldol and Mannich reactions. It was found that hydroxy acetones can be employed in these reactions to give *anti*-1,2-diols[26,27] and *syn*-1,2-aminoalcohols.[8]



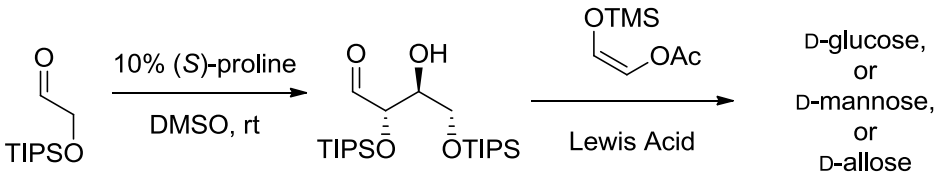
Scheme 4: Proline-catalysed aldol and Mannich reactions using hydroxyacetone.[8,26,27]

Protocols were also quickly established for the application of aldehydes as the pronucleophilic substrate in homo- and cross-aldol processes developed by the groups of Barbas[28] and MacMillan[29] respectively (Scheme 5). The analogous intramolecular reaction was also successfully developed.[30]



Scheme 5: Asymmetric aldol reactions with aldehyde pronucleophiles developed by the groups of Barbas[28] (top) and MacMillan[29] (bottom).

This use of aldehydes was also extended to α-hydroxyaldehyde equivalents,[31] which allowed an organocatalytic *de novo* synthesis of sugars (Scheme 6).[32] It has since been found that α-chloroaldehydes are viable pronucleophiles as well.[33]



Scheme 6: Two-step synthesis of sugars with an intermediate prepared by enamine catalysis; Different sugars can be prepared by variation of the conditions in the final step.[32]

Other notable advances in substrate scope have been achieved through variation of the electrophilic component of the reaction. The reaction of aldehydes with ethyl glyoxylate – which can be achieved with *anti*-[34] or *syn*-diastereoselectivity[35] – has been developed. Analogously, Mannich reactions can be performed with imines derived from ethyl glyoxylate with aldehyde[36] and ketone[37] nucleophiles. Certain activated ketones have also been found to be applicable to the role of electrophile, such as α-keto esters,[38,39] α-keto phosphonates,[40] and trifluoromethyl ketones.[41–44] The attainable products from the changes in the electrophile described here are displayed below in Figure 2.

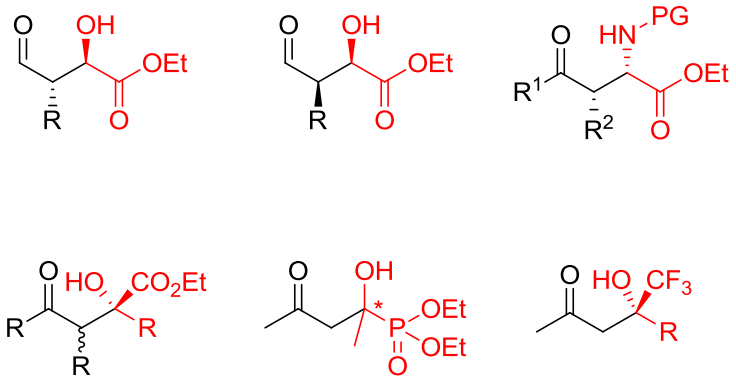


Figure 2: Products available from aldol and Mannich reactions with various electrophiles.

Many other, more esoteric, variants of organocatalytic aldol and Mannich reactions have been developed for cases in which the synthetic target demands certain functional groups for further derivatisation.

Research into enamine catalysis methodology for asymmetric conjugate addition reactions has been similarly thorough, and success has been found with a wide range of Michael acceptors.[45] More general alkylation reactions have presented a greater challenge; this is partly due to the incompatibility of alkylating agents with amine catalysts, which can themselves become alkylated.[46] However, much progress has been made through use of SOMO catalysis, an extension of enamine catalysis, which involves single electron oxidation of the enamine intermediate and subsequent radical-based transformation.[47] This allows asymmetric allylation,[47] benzylation,[48] enolation,[49] and trifluoromethylation[50] of carbonyl compounds. Complementary alkylation methods in enamine catalysis have also been developed with allylic,[51] benzylic,[52] and heteroaromatic[53] carbocations. Through the combination of enamine catalysis and copper catalysis, iodonium salts have very recently been applied as electrophiles in asymmetric trifluoromethylation,[54] arylation,[55] and vinylation[56] reactions. Asymmetric alkylation reactions possible through enamine catalysis are shown below in Figure 3.

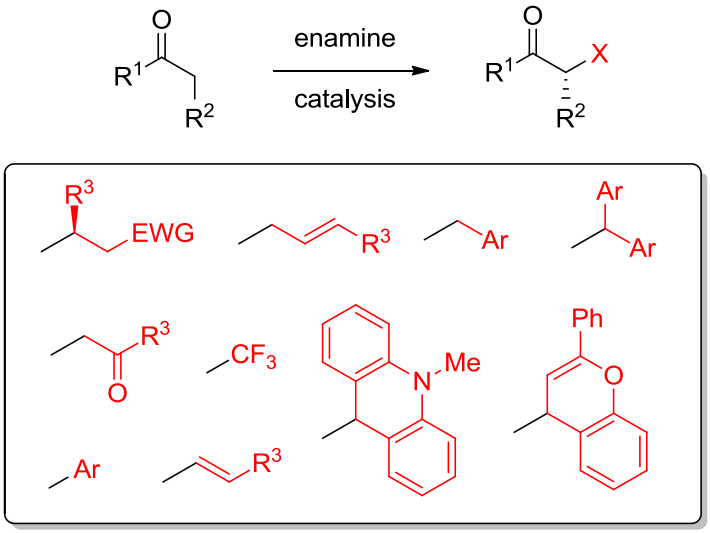
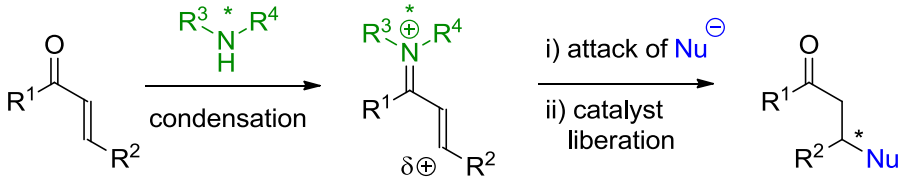


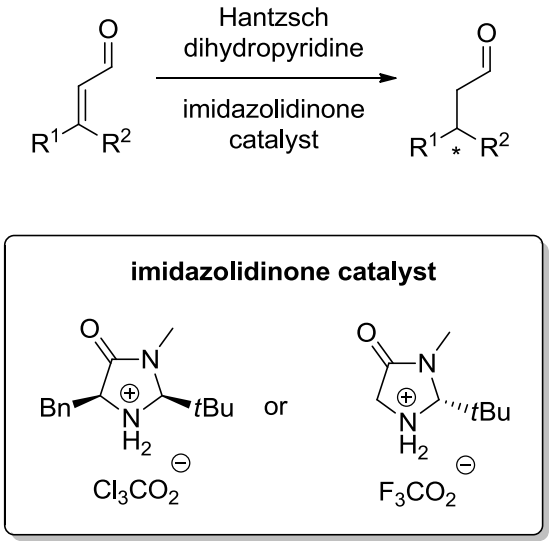
Figure 3: Alkylation products accessible through enamine catalysis; The groups highlighted in red are derived from the corresponding electrophile; R^1 = H or alkyl group, R^2 = alkyl group, R^3 = alkyl or aryl group, EWG = electron withdrawing group, Ar = aryl group.

In asymmetric iminium catalysis, carbonyl compounds are converted to iminium intermediates with chiral amines; unsaturated carbonyl substrates are employed and the intermediates generated undergo cycloaddition processes as in Scheme 2, or 1,4-addition with nucleophiles to give β-functionalised carbonyl compounds after catalyst liberation (Scheme 7).[57]



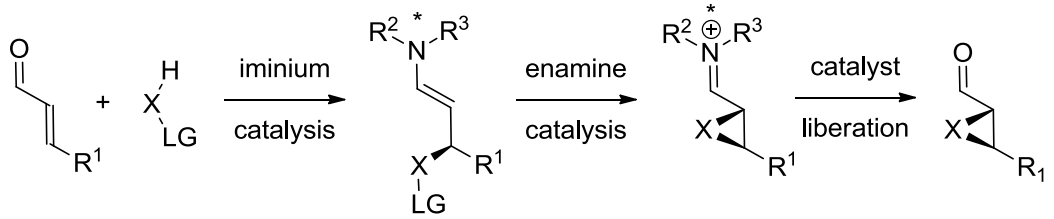
Scheme 7: General mechanism of asymmetric iminium catalysis; $R_3R_4NH^*$ = chiral primary or secondary amine; $Nu^{\ominus}$ = nucleophile (C-, N-, O-, P-, and S-based examples known).

A simple, but powerful, early application of this reactivity was shown in the transfer hydrogenation of enals developed independently by the groups of List[58] and MacMillan.[59]



Scheme 8: Asymmetric enal hydrogenation through iminium catalysis.[58,59]

Enamine and iminium catalysis are closely related because both types of intermediates are formed in both classes of organocatalysis – the only difference is which intermediate dictates the transformation. This bridge between the two modes of catalysis has been exploited in the development of domino reactions that involve both types of reactivity. This is demonstrated in the organocatalytic epoxidation[60] and aziridination[61] reactions (Scheme 9), in which oxygen and nitrogen compounds bearing a leaving group act as nucleophiles in an iminium catalysis cycle, and then as electrophiles in an enamine catalysis cycle.



Scheme 9: Organocatalytic epoxidation/aziridination reactions operating through a domino iminium/enamine process; X = O or NR; LG = leaving group.

1.3. Non-Covalent Catalysis – Ion-Pairs and Binders

Organocatalytic methods that rely on non-covalent interactions with reacting substrates have also been developed; these reactions are often complementary to those proceeding through covalent catalysis.

In asymmetric phase transfer catalysis (PTC) a chiral counter-ion becomes associated with an ionic substrate to generate a new chiral complex.[62] Shown in Figure 4 is a standard substrate-type used in PTC for generating enantioenriched amino acid derivatives upon reaction with an appropriate electrophile.

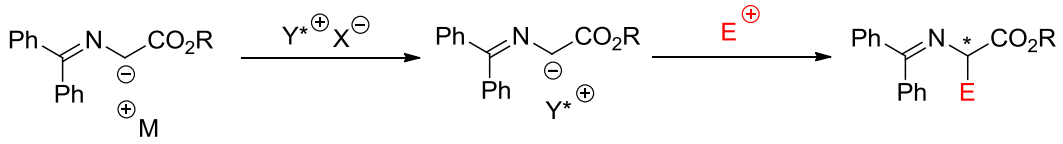


Figure 4: PTC applied to the synthesis of enantioenriched amino acid derivatives; Y*⊕ = chiral counter cation; E⊕ = electrophile.

Enolates of various types are the substrates typically utilised in PTC, but enantioselective reactions are also known that employ much simpler anions – such as peroxide in asymmetric Weitz-Scheffer epoxidations.[63] The organic chiral cations (Y*⊕) employed are usually quaternary ammonium species and some representative examples that have been shown to induce high levels of enantioselectivity are depicted in Figure 5. In recent times analogous phosphonium cations have gained increased attention.[64]

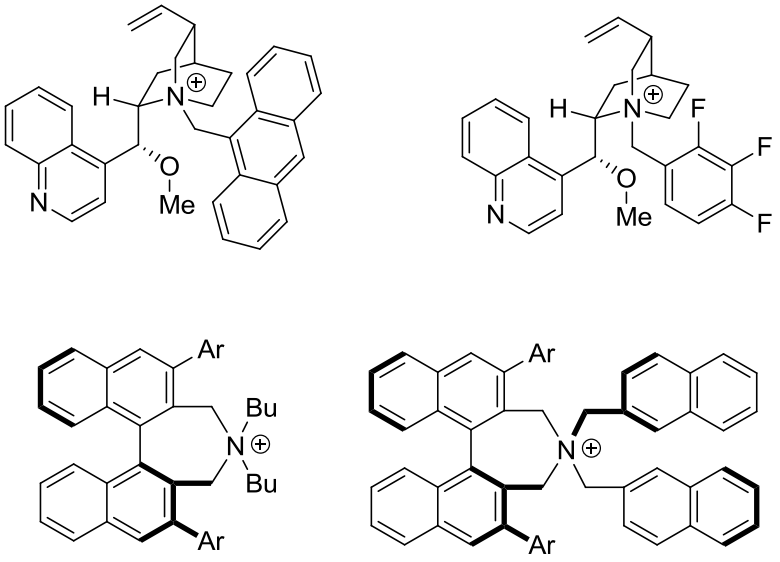
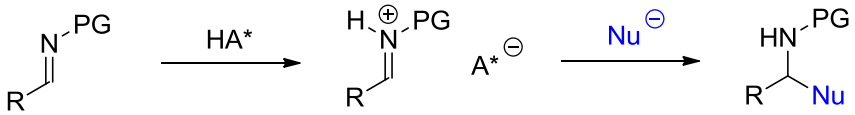


Figure 5: Chiral ammonium cations successfully applied in asymmetric PTC; Ar = 3,4,5-$F_3C_6H_2$; Clockwise from top left: introduced by the groups of Corey,[65] Jew and Park,[66] Maruoka,[67] and Marouka.[68]

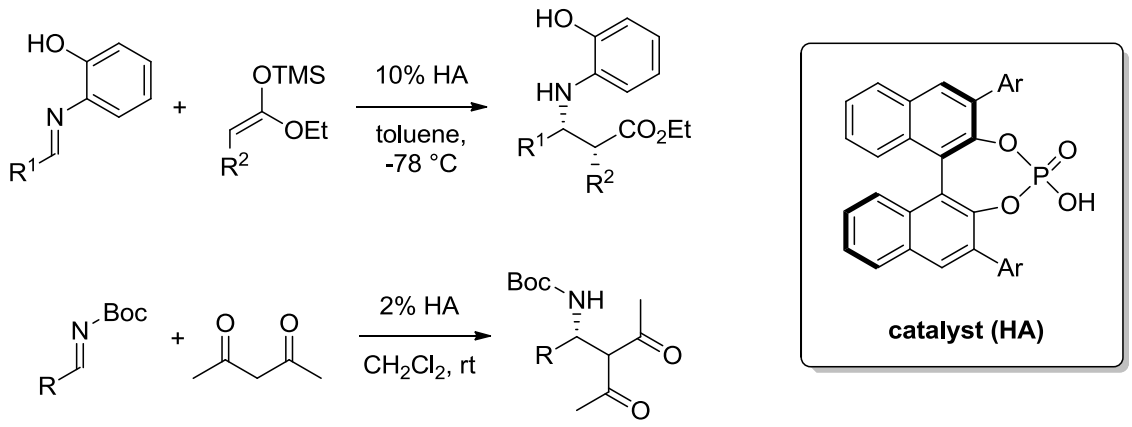
As well as creating a chiral environment for the ensuing reaction, the counter ion often serves to solubilise the substrate in the reaction medium. In fact, in many examples this is a central facet, as a biphasic reaction medium is employed and the catalyst shuttles the reagents between the phases, which reveals the origin of the PTC designation.

A similar ion-pairing mechanism operates in asymmetric Brønsted acid and base catalysis. A key protonation or deprotonation event yields an activated intermediate with a chiral counter-ion. The asymmetric Brønsted acid catalysis approach has found particular application in the activation of imines and imine fragments buried within other functional groups (such as in pyridine rings).



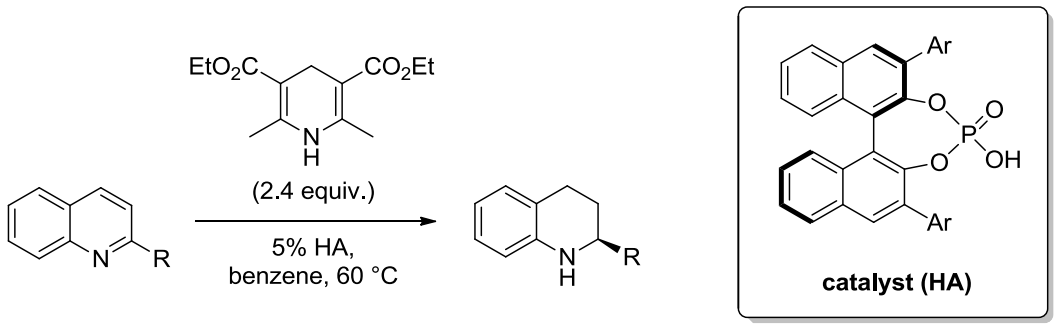
Scheme 10: Asymmetric Brønsted acid catalysis for the 1,2-addition to imines; $A^{*\ominus}$ = chiral conjugate base; $Nu^{\ominus}$ = nucleophile.

This reaction-type was discovered independently by the groups of Akiyama[69] and Terada[70] (Scheme 11). Axially chiral phosphorus-based catalysts employed in these reactions have been widely used since.



Scheme 11: First examples of chiral phosphoric acid-catalysed reactions; Top reaction: Akiyama group,[69] Ar = 4-nitrophenyl, R^1 = aryl, R^2 = Me, Bn, $OSiPh_3$; Bottom reaction: Terada group,[70] Ar = 4-(β-Naphthyl)phenyl, R = aryl.

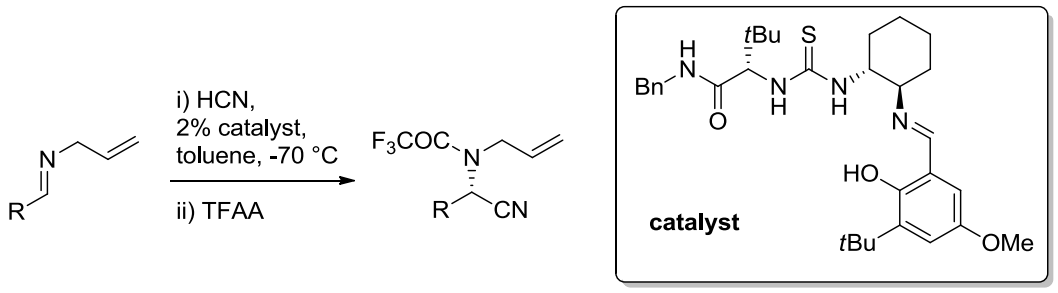
A striking example of this reactivity is shown in the synthesis of alkaloid natural products by transfer hydrogenation of quinoline substrates reported by Rueping and co-workers[71] (Scheme 12).



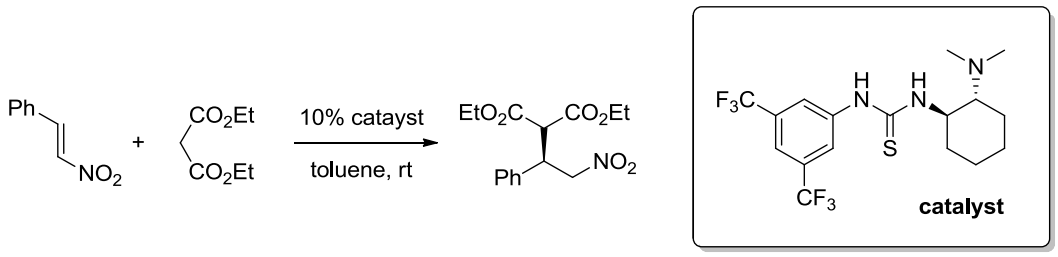
Scheme 12: Brønsted acid-catalysed transfer hydrogenation of quinolines reported by Rueping and co-workers; R = aryl, alkyl; Ar = 9-phenanthryl.

A wide variety of other catalyst structures and transformation types has been examined,[72] including processes that involve activation of carbonyl compounds.[73]

Other catalysts interact with substrates or key intermediates through non-bonding interactions, usually hydrogen bonds. Association purely through non-ionic intermolecular interactions is in some cases sufficient to activate and impart stereochemical information. Particular use has been made of catalysts bearing the thiourea functional group, exemplified by the seminal contributions made by the groups of Jacobsen[74] and Takemoto[75] (Scheme 13 and Scheme 14).



Scheme 13: Asymmetric Strecker reaction first reported by the group of Jacobsen.[74]



Scheme 14: Asymmetric conjugate addition reaction first reported by the group of Takemoto.[75]

These catalysts, and related species, have since been applied to a range of other reactions, and new catalysts and systems have been developed bearing different functional groups capable of activating a given substrate.[76] Catalysts based upon cinchona alkaloids have also proved to be particularly effective within this reaction framework.[77] Often, hybrid systems are employed in which the catalyst is additionally anchored by a covalent bond or ionic interaction. The general basis for non-covalent catalysis of this type is the incorporation of functional groups into the catalyst structure that form very strong and specific interactions with groups on the substrate.

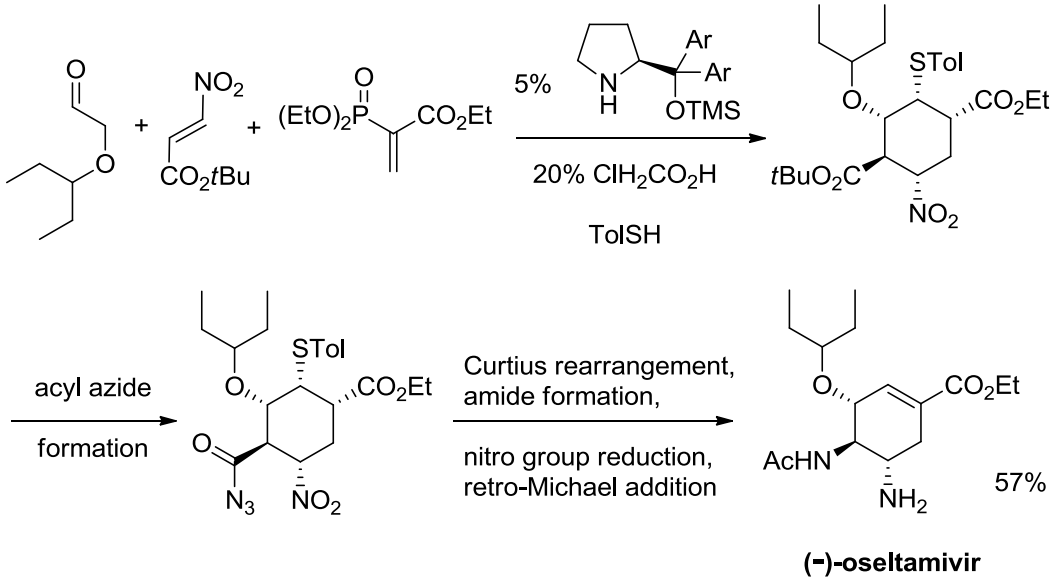
1.4. Achievements and Challenges

Organocatalysis offers several practical advantages over alternative methods. By definition, the catalysts do not contain toxic metals hazardous to human health or the environment. They are typically stable compounds that can be subjected to a range of different reaction conditions and have broad functional group tolerance. This stability presents the opportunity to use unactivated and unprotected substrates. There are also advantages from the point of view of the researcher: the active catalyst is not formed *in situ* and its structure is therefore unambiguous. This contrasts with the mixture of ligands with a transition metal catalyst precursor. Catalyst design and investigation into structure activity relationships are therefore made more straightforward.

Perhaps the major achievement in the field of organocatalysis has been the paradigm shift in the approach to synthetic chemistry research. Previously, the application of transition metal complexes would be the logical choice for a researcher interested in inventing new asymmetric catalytic transformations. This thinking is of course justified by the vast body of precedents from which inspiration can be drawn. Indeed the huge importance of asymmetric transition metal catalysis has been recognised by the award of the Nobel Prize to Noyori,[78] Knowles,[79] and Sharpless[80] for their contributions to the field. Now, a body of literature also documents precedents for the use of organic molecules as catalysts, so this approach can be considered with confidence too.

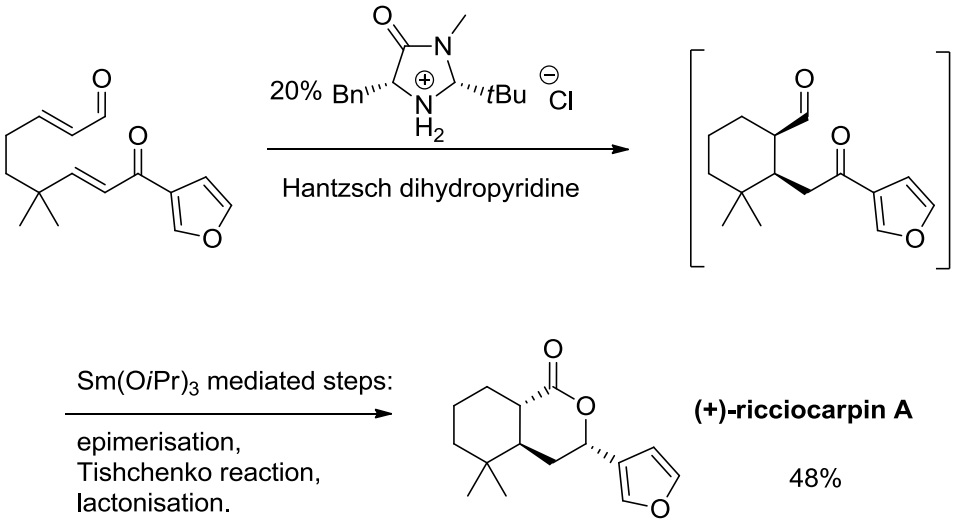
The practicality of organocatalytic methods is best demonstrated by the purpose they have found in application towards a range of synthetic goals. In addition, applications in an industrial setting should be attractive because the low cost and typically environmentally benign nature of the catalysts are major selling points. Organocatalysis has become quickly assimilated into the toolset of the synthetic chemist, and has been applied to a variety of total syntheses. Two examples are given below that demonstrate the improved access that can be achieved in the pursuit of important target molecules. A one-pot organocatalytic cascade, which installed all of the required stereochemistry, was used in the first step of the incredibly efficient

synthesis of the anti-influenza pharmaceutical (–)-oseltamivir (Tamiflu®) reported by Hayashi and co-workers (Scheme 15).[81]



Scheme 15: Hayashi's synthesis of (–)-oseltamivir involving a key, one-pot, organocatalytic cascade in the first step.

A domino organocatalytic transfer hydrogenation/Michael addition process was employed by List and Michrowski in the synthesis of the molluscicidal compound (+)-ricciocarpin A,[82] which has the potential to be used to control the spread of schistosomiasis (Scheme 16). With this method, it was also possible to prepare analogues, and one of these showed higher bioactivity.



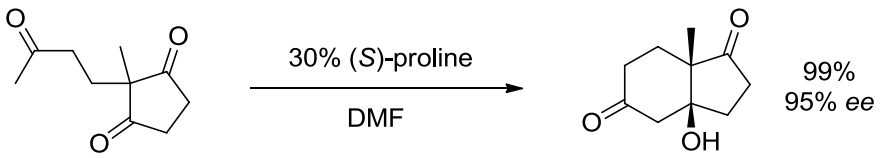
Scheme 16: List's synthesis of (+)-ricciocarpin A with formation of a key intermediate through an organocatalytic domino reduction/Michael reaction.

The application in catalytic cascade reactions highlights the flexibility that organocatalysts can often display.[83] These reactions have been used to target the core of a desired molecule as shown above, or in the general preparation of useful complex materials – typically heterocycles.

Alongside the positive aspects of organocatalysis, there still exist some major limitations. Organocatalytic processes are often catalytically inefficient, requiring high catalyst loadings and long reaction times compared with most transition metal-catalysed reactions. In contrast to the work that has been carried out to discover new reactions and catalysts, relatively few mechanistic studies have been performed. The information that has been acquired, however, has provided incredibly detailed descriptions of the way in which certain reactions work and differ from other, seemingly similar ones. In the opinion of this author, increased efforts to further unravel the mechanisms in organocatalysis will facilitate the improvement of many existing reactions, and precipitate the discovery of currently impossible ones.

2. Proline Catalysis

As discussed above, enamine catalysis has been extensively developed over the last 12 years. In this scientific progress, proline catalysis served as a major initial vehicle and it has continued to play a central role in further developments. This simple amino acid has been known as an asymmetric catalyst since the 1970s, when it was discovered that it could mediate the enantioselective intramolecular aldol reaction of triketones.[84–85] The reaction, termed the Hajos–Parrish–Eder–Sauer–Wiechert (HPESW) reaction after its discoverers, was once seen as a useful (but esoteric) transformation, but is now much more likely to be defined as the prototypical example of proline catalysis (Scheme 17).



Scheme 17: Hajos-Parrish-Eder-Sauer-Wiechert reaction.

In hindsight, it is amazing that further development of proline catalysis did not continue until over 20 years later, when the intermolecular aldol reaction was reported.[6] Importantly, this discovery showed that proline is not limited to the HPESW reaction but is much more generally applicable as a catalyst, and since then proline has been applied to a large number of reactions. A summary of the important transformations that can be catalysed by proline is shown in Figure 6; the absolute stereochemistry depicted is that obtained using (*S*)-proline.

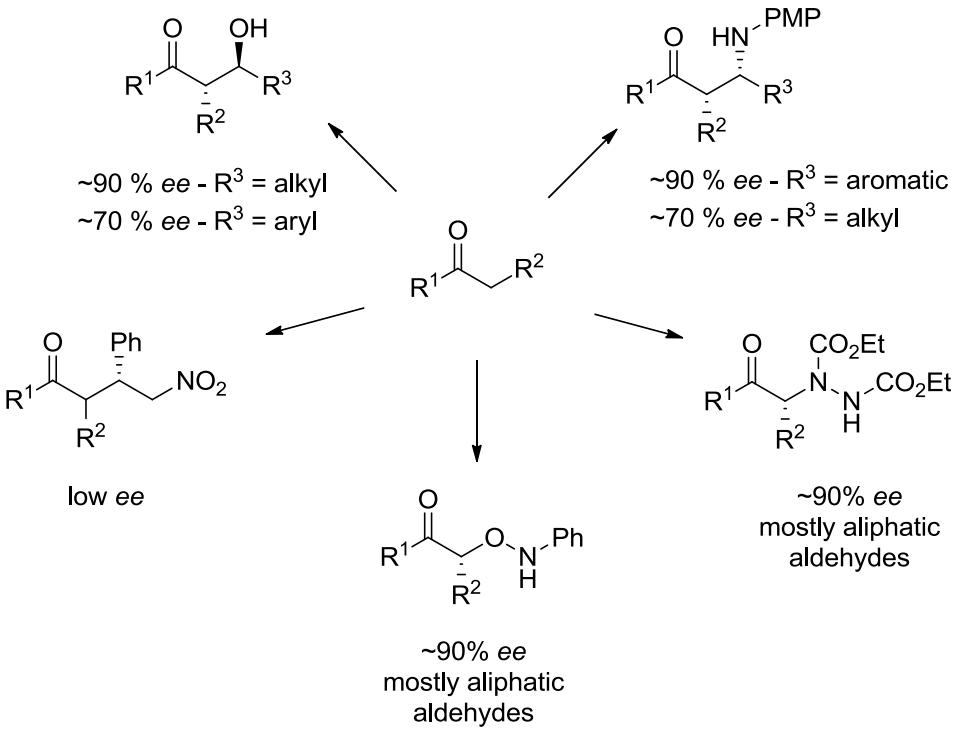


Figure 6: Asymmetric proline-catalysed transformations of enolisable carbonyl compounds; The stereochemistry of products obtained is that derived with (*S*)-proline.

Although proline is not always the best catalyst for a given reaction, it has a very wide applicability. This fact, coupled with its ready availability in both enantiomeric forms, means that proline is typically tested whenever a new process is investigated.

Many of the systems since developed to improve proline-catalysed transformations, or for new reactions, have employed catalysts structurally similar to proline. Direct analogues that have been introduced wherein the carboxylic acid group is replaced with another Brønsted acid have proved to be effective. Particular success has been seen with the development of catalysts with a tetrazole,[86–88] sulfonamide,[89] ammonium,[90,91] or amino alcohol group[92] (see Figure 7).

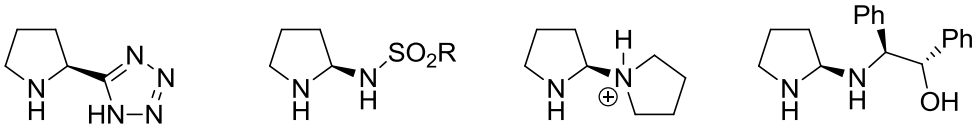


Figure 7: Proline analogues bearing Brønsted acids.

A feature that is particularly prevalent in catalyst design is the pyrrolidine framework, which is seen as a privileged structure in organocatalysis. The rigidity of the 5-ring system limits the conformational freedom of reactive intermediates and facilitates the transition of the nitrogen between sp^2 and sp^3 environments. This allows for efficient organisation of transition states, and limits access to alternative pathways.

The importance of the pyrrolidine unit is reflected in the comparable imidazolidinone structure of catalysts developed by MacMillan and co-workers.[7] Remarkably these species, which operate in the related field of iminium catalysis, were developed independently at the same time as the early research into proline catalysis. The effectiveness of these catalysts correlates to their bulk and, along with the conceptually similar prolinol silyl ether catalysts discovered independently by the groups of Jørgensen[93] and Hayashi,[94] they have also found use in enamine catalysis.

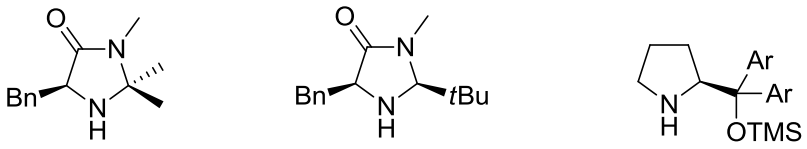


Figure 8: Organocatalysts with bulky substituents.

Strikingly, other *N*-heterocyclic carboxylic acids such as 2-azetidine carboxylic acid and 2-piperidine carboxylic acid (pipecolic acid) were found, early on, to be relatively inactive.[6]

Aside from its practical uses, and its influence seen in the design of other catalysts, proline is also hugely important in the field of enamine catalysis because it has played a central role in mechanistic studies. The functioning of a wide variety of reactions in enamine catalysis is related back to what is known about the proline reaction.

3. Mechanistic Debate

3.1. Mechanism of the HPESW Reaction

The mechanism of the HPESW reaction remained a matter of debate until the more recent reports of proline-catalysed reactions provided the impetus to resolve the matter. The different mechanisms proposed since the original discovery of the reaction are shown in Figure 9.

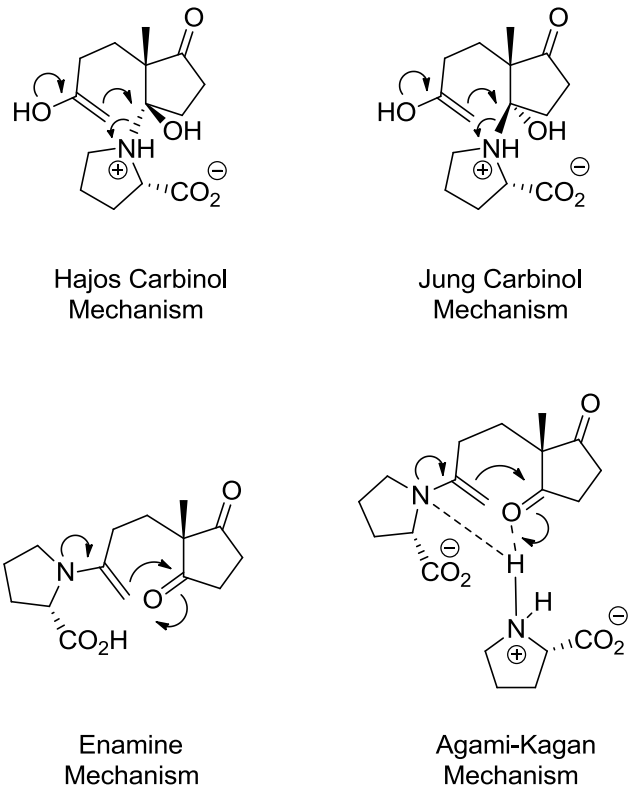


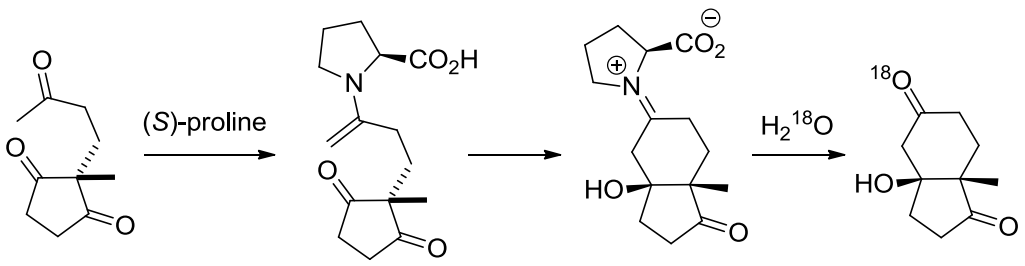
Figure 9: The different historical models proposed for the mechanism in the HPESW reaction.

Hajos initially proposed that the ketone undergoing nucleophilic attack is activated as a carbinol amine intermediate.[85] The mechanism was questioned by Jung, since the apparent substitution reaction would have to proceed with retention of stereochemistry to predict the correct product enantiomer. A revised mechanism was proposed in which the carbinol in question is generated by attack of proline onto the

opposite face of the ketone, and it was alternatively suggested that the reaction could proceed through an enamine intermediate.[95]

Agami and Kagan observed a non-linear relationship between catalyst and product *ee* and therefore proposed an enamine mechanism involving two proline molecules in the C-C bond-forming step.[96] It was suggested that one molecule of proline activates the nucleophilic ketone – transforming it into the enamine – while the second molecule acts as the proton-source for the forming alkoxide group. However, when List and co-workers re-examined the reaction mechanism they could find no evidence of non-linear effects;[97] the difference in results was suggested to be due to the use of chiral HPLC rather than the less reliable optical rotation method used by Agami and Kagan. This question of whether non-linear effects occur was addressed by Armstrong, Blackmond, and co-workers. They found that non-linear effects do occur when the reaction is carried out under conditions in which proline is not fully dissolved.[98] Under these conditions, the *ee* of proline in solution does not correlate linearly with the overall proline *ee*. This is because the eutectic composition of proline has a solution *ee* of around 50%. Therefore, the effective catalyst *ee* will be around 50% regardless of the total catalyst *ee*, other than in the cases where it is very high or low when all of the material accounted for.

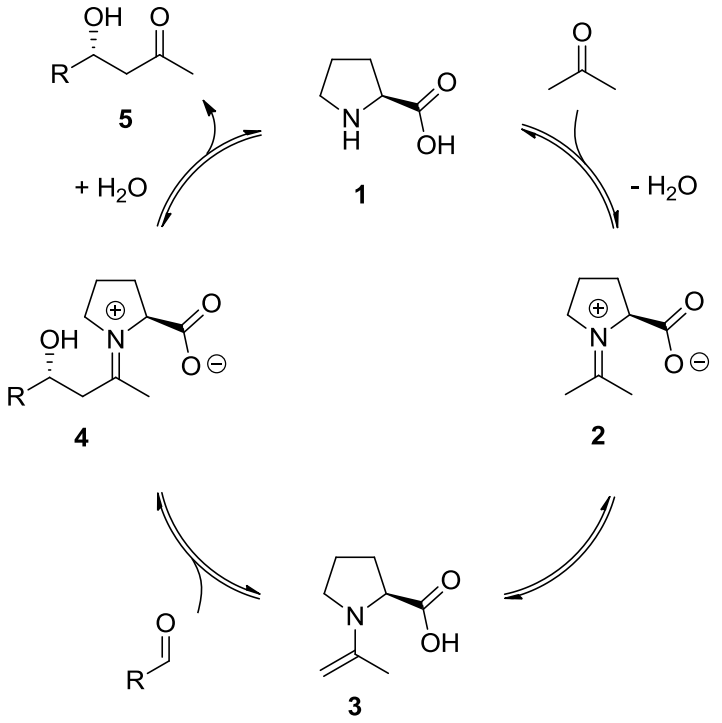
In further support for the enamine mechanism, it was found that when ^{18}O labelled water is introduced to the reaction, ^{18}O becomes incorporated into the final product in the nucleophilic carbonyl; this substitution would be required by the enamine mechanism, in the final hydrolysis of the iminium group generated (Scheme 18).[99] Thus, it is generally now accepted that the HPESW reaction proceeds through an enamine intermediate as was earlier proposed, and involves only one proline molecule in the catalytic cycle.



Scheme 18: Mechanism for ^{18}O labelling of the HPESW product.

3.2. Houk–List Model

This model for the HPESW reaction was subsequently extended to describe the mechanism of the proline-catalysed intermolecular aldol reaction, and the corresponding catalytic cycle is shown below in Scheme 19.



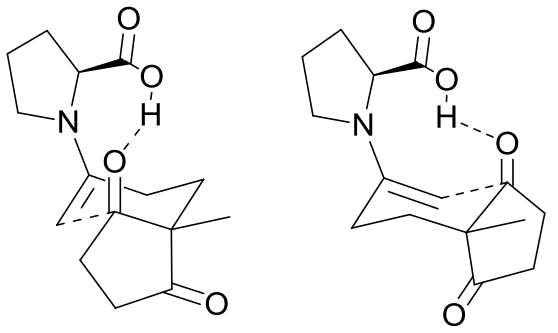
Scheme 19: The catalytic cycle of the Houk–List model for the proline-catalysed aldol reaction.

Proline (**1**) first forms an iminium ion intermediate (**2**) by condensation onto the pronucleophilic carbonyl compound. This intermediate then undergoes deprotonation to form the key enamine intermediate (**3**), which reacts with the aldehyde to form

another iminium intermediate (**4**); subsequent hydrolysis of **4** yields the product **5** and reforms the catalyst.

The methyl amide analogue of proline gives poor conversion in the intermolecular aldol reaction, and it was reasoned that the carboxylic acid side chain is essential.[6] The steps in the catalytic cycle can all potentially be facilitated by the ability of the carboxylic acid to quench negatively charged groups and, conversely, the ability of the carboxylate form to act as a base.

Much of the support for this mechanism, termed the Houk–List model, has come through computational studies. When the proposed mechanisms for the HPESW reaction (Figure 9) were assessed computationally, it was found that the enamine mechanism gave the lowest energy transition state in the C-C bond-forming step, supporting this general model.[100] The lowest energy transition states obtained for this mechanism (shown in Figure 10) involve concerted proton transfer from the carboxylic acid onto the forming alkoxide.[101] Thus the additional importance of the carboxylic acid group for the introduction of enantioselectivity was revealed.



anti-TS
E_{rel} = 0.0 kcal/mol

syn-TS
E_{rel} = 3.4 kcal/mol

Figure 10: The lowest energy transition states calculated by Houk for the HPESW reaction differentiated by an *anti*- or *syn*-relationship between the double bond and the acid group.

Calculated transition states not incorporating this form of intramolecular acid catalysis could not be found, and this is consistent with the previous finding that the transition

state energies of aldol reactions are greatly reduced when intramolecular stabilisation of the developing charges is possible.[102] The two lowest energy transition states depicted in Figure 10 are distinguished by the conformation of the enamine double bond relative to the carboxylic acid group. It was found that the transition state in with these groups bear an *anti*-disposition is lower in energy than the case with a *syn*-disposition. In the *syn*-TS, in order for the carboxylic acid group to attain sufficient proximity to the electrophilic ketone, the forming iminium ion becomes distorted from its ideal planar structure; in contrast, the iminium ion formed in the *anti*-TS does not deviate far from planarity.

This model was extended to the intermolecular reaction, and the conclusions were similar, with *anti*-TS energies calculated to be lower than the corresponding *syn*-TS energies due to differences in the planarity of the forming iminium ion.[103] The four lowest energy transition states calculated for the intermolecular reaction between acetone and acetaldehyde are shown in Figure 11. In this case, an additional factor is the orientation of the electrophile with respect to the bulk of the enamine.

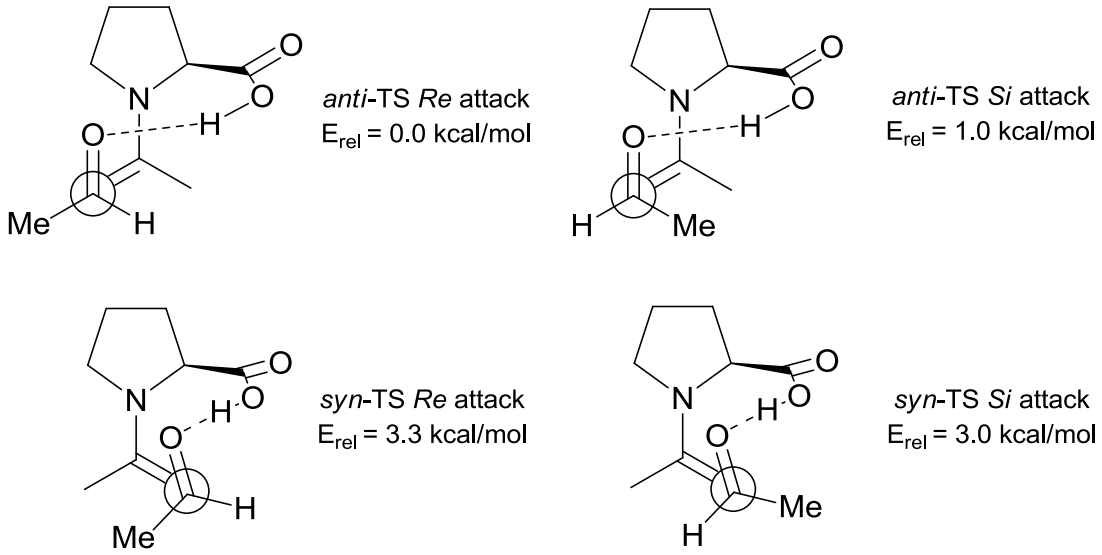


Figure 11: The calculated lowest energy transition states for the proline-catalysed intermolecular aldol reaction.

It was found that both *anti*-transition states are lower in energy than the *syn*-transition states. The calculated *anti*-TS that leads to attack at the *Re*-face of the aldehyde is lower in energy than that involving *Si*-face attack, as this orientation involves fewer steric interactions with the enamine. Application of the model to other reacting partners showed that the differences in energy between the respective *anti*-transition states (the predicted value of $\Delta\Delta G^{\ddagger}$) were in good agreement with the experimental results.

An interesting feature of these studies on the proline-catalysed intra- and intermolecular aldol reaction is the revelation that stabilisation of the forming alkoxide in the transition states is effected not only by the carboxylic acid proton, but also by the slightly acidic hydrogen atoms of the methylene group adjacent to the nitrogen atom. This interaction, depicted in Figure 12, stabilises the *anti*-transition states more effectively than the *syn*-transition states because the forming alkoxide is closer, and is an additional factor that accounts for the lower energies of *anti*-transition states.

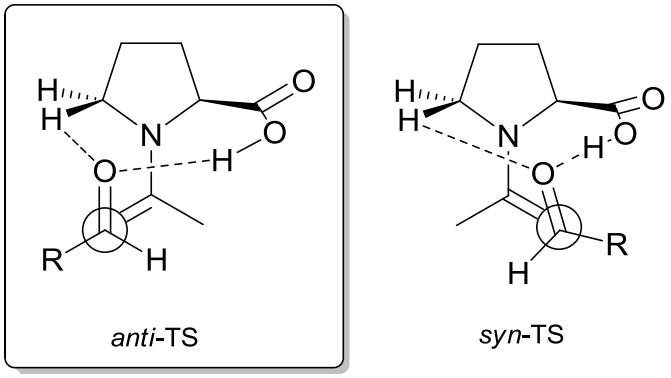


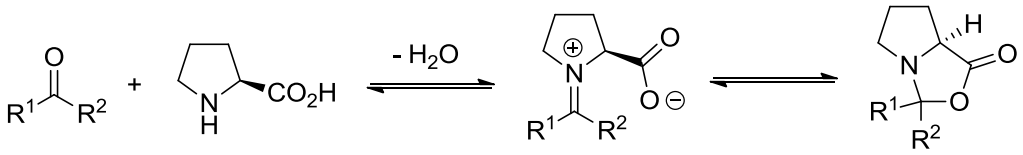
Figure 12: The NCH $\delta^{\oplus\cdots}$O $\delta^{\ominus}$ interaction can stabilise the transition states of proline-catalysed aldol reactions; The lowest energy TS is highlighted.

The existence of this interaction is supported by the observation that DMTC (5,5-dimethylthiazolidine-4-carboxylic acid) shows greater selectivity than proline in aldol reactions.[27] This is explained by the increased acidity of the methylene group that gives rise to the interaction.[104] Computational models for the mechanism of proline-

catalysed reactions have gained validity by the success that such models have had in predicting selectivity.[103 – 105]

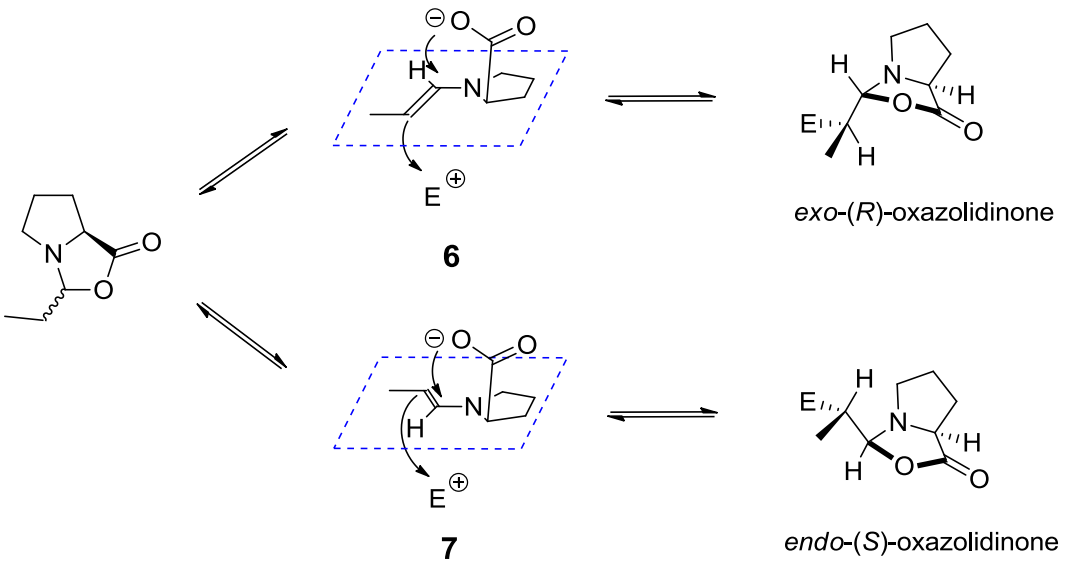
3.3. Seebach–Eschenmoser Model

Oxazolidinones, formed by reaction between the catalyst and one substrate unit, are species commonly observed in enamine catalysis, and their importance has proved to be a topic for debate. Oxazolidinone formation arises from the trapping of iminium intermediates as shown in Scheme 20; these compounds are readily observed by ^{1}H NMR spectroscopy carried out on mixtures of proline and carbonyl compounds.



Scheme 20: Formation of oxazolidinones by reaction of the catalyst with one substrate unit.

In the Houk–List picture, oxazolidinones are merely an off-cycle resting state for the catalyst in equilibrium with on-cycle intermediates. Seebach, Eschenmoser, and co-workers[106] contrastingly proposed a mechanism in which these species are part of the cycle, and also in which oxazolidinone formation occurs in the enantiodetermining step.

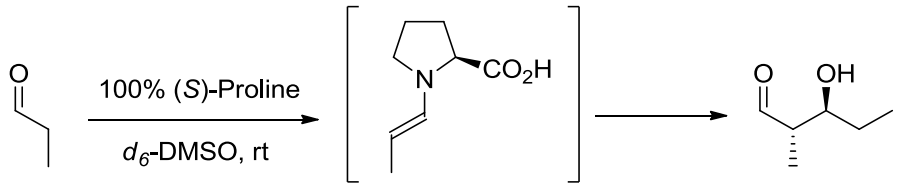


Scheme 21: Seebach-Eschenmoser model for enantiocontrol through oxazolidinone formation; E⊕: electrophile.[106]

The proposition is that in the C-C bond-forming step, an enamine carboxylate intermediate attacks the electrophile in a lactonisation process, giving the oxazolidinone form of the product directly. Unlike in the Houk–List model, the approach of the electrophile is from the face opposite the carboxylate group in the transition state (Scheme 21). It was argued that many electrophiles employed in proline catalysis do not require activation by intramolecular acid catalysis. The observed enantioselectivity in proline catalysis is accounted for by a lowest energy transition state in which the carboxylate and enamine groups are in a *syn*-disposition (**6**). This gives the *endo*-oxazolidinone form of the product whereas the alternative *anti*-attack (**7**) gives the less stable *exo*-oxazolidinone form; it is presumed that the transition state is product-like and hence **6** is the favoured pathway. It was additionally proposed that the key enamine carboxylate intermediate could be directly generated from oxazolidinone intermediates by base-induced elimination, thus placing these species on the catalytic cycle.

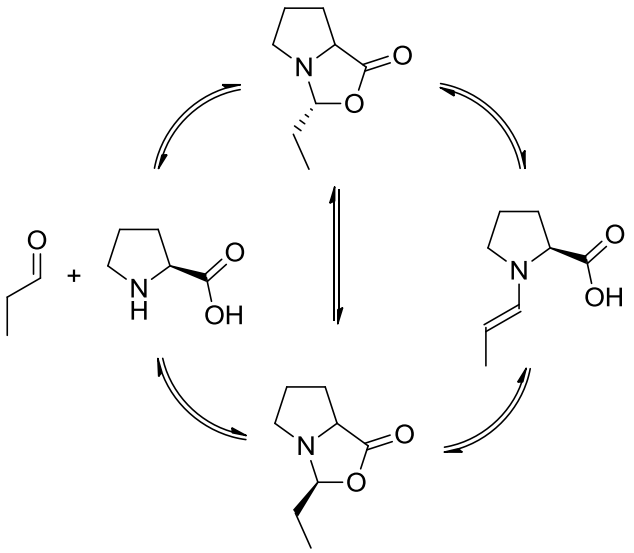
3.4. Enamine Detection and Analysis

Until relatively recently, a persistent criticism of the Houk–List model was that the key enamine intermediate is not observable. However, it has since been shown that this elusive intermediate can be seen under certain conditions. Gschwind, Zeitler, and Schmid reported the first such observation in the proline-catalysed homoaldol reaction of aliphatic aldehydes.[107] The generation of the enamine intermediate was achieved by the (crucial) application of a 100% catalyst loading.



Scheme 22: Gschwind conditions for observation of the enamine intermediate in the proline-catalysed homoaldol reaction of propanal.[107]

The usual oxazolidinone intermediate was still the major observable species derived from the catalyst. Interestingly, it was discovered that the oxazolidinone to enamine ratio was unaffected by catalyst loading; this indicates that under typical reaction conditions the enamine is present, but at a concentration too low to be detected by NMR spectroscopy. It was additionally found, through the application of EXSY experiments, that the enamine is in rapid equilibrium with both oxazolidinone diastereoisomers, but not with propanal. This suggests that enamine formation can only occur from the oxazolidinone form of the catalyst. An intermediate iminium species could not be detected, and the rate constants determined for formation of the starting material and enamine from the two oxazolidinone isomers were not indicative of its existence.



Scheme 23: Rapid catalyst resting state equilibria determined by EXSY.[107]

It was noted in this study that the enamine intermediate is only observable in polar aprotic solvents with high hydrogen-bond acceptor ability (β). The necessity of the latter solvent property was elucidated by calculations that showed considerable stabilisation of the enamine intermediate when an explicit molecule of DMSO was incorporated into the model.[108] Specifically, the carboxylic acid group is stabilised by coordination of the solvent as a Lewis base (Figure 13).



Figure 13: Enamine stabilisation by DMSO determined by computational analysis of explicit solvent effects.[108]

Proline-derived enamines can also be readily observed by NMR spectroscopy in the presence of bases, which shift the equilibrium away from oxazolidinone formation.[108,109] Spectroscopic studies were subsequently extended to prolinol and prolinol ether catalysts, which were found to give larger ratios of the enamine intermediate with respect to other species derived from the catalyst in question

(Figure 14).[110] The conformational preferences of such enamine intermediates were revealed by extensive NOESY analyses; notably the existence of enamines bearing a *cis*-relationship between the alkene group and the pyrrolidine ring substituent was observed for prolinol catalysts.[111]

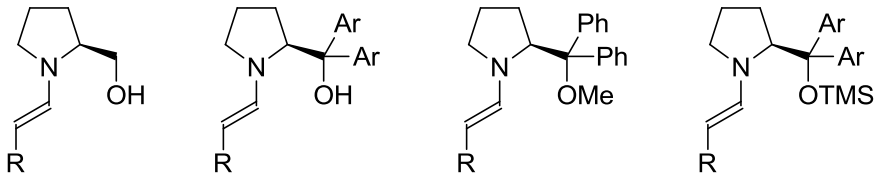
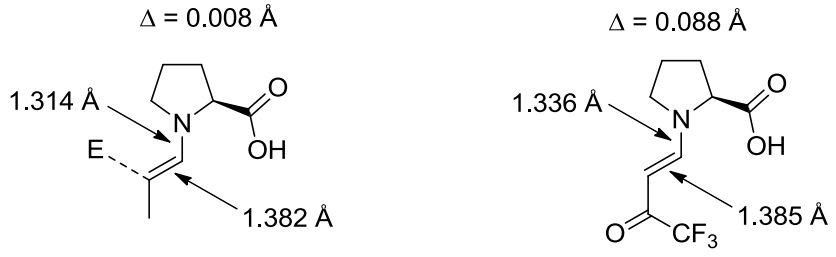


Figure 14: Further examples of enamine intermediates observed by Gschwind, Zeitler, and Schmid; Ar = Ph, 3,5-$(CH_3)_2C_6H_3$, 3,5-$(CF_3)_2C_6H_3$; R = Me or *i*Pr.[110]

Further analysis of enamine structure has been carried out by List and co-workers, who prepared isolable analogues and determined their molecular structures by X-ray crystallography.[112] It was found that trifluoromethyl enaminones contained bond lengths similar to those calculated for enamine catalysis transition states and could thus serve as transition state mimics. Another feature of these model compounds that corroborates the calculated structures in the Houk–List model is the lack of nitrogen pyramidalisation.



TS for enamine attack
(DFT calculation)

List enaminone TS mimic
(X-ray crystallography)

Figure 15: Comparison of bond lengths and N pyramidality (Δ) for enamine attack TS (determined by DFT calculation) and List enaminone TS model (determined by X-ray crystallography).

3.5. Additives Effects and Kinetic Investigations

A successful approach to elucidating features of organocatalytic mechanisms has been to apply Reaction Progress Kinetic Analysis (RPKA). In this methodology, the complete kinetic profile of a catalytic reaction is determined under different sets of conditions, and these data are used to assess the relative likeliness of different reaction mechanisms.[113] In particular, it has been found to be crucial to account for the behaviour of additives in order to uncover a complete picture of a given reaction.

3.5.1. Effect of Water on the Proline-Catalysed Aldol Reaction

Water is the most commonly investigated additive in enamine catalysis and, in addition, considerable efforts have been made to find conditions under which water can be used as a reaction medium.[114] Pihko and co-workers were the first to report an extensive study on the effect of water on the proline-catalysed aldol reaction.[115] It was found that added water had little effect on aldol reactions carried out with excess of nucleophile; however, when the reaction was performed under stoichiometric conditions, noticeable improvements in conversion were observed in the presence of one equivalent of water (Figure 16).

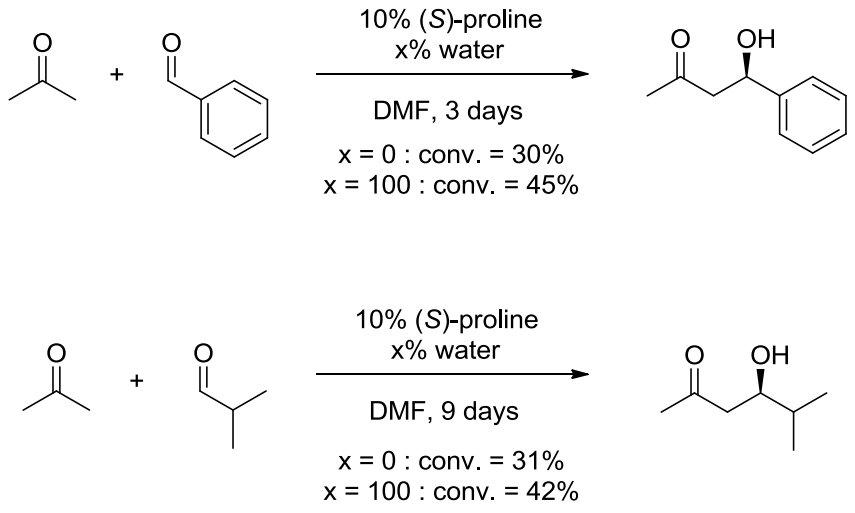


Figure 16: The effect of water on conversion in stoichiometric proline-catalysed aldol reactions.[115]

Under standard conditions, a large excess of the nucleophilic reaction partner is employed and it is often used as a cosolvent. In consequence, the reaction is not viable if the ketone or aldehyde being used as the nucleophile is either valuable or hard to remove. When reactions are performed with stoichiometric amounts of nucleophile and electrophile, reaction times are drastically lengthened. With water as an additive it was demonstrated that non-volatile ketones such as those shown in Figure 17 could be used as nucleophiles in stoichiometric aldol reactions.[115]

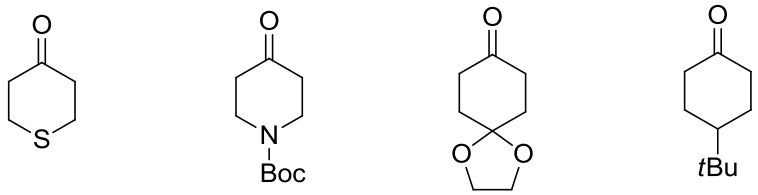


Figure 17: Non-volatile ketones shown to be viable nucleophiles in stoichiometric proline-catalysed aldol reactions, using water as an additive (1–5 equiv.).[115]

These observations were originally explained by invoking reaction acceleration caused by water,[116] and this assertion was used as evidence in the Seebach-Eschenmoser model that Brønsted acid activation by the proline carboxylic acid would not necessarily be needed.[106] It has since been shown by Armstrong, Blackmond, and co-workers that water actually suppresses the intrinsic rate of the reaction, but serves to lengthen the lifespan of the catalyst.[117] Proline is susceptible to deactivation by off-cycle processes (Figure 18) such as formation of spectator oxazolidinones (**8**) or azomethine ylides (**9**) that can undergo [3+2]-cycloaddition with the aldehyde present.

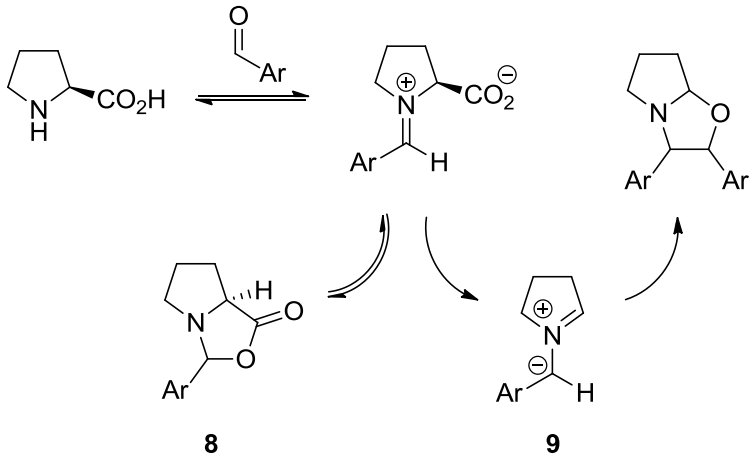


Figure 18: Off-cycle processes in the proline-catalysed aldol reaction lead to formation of oxazolidinones and azomethines; this serves to reduce the concentration of proline.[117]

The catalyst-stabilising effect of water was deduced by "same excess" experiments. In this framework, the reaction was repeated under different starting conditions, such that the concentrations of the reacting ketone and aldehyde were reduced while maintaining the same level of "excess".[ii] For a general case in which the reaction proceeds through 1:1 combination of two substrates, the second experiment mirrors the first experiment after a certain time period: if the new experiment is performed with half the amount of the limiting reagent, the conditions match those attained at the halfway point of the first reaction. This is because "excess" is maintained over the course of a reaction by the reaction stoichiometry. Because of this parallel, the relationship between concentration and rate measured in "same excess" experiments should be identical. If this is not the case, it indicates that catalyst degradation or product inhibition is occurring, and these scenarios can be deconvoluted by further experimentation. Addition of water acts to suppress the undesired catalyst degradation, but formation of iminium species **2** is also suppressed, and this is a key intermediate in the reaction. Overall therefore, water was found to have a negative order in the reaction – quantified as −0.7 by fitting the observed relationship between water concentration and pseudo first-order rate constants to a Michaelis–Menton rate law.[118]

ii) "Excess" here refers to the absolute difference in amount of two reagents rather than the relative excess, which does change over the course of a reaction unless a 1:1 mixture is used.

It was additionally determined that the reaction displayed positive order in the two substrates, acetone and aldehyde. This knowledge allowed the rate law for the proline-catalysed aldol reaction between acetone and an aldehyde to be written as shown in Equation 1.

$$\mathbf{rate} = \boldsymbol{k} \cdot [\mathbf{acetone}]^{\boldsymbol{m}} \cdot [\mathbf{aldehyde}]^{\boldsymbol{n}} \cdot [\mathbf{proline}] \cdot [\mathbf{H_2O}]^{-0.7}$$

Equation 1: The experimental rate law for the proline-catalysed aldol reaction between acetone and an aldehyde.

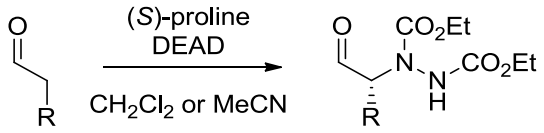
The values of these unknown powers were then determined by "different excess" experiments. For a catalytically stable system, this method involves performing the reaction under conditions in which the "excess" of reagents is changed. Mathematical comparison of the rate data allows for determination of the orders, and it was found that m = 0.58 and n = 0.9.[118]

The rate-determining step of the process can be identified by comparison of the experimental rate law with the different theoretical rate laws that would be apparent if a given step is indeed rate-determining. The matching comparison in this case is found with rate-determining C-C bond formation, i.e. the addition of enamine **3** to the aldehyde substrate. In additional support to this conclusion, the calculated H/D KIE for this step was in good agreement with the experimental value for the reaction. The k_H/k_D value of 2 is smaller than expected for a primary isotope effect because it involves a combination of an inverse and a normal isotope effect, due to enamine attack on the aldehyde and proton transfer from the carboxylic acid.

This work clearly demonstrates the value that understanding the effect of additives can have in mechanistic investigations. A similar case study is provided by the proline-catalysed amination reaction.

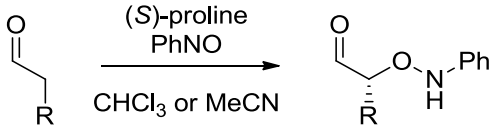
3.5.2. Rising Rate in the Proline-Catalysed Amination Reaction

The proline-catalysed amination[iii] of aldehydes was reported independently by the groups of Jørgensen[11] and List,[12] who found that the reaction between aliphatic aldehydes and azodicarboxylates proceeds with excellent enantioselectivity (Scheme 24).



Scheme 24: Proline-catalysed amination of aliphatic aldehydes developed independently by the groups of Jørgensen[11] and List.[12]

A closely related reaction which uses a similar high energy electrophile is the proline-catalysed aminoxylation reaction simultaneously discovered by the groups of MacMillan,[13] Hayashi,[14] and Zhong.[15] In this process, α-oxidation of aliphatic aldehydes is achieved by reaction with nitrosobenzene.

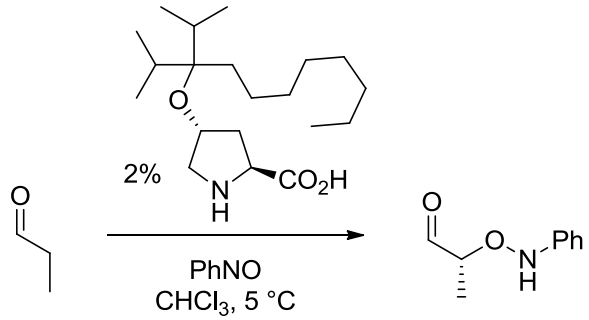


Scheme 25: Proline-catalysed aminoxylation of aliphatic aldehydes developed independently by the groups of MacMillan,[13] Hayashi,[14] and Zhong.[15]

In both the amination[119] and aminoxylation[120] reactions, kinetic investigation revealed a rising rate over the course of the reaction. This represents a stark contrast to the proline-catalysed aldol reaction in which, as is the typical case, the rate decays as substrates are consumed. Increased solubilisation of the catalyst over the course of the reaction was ruled out as a factor by application of a soluble proline analogue,

iii) Although the transformation is more correctly termed a hydrazination reaction, it will be referred to here as "amination" in accordance with conventional literature designation.

which displayed the same effect under completely homogeneous conditions – instead, the phenomenon was shown to be due to product-induced acceleration of the reaction (Scheme 26).[121]



Scheme 26: Aminoxylation reaction with soluble proline analogue.[121]

It was later discovered that protic additives including alcohols and carboxylic acids also gave corresponding rate enhancement, and again this finding was not observed for the aldol reaction.[118] In this report, the product acceleration was found to be due to the hydrazine and alkoxyamine functional groups acting similarly as protic activators. This was shown by the demonstration that above a given loading of product or other acidic additive, the same reaction profile occurs.

Importantly, it was determined that the electrophile in both reactions exhibits zero-order behaviour in the reaction, with the aldehyde displaying first-order behaviour.[121] The catalytic cycle is presumed to fit the Houk–List model and, within this framework, these reagent orders are consistent with rate-limiting enamine formation. Further support for this was provided by the measurement of a large primary kinetic isotope effect when deuterated propanal is employed.[122] Thus, the product and other protic additives are capable of accelerating this step. For the aldol reaction, overall rate enhancement in this way would be impossible, since the rate-determining step comes after enamine formation.

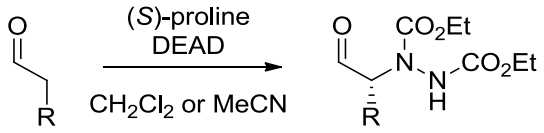
Through the studies described above, a complete picture of some important organocatalytic reactions has been attained. The work relied upon the discovery and

explanation of additives effects, showing their profound value as mechanistic probes. In the results reported below, this approach is extended to further additives effects and the mechanistic implications they present are revealed for the amination, intermolecular aldol, and HPESW reaction.

4. Amination

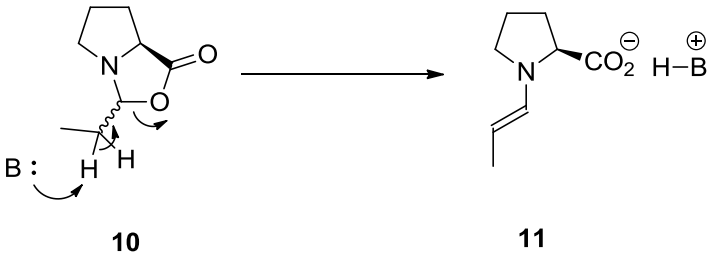
4.1. Introduction

As described above, the proline-catalysed amination reaction is accelerated by protic additives because they can increase the rate of enamine formation – the rate-determining step in the reaction.



Scheme 27: The proline-catalysed amination of aliphatic aldehydes.[11,12]

As an extension of this study, we were interested to assess the effect of basic additives on the amination reaction. Bases may also accelerate enamine formation; indeed, acid and base catalysis in transformations of carbonyl compounds are historic and underlying concepts in organic chemistry.[123] In addition, the Seebach–Eschenmoser model at the centre of the mechanistic debate in enamine catalysis implies that proline-catalysed reactions with active electrophiles, of which DEAD is an example, should be facilitated by base catalysis.[106] This is because conversion of oxazolidinone (**10**) to enamine carboxylate (**11**) – the proposed active species in this model – is suggested to be mediated by basic species present in the reaction medium (Scheme 28).



Scheme 28: The proposed generation of the key enamine carboxylate intermediate (11) from the oxazolidinone resting state (10) mediated by a base (B:).

In a preliminary experiment performed by our collaborators,[iv] it was incredibly found that introduction of DBU to the proline-catalysed reaction between propanal and DEAD caused an inversion in the stereochemical outcome. No such additive-induced reversal of enantioselectivity had previously been observed in an organocatalytic process. This exciting result warranted independent verification, and I proceeded to repeat the initial finding and perform further studies.

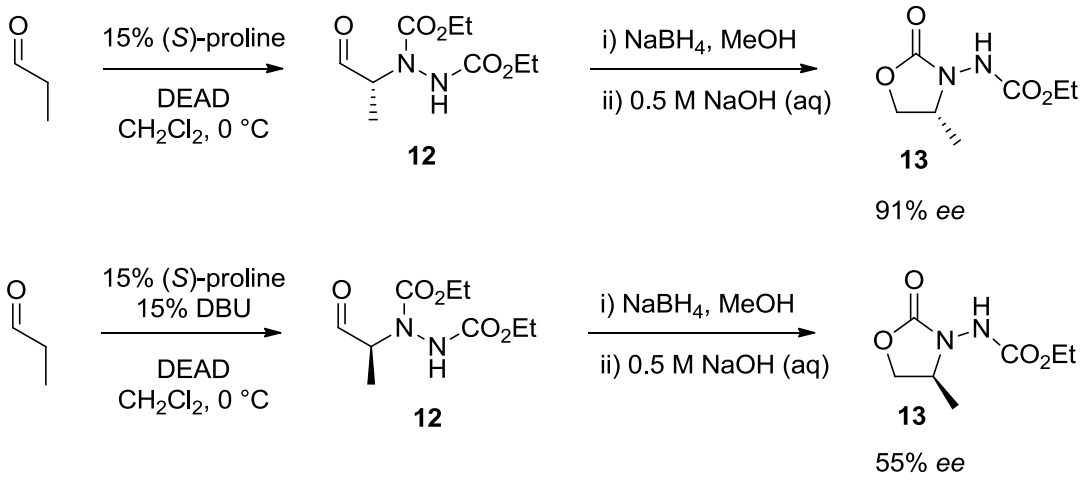
4.2. DBU as an Additive

The reaction protocol reported by Jørgensen and co-workers was adapted for the work reported hereafter: (*S*)-Proline and DBU were mixed in dichloromethane and allowed to equilibrate at 0 °C[v] for 20 minutes prior to addition of DEAD and propanal to initiate the reaction. Conversion was easily monitored by the disappearance of the orange colour of DEAD, which was employed as the limiting reagent.

An important practical point is that the aldehyde product **12** is reported to be unstable with respect to racemisation and hence, in the original publications and in subsequent work that built upon the methodology, the enantioenriched product is typically derivatised to an oxazolidinone (**13**) prior to analysis. After such derivatisation by methanolic borohydride reduction and subsequent base-induced cyclisation, the product was purified by flash column chromatography and the initial result of our collaborators was confirmed (Scheme 29). An attempt was made to perform the reaction at a lower temperature (–20 °C) but no product was formed after stirring for 4 days.

iv) Moran, A.; Blackmond, D. G. B.

v) The reaction temperature was changed from 5 °C for practical ease.

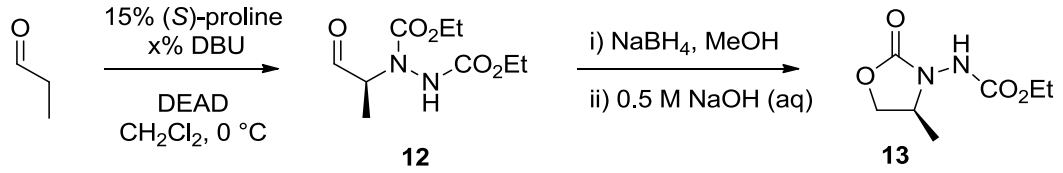


Scheme 29: Enantioselectivity in the proline-catalysed amination reaction between propanal and DEAD; when DBU is added, a reversal in selectivity is observed.

To further probe this effect, reactions were performed with different DBU to proline ratios. As expected, it was found that as the ratio was increased, the extent of reversal in enantioselectivity also increased (the results of this study are displayed in Figure 19 below). It is assumed that DBU completely deprotonates proline under these conditions. Evidence for this was provided by a control experiment in which a sample of enantioenriched amination product was treated with free DBU under the reaction conditions and became rapidly racemised; this indicates that free DBU would not be consistent with the observation of enantioselectivity in the DBU/proline-catalysed reaction.

Thus, when the DBU to proline ratio is between 0 and 1, a mixture of proline and its conjugate base will be present. Since the stereochemical outcome of the reaction is reversed in the presence of DBU, these two forms of the catalyst must give opposite enantiocontrol. The maximum selectivity of the proline-catalysed process is much higher than that of the competing reaction facilitated by its deprotonated form. However, stereochemical inversion was favoured even at low DBU to proline ratios. This clearly indicates that the prolinate catalyst has a higher turnover frequency (TOF).

The solid line on the plot shown in Figure 19 represents the expected relationship between product % *ee* and DBU to proline ratio if the TOF for prolinate catalysis is a factor of 14.3 greater than that of proline catalysis. This curve overlaps well with the results for experiments performed with a DBU to proline ratio greater than 0.4, but for lower ratios, the model underestimates the extent of stereochemical inversion.



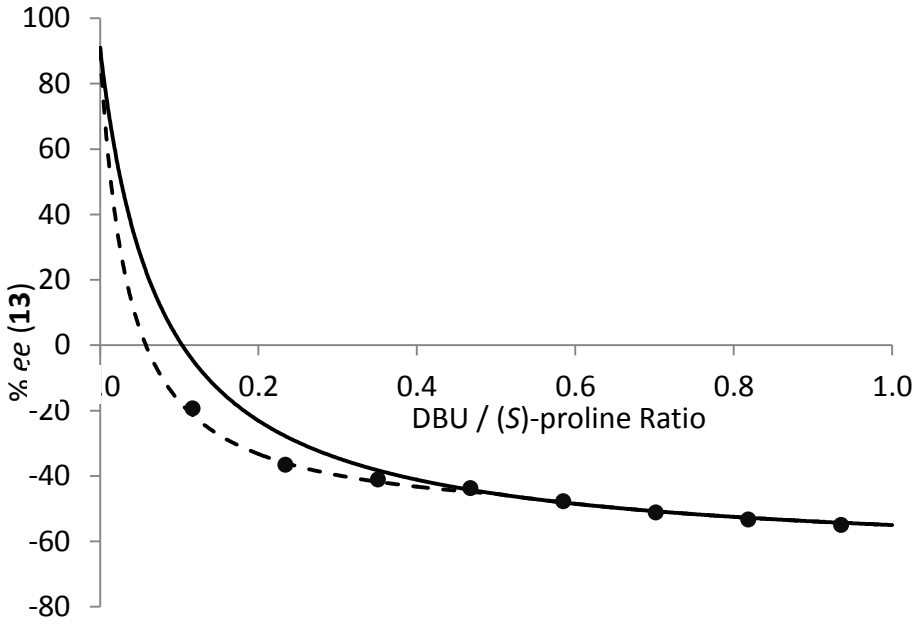


Figure 19: Relationship between % *ee* (positive for (*R*)-product) and DBU/proline ratio in the (*S*)-proline-catalysed amination reaction; Black circles – experimental data; Solid line – modelled relationship assuming a 14.3 factor difference in TOF for prolinate catalyst *vs*. proline catalyst; Dashed line – modelled relationship as for solid line with correction for the maximum proline concentration set at 7.5% loading.

A plausible explanation for this is the difference in solubility of proline and its conjugate base under these conditions. At lower ratios the greater amounts of free proline present could render the reaction solvent saturated, meaning that the prolinate to proline ratio in solution is higher than the overall DBU to proline ratio; the

extent of enantioselectivity reversal is thus greater than expected. The relationship between product *ee* and DBU to proline ratio taking this solubility effect into account is modelled by the dashed line in Figure 19. This shows how the curve changes if the proline saturation point is reached at 7.5% loading i.e. when the DBU to proline ratio is 0.5. In this simple model it is assumed that proline solubility remains the same over the course of the reaction.

4.3. Implication of DBU Effect

The finding that the conjugate base of proline catalyses the amination reaction with an opposite sense of enantioselectivity is highly significant mechanistically because it invalidates the Seebach–Eschenmoser model. In both the Seebach–Eschenmoser and Houk–List models, the reaction intermediate involved in the stereodetermining step is an enamine derived from proline and the pronucleophilic carbonyl compound. The only structural difference between these proposed intermediates is the form of the carboxylic acid side group, which is deprotonated in the Seebach–Eschenmoser model (Figure 20).

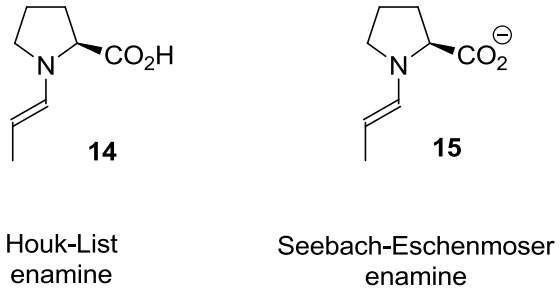


Figure 20: Enamine intermediates in the Houk–List and Seebach–Eschenmoser models derived from propanal.

Both models predict the same sense of enantioselectivity in proline-catalysed reactions but this cannot be the case since the deprotonated catalyst, which would also form enamine carboxylate **15**, gives the opposite sense. The reversal of selectivity could be due to the carboxylate acting as a blocking group in the manner proposed for the diaryl prolinol silyl ether catalyst,[124] which is known to give opposite selectivity

compared with proline[vi] in this reaction;[93] the different modes of reaction are displayed in Figure 21.

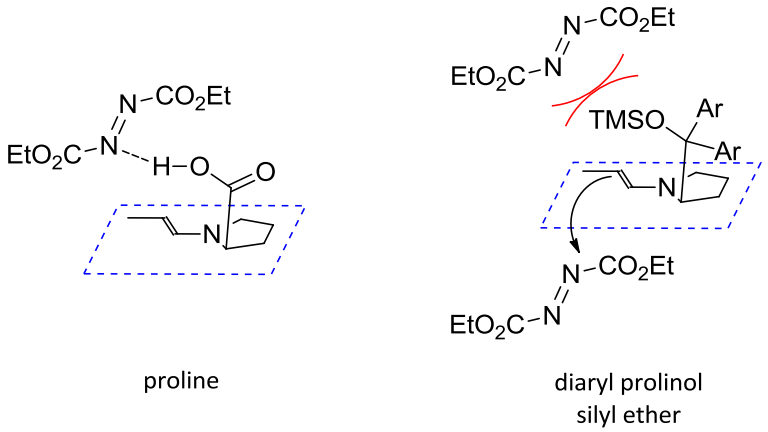


Figure 21: Rationalisation of differences in stereoselectivity between pyrrolidine catalysts; Directing group effect shown for proline; Blocking group effect shown for diaryl prolinol silyl ether.[124]

Possible lowest energy transition states with DEAD approaching from the opposite face to the carboxylate are shown below (Figure 22). The transformation could still involve concerted attack of the carboxylate group as suggested in the Seebach–Eschenmoser model, but the lowest energy transition state of this model must be adjusted to give an *anti*-relationship between the double bond and carboxylate group in the lowest energy transition state in order to give the correct enantioselectivity. In the postulation of this enamine carboxylate mechanism, it was originally noted that this configuration exhibits a favourable alignment of the reacting groups in terms of stereoelectronic effects.[106]

vi) This comparison is made with the configuration of proline from which the diaryl prolinol catalyst is derived.

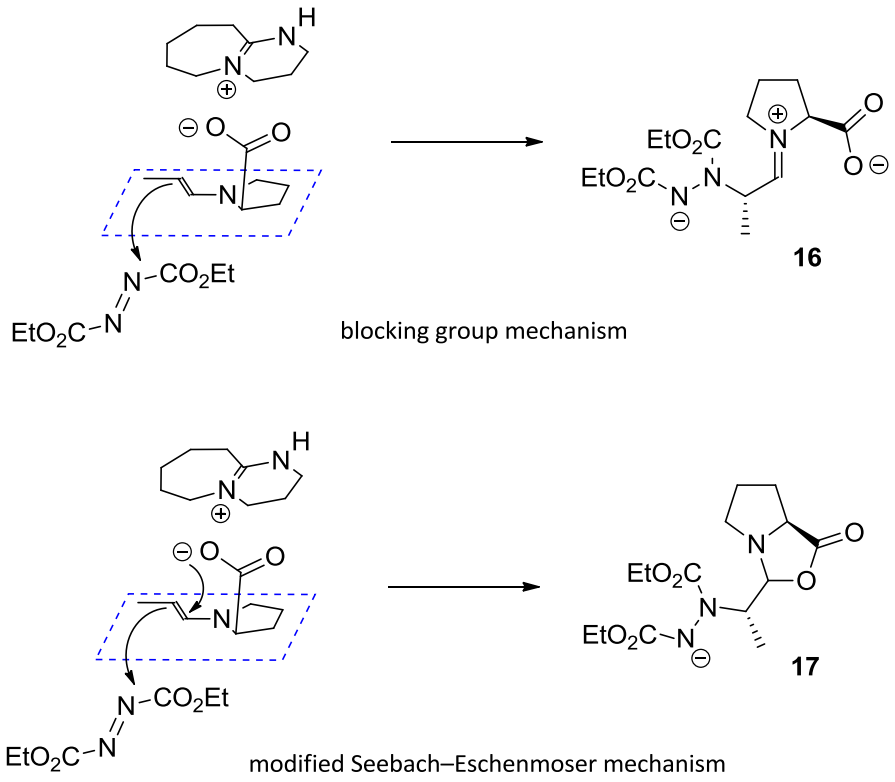


Figure 22: Transition state models that explain the observed stereochemical outcome of the prolinate-catalysed amination reaction; The carboxylate group could act as a blocking group (as in the diaryl prolinol silyl ether-catalysed reaction) or as an anchimeric assisting group (modified Seebach–Eschenmoser mechanism).

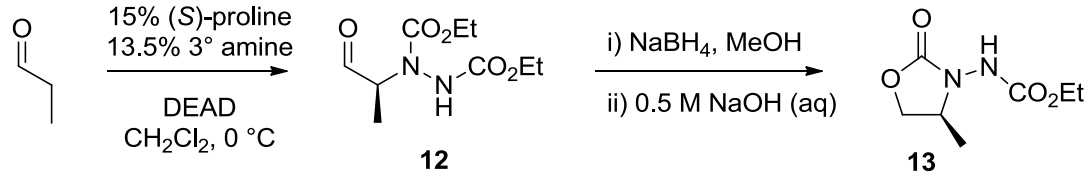
It would be very difficult to differentiate between the possibilities displayed in Figure 22 because if iminium intermediate **16** is formed, it would be likely to rapidly cyclise to form the oxazolidinone **17** in a separate step. This question has since been addressed computationally by Sunoj and Sharma and it was determined that involvement of the carboxylate group does not occur.[125]

4.4. Screen of Other Tertiary Amines

We were next keen to probe the generality of the additive effect by screening a range of other tertiary amines as additives in the proline-catalysed amination reaction. A base to proline ratio of 0.9 was chosen for this screen to avoid product racemisation, which could inadvertently be caused by the presence of excess base. By analogy to the

DBU to proline ratio study, this was expected to give a similar outcome to a reaction in which a 1:1 ratio is employed.

The bases tested showed the same reversal of selectivity as seen with DBU, and notably the selectivity induced by the different combinations (Table 1) was found to be dependent on the strength of the base.



tertiary amine	pK_a (H_2O)[vii]	*ee* / % (**13**)[a]
DBU	11.9[126]	55
DIPEA	11.4[127]	50
DBN	11.0[126]	46
quinuclidine	11.4[128]	28
DMAP	9.9[129]	33
DABCO	8.6[128]	28
NMM	7.4[130]	9

Table 1: Proline-catalysed amination reaction in the presence of tertiary amines; a) Determined by GC analysis of the purified product.

A plot of product *ee* against pK_a (Figure 23) shows the positive correlation between base strength and selectivity.

vii) In every instance where the pK_a of a base is given in this thesis, the value refers to the acid dissociation constant of the corresponding conjugate acid.

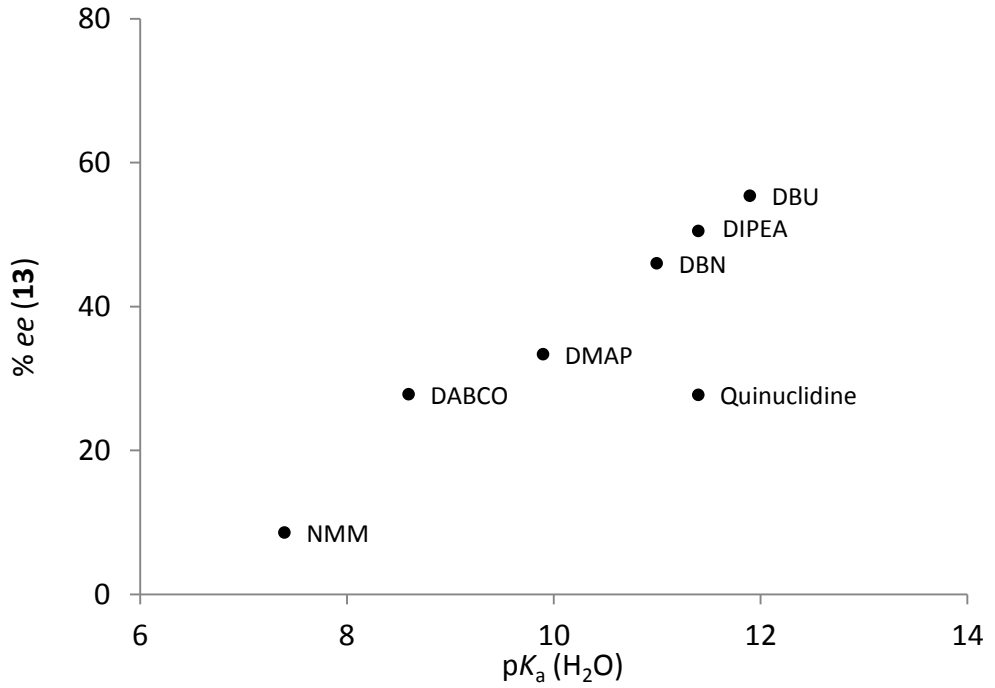


Figure 23: Plot of enantioselectivity (% *ee*) against base strength (pK_a) for the (*S*)-proline-catalysed amination reaction in the presence of tertiary amine bases; See Table 1 for conditions and raw data.

The only outlier apparent in Figure 23 is quinuclidine. This amine can become degraded over time by CO_2 absorption, which could offer a possible explanation for this observation. However, when the experiment was repeated with freshly sublimated quinuclidine, the same result was obtained. It was therefore rationalised that although the base strength appears to be a major factor governing selectivity, other properties also differentiate the bases. To gain more information about the relationship between additive base strength and selectivity, we next turned to the application of reagents even more basic than DBU.

4.5. Phosphazene Bases

Phosphazene compounds were developed as extremely strong, uncharged bases by Schwesinger and co-workers to bridge the gap in activity between other nitrogen-based organic bases and organometallic species.[131] These reagents were found to be readily tuned because the basicity of the central iminophosphorane group can be continually enhanced by homologation within the structure. Phosphazenes applied to

the proline-catalysed amination reaction are shown below in Figure 24; these species are all more basic than DBU.[viii]

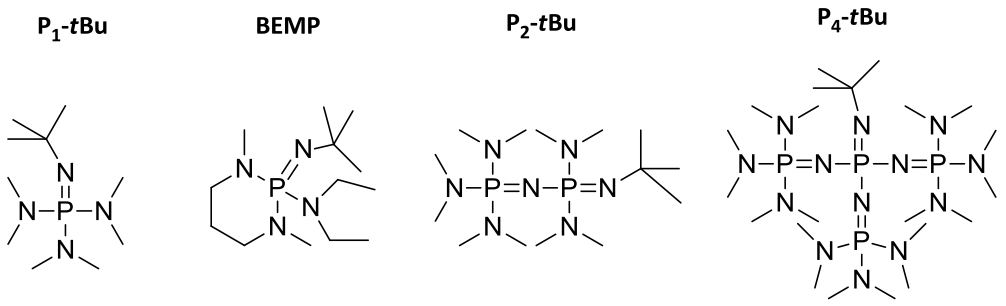
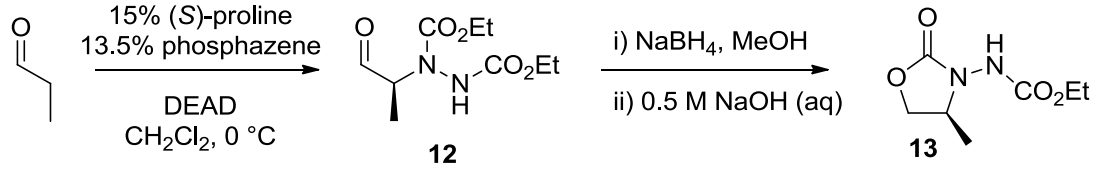


Figure 24: Phosphazene bases screened as additives in the proline-catalysed amination reaction.

Three of the phosphazene bases tested as additives (P_1–*t*Bu, BEMP, and P_2–*t*Bu) gave the same enantioselectivity reversal as seen previously. Disappointingly, the selectivity observed was not significantly higher than that seen with the simpler organic bases (Table 2). These results show that there is a limit to the amount that the enantioselectivity of the reaction can be enhanced with increasing additive basicity.



phosphazene	pK_a (MeCN)[131]	*ee* / % (**13**)[a]
P_1-*t*Bu	26.9	58
BEMP	27.6	57
P_2-*t*Bu	33.5	56
P_4-*t*Bu	41.9	–[b]

Table 2: Proline-catalysed amination in the presence of phosphazene bases; a) Determined by GC analysis of the purified product; b) Reaction failed.

viii) The pK_a of DBU in MeCN is 24.

The strongest phosphazene base tested, P_4–*t*Bu, gave none of the expected product. When a mixture of this reagent and proline was dissolved in dichloromethane, an instant discolouration and warming resulted. Side-reactions could have arisen through carbene generation resulting from deprotonation of the dichloromethane and α-elimination; although this process would typically be effected by carbanionic organolithium reagents, it has been shown that weaker bases such as NaHMDS can also be used.[132]

4.6. Guanidines – A Series of Isosteric Bases

Although the tertiary amine additives demonstrated the general trend between selectivity and basicity, the amines hitherto mentioned are a structurally diverse set and other properties – such as size, nucleophilicity, or solubility – could give rise to differences in selectivity. We therefore felt it was pertinent to reassess the relationship between selectivity and additive basicity with a series of isosteric bases. The compounds were envisaged to incorporate an aromatic group electronically linked to the basic centre. Variation of the substituent pattern on this moiety would then allow tunability of the basicity with minimal structural change. A number of structures that could meet this requirement were considered (Figure 25).

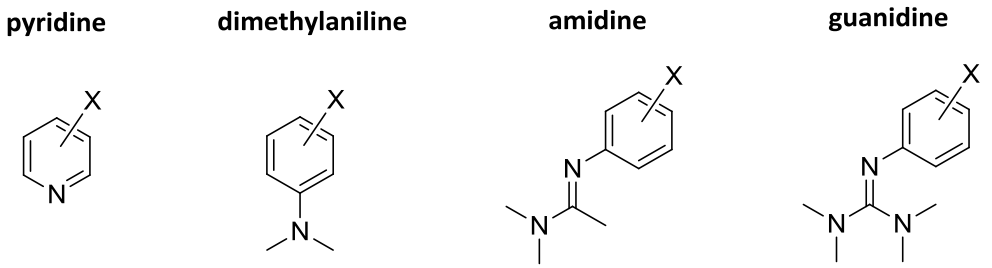


Figure 25: General structures of potential sets of isosteric bases.

This type of tunability is possible with substituted pyridines and dialkylanilines, but these species would be insufficiently basic for this purpose unless heavily functionalised. Monosubstituted examples are weak bases with aqueous *p*K_a values in the range 0–7 (Figure 26).[133,134]

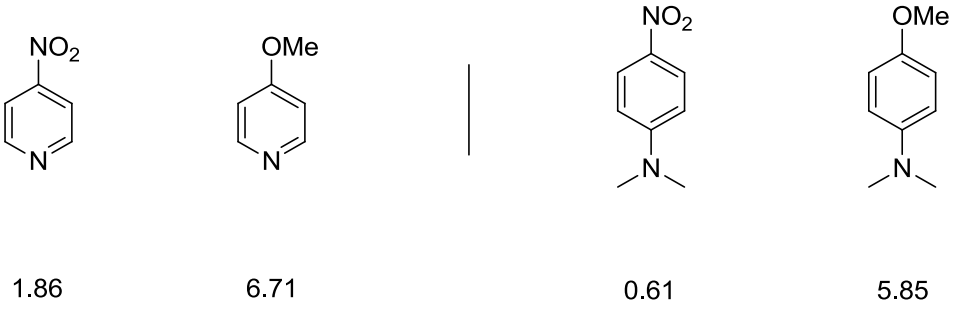


Figure 26: Aqueous pK_a values of substituted pyridines[133] and dimethylanilines.[134]

Monosubstituted 2-aryl-1,1-dimethylacetamidines and 2-aryl-1,1,3,3-tetramethylguanidines are examples of stronger bases that are similarly tuneable (Figure 27).[135,136]

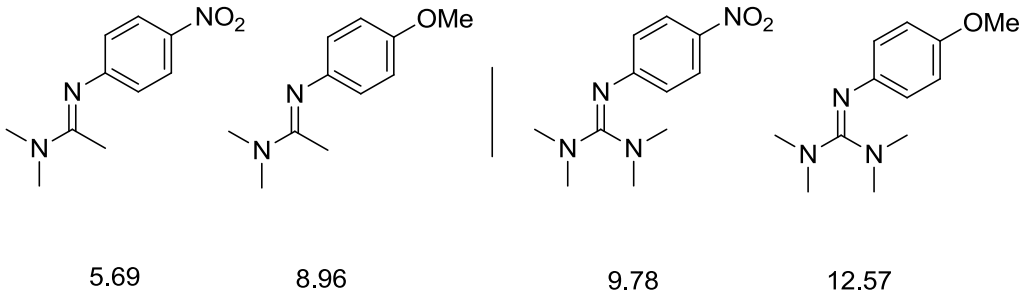
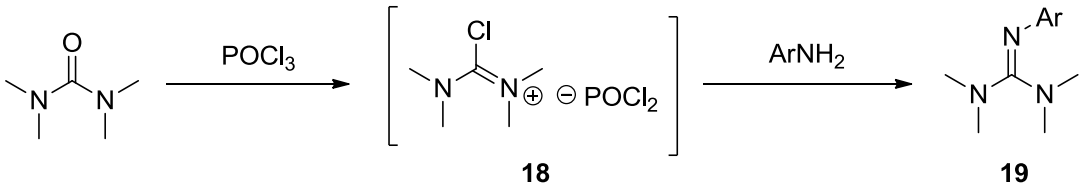


Figure 27: pK_a values of substituted 2-aryl-1,1-dimethylacetamidine (EtOH)[135] and 2-aryl-1,1,3,3-tetramethylguanidine (H_2O)[136] bases.

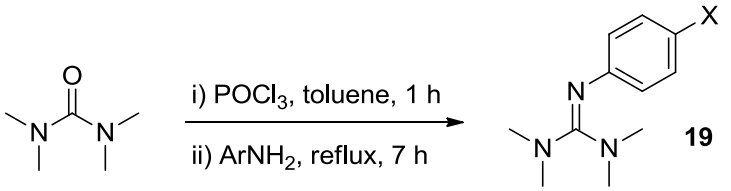
For a range of such compounds, pK_a values have been determined and synthesis can be achieved in one step from commercially available materials.[135,136] The 2-aryl-1,1,3,3-tetramethylguanidine (ArTMG) structure was selected due to the better match of pK_a range to the previously employed tertiary amines.

In order to prepare a set of ArTMGs, a protocol was adapted from previously reported methods.[136,137] This methodology involves condensation of anilines onto tetramethylurea with phosphorus oxychloride as an activating agent.



Scheme 30: Condensation approach employed to prepare ArTMG bases.

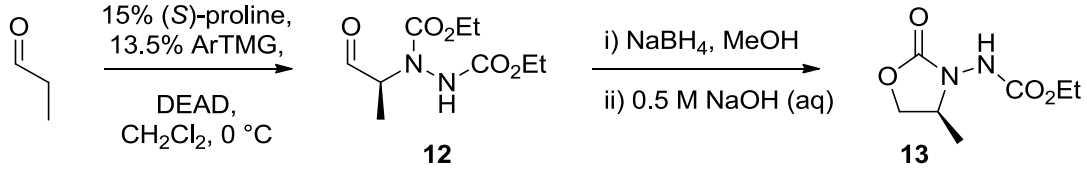
In previous syntheses, reaction times of 14 hours for the formation of the 2-chloroformamidinium intermediate **18** have been reported.[136,137] By contrast, generation of the analogous species in Vilsmeier–Haack protocols using DMF and phosphorus oxychloride has recently been reported to take as little as 5 minutes[138,139] and the reaction between *N*,*N*-dimethylacetamide (DMA) and phosphorus oxychloride is reported to take less than 1 hour.[140,141] Gratifyingly, it was found that modification of the procedure to shorten the time period for formation of intermediate **18** did not have an negative effect on the overall yield of PhTMG **19a** and, using this modification, the synthesis of ArTMG bases commenced. The preparation of a variety of *para*-substituted ArTMG bases is detailed in Table 3 alongside pK_a data, where available: for **19a–h** pK_a data have been determined in both water[136] and acetonitrile.[130]



ArTMG	X	Yield / %	pK_a (H_2O)[136]	pK_a (MeCN)[130]
19a	H	49	12.2	20.6
19b	MeO	74	12.6	21.0
19c	Me	61	12.4	20.9
19d	Cl	38	11.7	19.7
19e	Br	92	11.6	19.6
19f	CF_3	31	11.4	19.0
19g	CN	69	11.0	18.4
19h	NO_2	65	9.8	17.8
19i	NMe_2	72	–	–
19j	Et	65	–	–
19k	*t*Bu	50	–	–
19l	Bn	61	–	–
19m	CO_2Me	46	–	–
19n	CO_2Et	52	–	–

Table 3: ArTMG bases synthesised by condensation of substituted anilines onto tetramethylurea with Vilsmeier–Haack type activation; pK_a data is given where available.

The reaction was found to give moderate yields with a variety of 4-substituted anilines; comparatively low yields were observed with chloroaniline, which displayed poor solubility in the reaction medium, and trifluoromethylaniline, which was reported to be a poor substrate.[130] With this set of ArTMG bases in hand, their effect as additives in the proline-catalysed amination reaction could be explored (Table 4).



ArTMG	X[a]	pK_a (H_2O)[136]	pK_a (MeCN)[130]	Yield / % (**12**)[b]	*ee* / % (**13**)[c]
19b	MeO	12.6	21.0	74	66
19c	Me	12.4	20.9	58	63
19a	H	12.2	20.6	53	59
19d	Cl	11.7	19.7	48	57
19e	Br	11.6	19.6	91	56
19f	CF_3	11.4	19.0	83	54
19g	CN	11.0	18.4	80	56
19h	NO_2	9.8	17.8	77	48

Table 4: Proline-catalysed amination reaction with isosteric ArTMG bases as additives; a) ArTMG *para*-substituent (see Table 3); b) Determined by sampling and NMR analysis in comparison with an internal standard (PhCN); c) Determined by GC analysis of the purified product.

In keeping with previous findings, all ArTMG bases induced a switch in usual selectivity for the proline-catalysed amination reaction. The reactions proceeded in moderate to good yield and it can again be seen that higher selectivity is observed when more basic additives are used. The data are shown graphically in Figure 28.

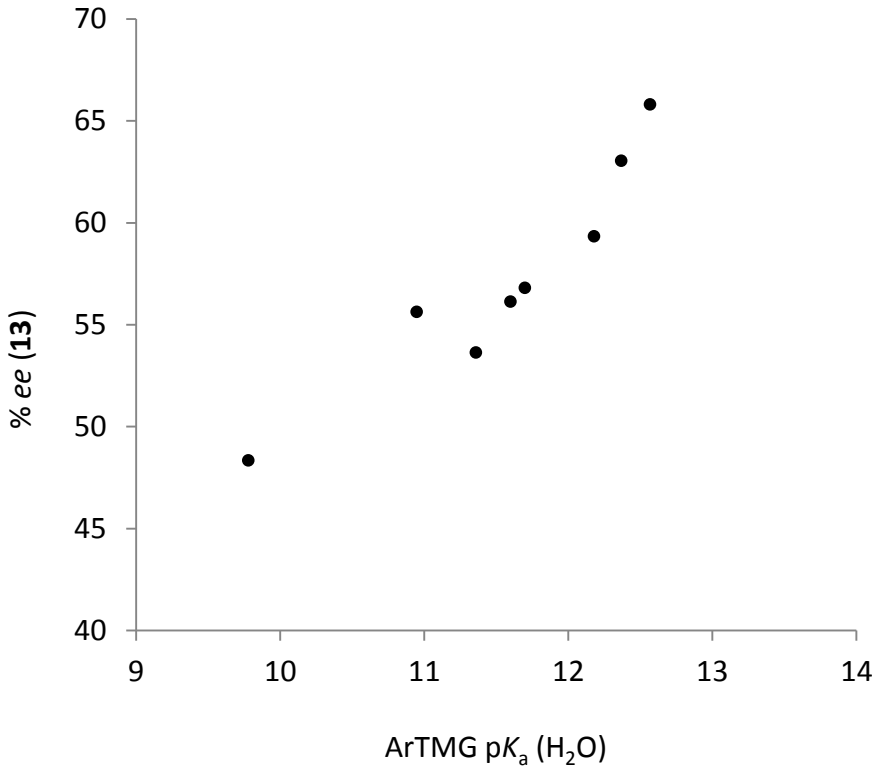


Figure 28: Plot of % *ee* against ArTMG pK_a (H_2O) for the proline-catalysed amination of reaction with ArTMG additives; See Table 4 for conditions and raw data.

As in the screen of tertiary amine additives, a positive correlation between enantioselectivity and additive base strength was found. The structural conformity of this set of bases means that many of the properties other than basicity are very similar. This study thus shows that additive basicity is indeed the major factor in determining the selectivity of the proline-catalysed amination reaction.

Examples that deviate from the rest of the data in the plot of % *ee* against pK_a could be in part due to the use of aqueous acid dissociation constants. The reactions are performed in dichloromethane, whose solvent properties differ from water in almost every way. It can be seen that if the results with guanidine additives are replotted using pK_a values obtained in acetonitrile, the appearance of the graph is altered (Figure 29).

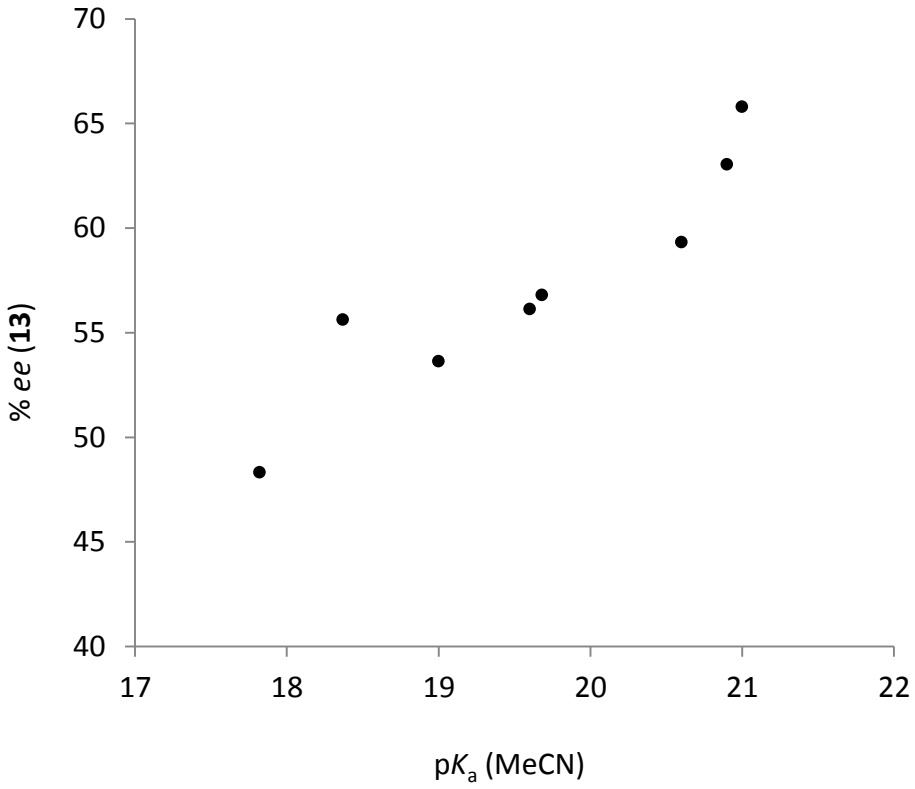
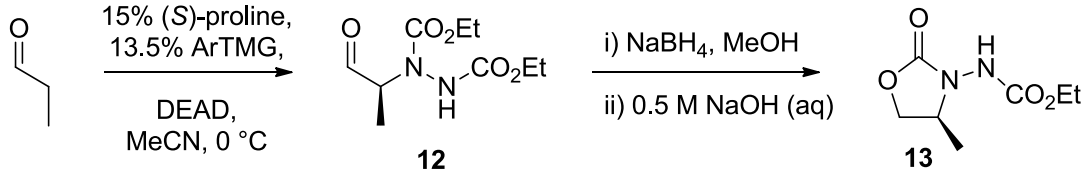


Figure 29: Plot of % *ee* against ArTMG pK_a (MeCN) for the proline-catalysed amination reaction with ArTMG additives; See Table 4 for conditions and raw data.

In order to assess this factor, the proline-catalysed amination reactions with ArTMG additives were performed in acetonitrile, a solvent in which pK_a data have been obtained. The same switch in enantioselectivity with respect to proline was observed in all cases. However, the difference in selectivity induced between the additives was found to be much less pronounced.



ArTMG	X[a]	pK_a (MeCN)[130]	Yield / % (**12**)[b]	ee / % (**13**)[c]
19b	MeO	21.0	44	51
19a	H	20.6	56	52
19d	Cl	19.7	48	51
19e	Br	19.6	58	47
19f	CF_3	19.0	71	47
19g	CN	18.4	60	48
19h	NO_2	17.8	55	45

Table 5: Proline-catalysed amination reaction with isosteric ArTMG bases as additives in MeCN; a) ArTMG *para*-substituent (see Table 3); b) Determined by sampling and NMR analysis in comparison with an internal standard (PhCN); c) Determined by GC analysis of the purified product.

The plot of selectivity against basicity shown in Figure 30 shows that in acetonitrile there is no strong dependence between enantioselectivity and basicity. Instead, the trend in data appears more like a plateau around a similar level of selectivity, suggesting that the factor which differentiates the bases is largely attenuated in this solvent.

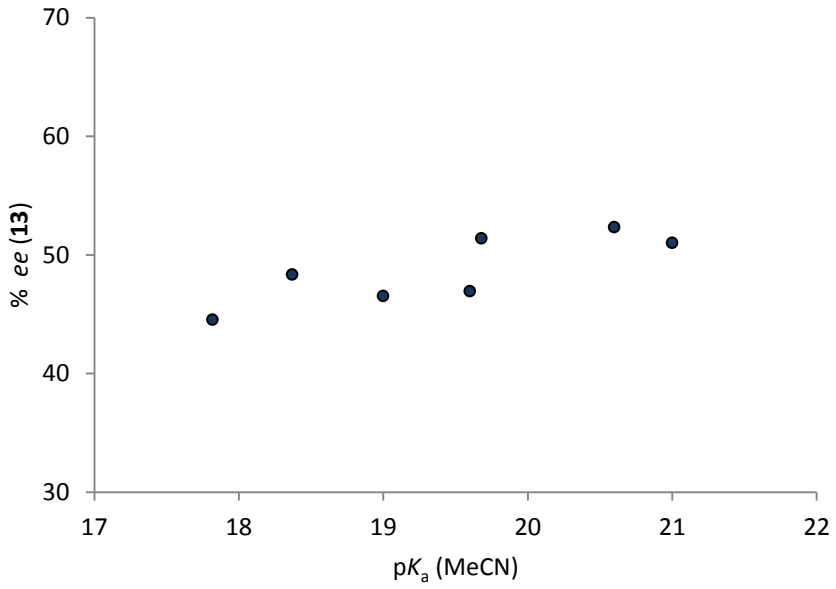
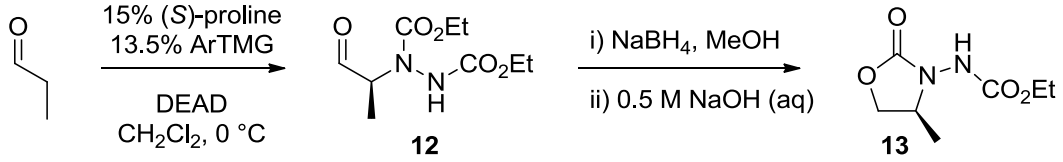


Figure 30: Plot of % *ee* against ArTMG pK_a (MeCN) for the proline-catalysed amination reaction in MeCN with ArTMG additive; See Table 5 for conditions and raw data.

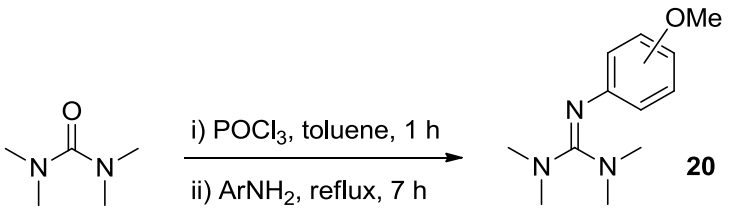
The remaining guanidines – those without reported pK_a data – were also applied as additives in the amination reaction (Table 6). The corresponding mixtures of proline and ArTMG bases effected selectivity as expected with respect to their electronic properties, with the exception of the ester-substituted examples. These results confirm that the size of the substituent (X) on the ArTMG does not greatly affect the selectivity, since the reaction with **19k** (X = *t*Bu) did not show large variation from the expected enantioselectivity. Disappointingly, the dimethylamino-substituted ArTMG (**19i**) did not give rise to a larger inversion than previously observed.



ArTMG	X[a]	Yield / % (**12**)[b]	*ee* / % (**13**)[c]
19i	NMe_2	45	58
19j	Et	39	59
19k	*t*Bu	37	57
19l	Bn	49	55
19m	CO_2Me	48	56
19n	CO_2Et	52	55

Table 6: Proline-catalysed amination reaction with isosteric ArTMG bases (without reported pK_a data) as additives; a) ArTMG *para*-substituent (see Table 3); b) Determined by sampling and NMR analysis in comparison with an internal standard (PhCN); c) Determined by GC analysis of the purified product.

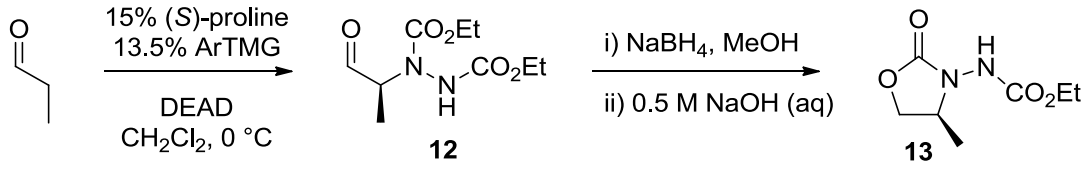
The effect of the ArTMG substitution pattern was next investigated. Methoxy-substituted ArTMG bases were prepared and applied as additives in the amination reaction. The 2-methoxy and 3-methoxy compounds were synthesised in good yields as expected, but the 3,4,5-trimethoxy guanidine was formed in reduced yield.



	Ar	Yield / %	pK_a (H_2O)[136]	pK_a (MeCN)[130]
20a	2-MeO-C_6H_4	64	12.2	21.0
20b	3-MeO-C_6H_4	70	12.0	20.4
20c	3,4,5-$(MeO)_3$-C_6H_2	45	–	–

Table 7: ArTMG bases synthesised by condensation of substituted anilines onto tetramethylurea with Vilsmeier–Haack type activation; pK_a data are given where available.

The substitution position of the monosubstituted guanidine aryl group was found to have little effect on the selectivity of the ArTMG/proline-catalysed amination reaction. ArTMG additives with substitution at the 2- and 3- positions on the aromatic moiety displayed selectivity in keeping with the previous results, given the differences in pK_a. However, the trisubstituted ArTMG additive (**20c**) was found to induce only 52% *ee* when applied to the reaction; it was expected that this base would be stronger than the others synthesised, but pK_a data were not available to confirm this assertion.



	ArTMG	pK_a (H_2O)[136]	pK_a (MeCN)[130]	Yield / % (**12**)[a]	*ee* / % (**13**)[b]
19b	4-MeO	12.6	21.0	65	66
20a	2-MeO	12.2	21.0	61	58
20b	3-MeO	12.0	20.4	34	53
20c	3,4,5-$(MeO)_3$	–	–	35	52

Table 8: Proline-catalysed amination reaction with isosteric ArTMG bases as additives; a) Determined by sampling and NMR analysis in comparison with an internal standard (PhCN); b) Determined by GC analysis of the purified product.

Lastly, 2-phenyl-1,1,3,3-tetraethylguanidine (**21**) was prepared and tested as an additive to assess the effect of bulk at the amino groups.

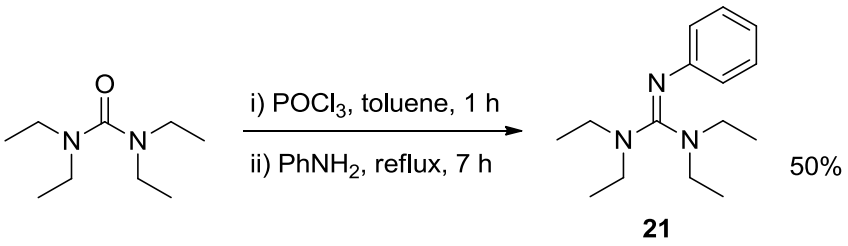
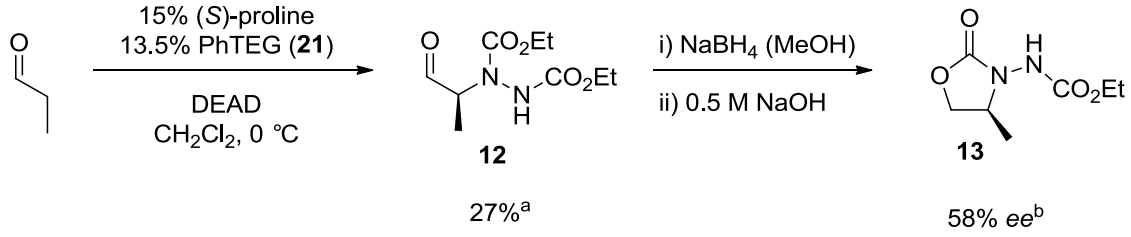


Figure 31: Synthesis of 2-phenyl-1,1,3,3-tetraethylguanidine (PhTEG).

When PhTEG (**21**) was applied as an additive in the amination reaction, the enantioselectivity observed was very similar to that seen with PhTMG (**19a**). This result suggests that not only does additive basicity dictate selectivity in the proline-catalysed amination reaction, but that additive bulk is a much less significant factor.



Scheme 31: Proline-catalysed amination reaction in the presence of PhTEG; a) Determined by sampling and NMR analysis in comparison with an internal standard (PhCN); b) Determined by GC analysis of the purified product.

Synthesis of a guanidine bearing diisopropyl amino groups was attempted to further examine the effect of size, but this was unsuccessful.

4.7. Dependence on Basicity

The observed link between selectivity and additive basicity could either be caused by the ability of the additive to deprotonate the stereodetermining intermediate, or by the involvement of its conjugate acid in product formation. These possibilities are discussed below:

The extent of deprotonation of the key enamine intermediate will dictate how much the reaction proceeds through prolinate catalysis and therefore how much of the product is derived from the transition state depicted earlier in Figure 22. Any enamine intermediate present that is not deprotonated will react by the standard proline pathway, and erode overall selectivity as observed in the DBU to proline ratio study. Alternatively, enantioselectivity could be eroded by increased preference for a different transition state. In the second lowest energy transition state for enamine catalysis with diaryl prolinol silyl ethers, the reacting electrophile is proposed to approach from the opposite face to the bulky ring substituent; the difference from the lowest energy transition state is that the double bond of the enamine has a *cis*-relationship to the bulky substituent and thus the opposite face of the enamine

undergoes reaction.[124] This transition state is depicted in Figure 32, alongside its analogue in prolinate catalysis.

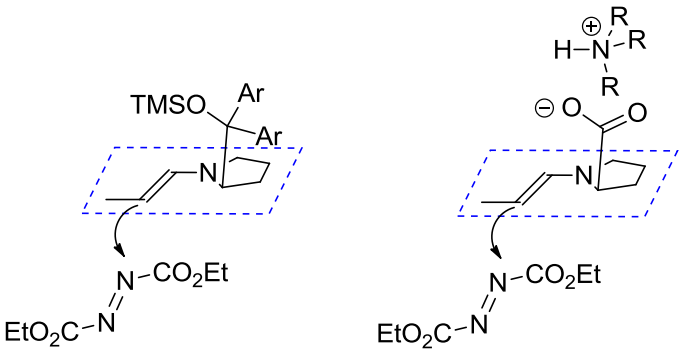


Figure 32: Second lowest energy transition state for diaryl prolinol silyl ether-catalysed amination reaction alongside the analogous transition state for the ammonium prolinate-catalysed reaction.

For prolinate catalysis, it is unlikely that weaker bases will reduce the energy gap between this transition state and the lowest energy transition state ($\Delta\Delta G^{\ddagger}$). The necessarily weaker conjugate acids of stronger bases could engage in stronger directional coordination to the carboxylate group. However, the major intermolecular interaction between the two species is the ionic bond, and ion-pair separation should be similar for the bases tested.

An alternative transition state that would be greatly affected by the basicity of the additive would involve coordination of the reacting DEAD by the conjugate acid; for weaker bases, this interaction would be stronger. Induction of enantioselectivity through an ammonium fragment acting as a directing group has been shown to be possible with catalysts developed by Yamamoto and co-workers.[90] However, within these catalysts the ammonium group is covalently bound and therefore more likely to be productively organised in a transition state than the more loosely associated counter cation. Even if this is the lowest energy transition state that leads to the minor enantiomer in some cases, it cannot be so in all cases because, as shown by the application of phosphazenes, the enantioselectivity cannot be continually increased with stronger bases.

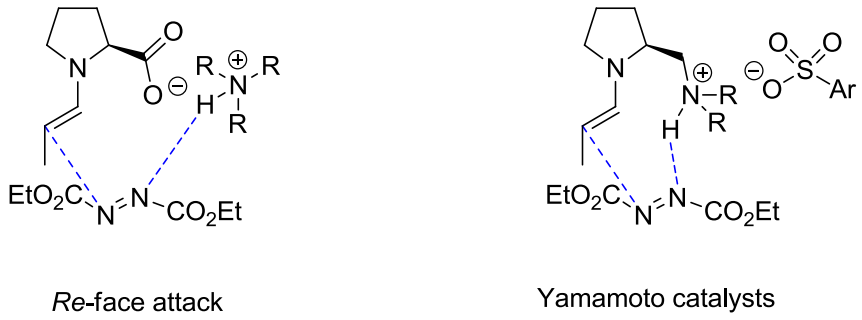
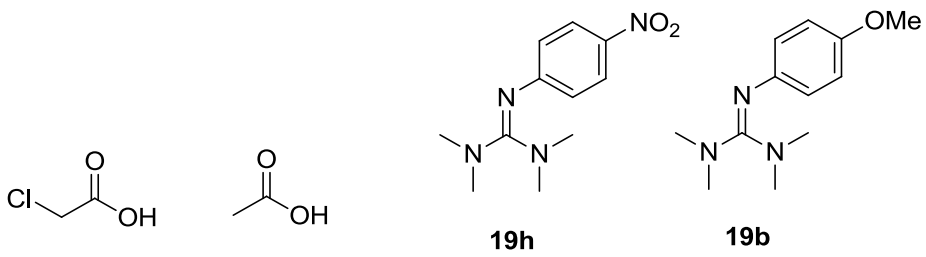


Figure 33: Alternative, directing group transition state in prolinate catalysis shown alongside the analogous transition state with Yamamoto catalysts.

To investigate these possible explanations further, it is first necessary to determine the degree to which the key enamine intermediate is deprotonated by the various bases assayed. Thus far, the effect of basic additives has been analysed and discussed in terms of the pK_a values of the bases in question. A problem with this approach is that the vast majority of pK_a data has been determined in water, alcohols, DMSO, DMF, and acetonitrile; these are highly polar solvents, the properties of which are dissimilar to the majority of more commonly used organic solvents such as dichloromethane, chloroform, diethyl ether, THF, and hexane.

It is assumed that the trends in basicity within a class of similar compounds, such as tertiary amines, should be roughly the same in any solvent. However, it is not immediately apparent whether comparison of pK_a values between different types of functional groups is valid in solvents other than that used to acquire the pK_a data. In water, tertiary amines such as those used in the experiments described above are expected to fully deprotonate simple aliphatic carboxylic acids. In acetonitrile, pK_a data suggest that not all of such amines will be expected to do so. This is illustrated in Figure 34 with pK_a data for acetic acid and chloroacetic acid, and the strongest and weakest ArTMG tested as additives in the amination reaction.



pK_a (H_2O)	2.86	4.76	9.78	12.57
pK_a (MeCN)	19.45	21.57	17.8	21.0

Figure 34: pK_a values for chloroacetic acid and acetic acid (in H_2O[142] and MeCN[143]) and for the conjugate acids of 19h and 19b (in H_2O[136] and MeCN[130]).

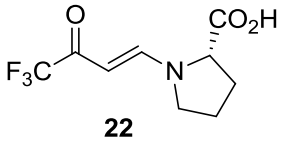
Chloroacetic acid has been shown to be an acid of comparable strength to proline;[108] in water it is seven orders of magnitude more acidic than the conjugate acid of **19h** (the weakest ArTMG base tested), but strikingly in acetonitrile its acidity is between that of the conjugate acids of **19b** and **19h**.

In dichloromethane, the solvent for the amination reaction, pK_a data are virtually non-existent. Measurement of pK_a in organic solvents like dichloromethane is not straightforward due to the inability of the solvent, under usual conditions, to become protonated to form the corresponding lyonium ion, the relative concentration of which defines the dissociation constant. Therefore, to determine whether certain acids will be deprotonated by certain bases in lieu of such information, a useful approach is titration.

Although proline is the catalyst for the process, this is not necessarily the most important species with respect to additive-induced deprotonation. The key reaction intermediate is the enamine, or more precisely the key component is the transition state of enamine attack. Extent of deprotonation of these species will dictate which reaction pathway – proline or prolinate – will dominate. Due to the instability of the

propanal enamine intermediate in organic solvents, this is not a suitable substrate for a titration experiment.

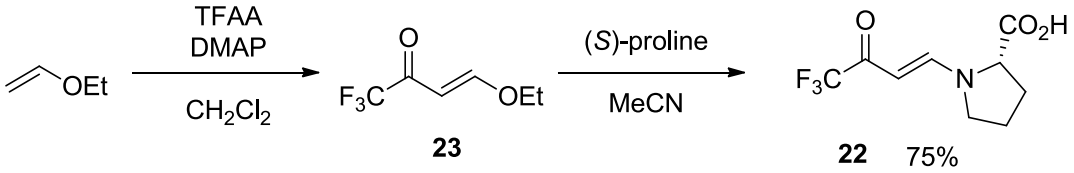
As discussed earlier, it has been reported that a proline-derived enaminone (**22**) is a good model for the transition state in enamine catalysis with bond lengths and N pyramidality that match the calculated transition state for a proline-catalysed aldehyde transformation.[112]



22

Figure 35: List enaminone TS model.[112]

This model compound was therefore the most applicable substrate for the titration experiment, and it was synthesised according to method of Andrew and Mellor (Scheme 32).[144] A vinylogous ester intermediate (**23**) was prepared by trifluoroacetylation/deprotonation of ethyl vinyl ether and subsequently converted to enaminone **22** by an addition-elimination reaction with (*S*)-proline in 75% overall yield over the two steps.



23 **22** 75%

Scheme 32: Synthesis of model enaminone compound.

With the enaminone in hand, it was possible to determine the extent of deprotonation with a given base through a spectroscopic titration experiment. The most clearly resolved resonances in the ^{1}H NMR spectrum of enaminone **22** correspond to the

protons labelled in Figure 36; as depicted, two conformers of the compound are observed and this remained the case for the deprotonated form.

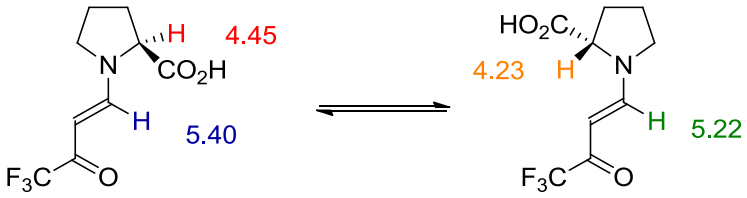


Figure 36: Clearly resolved ^{1}H NMR resonances of enaminone 22 monitored in base titration experiments.

The titration experiment was performed by sequential addition of aliquots of base to a sample of enaminone **22** in $CDCl_3$. NMR spectra from the titration of enaminone **22** against DBU are shown in Figure 37. It can be seen from the overlay of spectra that DBU completely deprotonates the substrate as the spectra corresponding to 1.0 and 1.2 equivalents of added base are identical.

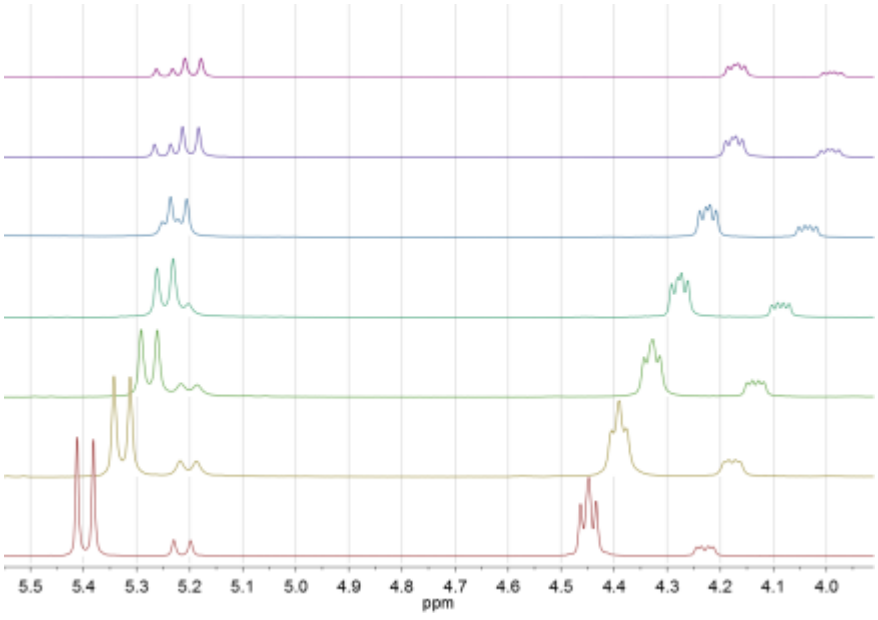


Figure 37: NMR spectroscopic titration of enaminone 22 against DBU; From bottom, spectra show: 0, 0.2, 0.4, 0.6, 0.8, 1.0, and 1.2 equiv. base added.

Titrations were next carried out for a selection of ArTMG bases. For the stronger bases **19a** and **19b**, the enaminone spectrum remains unchanged after the addition of one equivalent of base, again indicating complete deprotonation. However, for **19g** it was found to be necessary to add 1.8 equivalents of base in order to attain the spectrum of the deprotonated form of the enaminone. For the weakest ArTMG base (**19h**), even addition of 2 equivalents was insufficient to achieve this.

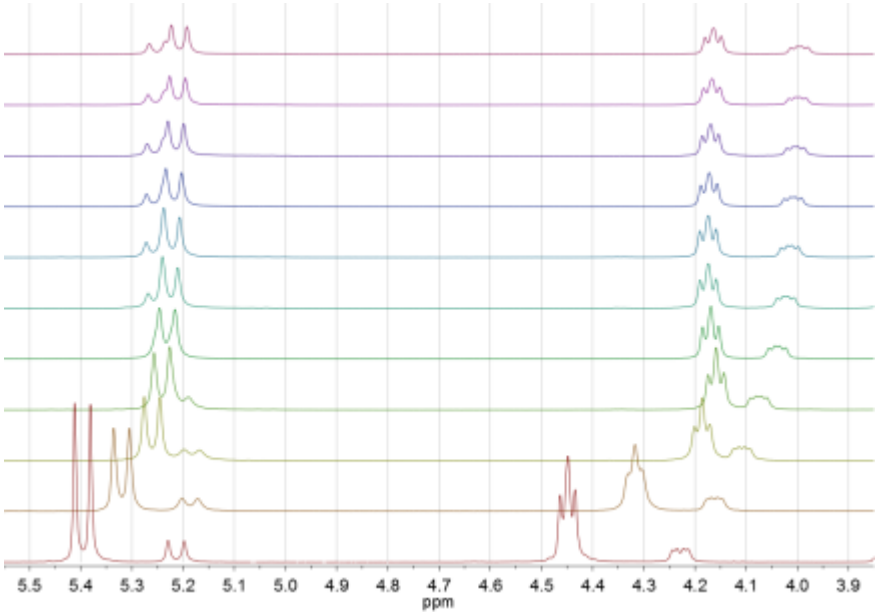


Figure 38: NMR spectroscopic titration of enaminone 22 against ArTMG 19g at 296 K; From bottom, spectra show: 0, 0.2, 0.4, 0.6, 0.8, 1.0, 1.2, 1.4, 1.6, 1.8, and 2.0 equiv. base added.

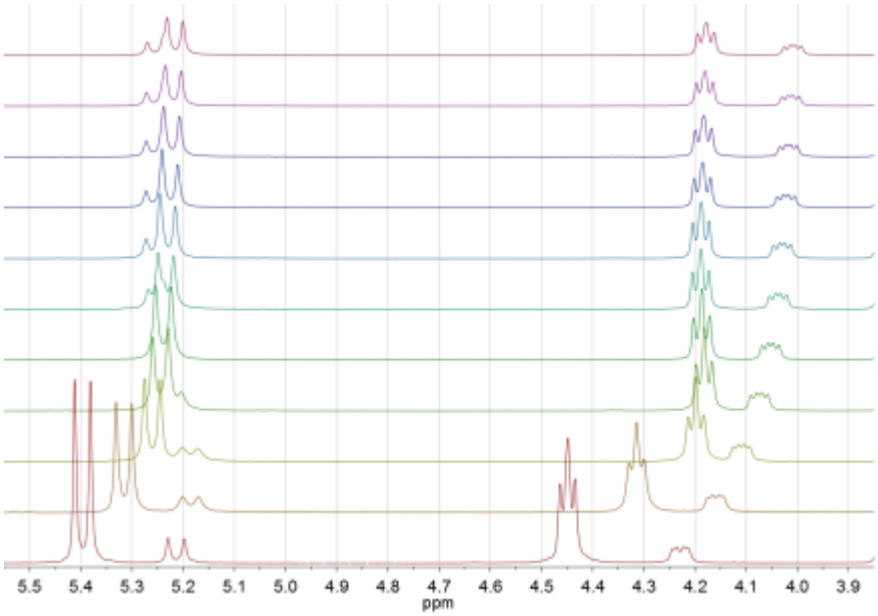


Figure 39: NMR spectroscopic titration of enaminone 22 against ArTMG 19h at 296 K; From bottom, spectra show: 0, 0.2, 0.4, 0.6, 0.8, 1.0, 1.2, 1.4, 1.6, 1.8, and 2.0 equiv. base added.

For the ArTMG bases, the titration experiments do not show a uniform shift of resonances from the natural state of the enaminone to the deprotonated form. Unlike in the DBU titration, the peaks for the two conformers appear to coalesce on addition of the base. Nevertheless, the chemical shifts still change upon each addition of base.

Thus, the titration experiment shows that strong bases such as DBU, **19a**, and **19b** completely deprotonate the transition state mimic **22** under this set of conditions, but the weaker bases **19g** and **19h** do not. This is therefore the reason for the dependency of additive basicity on selectivity in the proline-catalysed amination reaction. The loss of dependency seen in acetonitrile is explained by either the greater basicity of tertiary amines in this solvent or the reduced acidity of the enamine intermediate, relative to the case in dichloromethane. Since the bases tested all have a similar capability to deprotonate the catalyst, little variation in selectivity is observed.

It can also be assumed therefore that the proposed transition state in which the conjugate acid of the basic additive acts as a directing group is not the major source of the minor enantiomer. The lowest energy pathway to this product is likely to be that

shown in Figure 32, in which the electrophile attacks the face of the enamine that is on the opposite side of the carboxylate group, and the carboxylate and double bond bear a *syn*-relationship. The transition state in question is redisplayed below in Figure 40 along with the pathway that leads to the major enantiomer.

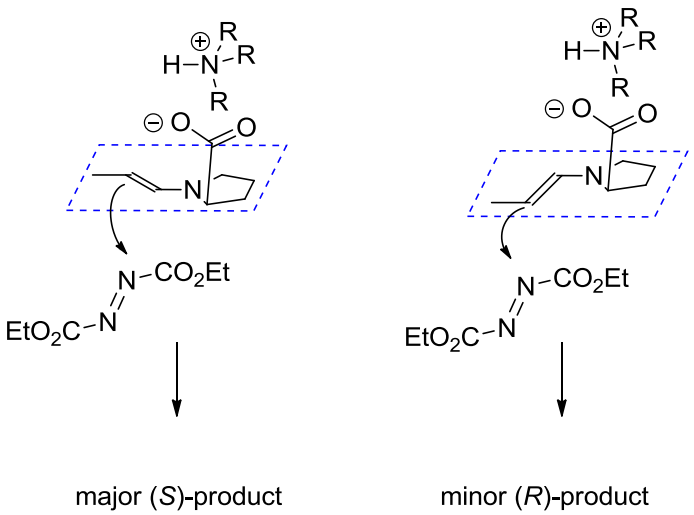


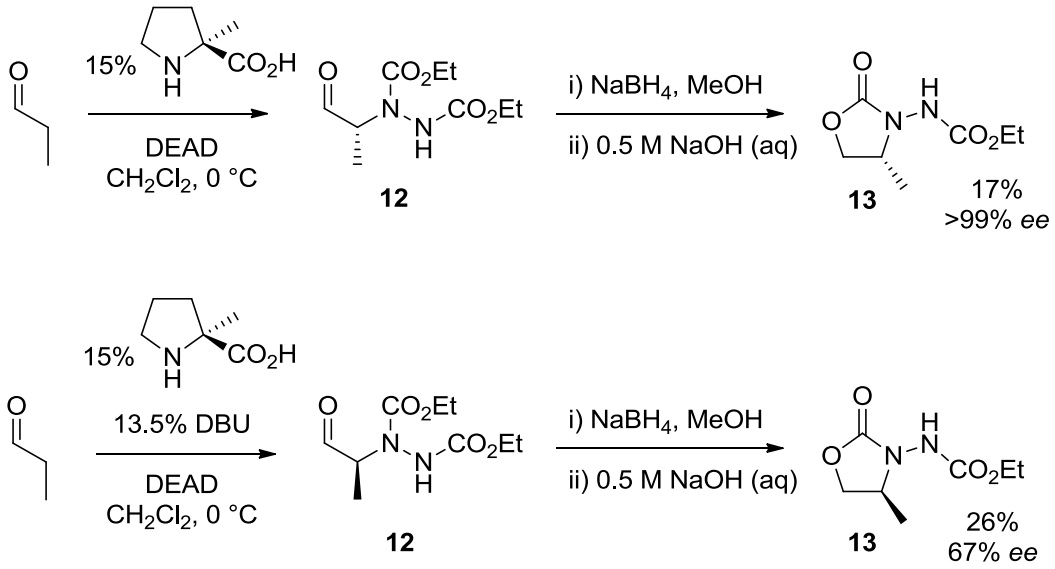
Figure 40: Lowest energy transition states leading to the major and minor enantiomers in the prolinate-catalysed amination reaction.

Therefore, in order to increase enantioselectivity in the prolinate-catalysed amination reaction it is necessary to disfavour the *syn*-conformation between these groups. This should be achievable with increased bulk, which would lead to greater steric interactions in this conformation.

4.8. Different Catalysts with DBU Additive

We sought to further probe the importance of conformational preference in the prolinate transition state by application of catalysts with different steric biases. α-Methylproline is perhaps the simplest example that fits this criterion. It is a catalyst that has previously been reported to show superior ability in certain organocatalytic processes when compared with proline; examples of this include α-hydroxylation of aldehydes with molecular oxygen[17] or *N*-tosyl-3-phenyloxaziridine,[145] and intramolecular α-alkylation of aldehydes.[46] In the amination reaction too,

enantioselectivity was increased and with added DBU the extent of inversion in enantioselectivity was also increased (Scheme 33).



Scheme 33: α-Methylproline-catalysed amination reaction in the absence and presence of DBU; % *ee* determined by GC analysis of the purified product.

The increased inversion can be explained by the additional bulk of the methyl substituent. In the presence of the basic additive, the higher energy *Si*-transition state for prolinate catalysis should be further disfavoured because in this transition state both the enamine double bond and DEAD will experience additional steric clashes with the methyl group (Figure 41).

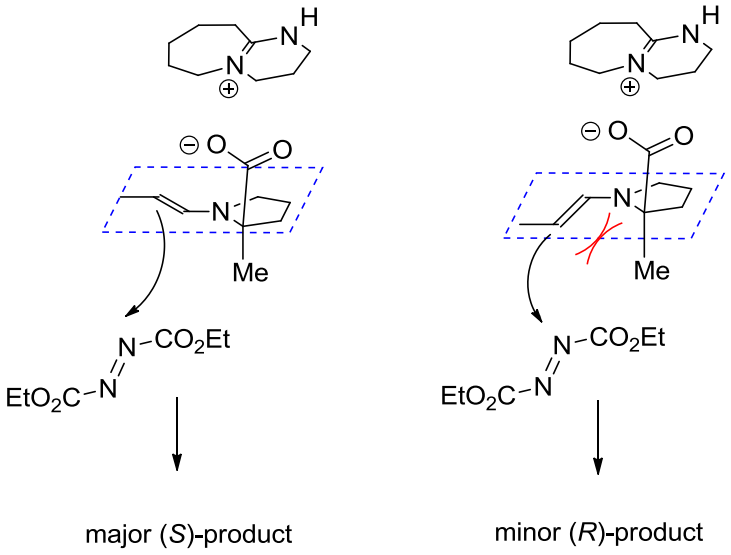
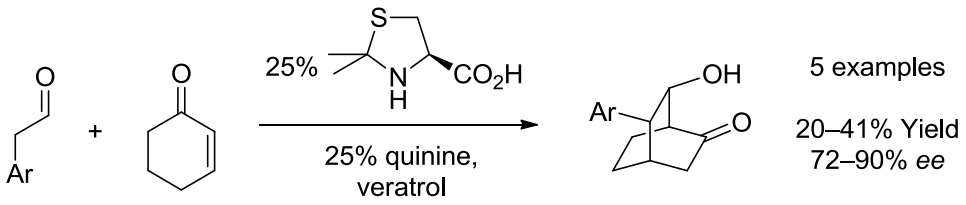


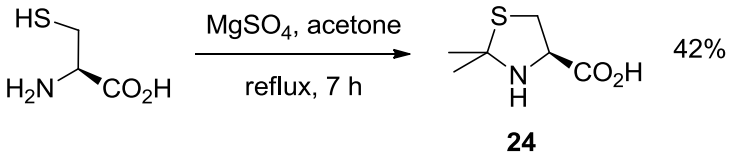
Figure 41: Lowest energy transition states for the α-methylproline-catalysed amination reaction in the presence of DBU.

Another proline analogue with a different steric bias is (*R*)-2,2-dimethylthiazolidine-4-carboxylic acid (**24**). Interestingly, this catalyst has been shown to have enhanced activity with added bases in an organocatalytic Diels–Alder reaction between enolisable aldehydes and enones;[146] the best improvement in selectivity was observed upon application of the chiral tertiary amine quinine (Scheme 34).



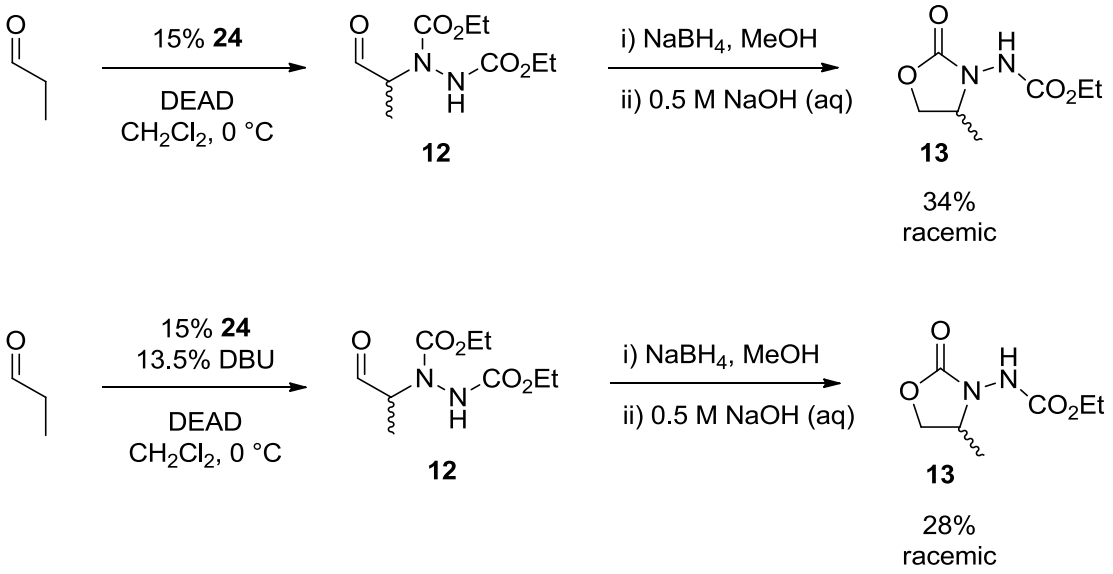
Scheme 34: Quinine-assisted, DMTC-catalysed Diels–Alder reaction between aldehydes and enones reported by Bella and co-workers;[146] The lithium carboxylate salt of 24 gave lower enantioselectivity.

The catalyst was synthesised by condensation of (*R*)-cysteine onto acetone with the aid of $MgSO_4$ as a desiccant; recrystallisation ensured complete removal of unreacted cysteine.



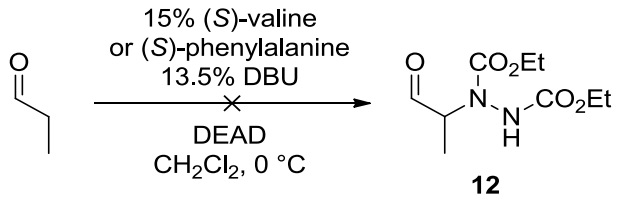
Scheme 35: Synthesis of (*R*)-2,2-dimethylthiazolidine-4-carboxylic acid by condensation of (*R*)-cysteine onto acetone in the presence of $MgSO_4$.

Unfortunately, although the catalyst effected product formation, the amination reaction proceeded without selectivity with and without DBU.



Scheme 36: 24-catalysed amination reaction in the absence and presence of DBU; % *ee* determined by GC analysis of the purified product.

Although they are less generally applicable than proline, simple primary amino acids are also used as organocatalysts, typically in aldol and Mannich reactions.[147] Due to the dramatic change in reactivity observed with proline in the presence of bases, we were interested to see if a catalytic turnover could be achieved with primary amino acids in the amination reaction upon addition of DBU. Unfortunately, the two primary amino acids tested proved to be catalytically inactive in the amination reaction with or without DBU.

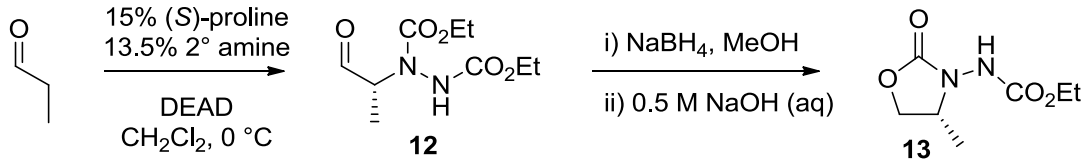


Scheme 37: Attempted primary amino acid-catalysed amination reaction.

4.9. Secondary Amines as Additives

Some secondary amines were next applied as additives to the amination reaction. These additives display similar basicity to the previously tested tertiary amines and therefore could be expected to show a similar effect. A complication is the potential for enamine formation between the aldehyde and the additive itself, however in a control experiment it was found that pyrrolidine is inactive as a catalyst in the reaction within the typical time period for proline- or amine/proline-catalysed reaction. The result of the screen of three secondary amines and one primary amine in the proline-catalysed amination reaction is shown below in Table 9.

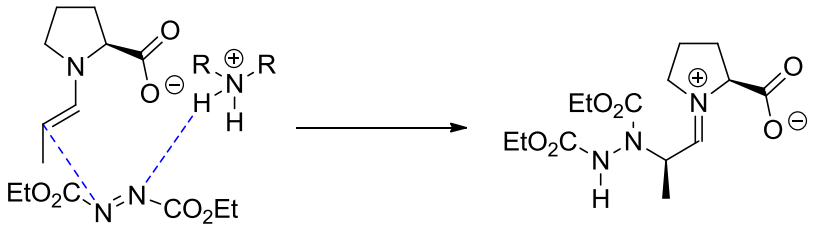
In all cases, and in stark contrast to the activity of tertiary amines, the same selectivity as proline was observed. Since these additives represent a range of basicity similar to that of the tertiary amines, it can be assumed that deprotonation of the catalyst does take place. However the resulting catalytic activity of the prolinates generated is clearly very different.



secondary amine	pK_a (H_2O)[148]	*ee* / % (**13**)[a]
pyrrolidine	11.32	76
dimethylamine	11.05	37
N-methylhydroxylamine	6.24	71
hydroxylamine	5.97	11

Table 9: Proline-catalysed amination reaction in the presence of secondary amines; a) Determined by GC analysis of the purified product.

As previously discussed, a possible transition state in prolinate catalysis would involve the conjugate acid of the basic additive acting as a directing group. Although this was discounted for prolinates generated from tertiary amines, for secondary amines this reactivity is statistically favoured because the conjugate acid bears an extra proton to coordinate and quench the electrophile (Figure 42).



directing group TS

Figure 42: Possible competing transition state in the prolinate-catalysed amination reaction in the presence of secondary amines.

Another possibility is that the ability of secondary amines to condense onto the aldehyde starting material, to form iminium and enamine products, sequesters the

additives and liberates free proline. This would depend upon the position of an equilibrium such as shown in Figure 43.

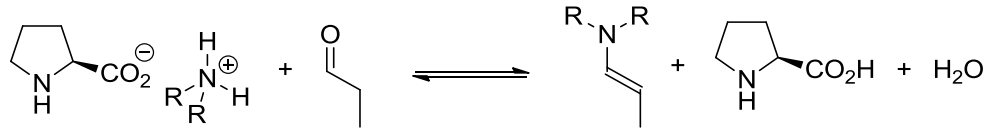


Figure 43: Equilibrium through which secondary amine additives could become sequestered in the proline-catalysed amination reaction.

4.10. Preformed Prolinates

Having ascribed selectivity in the base-assisted proline-catalysed amination reaction to a carboxylate group blocking effect, we were curious to see whether preformed prolinate salts would give rise to a similar phenomenon. Such compounds have been applied in asymmetric iminium catalysis for the conjugate addition of malonates[149,150] and nitroalkanes[149] to enals, and in asymmetric enamine catalysis in the HPESW reaction.[150]

Synthesis of prolinate salts (**25**) was initially attempted by stoichiometric combination of proline and metal hydroxides as shown in Figure 44. These salts were then isolated by evaporation of the reaction solvent and generated water, but it was found that such salts were highly hygroscopic: when freeze-dried, the salts appeared to be crystalline solids, but on contact with the atmosphere they rapidly turned into viscous oils.

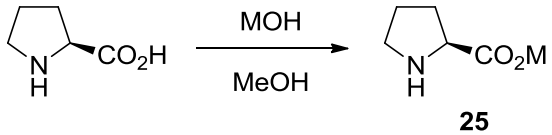
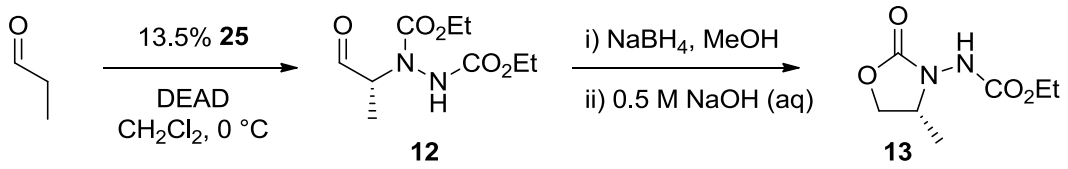


Figure 44: Formation of prolinate salts from proline and hydroxides; M = Li, Na, K, Cs, Bu_4N.

In order to assess the catalytic activity of these salts, an experimental procedure was designed such that the required amount of prolinate catalyst could be formed in the

reaction vessel for the subsequent amination reaction, minimising handling and the chance for deliquescence to occur. Surprisingly, the salts were found to be readily soluble in dichloromethane and the results are detailed below in Table 10. Prolinate salts of group 1 metals showed no selectivity in the reaction, although consumption of DEAD was complete within a time comparable to the DBU/proline-catalysed reaction.



M	Yield / % (**12**)[a]	*ee* / % (**13**)[b]
Li	33	<5
Na	68	<5
K	68	<5
Cs	61	16
Me_4N	58	46
Et_4N	42	58
Bu_4N	45	59

Table 10: Prolinate-catalysed amination reactions using preformed prolinate salts; a) Determined by sampling and NMR analysis in comparison with an internal standard (PhCN); b) Determined by GC analysis of the purified product.

However, prolinate salts with tetraalkylammonium counter cations were found to catalyse the reaction with selectivity in the same sense as when tertiary amines are applied as additives.[ix] For the preformed prolinates, all of the reaction intermediates necessarily bear carboxylate groups, and the reversal of selectivity seen supports the conclusion that enamine carboxylates are the stereodetermining intermediates in

ix) In control experiments it was shown that the simple presence of a high salt concentration, achieved through adding tetraalkylammonium halides at different loadings, does not affect the enantioselectivity of either the proline- or DBU/proline-catalysed amination reaction.

proline-catalysed reactions with basic additives. The tetraalkylammonium prolinates appear to show increased selectivity with increased counter cation size. This fits the transition state model described earlier (Figure 40), which predicts that increase in the effective size of the carboxylate group will enhance selectivity.

The non-selectivity of group 1 prolinates could be due to the possibility of the metal cation directing the approach of the electrophile by stabilising the generated negative charge (Figure 45). The flexibility of the metal cation in organising various transition states would give a racemic product.

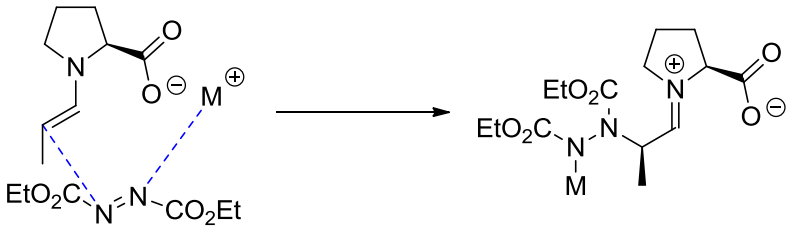


Figure 45: Possible competing transition state type in the group 1 prolinate-catalysed amination reaction.

This would be consistent with the small degree of enantioselectivity observed with cesium prolinate, because among the alkali metal cations applied, cesium has the poorest coordinating ability on account of its smaller charge density. Tetraalkylammonium cations, which show much higher selectivity, are very poorly coordinating and such a transition state would therefore be unlikely. The zinc prolinate-catalysed aldol reaction reported by Darbre and co-workers is proposed to operate through a similar transition state.[151] They found that in this reaction, shown in Figure 46, low enantioselectivity was observed in a number of cases, demonstrating the facility with which prolinate-catalysed reactions of this type can proceed through different pathways.

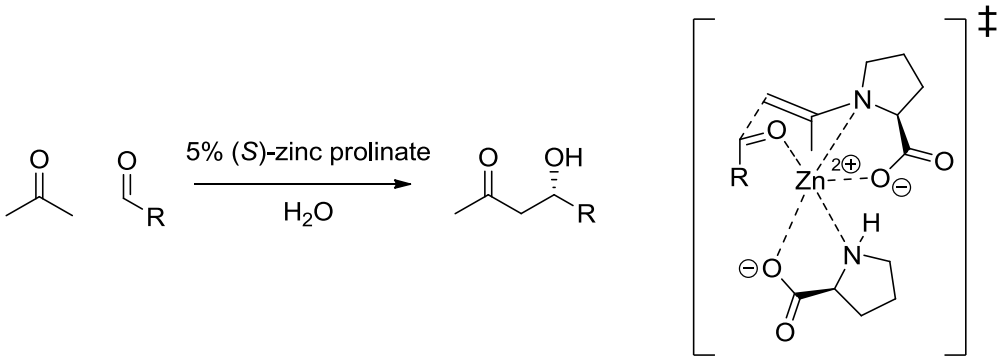
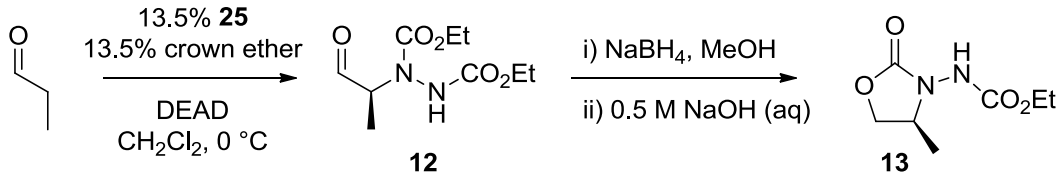


Figure 46: Zinc prolinate-catalysed aldol reaction reported by Darbre and co-workers with proposed transition state shown.[151]

We reasoned that sequestering the metal cation might attenuate the impact of such an alternative pathway. Thus, in an attempt to render a greater degree of ion-pair dissociation in the prolinate intermediate, crown ethers were applied to the appropriate metal prolinate-catalysed amination reactions. It was found that with the matching crown ether present, metal prolinates catalysed the reaction with the expected reversal of selectivity with respect to proline.



M	crown ether	Yield / % (**12**)[a]	*ee* / % (**13**)[b]
Li	12-crown-4	33	54
Na	15-crown-5	38	59
K	18-crown-6	36	67
K	dibenzo-18-crown-6	38	61
K	Kryptofix 222	36	65

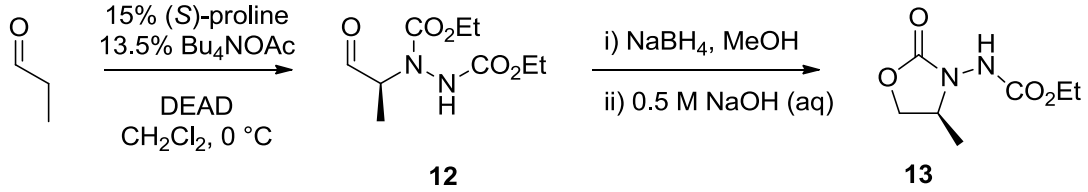
Table 11: Group 1 metal prolinate-catalysed amination reactions in the presence of the corresponding crown ether; a) Determined by sampling and NMR analysis in comparison with an internal standard (PhCN); b) Determined by GC analysis of the purified product.

Surprisingly, differences in selectivity were observed when different metal/crown ether combinations were employed. The counter cation therefore retains some degree of influence over the reactivity of the catalyst and this implies that only partial ion-pair separation is achieved. It is likely that such separation is not favoured by the reaction solvent, since dichloromethane has poor ion stabilisation ability. This hypothesis has previously been suggested for a metal prolinate catalyst with Yamaguchi and co-workers positing that the application of a crown ether increases the effective bulk based upon its altered reactivity.[150]

4.11. Preparation of Bulkier Prolinates

Having seen a limited trend between cation size and enantioselectivity in the prolinate-catalysed amination reaction, we were keen to extend the number of catalysts screened to examine the effect more fully. In particular we were interested in the activity of other ammonium prolinates and analogous phosphonium prolinates.

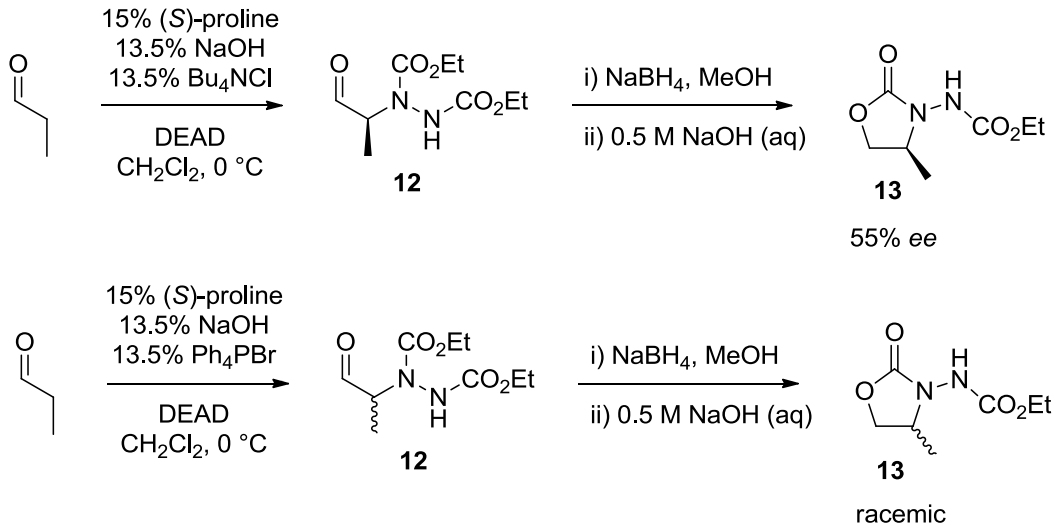
Unfortunately, screening such counter cations with our methodology was hindered by the limited availability of the required hydroxide salts needed to prepare prolinate catalysts. It had been demonstrated by our collaborators that prolinate catalyst could also be accessed *in situ* by mixing proline with the required acetate – since acetate is a stronger base than prolinate.[x]



Scheme 38: Prolinate-catalysed amination reaction with *in situ* prolinate generation with Bu_4NOAc demonstrated by our collaborators.[x]

The desired acetate salts were also found to be largely unavailable. However, a much wider range of halide salts are either commercially available or synthetically accessible. Ion-exchange was attempted to convert tetraphenylphosphonium bromide to the corresponding acetate but this proved unsuccessful. A procedure for *in situ* generation of a desired prolinate by cation exchange was investigated with mixed success. The result of the amination reaction catalysed by tetrabutylammonium prolinate was replicated by the catalyst generated from proline, sodium hydroxide, and tetrabutylammonium chloride. However, when the protocol was attempted using tetraphenylphosphonium bromide, racemic product resulted (Scheme 39).

x) Hein, J. E.; Blackmond, D. G.



Scheme 39: Attempted *in situ* cation exchange for in the prolinate-catalysed amination reaction; % ee determined by GC analysis of the purified product.

A lack of selectivity with the phosphonium prolinate catalyst would be unlikely given the previous results obtained with ammonium prolinates, therefore it was reasoned that cation exchange did not take place when the phosphonium bromide was employed. Thus, only sodium prolinate was formed and the reaction proceeded unselectively, as expected.

We next turned our attention to the use of silver salts. It was proposed that if silver prolinate could be formed, it should undergo cation exchange with a halide salt driven by the formation of an insoluble silver halide. Silver prolinate was formed by mixing proline and silver acetate in dichloromethane and, on addition of an equivalent of tetraphenylphosphonium bromide, a pale yellow precipitate was instantly formed indicating a successful cation exchange.

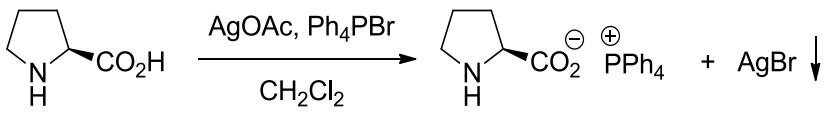
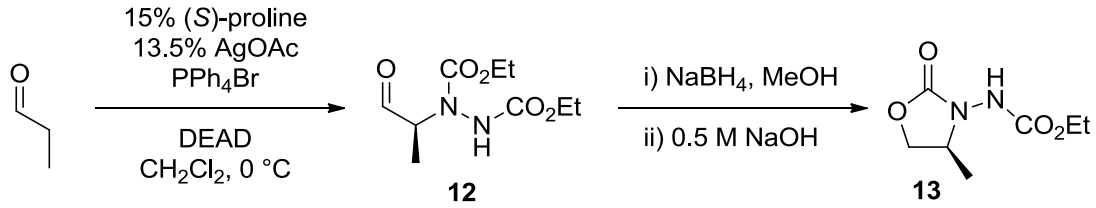


Figure 47: Formation of tetraphenylphosphonium prolinate using silver salts.

Tetraphenylphosphonium prolinate formed in this manner catalysed the amination reaction giving the expected inverted selectivity with respect to proline (60% *ee*). The effect of changing the loading of the phosphonium bromide salt was examined to ensure that complete cation exchange occurred. It was found that no improvement in enantioselectivity is observed with higher loadings, and a 1:1 Ph_4Br to AgOAc ratio is sufficient to achieve complete formation of the desired phosphonium prolinate.



PPh_4Br / AgOAc ratio	Yield / % (**12**)[a]	*ee* / % (**13**)[b]
1.0	79	60
1.5	83	60
2.0	82	60
2.5	83	61
5.0	78	60

Table 12: Tetraphenylphosphonium prolinate-catalysed amination reaction; a) Determined by sampling and NMR analysis in comparison with an internal standard (PhCN); b) Determined by GC analysis of the purified product.

As a control experiment, the amination reaction was also carried out with AgOAc alone, generating silver prolinate; this also catalysed the reaction, but gave the same sense of enantioselectivity as proline. This confirms that the cation exchange with tetraphenyl phosphonium bromide is successful.

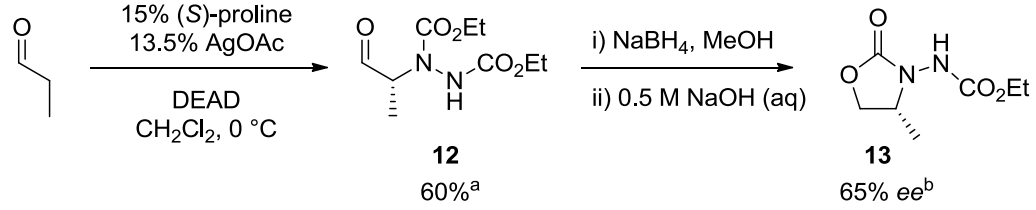
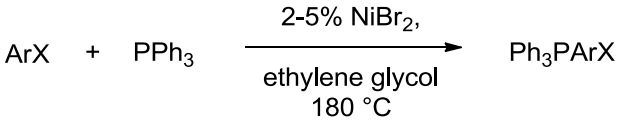


Figure 48: Silver prolinate-catalysed amination reaction; a) Determined by sampling and NMR analysis in comparison with an internal standard (PhCN); b) Determined by GC analysis of the purified product.

Five further phosphonium halides were screened in this reaction: PPh_3MeBr, PPh_3EtBr, and PPh_3iPrBr were commercially available, while two further examples were synthesised. This was achieved through the cross-coupling reaction developed by Charette and co-workers.[152] In this methodology, a wide range of phosphonium halides are accessible from triphenylphosphine and aryl halides through nickel catalysis in ethylene glycol, which serves as a ligand as well as the reaction solvent.



Scheme 40: Ni-catalysed cross-coupling approach to phosphonium halides reported by Charette and co-workers.[152]

As detailed below in Figure 49, preparation of triphenyl-3-tolylphosphonium iodide (**26**) and 2-naphthyl-triphenylphosphonium bromide (**27**) was successful.

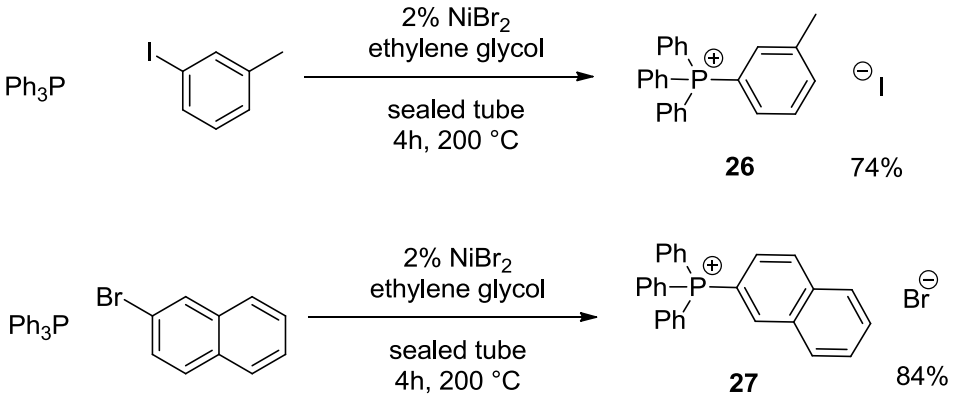
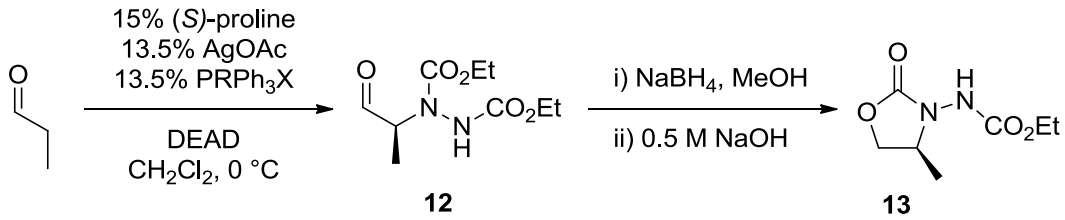


Figure 49: Charette Ni-catalysed phosphonium halide synthesis applied to bulky phosphonium cation formation.

Phosphonium salts were also synthesised from mesityl iodide and 1-naphthyl iodide, but purification by trituration or recrystallisation proved impossible. Phosphonium salt formation from the more hindered tris(2-tolyl)phosphine was unsuccessful even after prolonged heating, with 87% recovery of starting material.

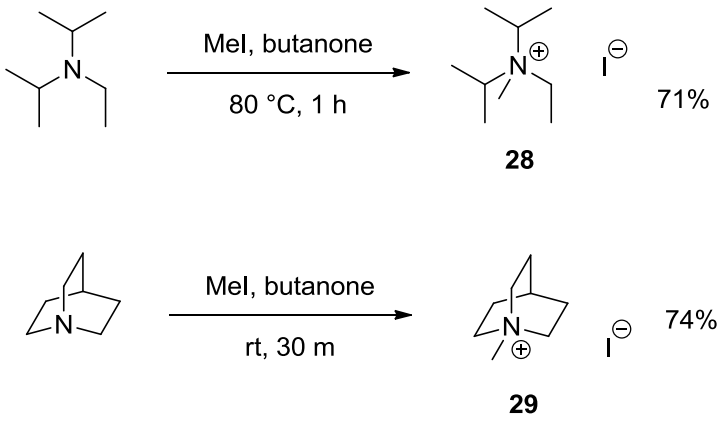
The additional phosphonium cations all showed very similar enantioselectivity when applied as counter ions in the prolinate-catalysed amination reaction. The results are shown in Table 13, including that previously found for PPh_4Br.



R	X	*ee* / % (**13**)[a]
Me	Br	57
Et	Br	61
*i*Pr	Br	60
Ph	Br	60
3-Tol	I	58
2-Nap	Br	60

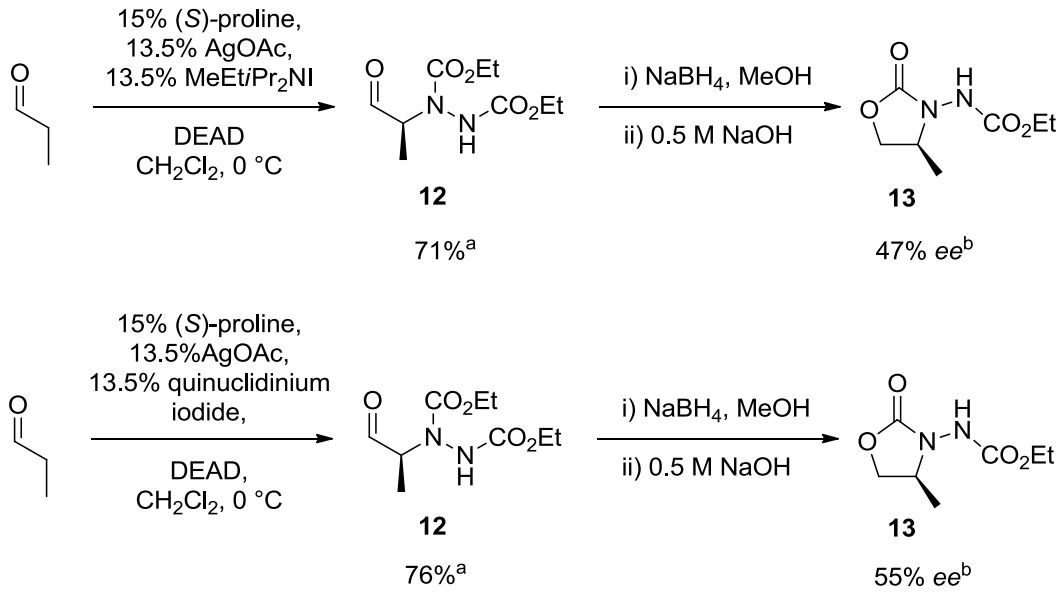
Table 13: Phosphonium prolinate-catalysed amination reaction with a range of phosphonium counter cations; a) Determined by GC analysis of the purified product.

Some additional tetraalkylammonium halides where also made for testing with the AgOAc method. Ethyldiisopropylmethylammonium iodide (**28**) and *N*-methylquinuclidinium iodide (**29**) were prepared in good yields by quaternisation of the corresponding tertiary amines with methyl iodide.



Scheme 41: Preparation of ammonium salts by quaternisation of tertiary amines with MeI.

These cations were applied as counter ions in the prolinate-catalysed amination reaction in the same way as the phosphonium species had been, and showed comparable selectivity in the reaction to tetraalkylammonium prolinates previously generated from the corresponding hydroxide salts.



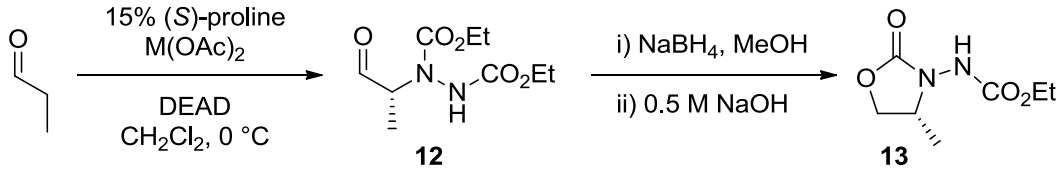
Scheme 42: Tetraalkylammonium prolinate-catalysed amination reactions using AgOAc exchange method; a) Determined by sampling and NMR analysis in comparison with an internal standard (PhCN); b) Determined by GC analysis of the purified product.

Overall it was shown that small variations to the structures of counter cations, within a given type of prolinate catalyst, does not have a major impact on the selectivity of the amination reaction. Future developments of bulky prolinate will therefore require much larger alterations in cation size.

4.12. Prolinates of Other Metals

In the studies detailed above, most of the prolinate counter cations have been weakly coordinating species expected to only act as blocking groups. Nevertheless, certain examples display selectivity, or lack thereof, which suggests the possibility for transition states in which the cation can direct the electrophile. We were therefore interested in studying the activity of some prolinates with counter cations known to coordinate other groups.

Metal prolinates were formed from the corresponding metal acetates in an analogous fashion to the application of AgOAc. The four metal cations chosen were dicoordinate, and the prolinate-catalysed amination reaction was carried out with two different proline to metal ratios in each case, in order to gauge the possible importance of metal diprolinate species and metal monoprolinate species, e.g. M(prolinate)$_2$ *vs* M(OAc)(prolinate). In all of the examples tested, the dicoordinate metal prolinates catalysed the reaction with the same sense of selectivity as proline.



M	proline:$M(OAc)_2$	Yield / % (**12**)[a]	*ee* / % (**13**)[b]
Mg	1:1	86	36
Mg	2:1	80	36
Cu	1:1	<1	70
Cu	2:1	89	>95
Pd	1:1	17	43
Pd	2:1	89	52
Ni	1:1	86	50
Ni	2:1	89	81

Table 14: Dicoordinate metal prolinate-catalysed amination reaction; a) Determined by sampling and NMR analysis in comparison with an internal standard (PhCN); b) Determined by GC analysis of the purified product.

Magnesium prolinate induced a rapid reaction which proceeded in high yield but relatively low selectivity. Copper prolinate gave a high yield and excellent selectivity but only when a 2:1 mixture of proline and $Cu(OAc)_2$ was applied. Palladium prolinate also gave good yields when a 2:1 proline to metal ratio was applied but induced lower selectivity. With nickel prolinate both the 1:1 and 2:1 mixtures were capable of catalysing the reaction in high yield but the 2:1 mixture gave much improved selectivity. The generally higher activity seen with a 2:1 proline to metal ratio could indicate that under these conditions free proline is present, but this would contradict the literature precedent for the formation of metal diprolinate species.[151]

The demonstration here and by Darbre and co-workers[151] of the activity of a range of metal prolinates suggests a conceptual design for bifunctional catalysts. The

incorporation of a coordinating metal lends the opportunity to apply ligands to tune activity. Thus, the advantages of prolinate catalysis – reactivity and capability to activate unreactive pronucleophiles – could be augmented by the advantages of transition metal catalysis, particularly the ease of modification with ligands.

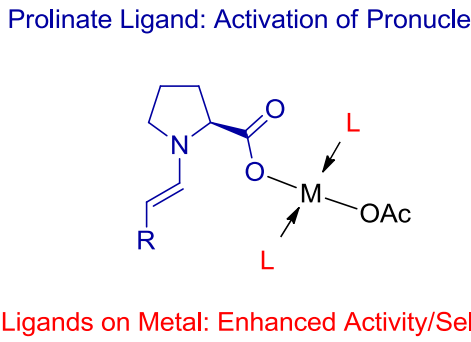


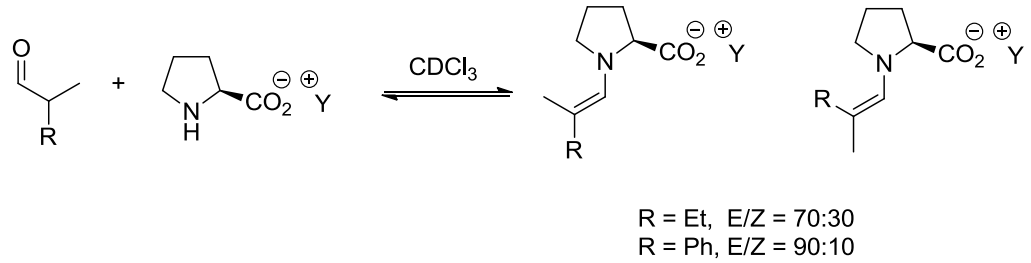
Figure 50: Conceptual bifunctional prolinate catalyst.

Recently, efforts have been made to combine organocatalysis and transition metal catalysis, but the metal usually serves to activate a reacting substrate rather than the catalyst itself.[153,154]

4.13. Steric Probe for Comparison of Prolinate Catalysts

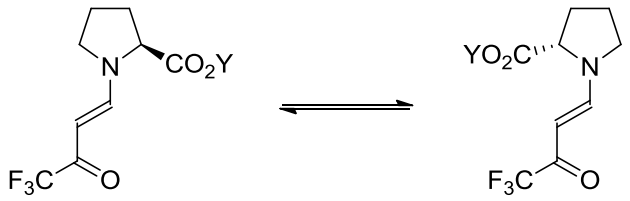
As has been detailed above, in the course of studying the prolinate-catalysed amination reaction, efforts have been made to assess the effect of changing the size of the counter cation. Through this approach, the limits to which different types of counter cations can be tuned have been discovered. However, it is desirable to find a more quantitative approach to the problem of the assessment of catalyst bulk. A remarkable feature of prolinate-catalysed reactions of aldehydes is how readily observable enamine intermediates are.[108,109] This leads to the possibility that enamine carboxylate species, generated from α-branched aldehydes and prolinate catalysts, could be used to determine the effective size of the catalyst since the E/Z ratio observed will be affected by this parameter. Enamines were formed from 2-phenylpropanal and 2-ethylpropanal adding stoichiometric quantities of prolinate catalysts and the E/Z ratios were determined. Disappointingly, it was found that this

isomeric ratio was unaffected by the identity of the counter cation; presumably the carboxylate is too far from the enamine double bond to influence its preferred configuration.



Scheme 43: Formation of enamines from prolinate catalysts and α-branched aldehydes with a range of counter cations.

However, another possible probe became apparent serendipitously with the choice of enaminone **22** for the base-titration study. In the ^{1}H NMR spectrum of this compound, two distinct conformers are clearly resolved. The conformers in question are the forms of the compound in which the relationship between the double bond and the carboxylic acid are *anti* and *syn* respectively as shown in Figure 36.[144] Gratifyingly, conversion of this enaminone carboxylic acid into a variety of corresponding enaminone carboxylates demonstrated that with different counter cations, the ratio of these conformers is changed.



anti-**30** *syn*-**30**

Y	*anti*-**30** / *syn*-**30**	amination *ee* / %[a]
H	83 : 17	-
DBUH	71 : 29	55
PhTMGH	72 : 28	59
Bu_4N	78 : 22	59
Ph_4P	74 : 26	60
Na + 15-crown-5	79 : 21	59
K + 18-crown-6	86 : 14	67
K + dibenzo-18-crown-6	83 : 17	61

Table 15: Conformational ratio of 30 with various different counter cations (Y); a) % *ee* of the amination reaction between propanal and DEAD of the corresponding prolinate.

A good match was found between the observed *anti*-**30** / *syn*-**30** ratio and the enantioselectivity of the corresponding prolinate-catalysed amination reaction. The finding that combinations of metal counter cations and crown ethers give the highest ratios supports our earlier claim that the complexed cation remains close enough to the carboxylate group to influence the activity of the catalyst.

Since the enaminone (**22**) used as a probe in this reaction is a model for the transition state of proline-catalysed reactions, it is a perfect fit to act as a probe for the effect of catalyst bulk. The conformational preference of **30** is expected to mirror the conformational preference of the transition state in prolinate catalysis. For catalysts that induce enantioselectivity through bulk rather than coordination of an electrophile,

this conformational preference is very likely to correlate closely with enantioselectivity. Therefore this approach could be extended to a range of different catalysts by preparation of the corresponding enaminone and determination of the ratio of the *anti* and *syn* conformers. Some obvious examples of such compounds are shown in Figure 51.

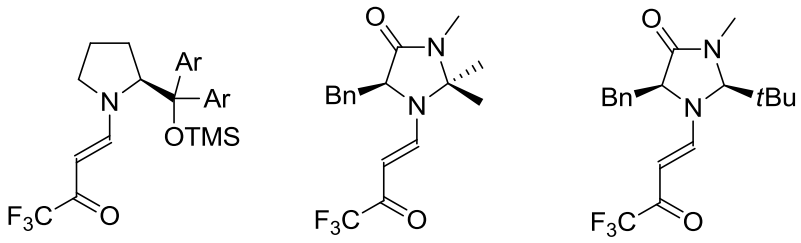


Figure 51: Proposed enaminone structures for determining the conformational preferences of known bulky catalysts.

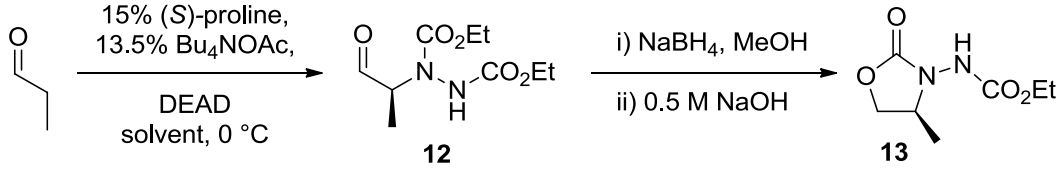
This approach could also be used to screen potential new catalysts to find structures that effect the greatest conformational bias. Preparation of such probes would be facilitated by the fact that a common intermediate would be used in the final step.

4.14. Prolinate-Catalysed Amination Solvent Screen

Given the remarkable solubility of prolinate salts in dichloromethane, we were interested to see if the catalyst would operate in different solvents. Another reason we were keen to perform such experiments was the potential for altering the degree of ion-pair association in the catalyst, and hence the observed activity.

In all of the solvents tested, the reaction with tetrabutylammonium prolinate gave the opposite sense of enantioselectivity to proline. The prolinate selectivities observed were similar to those seen in dichloromethane, except for in DMSO in which poor selectivity was observed with both proline and prolinate catalysis. For two of the solvents screened (*n*-hexane and THF) the absolute enantioselectivity of the prolinate catalyst exceeded that of proline, and this was the first such observation in this work.

In diethyl ether, the proline-catalysed reaction failed completely while the prolinate catalyst successfully gave product in moderate enantioselectivity. The slightly lower enantioselectivity observed in the prolinate-catalysed reaction in acetonitrile – compared with the reaction in dichloromethane – is consistent with the degree of enantioinduction seen in the reactions carried out in this solvent with proline and ArTMG bases (Table 5).



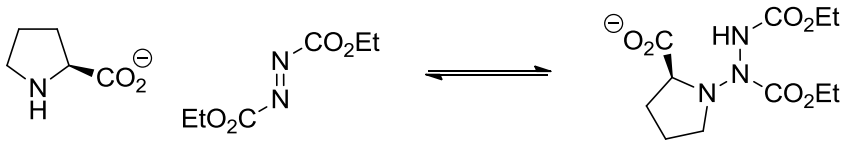
solvent	catalyst	*ee* / % (**13**)[a]	config.
n-hexane	(*S*)-proline	41	(*R*)
n-hexane	Bu_4N (*S*)-prolinate	53	(*S*)
Et_2O	(*S*)-proline	-	(*R*)
Et_2O	Bu_4N (*S*)-prolinate	57	(*S*)
THF	(*S*)-proline	36	(*R*)
THF	Bu_4N (*S*)-prolinate	60	(*S*)
CH_2Cl_2	(*S*)-proline	93	(*R*)
CH_2Cl_2	Bu_4N (*S*)-prolinate	60	(*S*)
MeCN	(*S*)-proline	90	(*R*)
MeCN	Bu_4N (*S*)-prolinate	49	(*S*)
DMSO[b]	(*S*)-proline	11	(*R*)
DMSO[b]	Bu_4N (*S*)-prolinate	8	(*S*)

Table 16: Proline- and Bu_4N prolinate-catalysed amination reaction in different solvents; a) Determined by GC analysis of the purified product; b) Reactions performed at rt to avoid solvent freezing.

The minimal variations in observed enantioselectivity in the prolinate-catalysed reactions indicate that changes in the ion-pair association achievable with different solvents do not give rise to a clear trend in altered activity. Nevertheless, a distinctive property of prolinate catalysis was clearly demonstrated: the wide range of solvent tolerance.

4.15. Kinetics

Over the course of these investigations into prolinate catalysis, the reaction kinetics of the tetrabutylammonium prolinate- and DBU/proline-catalysed amination were studied by our collaborators.[155] An unusual reaction profile was observed with a rapid initial rate followed by period of zero-order kinetics before the reaction suddenly halted. They discovered that under the normal reaction conditions, DEAD undergoes an addition reaction with the catalyst. This process is reversible but it results in removal of prolinate from the catalytic cycle.



Scheme 44: Off-cycle equilibrium involving an addition reaction between the prolinate catalyst and DEAD.[155]

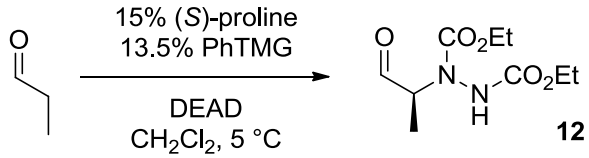
With this information, the reaction profile was fully explained: the reaction is rapid until the catalyst reaches equilibrium in its reaction with DEAD, after which the positive order in propanal is cancelled by an apparent negative order in DEAD, observed due to this deactivation of the catalyst. This region of the reaction profile dominates until the end point is approached when no further starting materials are available and the reaction abruptly ceases. The off-cycle can be suppressed by the addition of acid, and this can be achieved by forming prolinate catalysts from acetate salts to leave an equivalent of acetic acid. With these intriguing findings revealed, we

were interested in how these effects might be replicated under some of the conditions that we had explored.

The kinetic data for the amination reaction reported here were obtained by reaction calorimetry (RC). In this technique, the reaction under investigation is performed in an adiabatic chamber at a constant temperature. The energy required to maintain the constant temperature is directly related to the heat flow evolved or consumed by the reaction. This heat flow is in turn directly related to reaction rate, so the output is in effect a plot of rate against time. From the area under the curve of a given plot, the heat of reaction (ΔH_{rxn}) can be determined.

The reaction profile generated by RC for the proline-catalysed amination reaction in the presence of PhTMG is shown below in Figure 52. This exemplifies the unusual reaction profile that was described in the discussion of our collaborators' investigations, and the graph is annotated to highlight the key features. Beneath this, in Figure 53, is shown the effect of adding acetic acid to this reaction under otherwise matching conditions. The reaction rate is massively increased, no zero-order region is observed, and the result is that the reaction is complete after 10 rather than 30 minutes.

It is unsurprising that the catalyst generated from proline and PhTMG displays similar reaction kinetics to those obtained from mixing proline and DBU, but we were interested to see how the profile would differ in the presence of weaker bases.



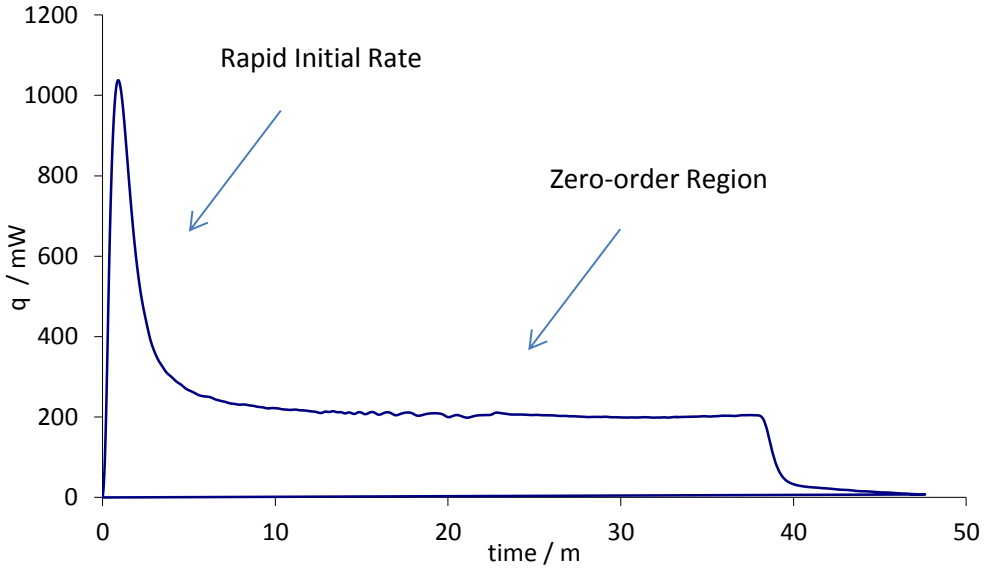


Figure 52: RC monitoring of the proline-catalysed amination reaction in the presence of PhTMG.

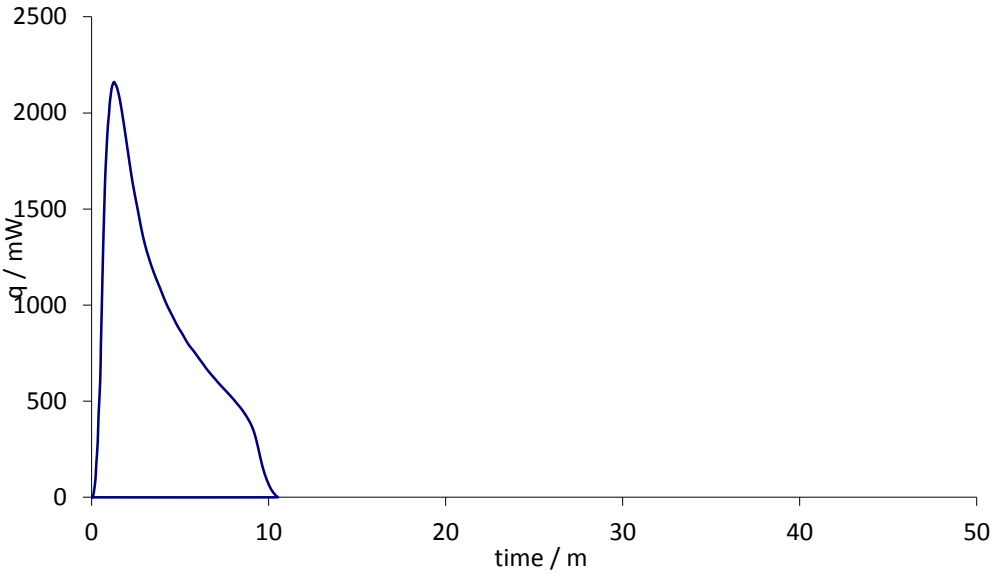


Figure 53: RC monitoring of the proline-catalysed amination reaction in the presence of PhTMG with added AcOH (13.5%).

The proline-catalysed amination reaction was monitored in the presence of **19f**, **19g**, and **19h** (the weakest ArTMG bases previously studied). These reactions were conducted in the presence of acetic acid to give the intrinsic rate of the amination reaction. From the RC data, it is clear that the weaker ArTMG bases give a slower reaction rate at all times during the course of the amination reaction.

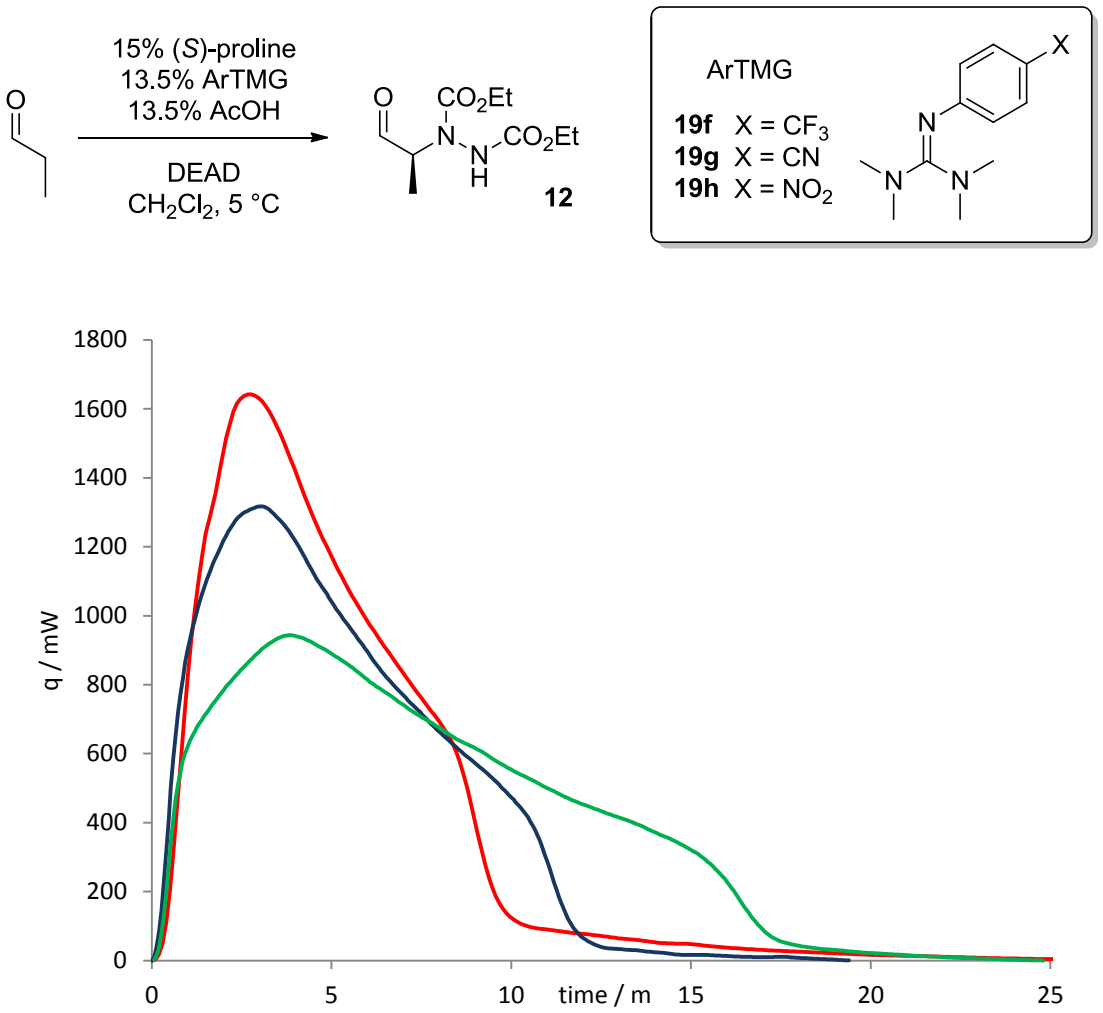


Figure 54: RC monitoring of the proline-catalysed amination reaction in the presence of ArTMG bases with added acetic acid; 19f (red line), 19g (blue line), 19h (green line).

This can be simply explained by the decreased amount of prolinate catalyst that is present with the weaker bases due to incomplete deprotonation of proline. The result displays further strong evidence that the differences in selectivity when bases are added are due to different degrees of deprotonation of the catalyst, rather than the

alternative explanation that the conjugate acid of the base lowers the energy of a competing transition state. If the latter explanation was true and each of the ArTMG bases was capable of fully deprotonating proline, then minimal difference in the reaction rate would be expected.

We also wanted to probe the effect of the crown ether additive on the kinetics of the metal prolinate-catalysed amination reaction (Figure 55).

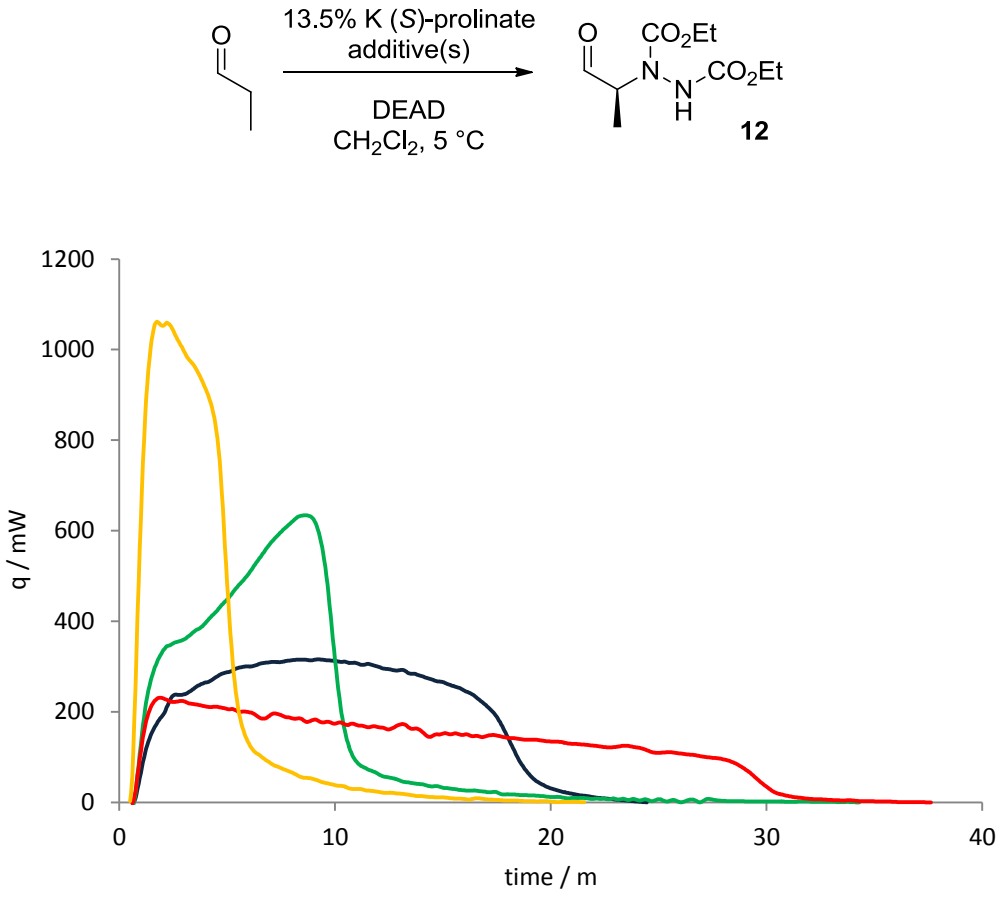


Figure 55: K prolinate-catalysed amination reaction in the presence of no additive (blue line), AcOH (13.5%) (green line), 18-crown-6 (13.5%) (red line), 18-crown-6 (13.5%) and AcOH (13.5%) (yellow line).

In the reaction, potassium prolinate readily forms the adduct with DEAD as evidenced by the zero-order region of the reaction profile, and in the presence of 18-crown-6 this is even more pronounced; presumably the nucleophilicity of the catalyst is increased

by its greater effective negative charge. When acetic acid is added, the change in reactivity is dramatic, with the crown ether-modified prolinate giving rise to a very rapid reaction. When just acetic acid is added, the reaction displays a rising rate as seen previously when product-induced reaction acceleration is operating.

The kinetic investigations into prolinate catalysis display the increased nucleophilicity these catalysts exhibit. In response to the publication of our work on prolinate catalysis and the work of our collaborators,[108,155,156] the nucleophilicities of prolinate catalysts were investigated by Mayr and co-workers.[157] According to the usual approach of the Mayr group, reaction rates were determined with a set of electrophiles with known electrophilicity parameters (E), such that the data obtained could be fitted to Equation 2, and the nucleophilicity parameters s_N and N could be determined. Knowledge of these values allows for semi-quantitative comparison with the reactivity of other species for which these parameters have been determined.[158]

$$\log k = s_N(N + E)$$

Equation 2: Mayr nucleophilicity equation; s_N = nucleophile specific sensitivity parameter, N = nucleophilicity parameter, E = electrophilicity parameter.

The reactions between benzhydrylium salts and the enamines derived from cyclohexanone were investigated for methyl proline ester, pyrrolidine, and prolinate.

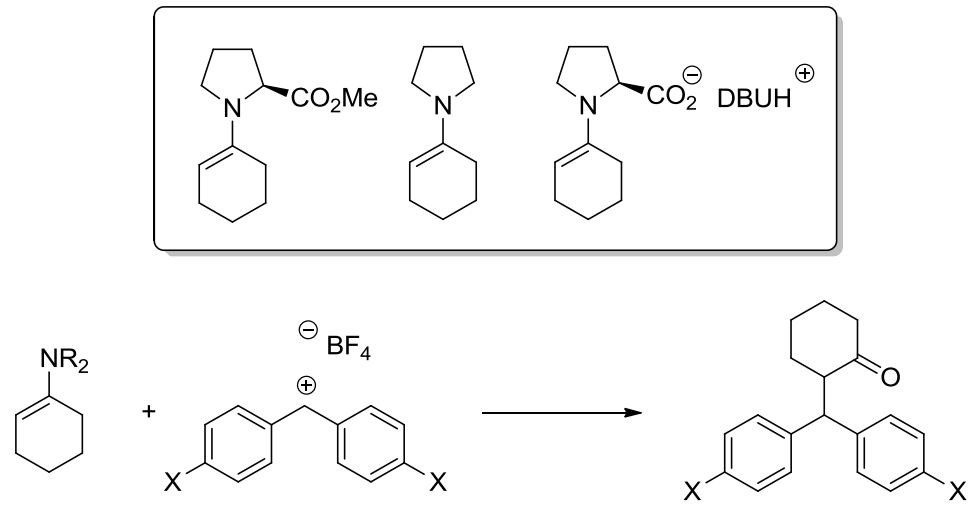


Figure 56: Reactions with benzhydrylium ions employed by Mayr and co-workers to determine nucleophilicity parameters for the enamines shown.

In their study it was determined that the enamine derived from prolinate was 50–60 times more reactive than that derived from pyrrolidine and 800–900 times more reactive than that derived from proline methyl ester. It was also shown, however, that the difference in reactivity is dramatically altered by the electrophile in question; in the reaction with β-nitrostyrene, the prolinate-derived enamine is 107 times more reactive than that derived from pyrrolidine, however with DEAD the difference is only a factor of 6. The authors conclude that the increased reactivity is due to anchimeric assistance provided by the naked carboxylate, but another explanation is simply increased nucleophilicity owing to the presence of a neighbouring negative charge.

4.16. Concluding Remarks

In this chapter, investigations into a variety of facets of the prolinate-catalysed amination reaction have been detailed. The factors that dictate stereoselectivity were analysed by application of an isosteric set of guanidine bases and by variation of the prolinate counter cation.

The demonstration of the high nucleophilicity of prolinate catalysts, in addition to the wide solubility profile and inherent tunability, shows the potential such species have

for further application. The results show the worth of applying additives in the process of catalyst screening.

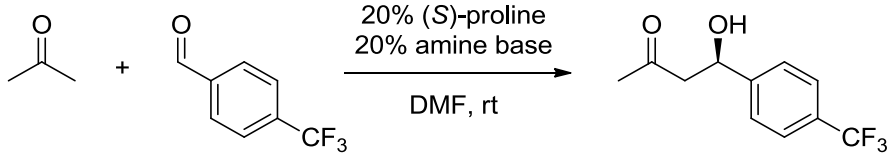
The observed ability to reverse the reaction selectivity on addition of an additive is interesting from a fundamental view of reaction design: the additive could be applied as a switch to sequentially achieve different reactivity from the same catalyst precursor. This general concept was achieved by Feringa and co-workers using a nucleophilic catalyst with an appended molecular motor;[159] in this report, application of light or heat switched the enantioselectivity, but it is notable that the enantioselectivity achieved was lower in both cases than the best achievable in the amination reaction with proline- or prolinate-catalysis.

The extension of prolinate catalysis to other reactions is an obvious goal, and in the next chapter, exploratory studies into its application to the aldol reaction are described.

5. Aldol

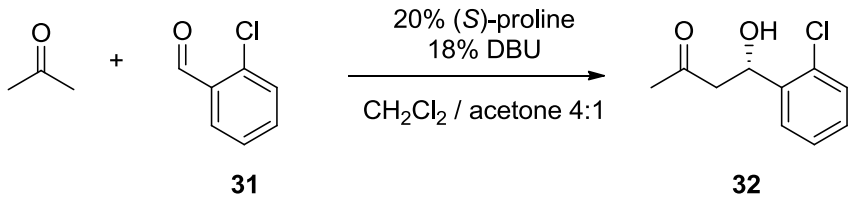
5.1. Base Effect in the Aldol Reaction

Following on from the discovery of the remarkable effect of basic additives on the proline-catalysed amination reaction, we were keen to investigate whether similar effects would be seen when bases are applied to the aldol reaction. It was reported by Pihko and co-workers that the addition of amine bases does not affect conversion in the proline-catalysed aldol reaction, but can lead to diminished enantioselectivity and, in the case of DBU, the product obtained was racemic.[115]



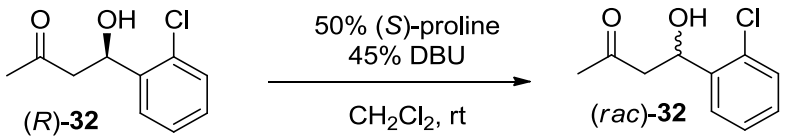
Scheme 45: Proline-catalysed aldol reaction studied in the presence of amine bases by Pihko and co-workers.[115]

The model aldol reaction chosen with which to investigate basic additives, in this thesis, was that between acetone and 2-chlorobenzaldehyde; this reaction has been extensively studied in the Armstrong group in the past, and as such conditions for performing and analysing the process had previously been established. We also decided to perform the reactions in dichloromethane to keep the conditions employed for prolinate catalysis as similar as possible to those in the amination reaction. During preliminary studies into the effect of DBU on the proline-catalysed aldol reaction, results were found to be difficult to reproduce: the additive appeared to effect stereochemical inversion, as it does in the amination reaction, on some occasions but at other times the product obtained was racemic.



Scheme 46: Proline-catalysed aldol reaction in the presence of DBU.

Reproducibility was not improved by variation of solvent, temperature, or aromatic aldehyde substrate. Due to these issues, an investigation was carried out to determine the product stability in the presence of proline and DBU, and it was found that an enantioenriched sample of the aldol product suffers racemisation under these conditions. Control experiments showed that proline and DBU alone are incapable of effecting such a dramatic change, although slight erosion in enantioenrichment was observed in the presence of DBU.



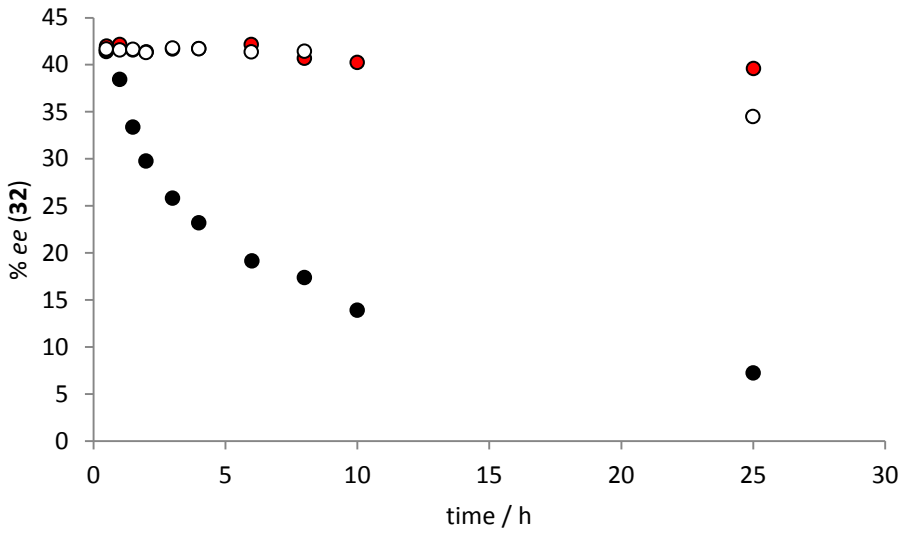
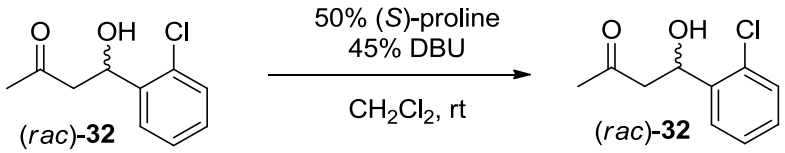


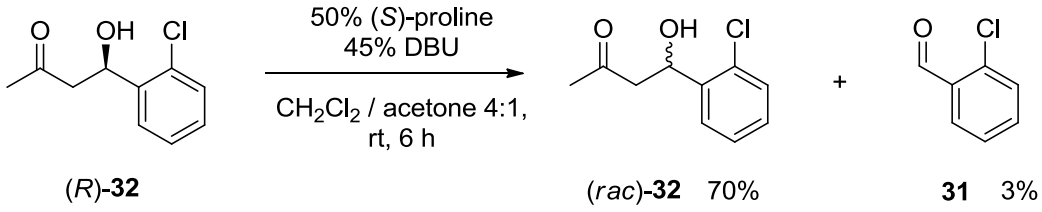
Figure 57: % *ee* of aldol product (32) over time in the presence of proline (red circles), DBU (white circles) and a 0.9 ratio mixture of DBU and proline (black circles); % *ee* determined by sampling/HPLC analysis.

Such loss of stereochemical information could be caused by kinetic resolution if one enantiomer is selectively destroyed. Such a process could explain the occasional observation of enantioselectivity. This was ruled out, however, by a further control experiment which showed that a racemic sample of the aldol product underwent no change in enantioenrichment over time, confirming that the results displayed in Figure 57 do indeed represent a racemisation process rather than an overall reversal of the absolute configuration by resolution.



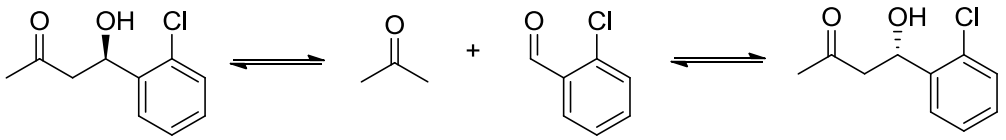
Scheme 47: Control experiment carried out with racemic aldol product (*rac*)-32 showing that kinetic resolution does not occur.

The racemisation is unlikely to result from a simple deprotonation/protonation sequence because the hydrogen attached to the stereocentre is not acidic. A clue was provided by the observation of 2-chlorobenzaldehyde (**31**), which was formed in the racemisation study. The presence of this material indicates that a retroaldol reaction must take place and that the proline-catalysed aldol reaction is therefore reversible in the presence of DBU; no detectable aldehyde formation is observed when hydroxyketone **32** is treated with proline or DBU alone. To quantify this result, the reaction was repeated in the presence of an internal standard, and it was found that the aldehyde had formed in a 3% yield after 6 hours. Strikingly, it was also found that the amount of aldol product had become depleted to 70% of the initial amount.



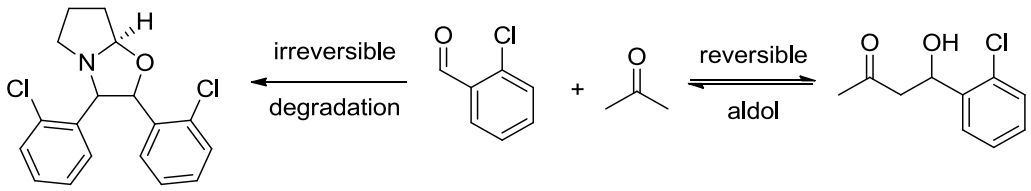
Scheme 48: DBU/proline-catalysed retroaldol reaction of hydroxy ketone 32; Reaction composition determined after 6 h by sampling/HPLC analysis.

This observation of a retroaldol process explains both the racemisation and the problems of reproducibility initially observed in determining the enantioselectivity of the forward reaction. Enantioselectivity may be observed at first, but over time the reversible aldol reaction reaches equilibrium. Since the starting material and product are in equilibrium, the two enantiomers of the product are also in equilibrium and necessarily, a racemate results.



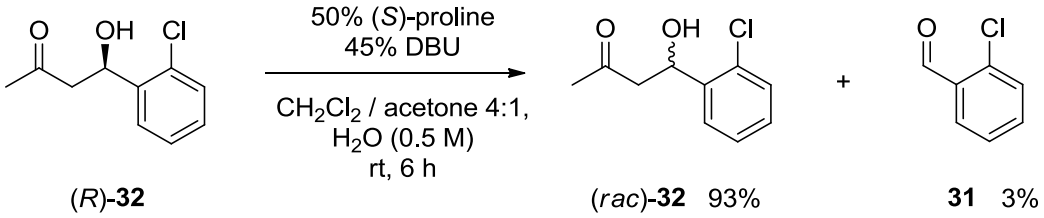
Scheme 49: Reversible aldol reaction results in racemic product at equilibrium.

The overall loss of material observed in the retroaldol process can be explained by the known proline degradation pathway which would deplete the amount of aldehyde and therefore also deplete the amount of aldol product, since the two species are in equilibrium.



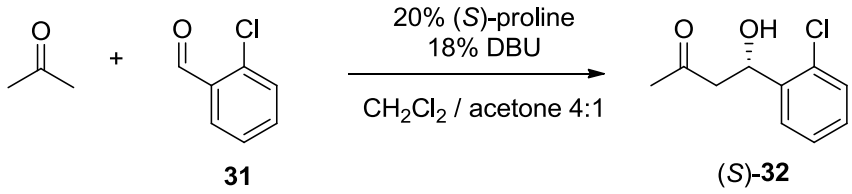
Scheme 50: Depletion of aromatic aldehyde and hence aldol product by known catalyst degradation pathway.

It is known that the degradation pathway can be suppressed in the presence of water, and it was found to be the case that addition of water prevented material loss (Scheme 51); erosion of enantioenrichment still occurred as would be expected since the racemisation pathway is unaffected.

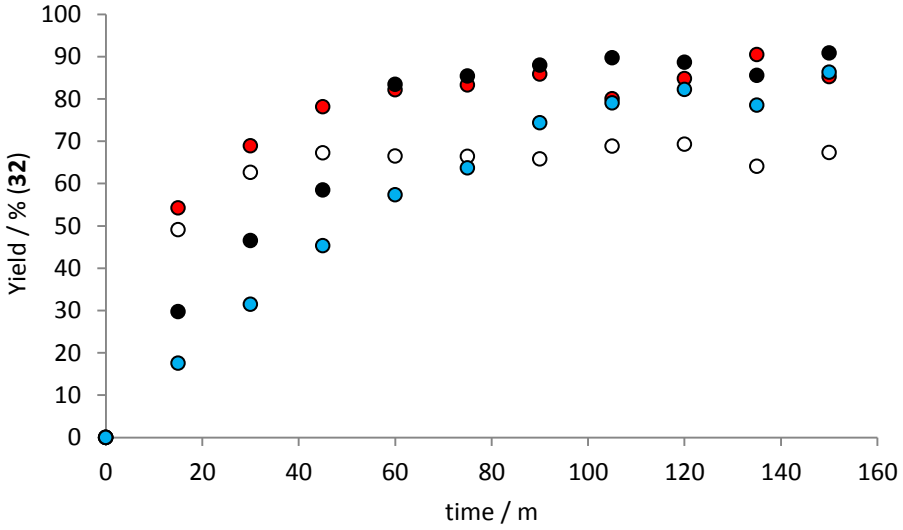


Scheme 51: DBU/proline-catalysed retroaldol reaction of hydroxy ketone 32 in the presence of water; Reaction composition determined after 6 h by sampling / HPLC analysis.

Armed with the information garnered from the retroaldol studies, the forward reaction was reinvestigated by a sampling approach to determine how yield and product % *ee* change over time. It was found that reaction progress stops at around 70% after 45 minutes. Addition of water results in a higher maximum yield (around 90%) but slows the reaction. With and without water, the % *ee* is around 20% at the start of the reaction but decreases over time. The racemisation occurs at a slower rate in the presence of water, however, indicating that under these conditions it takes longer for the product enantiomers to reach equilibrium.



31 (*S*)-**32**



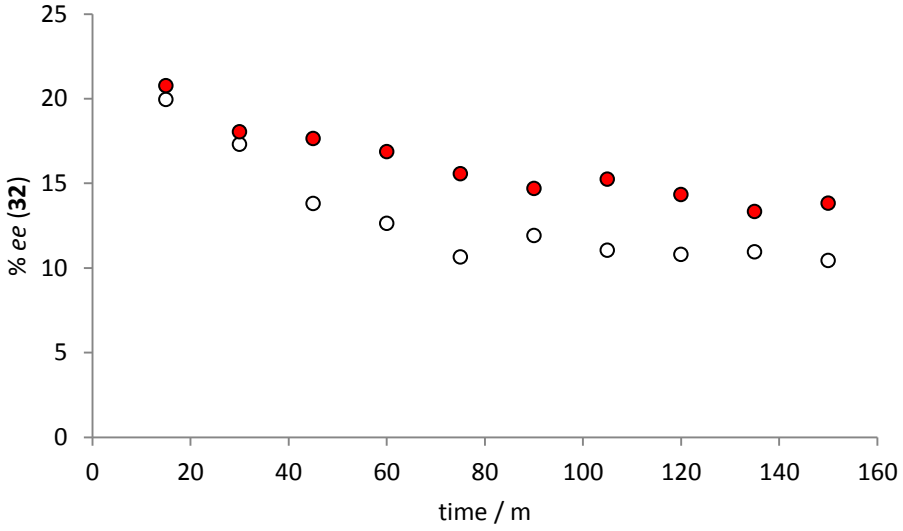


Figure 58: Proline-catalysed aldol reaction in the presence of DBU; White circles – no added water; Red circles – 1 equiv. added water; Black circles – 2 equiv. added water; Blue circles – 3 equiv. added water; Yield determined by sampling/HPLC analysis with respect to an internal standard (PhCN); % *ee* determined by sampling/HPLC analysis.

This study also shows that the product obtained is initially enantioenriched and becomes racemised over time. In addition it is confirmed that the sense of enantioselectivity is the reverse of that induced by proline.

Next, the DBU/proline-catalysed reaction was compared to some analogous systems (Figure 59). It was found that tetraalkylammonium prolinate catalysed the reaction at a similar rate, and in addition gave the same initial inverted sense of enantioselectivity at around the same level. The proline-catalysed reaction, which, as expected, gave (*R*)-**32** (58% *ee*) was comparatively much slower. Notably, when triethylamine was applied, the reaction was much more like the case with no additive than with added DBU – a slow reaction ensued and gave product that had the proline sense of chirality, albeit in diminished enantioselectivity (47% *ee*).

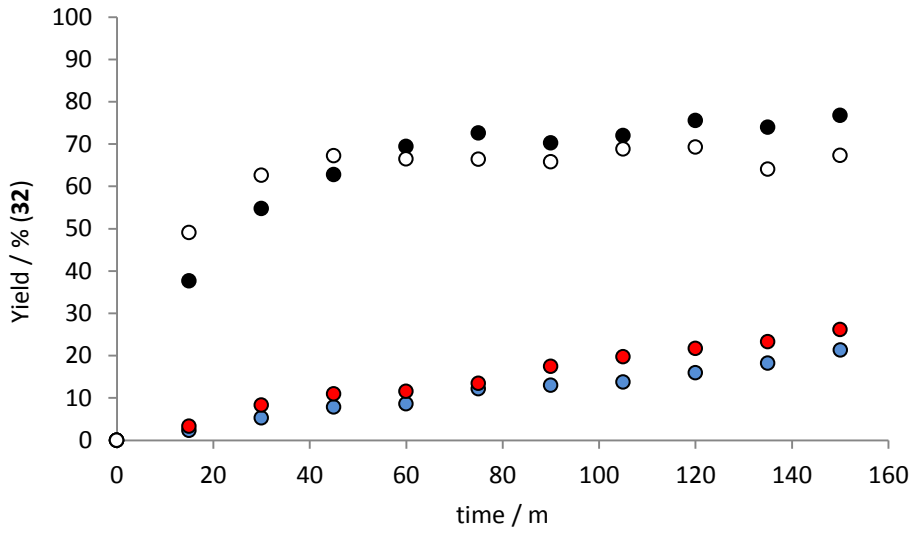


Figure 59: Reaction profile for the aldol reaction between acetone and 31 catalysed by DBU/proline (white circles), Bu_4N prolinate (black circles), Et_3N/proline (red circles), and proline with no additive (blue circles); Yield determined by sampling/HPLC analysis with respect to an internal standard (PhCN).

These results indicate that while prolinate catalysis is in operation when DBU is applied as a base, triethylamine is unable to induce prolinate catalysis under these conditions. The catalysts demonstrated different solubilities at the start of the reaction, which complicates the analysis; however, over the course of the proline-catalysed intermolecular aldol reaction, this becomes a smaller factor due to conversion of the catalyst to its oxazolidinone resting state.

It was found that even at a 4% loading of DBU and proline, a quicker reaction was achieved compared with that of the proline-catalysed reaction at 20% loading.

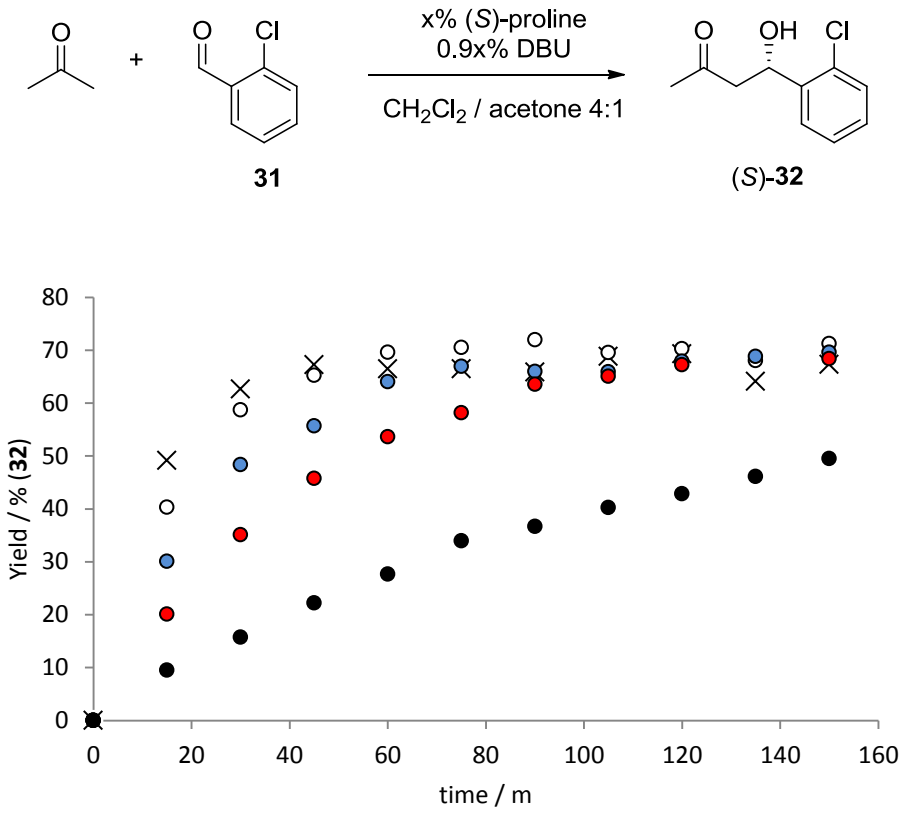


Figure 60: Proline-catalysed aldol reaction in the presence of DBU; Catalyst loading: 20% (crosses), 16% (white circles), 12% (blue circles), 8% (red circles), 4% (black circles); Yield determined by sampling/HPLC analysis with respect to an internal standard (PhCN).

With these lower catalyst loadings, the same observation was made of initially enantioenriched product – with configuration opposite to that obtained by proline-catalysis – that becomes racemised over time.

5.2. Explanation for Selectivity Reversal

Although base-induced reversal of stereoselectivity had previously been observed in the proline-catalysed amination reaction, its occurrence in the aldol reaction between acetone and 2-chlorobenzaldehyde is still somewhat surprising since the prochiral component is in this case the electrophile. In the proline-catalysed reaction, positioning of the aldehyde is governed by its orientation with respect to the carboxylic acid group. In the prolinate-catalysed reaction too, this orientation is likely to dictate the enantioselectivity. It is assumed, analogously to the prolinate-catalysed amination reaction, that the electrophile – in this case 2-chlorobenzaldehyde – approaches from the opposite face of enamine to the carboxylate group, which acts as a blocking group. The observed enantiomer would then be formed by attack on the *Si*-face of the aldehyde so that the aryl group is oriented away from the catalyst. The orientation of the aldehyde nucleophilic attack should be reasonably flexible since it will experience few steric clashes, and this is reflected by the low level of asymmetric induction.

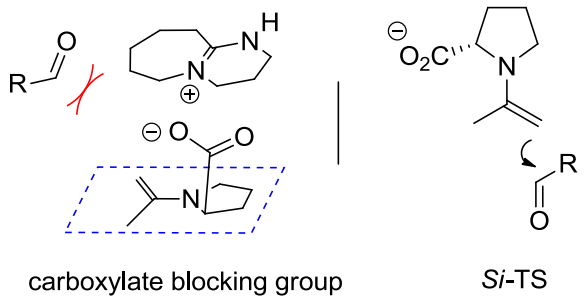
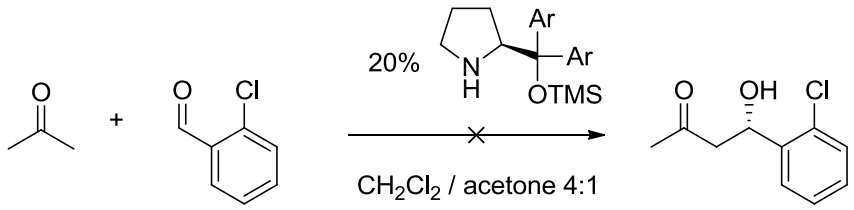


Figure 61: Proposed lowest energy transition state for the prolinate-catalysed aldol reaction.

We were interested to see how a diaryl prolinol silyl ether catalyst[xi] would perform in the reaction, since inversion of selectivity had again been observed, with the most probable explanation being provided by invocation of a blocking group effect. The catalyst was employed under the same conditions as for proline, but no conversion was observed within 2.5 hours, the same time period required for complete reaction in the DBU/proline case.

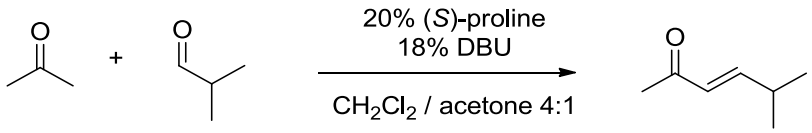


Scheme 52: Failed diaryl prolinol silyl ether-catalysed aldol reaction between acetone and 2-chlorobenzaldehyde; Ar = 3,5-$(CF_3)_2$-C_6H_3.

This result strikingly displays the greater reactivity of the DBU/proline catalyst compared with the prolinol ether. The aldehyde electrophile is less reactive than DEAD, and the proline-catalysed aldol reaction is possible due to activation of the electrophile by the carboxylic acid group, but the prolinate catalyst is sufficiently nucleophilic to catalyse the reaction without this form of activation.

It was also of interest to determine the effect of changing the electrophile to an aliphatic aldehyde. The branched substrate isobutyraldehyde was chosen for this purpose because although it is enolisable, it wouldn't readily undergo homoaldol reaction in the presence of the prolinate catalyst. However, in this reaction only the aldol condensation product was observed (Scheme 53). With pivaldehyde no conversion was observed.[xii]

xi) A sample of the catalyst used was synthesised and generously donated by D. P. Emmerson.
xii) In both cases, the reactions with aliphatic aldehydes were monitored by sampling / ^{1}H NMR analysis.

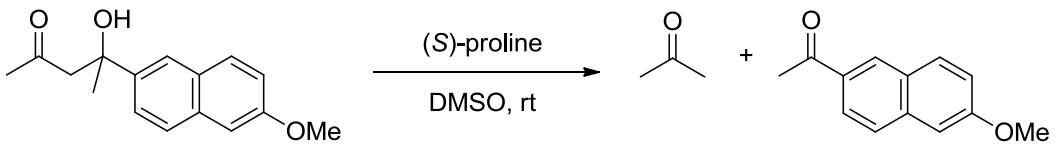


Scheme 53: Prolinate-catalysed aldol condensation reaction between acetone and isobutyraldehyde.

While it is interesting that the change in aldehyde substrate resulted in a contrasting reaction pathway, the product of the reaction is achiral and no inferences concerning the stereoselectivity of prolinate-catalysed reactions can be made, and so the reaction was not further investigated.

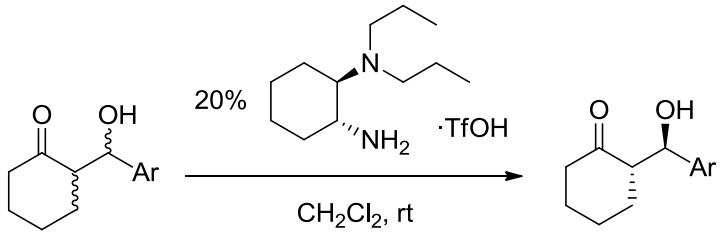
5.3. Retroaldol

As demonstrated above, prolinates are capable of catalysing the retroaldol reaction of hydroxyketone **32**. The selectivity initially seen in the forward reaction indicates that the retroaldol reaction is also selective due to microscopic reversibility. This selectivity is not directly observable however, due to the reversibility of the reaction and the energetic preference for the aldol product side of the equilibrium. We were interested to see if under other circumstances a prolinate catalyst could catalyse a retroaldol process stereoselectively as this could potentially give resolution of a racemic aldol product. In order for this to work, it would be necessary for the corresponding aldol reaction to be very slow so that reversibility does not occur. A tertiary keto alcohol – the formal aldol product of two ketones – would be ideally suited for this purpose. It has been shown by List and co-workers[97] that proline can catalyse the retroaldol reaction of a substrate of this type (Scheme 54).



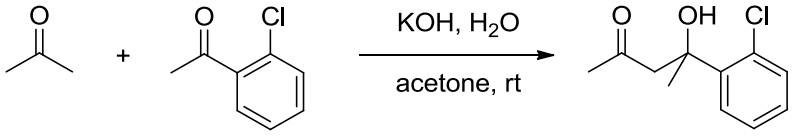
Scheme 54: Proline-catalysed retroaldol process reported by List and co-workers.[97]

In this reaction, only the initial rates at a range of different concentrations were recorded, and the enantioselectivity of the process was not determined; it had previously been reported that proline does not catalyse such reactions enantioselectivity.[27] However, the asymmetric retroaldol reaction has been reported with use of a primary amine organocatalyst (Scheme 55).[160]



Scheme 55: Primary amine-catalysed asymmetric retroaldol reaction reported by Luo, Cheng, and co-workers.[160]

We decided to test the retroaldol capability of prolinate catalyst on the same methoxynaphthyl substrate used by List.[97] It was initially attempted to synthesise the required hydroxyketone by a potassium hydroxide-catalysed aldol reaction. For the reaction between acetone and 2-chloroacetophenone, this method gave the desired product (*rac*)-**35**, albeit in a very low yield.



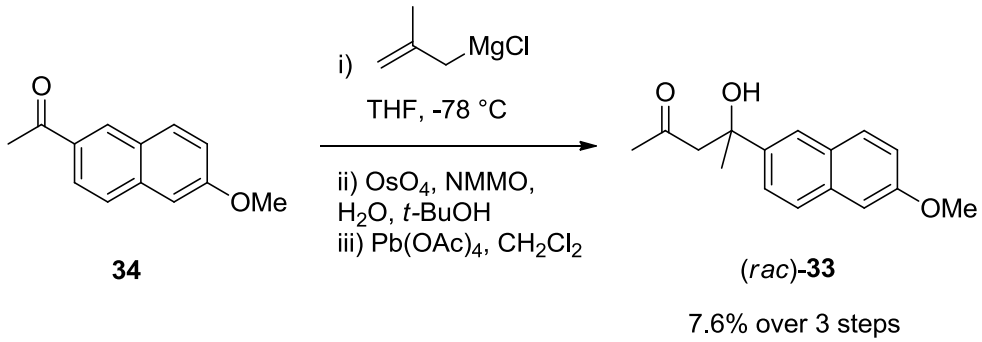
(*rac*)-**35**

0.5%

Scheme 56: KOH-catalysed aldol reaction between acetone and 2-chloroacetophenone; 79% recovery of unreacted 2-chloroacetophenone.

However, this procedure was completely unsuccessful for the formation hydroxyketone **33**. Therefore it was necessary to make the substrate in an indirect route; to this effect the three step synthesis of List, Lerner, and Barbas was employed.[161] The desired substrate was thus synthesised from the 6-methoxy-2-

acetonaphthone by 1,2-addition of an allyl Grignard reagent, Upjohn dihydroxylation, and lead tetraacetate-mediated oxidative cleavage.



Scheme 57: Synthesis of hydroxyketone from 6'-methoxyacetonaphthone by a Grignard addition, Upjohn dihydroxylation, oxidative cleavage sequence.

The major loss of material in this synthesis occurred in the final step, during which the desired product underwent retroaldol reaction as evidenced by the re-isolation of 6-methoxy-2-acetonaphthone, which accounted for 67% of the product loss. Nevertheless, the process yielded sufficient quantities for the retroaldol study.

An HPLC assay was developed that allowed resolution of the two enantiomers of **33** and 6-methoxy-2-acetonaphthone (**34**). The assay also allowed resolution of benzonitrile, an internal standard, and relative response factors for **33** and **34** were determined to allow calibration of HPLC data.[xiii] The prolinate-catalysed retroaldol reaction was then monitored by sampling and HPLC analysis. It was found that the DBU/proline combination could catalyse the transformation, but disappointingly the hydroxyketone remained racemic during the course of the reaction indicating that the process is not selective.

xiii) This is necessary because the detection method is UV spectroscopy and the different components have different UV activity.

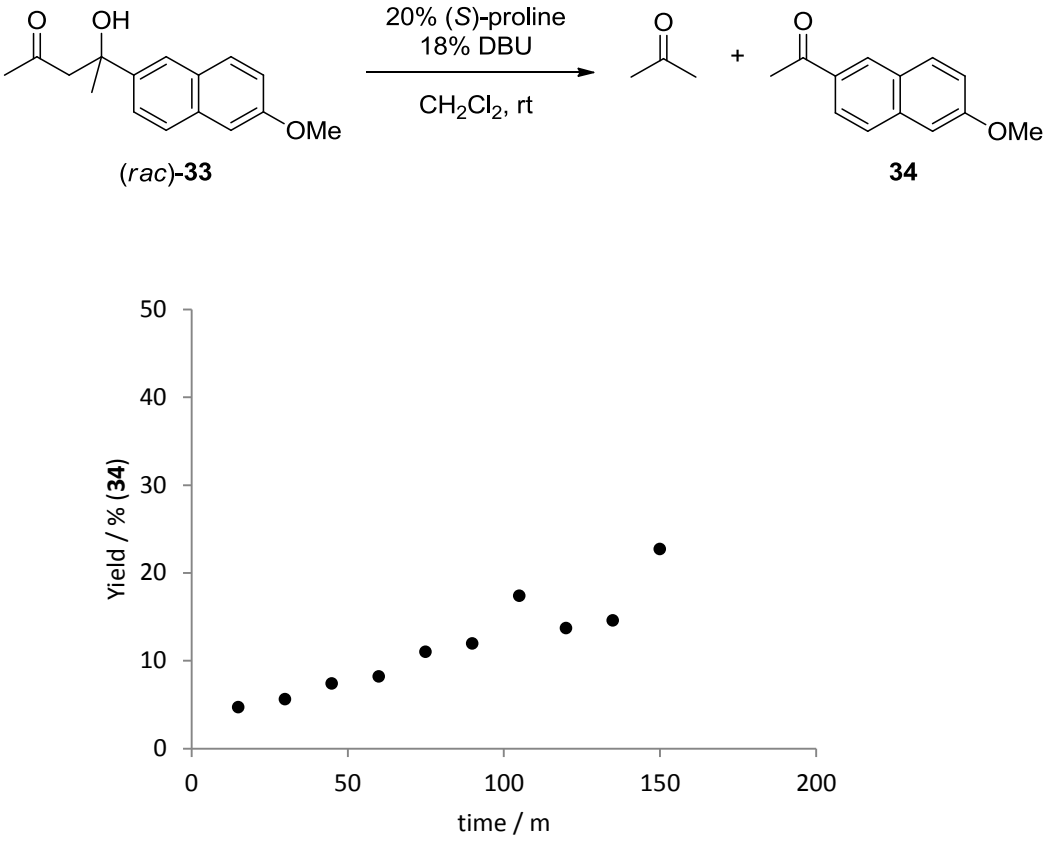


Figure 62: DBU/proline-catalysed retroaldol reaction of hydroxyketone 32 monitored by sampling/HPLC analysis; Yield determined with respect to an internal standard (PhCN).

Interestingly, under these conditions proline alone was not capable of catalysing the retroaldol process, in contrast to its reactivity in DMSO.

5.4. Dicarboxylic Acid Catalyst

Surprisingly, given the marked impact that we have observed of bases in enamine catalysis, literature reports on such phenomena are scarce. One notable example is the observation by Wu and co-workers that a rate enhancement occurs when triethylamine is added to aldol reactions catalysed by (2*S*,5*S*)-pyrrolidine-2,5-dicarboxylic acid.[162]

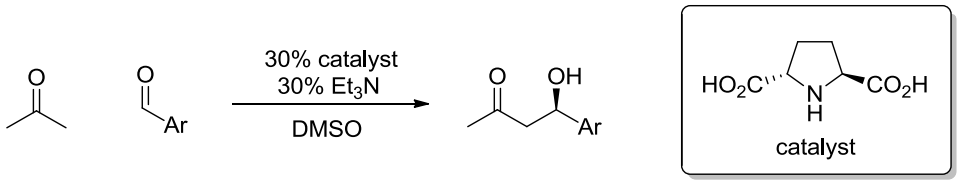
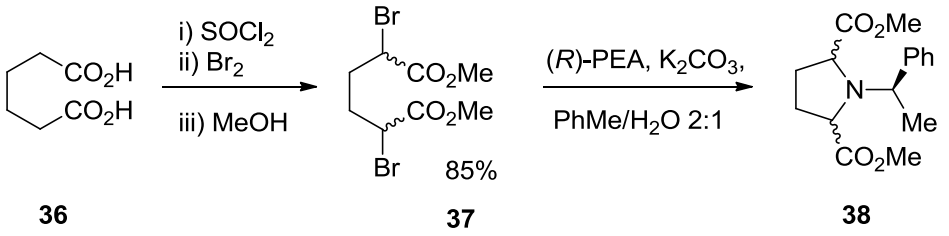


Figure 63: Dicarboxylic acid-catalysed aldol reaction, accelerated by Et_3N additive.

While a yield of 22% is obtained without added triethylamine, application of the additive results in a yield of 60% after 3 hours. The origin of this enhancement was unexplained and given our interest in prolinate catalysis, we were keen to investigate.

5.4.1. Synthesis of the Catalyst

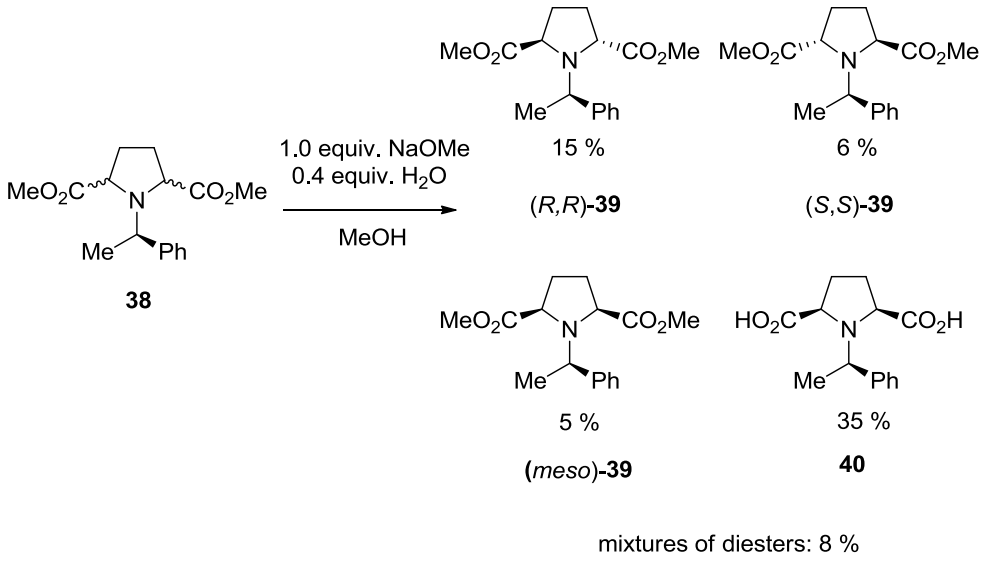
The required catalyst was synthesised from adipic acid (**36**) by a modified version of the method of Yamamoto and co-workers.[163] This method allows access to both enantiomers of the catalyst by introducing a chiral auxiliary in the pyrrolidine ring-forming step. The synthesis commenced with conversion of both carboxylic acid groups present in adipic acid to the corresponding acid chlorides. This intermediate was then dibrominated in a Hell–Vollhard–Zelinsky reaction and converted to the corresponding diester by addition of methanol. This gave dimethyl 2,5-dibromoadipate **37** as a mixture of diastereomers in 85% yield (over three steps). Double S_N2 substitution was then performed with a chiral primary amine to give pyrrolidine **38**.



Scheme 58: Formation of the pyrrolidine ring and introduction of an auxiliary to allow resolution.

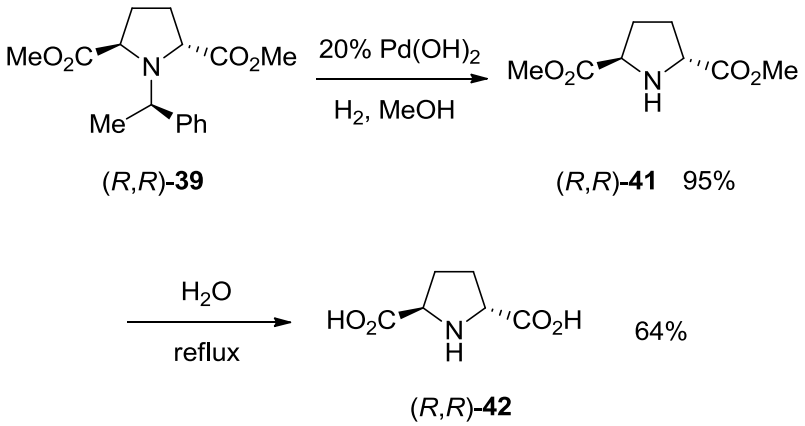
The mixture of pyrrolidine diester isomers was treated with sodium methoxide to which was added sufficient water to achieve hydrolysis of the *cis*-diester; this method

relies on the generation of a small concentration of sodium hydroxide and the greater susceptibility of the *cis*-isomer towards hydrolysis. The faster observed rate of hydrolysis for 2,5-*cis*-pyrrolidine diesters compared with the *trans*-counterparts has been attributed to greater solvent stabilisation for the forming tetrahedral intermediate in the transition state.[164] Following hydrolysis, the *cis*-isomer, as the diacid, can be removed by washing and this facilitates the chromatographic separation of the two *trans*-isomers. Thus (*R*,*R*)-**39** and (*S*,*S*)-**39** were obtained in 15 % and 6 % yield (over two steps) as shown in Scheme 59.



Scheme 59: Selective hydrolysis and separation of the diastereomeric mixture of pyrrolidine diesters; Yields shown are those obtained over two steps (from 37).

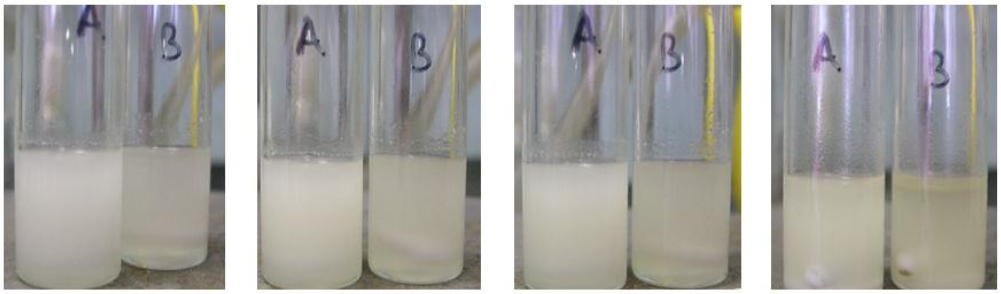
Diesters (*R*,*R*)-**39** and (*S*,*S*)-**39** were then separately converted into the two enantiomers of the dicarboxylic acid catalyst by successive hydrogenolysis and hydrolysis; the sequence is show in Scheme 60 for the conversion of (*R*,*R*)-**39** to (*R*,*R*)-**42**.



Scheme 60: Final stages of the synthesis: hydrogenolysis and hydrolysis yields the catalyst.

5.4.2. Analysis of the Base Effect

In initial attempts to study the catalyst, it became immediately apparent that the compound displays very poor solubility, and we suspected that the rate enhancement observed with added triethylamine is simply due to catalyst solubilisation. To investigate this hypothesis, the solubility of the catalyst in DMSO and in DMSO with triethylamine was assessed by ^{1}H NMR with use of an internal standard (2,5-dimethylfuran). Mixtures were prepared of the catalyst in deuterated DMSO with and without triethylamine; these were stirred for 1.5 hours and samples were filtered and analysed by ^{1}H NMR spectroscopy. While stirring, it became apparent on visual inspection that the catalyst was more soluble in the mixture containing triethylamine (see Figure 64).



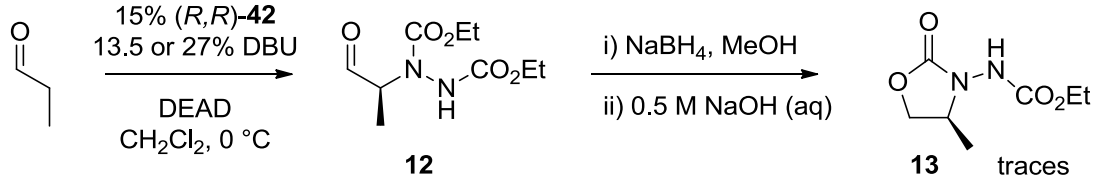
15 m 30 m 45 m 60 m

Figure 64: Appearance of mixtures after a given amount of stirring; A = d_6-DMSO without triethylamine, B = d_6-DMSO with triethylamine.

Comparison of the resulting spectra showed that in the presence of triethylamine the concentration of the catalyst is roughly doubled. Thus, it was concluded that the reaction experiences a rate enhancement with triethylamine additive due to solubilisation of the catalyst. Analysis of any intrinsic effects that may be caused by the presence of triethylamine proved impossible to determine because, even in the presence of triethylamine, the catalyst is so poorly soluble. It might be expected that the solubilisation is effected by deprotonation of the catalyst. However, in DMSO the trialkylammonium species and acetic acid derivatives have comparable acidity, and the case may not be so clear cut.

To determine the effect of genuine prolinate-type catalysis with the dicarboxylic acid catalyst, it was subjected to the amination reaction in the presence of DBU. On account of the presence of the two acid groups, this reaction was carried out with 0.9 and 1.8 equivalents of base relative to catalyst loading. Under both conditions the catalyst performed very poorly, giving only trace amounts of product (<1%). The sense of enantioselectivity reflected that expected from proline catalysis.[xiv]

xiv) In this case comparison must be made with the selectivity of (*R*)-proline because (*R*,*R*)-**42** was used.



Scheme 61: (*R*,*R*)-42-catalysed amination reaction in the presence of DBU.

When proline is applied under these reaction conditions, prolinate catalysis dominates: the reaction proceeds rapidly and with reversal of enantioselectivity. By analogy, the dicarboxylic acid catalyst (*R*,*R*)-**42** is expected to be deprotonated by DBU but the enhanced nucleophilicity expected is not apparent. The aldol reaction has an even weaker electrophile, and therefore the greater reaction rate in the presence of triethylamine is unlikely to be explained by the occurrence of prolinate catalysis. In the absence of DBU, (*R*,*R*)-**42** did not even generate traces of product – the most likely explanation for this is its poor solubility. Formation of small amounts of product in the presence of DBU could be due the action of non-deprotonated (*R*,*R*)-**42**, which is solubilised by DBU but has its concentration suppressed by the acid-base equilibrium.

5.5. Concluding Remarks

Overall, it has been demonstrated that in contrast to acids, basic additives can have a massive impact in the intermolecular proline-catalysed aldol reaction. These effects are not merely limited to altering the enantioselectivity but they can change the entire mechanism and outcome of the reaction. Further study will require the discovery of substrate combinations and base effects that are somewhat more stable. The next chapter will focus on an aldol reaction for which literature precedent suggested acidic additives could alter reactivity.

6. Hajos-Parrish-Eder-Sauer-Wiechert Reaction

6.1. Introduction

The HPESW reaction, introduced earlier, is the prototypical reaction in asymmetric enamine catalysis. As well as taking a central role in the history of organocatalysis, it remains a useful synthetic method to access the Wieland–Miescher ketone, which has found widespread use as an intermediate in the synthesis of a diverse range of complex molecules.[165]

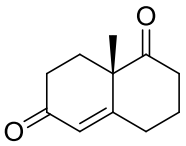


Figure 65: The Wieland–Miescher ketone accessible through the HPESW reaction.

Nevertheless, this reaction has certain limitations: high catalyst loading and lengthy reaction times are often required. In order to address these problems of catalyst efficiency, it is necessary to determine the rate-limiting step in the process. A study by Meyer, Houk, and co-workers attempted to resolve this question utilising the Singleton NMR method for revealing kinetic isotope effects.[166] The results of their investigation showed that ^{13}C enrichment only occurs at the acyclic carbonyl carbon of unreacted starting material after isolation from reactions taken to high conversion. The absence of enrichment at other positions – that are involved in other steps – suggests that the rate-limiting step precedes enamine formation. Strikingly, this contrasts with the intermolecular reaction, for which the rate-determining step is C-C bond formation, which occurs after enamine formation.[118]

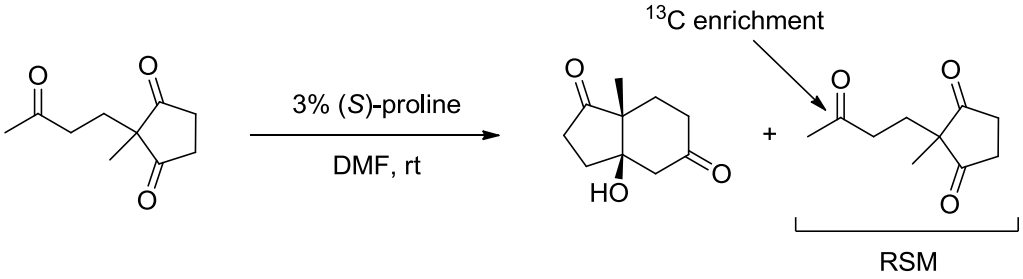
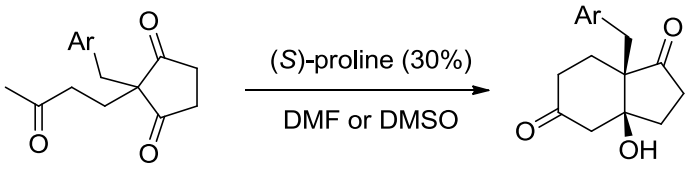


Figure 66: Singleton NMR experiment performed on the HPESW reaction by Meyer, Houk, and co-workers.

It has previously been shown in proline-catalysed reactions that the steps prior to C-C bond formation can be accelerated by acidic additives, as shown in the proline-catalysed amination reaction.[122] In addition, the stabilisation of transition states in all steps leading to enamine formation between acetaldehyde and dimethylamine by intrinsic involvement of methanol is supported computationally.[167] It was therefore of interest to us to investigate the possibly beneficial effect of acidic additives on the HPESW reaction.

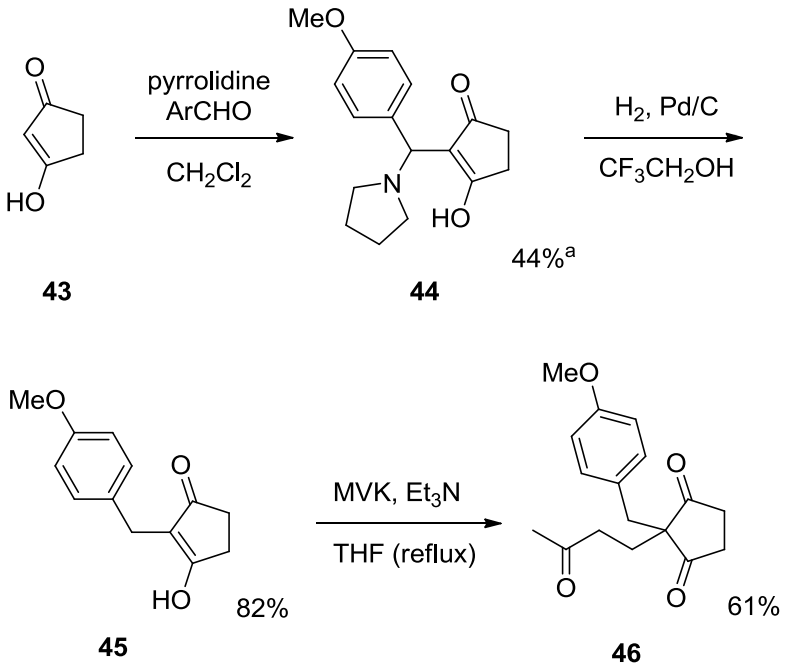
6.2. Model HPESW Reaction

As mentioned above, HPESW reactions are somewhat sluggish with many procedures reporting reaction times of 5–7 days. Owing to this, it was decided to study the reaction by sampling techniques rather than by performing *in situ* reaction measurements. It was desirable to analyse samples taken by chiral HPLC, since this would allow monitoring of not only product yield but also *ee* over the course of the reaction. However, the UV-detection method of the HPLC machine to be employed necessitated use of a substrate bearing a chromophore. Fortuitously, it has been reported that the reaction can be performed with aryl-substituted triketones[168] (Scheme 62) and such a compound with an appropriately UV-active aromatic substituent would be an ideal substrate for the model reaction.



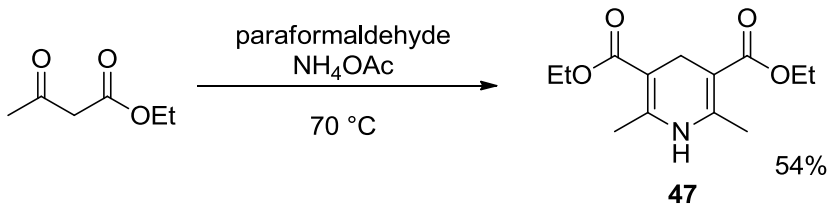
Scheme 62: HPSEW reaction of substrates with benzylic substituents reported by Brittain and co-workers.[168]

Following the method of Brittain and coworkers[168] the substrate required was synthesised in three steps. Firstly, Mannich base **44** was formed by reaction of 4-methoxybenzaldehyde with pyrrolidine and 3-hydroxycyclopent-2-enone (**43**). This was then converted to diketone **45** by palladium-catalysed hydrogenation and subsequently alkylated in Michael reaction with methyl vinyl ketone to yield the HPESW substrate, triketone **46**.

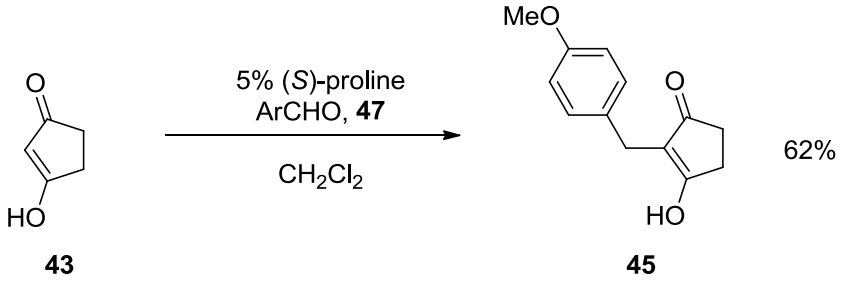


Scheme 63: Formation of triketone 46 from 3-hydroxycyclopent-2-enone (43) by the method of Brittain and coworkers;[168] a) 7% Mannich condensation product was formed, which could also be used in the next step.

It was later found that intermediate **46** could be prepared in greater overall yield by the method of Ramachary and Kishor in which 4-methoxybenzaldehyde undergoes one-pot Knoevenagel condensation/organocatalytic transfer hydrogenation, which had been reported for the synthesis of similar compounds.[169] The required Hantzsch dihydropyridine reducing agent (**47**) was synthesised by the method of Charette and co-workers (Scheme 64).[170]

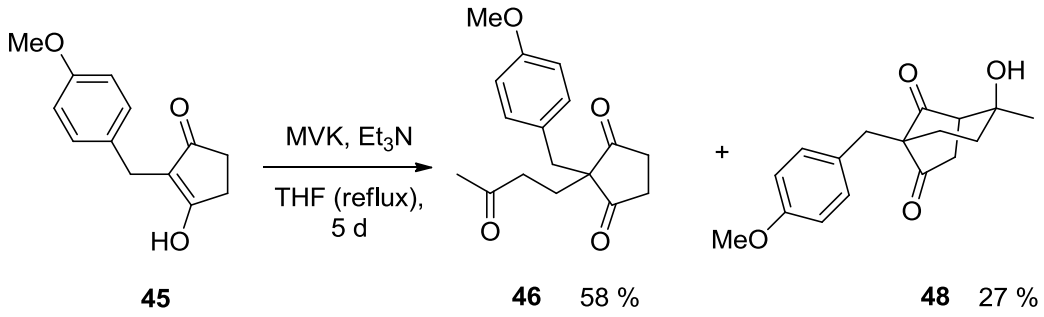


Scheme 64: Synthesis of Hantzsch dihydropyridine 47 by the method of Charette and co-workers.[170]



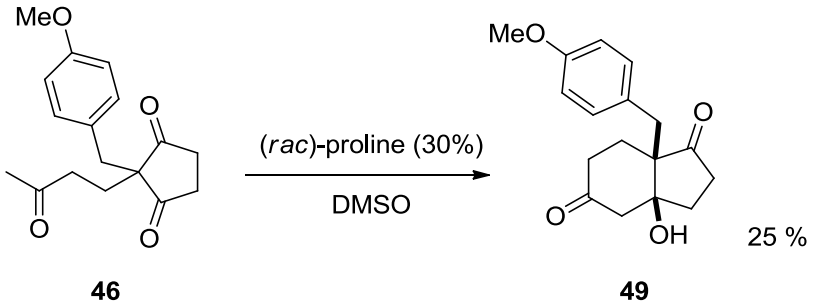
Scheme 65: Formation of 45 by the method of Ramachary and Kishor;[169] Ar = 4-MeOC$_6$H$_4$.

It was also found that in the final alkylation step, longer reaction time does not increase reaction yield, but instead formation of a by-product (**48**) resulting from cyclisation of the desired product occurs. The yield of triketone is similar to that obtained with shorter reaction times. This alkylation/cyclisation process is known to take place for 3-hydroxy-2-methyl-2-cyclopentene when high pressure is applied to the same reaction conditions.[171] Synthesis of an alternative substrate with a 4-nitro group in place of the 4-methoxy group of **46** was unsuccessful as the alkylation step with methyl vinyl ketone failed.



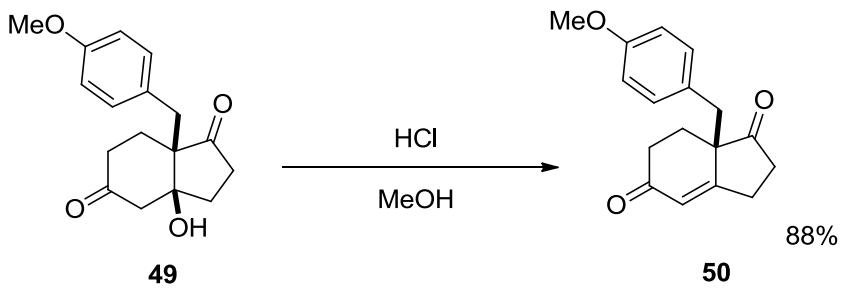
Scheme 66: Formation of cyclised by-product (48) observed with prolonged reaction times.

In order to monitor the HPESW reaction of the prepared triketone, an HPLC assay was devised so that periodically taken samples could be quantitatively analysed. A sample of the cyclised HPESW product **49** was prepared (Scheme 67) and with a chiral column, clean separation was achieved of the staring material, the enantiomers of the product, and benzonitrile (an internal standard).



Scheme 67: HPESW reaction of triketone 46 to prepare 49 for HPLC assay development.

Since the HPLC detection method employed is UV spectroscopy, response factors were determined relative to the internal standard to allow for calibration of HPLC data. Retention times and response factors were also determined for potential reaction by-products: hydroxyketone **48** and enone **50**, which was prepared by dehydration of **46** as shown in Scheme 68.

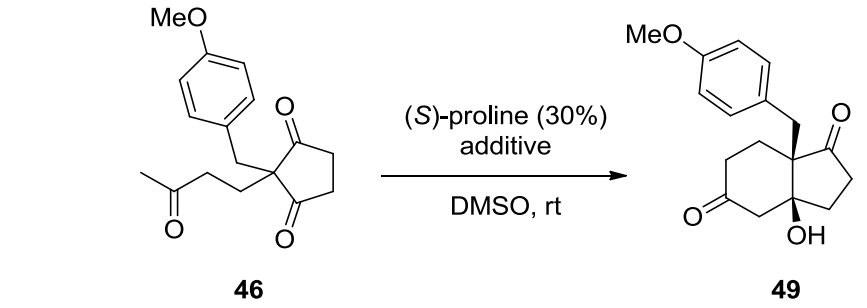


49 **50**

Scheme 68: Dehydration of HPESW product 49 to give enone 50.

6.3. Heterogeneous HPESW System

Preliminary testing was conducted with a 30% catalyst loading to show the viability of the model reaction and reaction monitoring system for this investigation. Under these conditions, it was found that the reaction proceeds to 40% yield over 6 hours. Addition of methanol in a 1% loading by volume resulted in a similar reaction profile, while addition of 1% acetic acid gave a slight increase in the reaction rate (Figure 67).



46 **49**

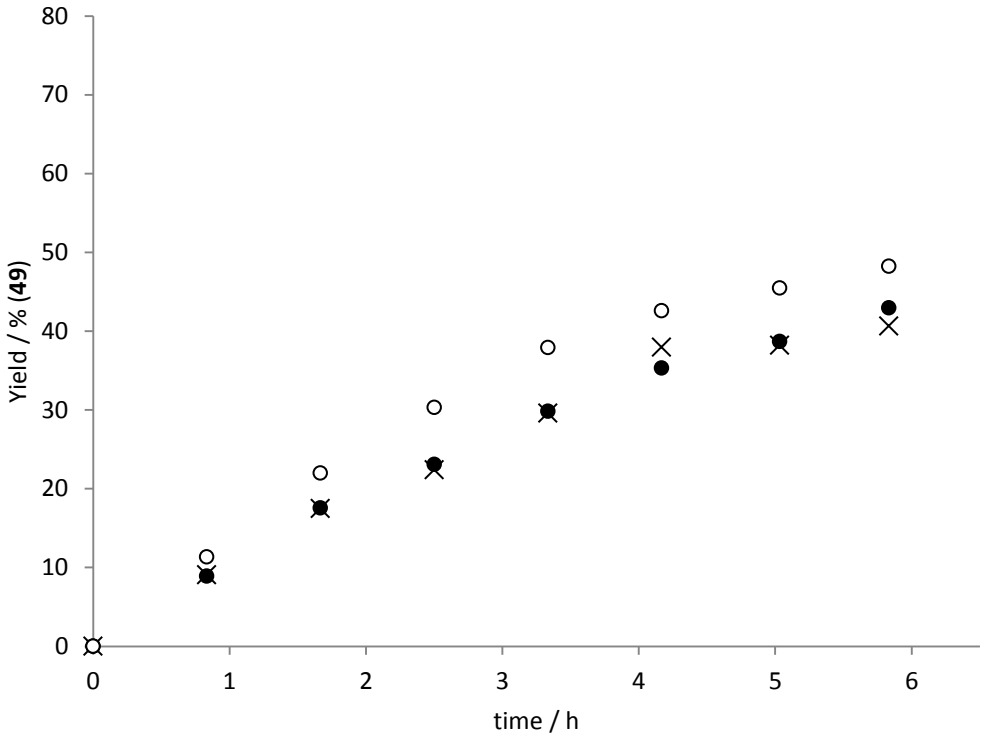
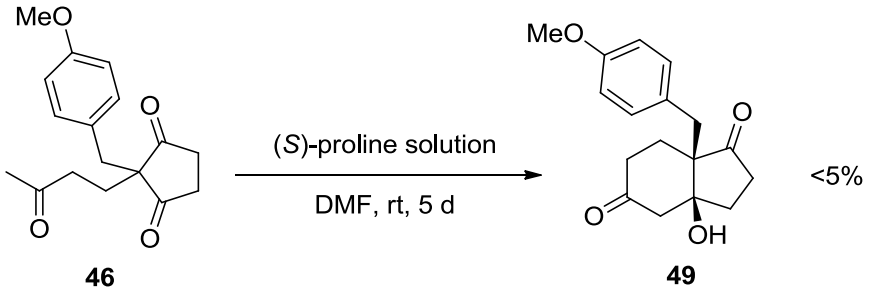


Figure 67: Proline-catalysed HPESW reaction of triketone 46 with no additive (crosses), 1 vol% MeOH added (black circles), 1 vol% AcOH added (white circles); Yield determined by sampling/HPLC analysis with respect to PhCN (I. S.).

However, in order to investigate whether any additive effects are intrinsically related to the reaction mechanism, it is desirable to work under fully homogeneous conditions so that solubility effects can be eliminated.

6.4. Proline Solutions

At first, an attempt was made to carry out the reaction using a solution of (*S*)-proline in DMF obtained as follows: proline was stirred in DMF for 20 minutes and after this time, the suspension was filtered. The reaction was initiated by adding this solution to the HPESW substrate (**46**). However, it was found that the proline solution-catalysed reaction was too slow to monitor.



Scheme 69: HPESW reaction carried out with (*S*)-proline solution in DMF; It was found that the reaction was too slow to be monitored in this way.

It was found that no increase in proline concentration could be achieved by grinding the catalyst. Stirring proline in DMF for 24 hours prior to filtration gave some improvement in the catalytic effectiveness of the proline solution, but the rate was still sluggish and we were concerned about the reproducibility of obtaining the solution over this time period. In addition, changing the reaction solvent for the study did not give any improvement. DMSO and acetonitrile proved similarly poor at dissolving proline, whereas when the reaction was performed in methanol many side-products were observed in the resulting HPLC analysis.

A solution to the solution problem was eventually found by employing solubilising agents: proline was stirred in a mixture of DMF and an additive for 20 minutes before filtering as before. The co-solvents tested for this purpose were acetic acid, trifluoroethanol (TFE), and methanol, and they were applied in a 1 vol% loading. It was found that the solutions thusly prepared were sufficiently concentrated to give a

reaction which could be monitored over a relatively short time period. The catalyst solutions prepared with different solubilising agents gave different rates when applied to the HPESW reaction; it was found that more acidic additives gave faster reactions.

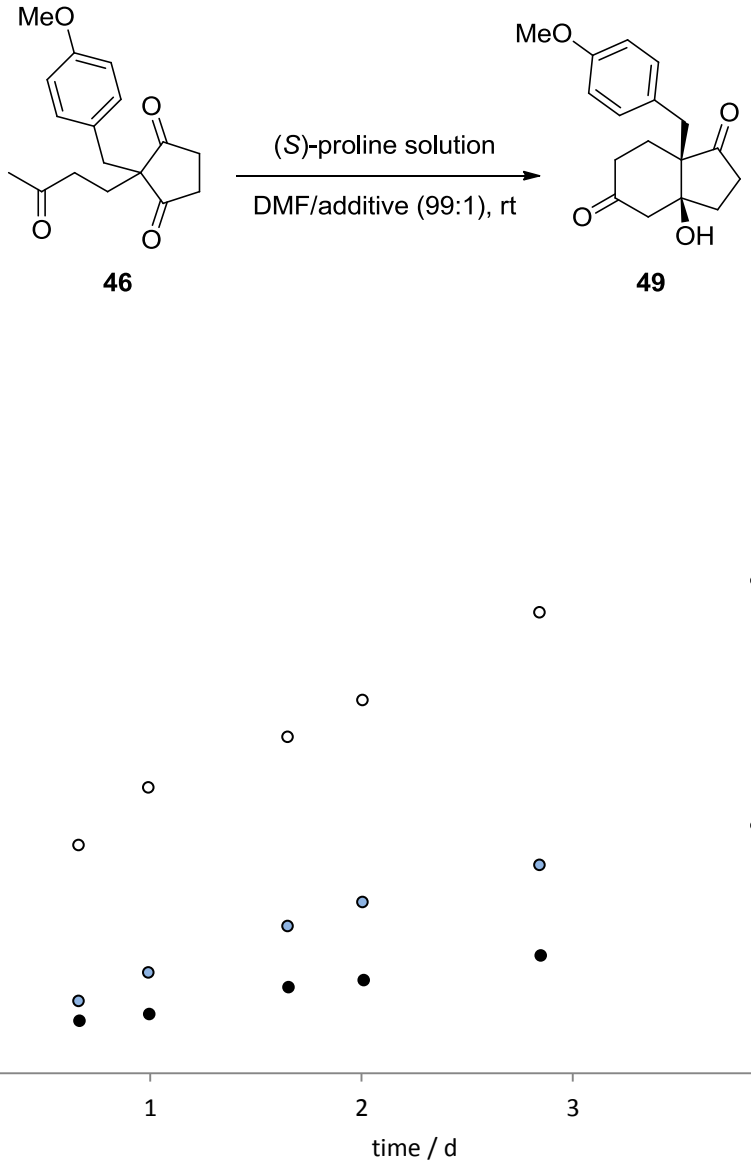
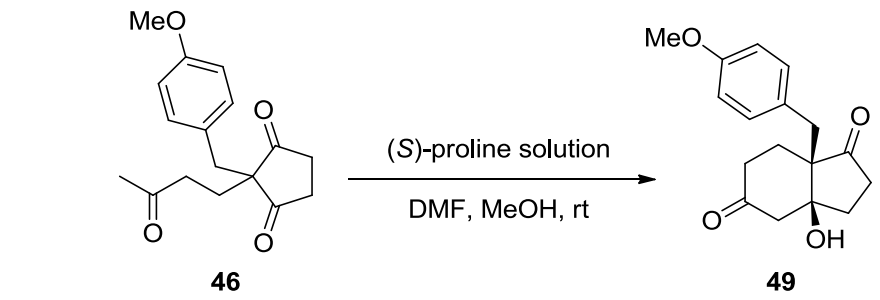


Figure 68: Proline-catalysed HPESW reaction of triketone 46 using a proline solution prepared in DMF/MeOH (black circles), DMF/TFE (blue circles), and DMF/AcOH (white circles); Solvent mixture = 99:1 DMF/additive; Yield determined by sampling/HPLC analysis with respect to PhCN (I. S.).

A solution prepared with 10 vol% methanol in DMF gave an even higher conversion over the same time period without the appearance of by-products previously observed

in pure methanol. Having established that such solutions were viable for performing the reaction monitoring experiment, additive effects not related to solubility were investigated. To achieve this, further quantities of additive were added to the saturated proline solution which had been prepared using that same additive as a solubilising agent; thus the total additive loading could be adjusted to greater values than the base-level of 1% by volume. These adjusted catalyst solutions were then applied to the reaction as before.

In the case of methanol it was found that increasing the additive loading above this base level had very little effect on the reaction rate. Reactions with loadings of 2–4% by volume all showed the same level of performance. When a much increased loading of 10 vol% was applied, the reaction rate in fact became suppressed. This could be due to the change in the macroscopic properties of the solvent system rather than any implicit molecular involvement of the cosolvent.



46 49

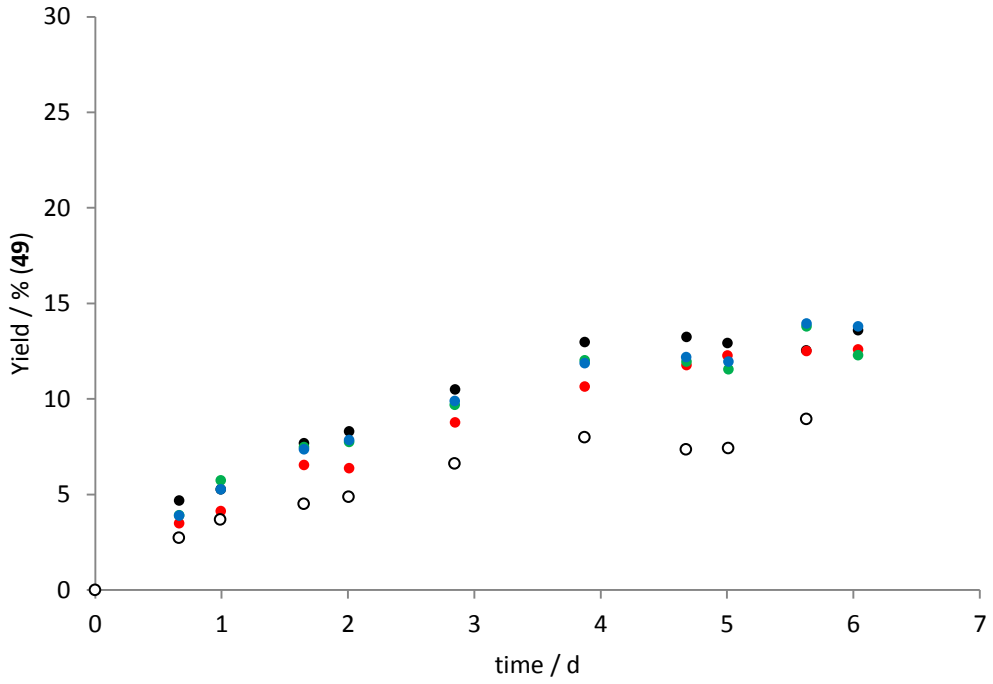


Figure 69: Proline-catalysed HPESW reaction of triketone 46 using a proline solution prepared in 99:1 DMF/MeOH with total MeOH loading of 1 vol% (black circles), 2 vol% (red circles), 3 vol% (green circles), 4 vol% (blue circles), 10 vol% (white circles); Yield determined by sampling/HPLC analysis with respect to PhCN (I. S.).

When the experiments were repeated with acetic acid as the additive, similar results were observed. In this case the drop in rate with increased additive loading was even more pronounced.

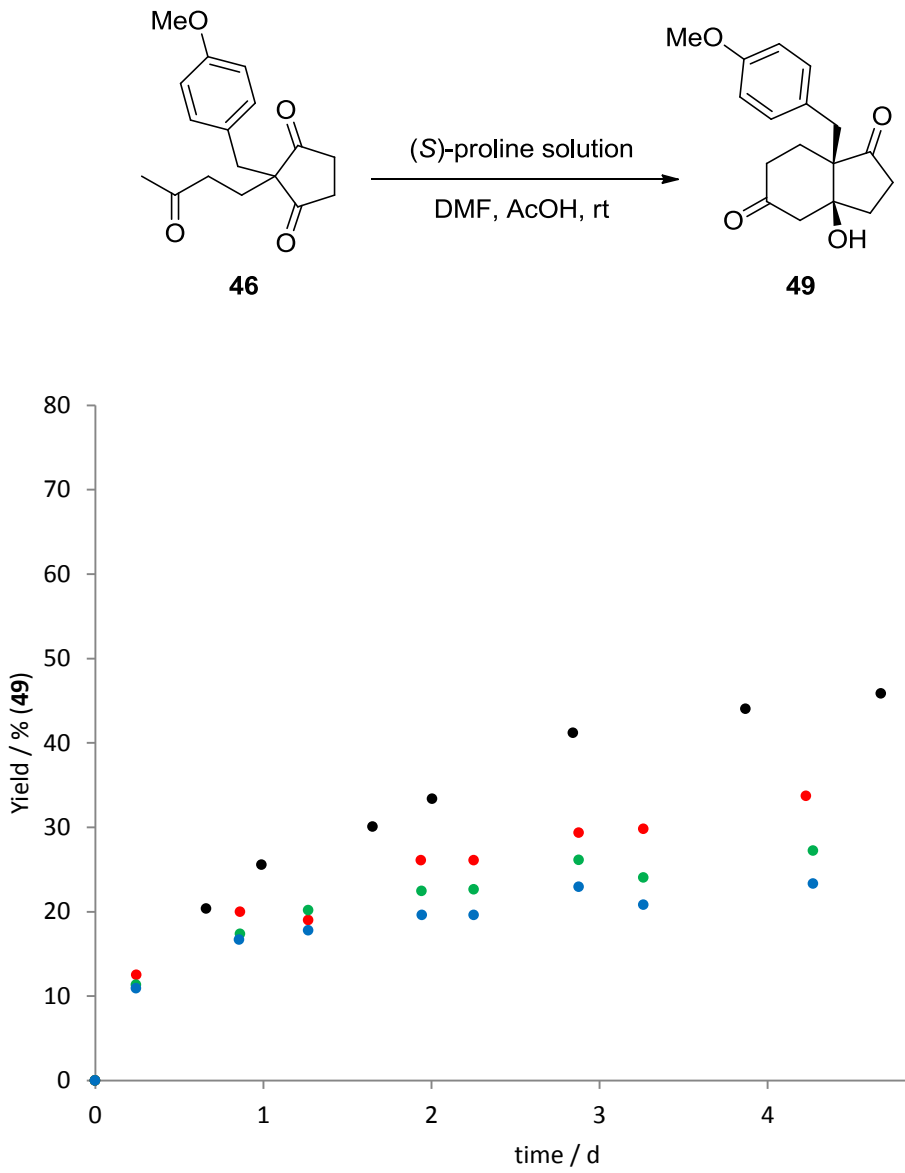


Figure 70: Proline-catalysed HPESW reaction of triketone 46 using a proline solution prepared in 99:1 DMF/AcOH with total AcOH loading of 1 vol% (black circles), 2 vol% (red circles), 3 vol% (green circles), 4 vol% (blue circles); Yield determined by sampling/HPLC analysis with respect to PhCN (I. S.).

Overall, the results show that increasing the loading of acidic additives above a base-level of 1 vol% does not increase the rate of the HPESW reaction. However, the experimental procedure fails to offer a comparison with the standard case in which no additive is present at all. This comparison could be obtained if an alternative catalyst – a proline analogue with greater solubility – is employed in the reaction.

6.5. Soluble Proline Analogues

The poor solubility of proline in organic solvents is a major limitation to its practicality. A screen of alternative catalysts[xv] was carried out for monitoring the HPESW reaction. As before, catalysts were stirred in DMF for 20 minutes and then filtered to generate a stock solution. In the screening process, reactions were monitored over 6 hours; while this time period was not expected to be sufficient for the observation of a complete reaction, it would reveal enough of the reaction profile to assess the suitability of the catalyst under investigation.

Two proline analogues with alternative Brønsted acid substituents were first assessed. Proline tetrazole **51** has become the most widely used analogue of this type since its introduction by the groups of Ley,[86] Saito and Yamamoto,[87] and Arvidsson.[88] Sulfonamide-containing proline analogues, such as **52**, were designed specifically to address the problem of proline solubility.[89] When applied to the HPESW reaction, these catalysts not only proved to be active, but the catalyst solutions were also more effective than the previously tested proline solution in DMF.

xv) Samples of catalysts used in this section were synthesised and generously donated by M. Klussmann and D. G. Blackmond.

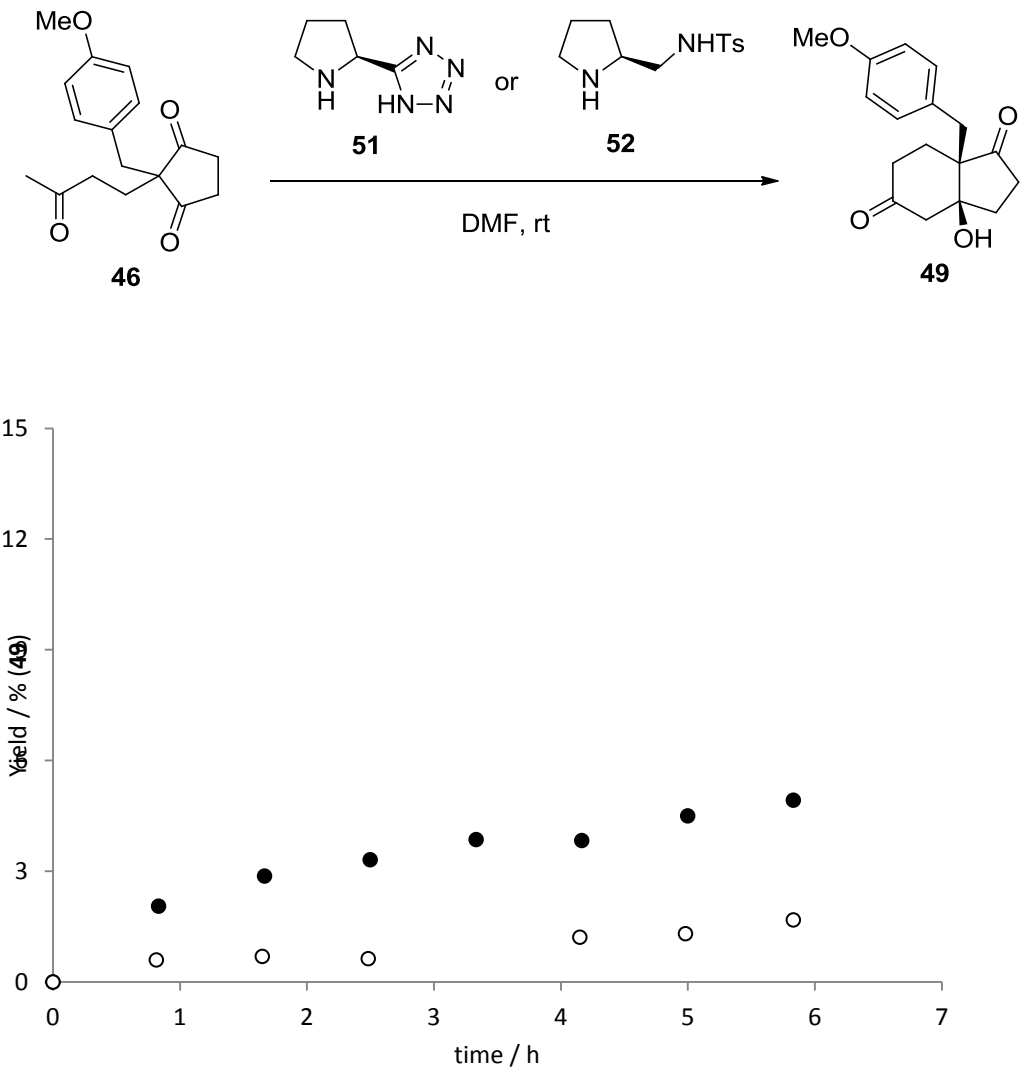
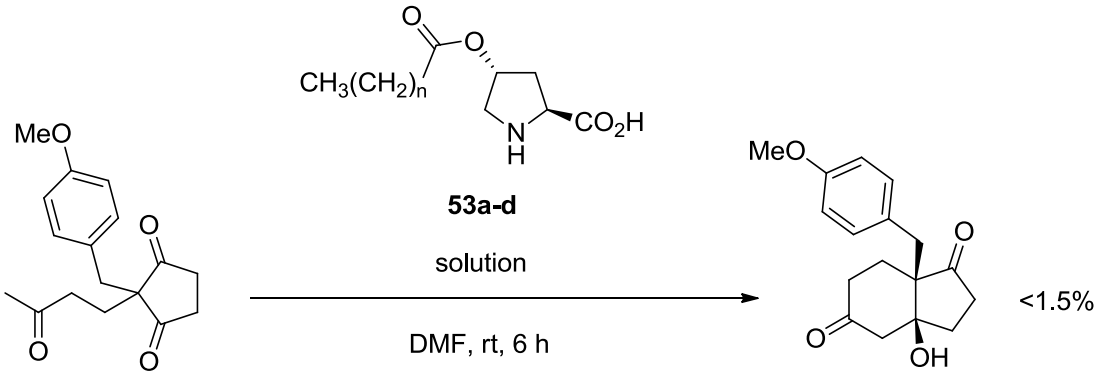


Figure 71: HPESW reaction of triketone 46 using a solution of catalyst 51 (black circles) or catalyst 52 (white circles); Yield determined by sampling/HPLC analysis with respect to PhCN (I. S.).

Next, catalysts were assessed that have an additional substituent on the pyrrolidine framework of proline to assist dissolution. Catalysts bearing linear aliphatic chains incorporated into the proline structure at the 4-position as part of an ester substituent showed promisingly increased solubility. However, solutions of these catalysts gave poor activity in the HPESW reaction (Scheme 70).



Scheme 70: HPESW reactions of triketone 46 using a solution of catalysts 53a (n = 3), 53b (n = 6), 53c (n = 10), 53d (n = 12).

Catalysts bearing a trialkylsiloxy substituent at the 4-position of proline were also specifically designed to give improved solubility compared with proline, and have been shown to have greater activity at lower loadings than proline in the aminoxylation and Mannich reactions.[172] This type of catalyst has since also been found to catalyse aldol reactions in water in excellent selectivity;[173] proline itself is not capable of doing this with enantioselectivity. Solutions prepared of two such catalysts proved to be the most effective tested: reactions with both TBS-hydroxyproline (**54**) and TIPS-hydroxyproline (**55**) exhibited significantly higher turnover than the other catalysts tested. The TIPS-substituted catalyst (**55**) was selected over the TBS-substituted catalyst (**54**) as the soluble proline analogue for further work because it gave better enantioselectivity (95% vs. 60% *ee*) and therefore appeared to be a closer match to proline (95% *ee*).

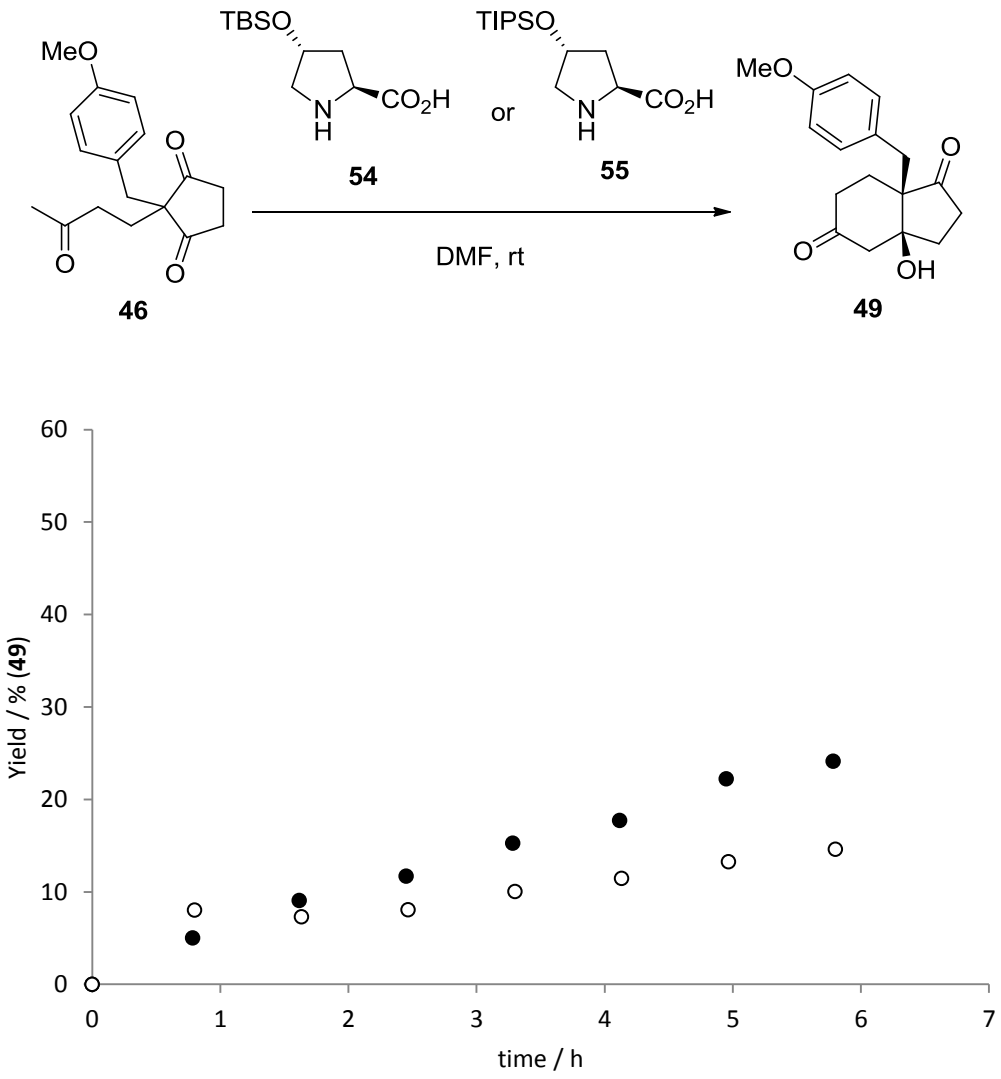
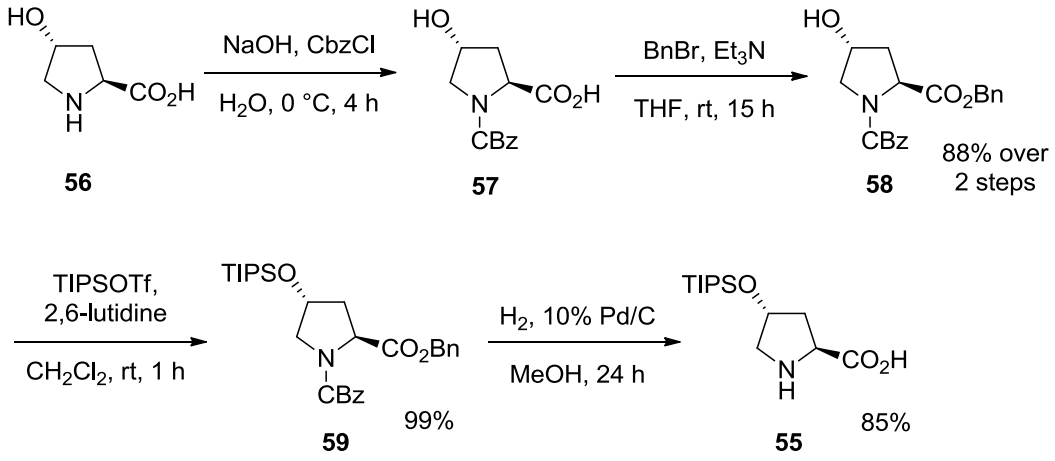


Figure 72: HPESW reactions of triketone 46 using a solution of catalyst 54 (black circles) or catalyst 55 (white circles); Yield determined by sampling/HPLC analysis with respect to PhCN (I. S.).

In order to undertake a full investigation of the HPESW reaction, a batch of catalyst **55** was synthesised according to the method of Hayashi and co-workers.[173] Two protecting groups were first installed onto (2*S*,4*R*)-4-hydroxyproline (**56**) by sequential conversion of the amino group to the benzyl carbamate and the acid group to the benzyl ester. The alcohol group of the doubly protected compound (**58**) was then silylated to furnish compound **59**, which was converted to the desired catalyst **55** by palladium-catalysed hydrogenolysis to remove the protecting groups.



Scheme 71: Synthesis of (triisopropyl)silyloxyproline catalyst (55).

The study of the HPESW reaction with this more soluble catalyst was then carried out in the same fashion as before. Stock catalyst solutions were prepared and directly applied to the reaction. Once again, additives were added prior to initiation of the reaction. Under these conditions, it was once more observed that methanol does not affect the rate of reaction.

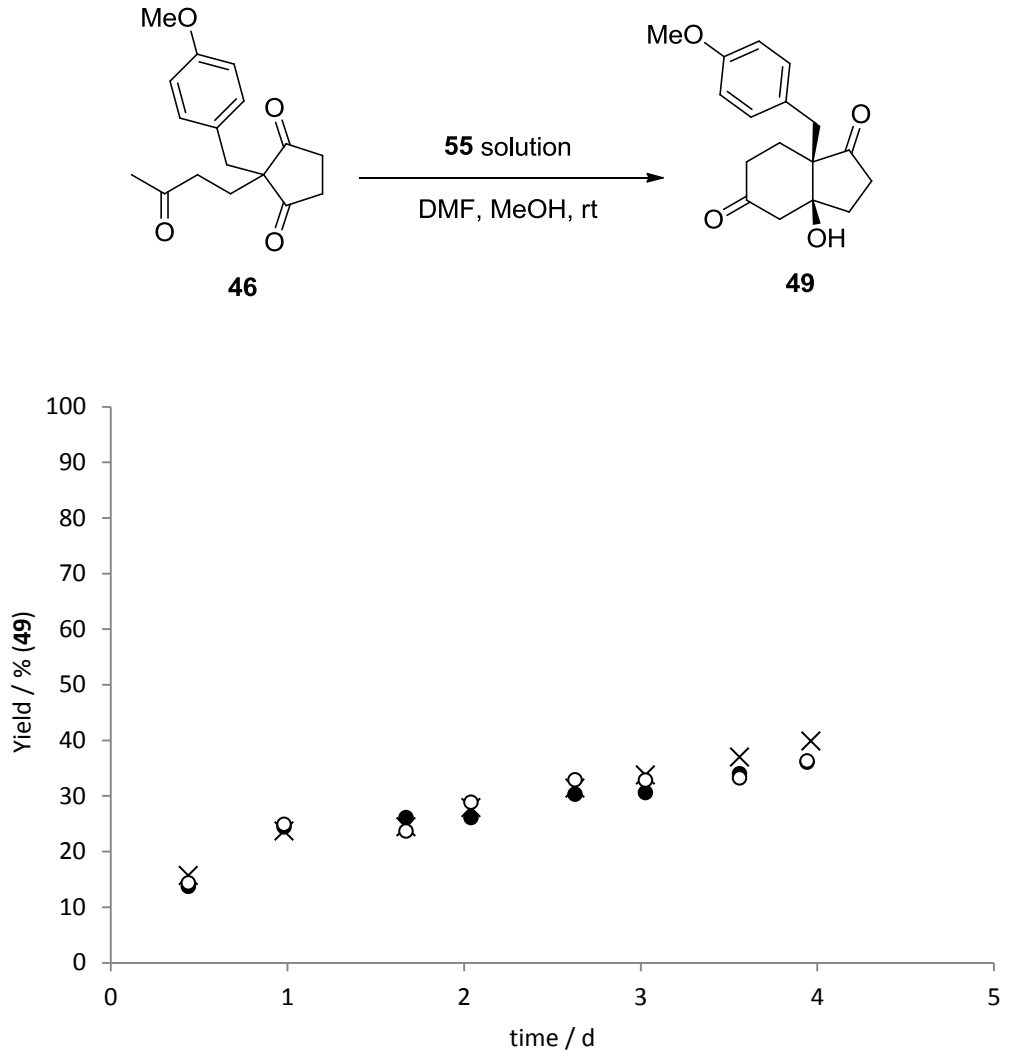


Figure 73: 55-catalysed HPESW reactions of triketone 46 using 55 solution in DMF with no additive (crosses), 1 vol% added MeOH (black circles), and 2 vol% added MeOH (white circles); Yield determined by sampling/HPLC analysis with respect to PhCN (I. S.).

Likewise with added acetic acid, the reaction profile was found to be unchanged (Figure 74). The results of these studies definitively show that acidic additives have no intrinsic effect on the rate of the 4-triisopropylsiloxyproline-catalysed HPESW reaction when solubility factors are excluded. By analogy, this of course strongly indicates that the same is true of the proline-catalysed process. This could be due to the incapability of the additives tested to influence the steps prior to enamine formation or because this step is in fact not rate-determining.

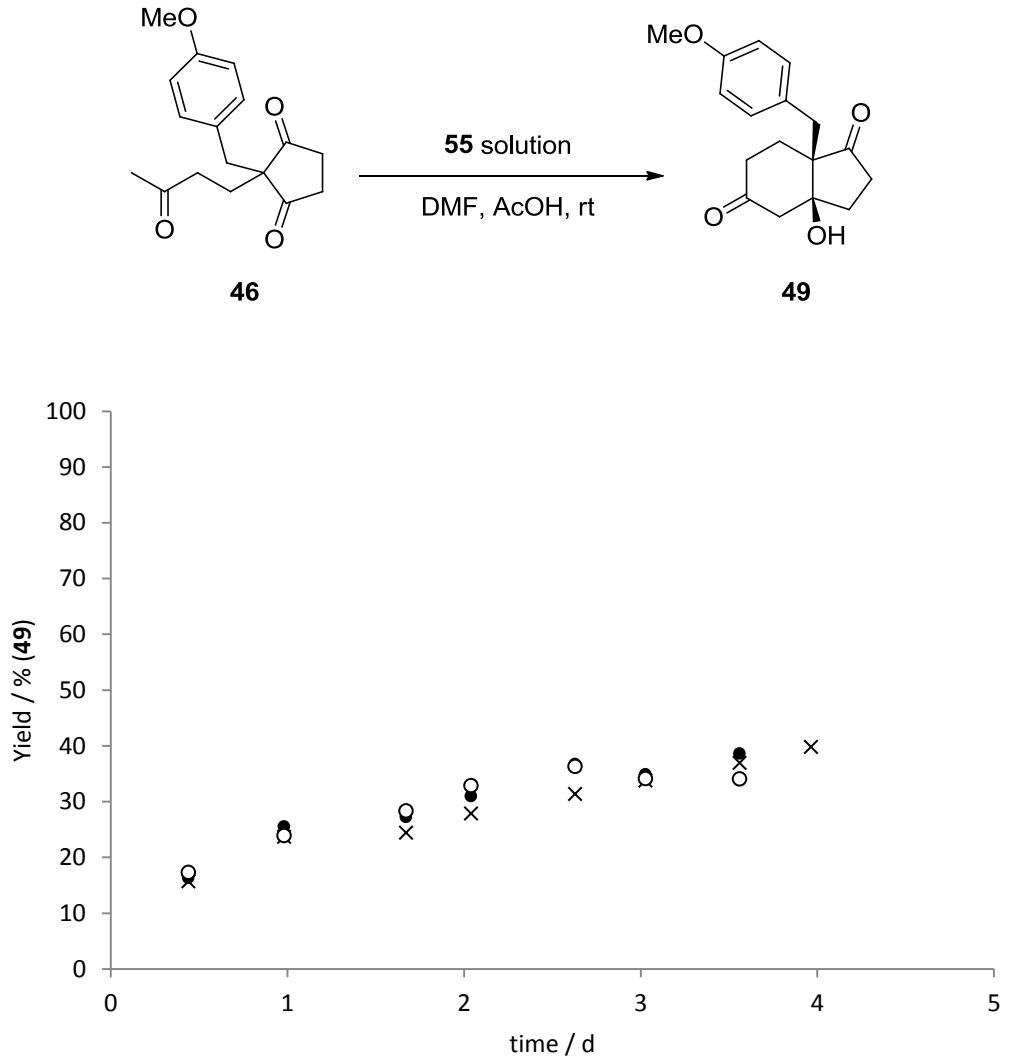


Figure 74: 55-catalysed HPESW reactions of triketone 46 using 55 solution in DMF with no additive (crosses), 1 vol% added AcOH (black circles), and 2 vol% added AcOH (white circles); Yield determined by sampling/HPLC analysis with respect to PhCN (I. S.).

6.6. Basic Additives

Another potential way to accelerate the steps that precede enamine formation is through the use of basic additives. Performing the HPESW reaction under heterogeneous conditions showed a large increase in reaction rate when triethylamine was added and a smaller increase in rate with added DBU.

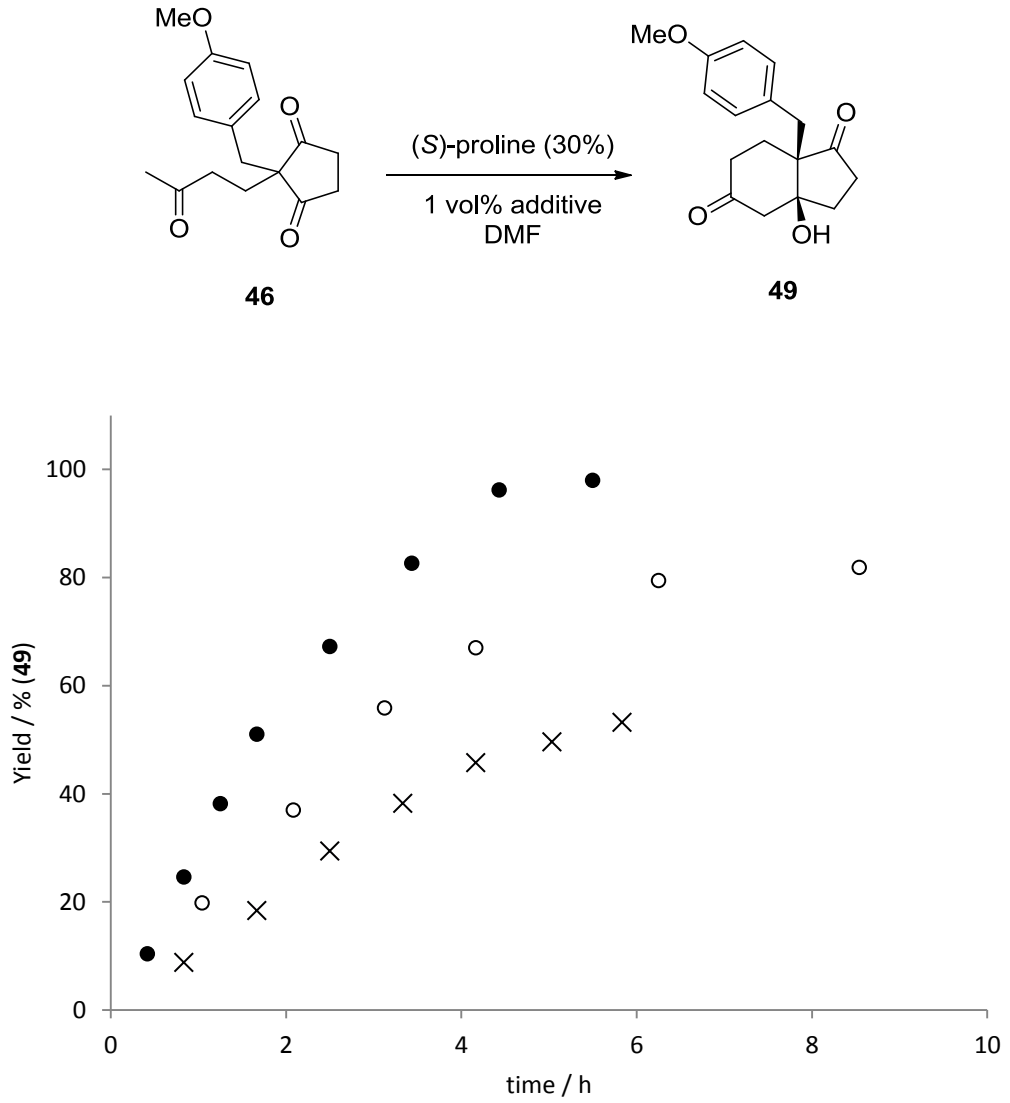


Figure 75: Proline-catalysed HPESW reactions of triketone 46 with no additive (crosses), 1 vol% Et_3N added (black circles), and 1 vol% DBU added (white circles); Yield determined by sampling/HPLC analysis with respect to PhCN (I. S.).

Although rate enhancement is observed, the enantioselectivity of the reaction is reduced with both catalysts from 95% with no additive to 84% in the presence of triethylamine and 26% in the presence of DBU; the same sense of enantioselectivity was still observed.

Again, solubility effects need to be excluded to determine if this rate enhancement has any intrinsic mechanistic basis, and solutions of the soluble proline analogue **55** were

employed once more to address this question. Under these conditions the rate enhancement with triethylamine is lost, with the reaction rate showing no discernible difference with or without the additive.

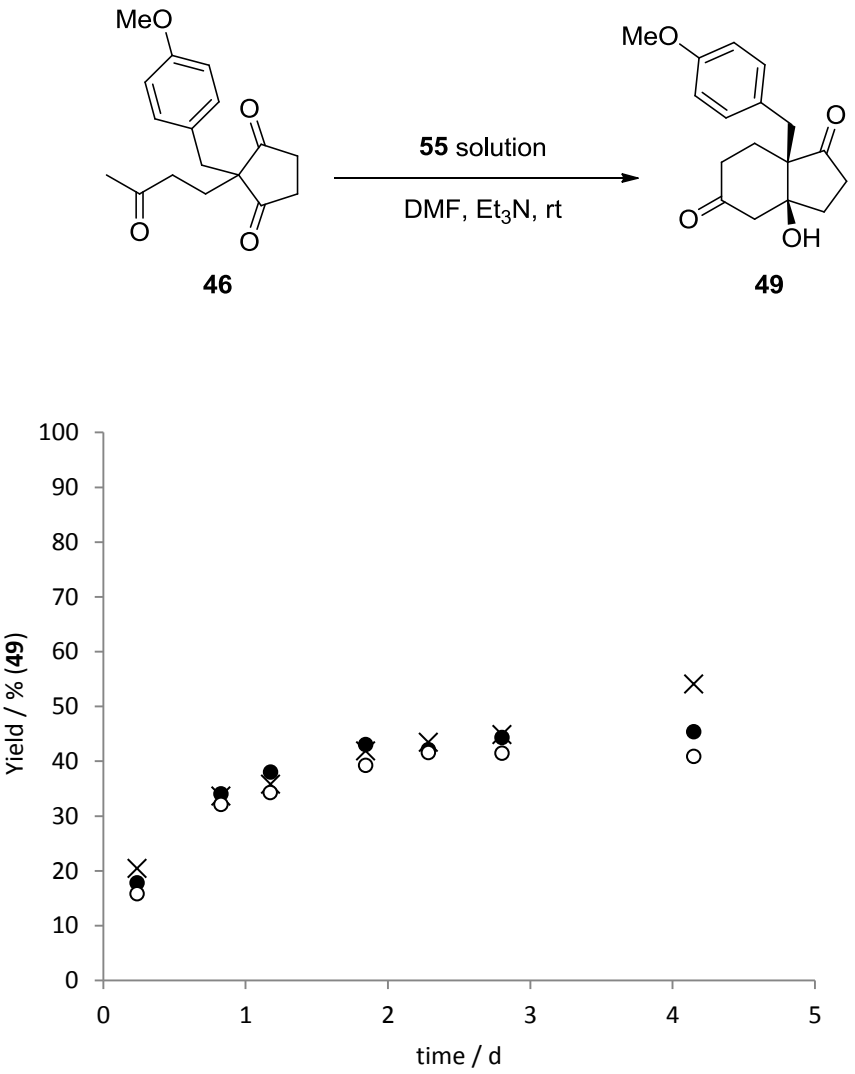
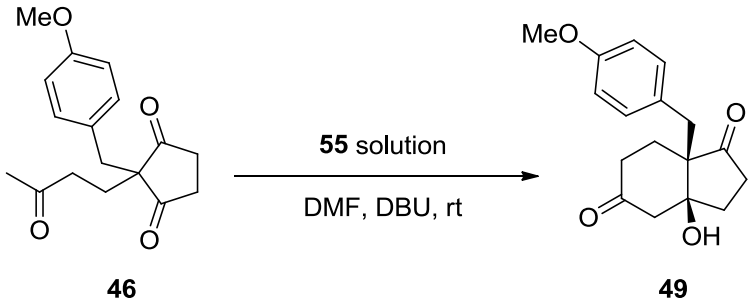


Figure 76: 55-catalysed HPESW reactions of triketone 46 using a solution of 55 in DMF with no additive (crosses), 1 vol% Et_3N added (black circles), and 2 vol% Et_3N added (white circles); Yield determined by sampling/HPLC analysis with respect to PhCN (I. S.).

The enantioselectivity was once more reduced from 95% with no additive, to 84% with 1 vol% added triethylamine, and to 77% with 2 vol%. This observation provides support for the rate-limiting step preceding C-C bond formation. Since this is the

enantiodetermining step, it is clearly affected by the additive and it would be unlikely that the reaction rate would be unaffected if this was also the rate-determining step.[xvi]

When the effect of DBU was reassessed using the fully homogeneous reaction system, a 0.5 vol% loading was sufficient to significantly suppress the reaction and with higher loadings only trace amounts of the product (**49**) were seen.



46 **49**

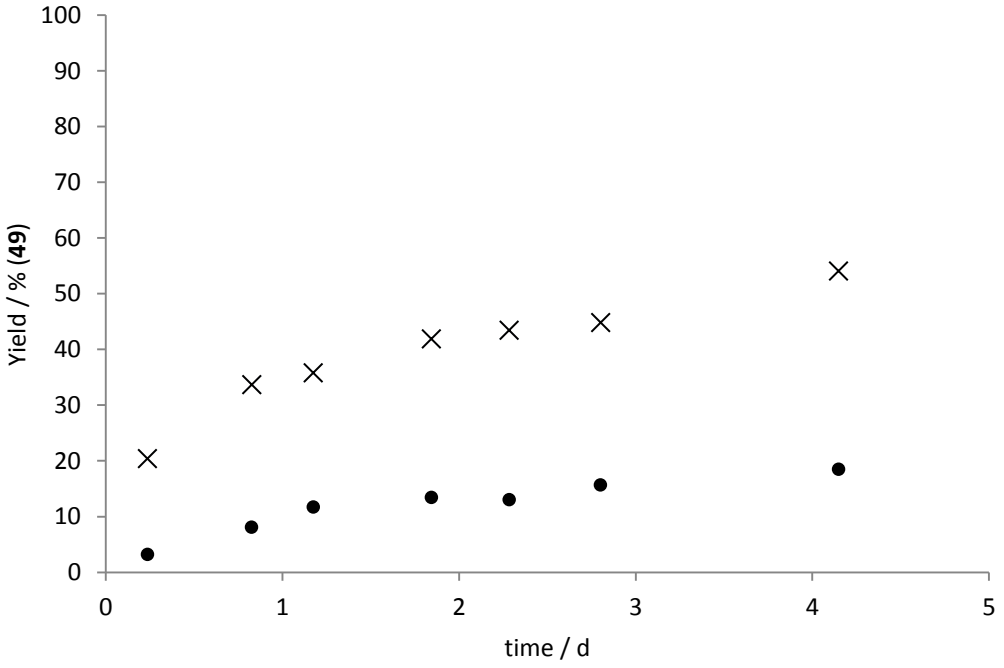
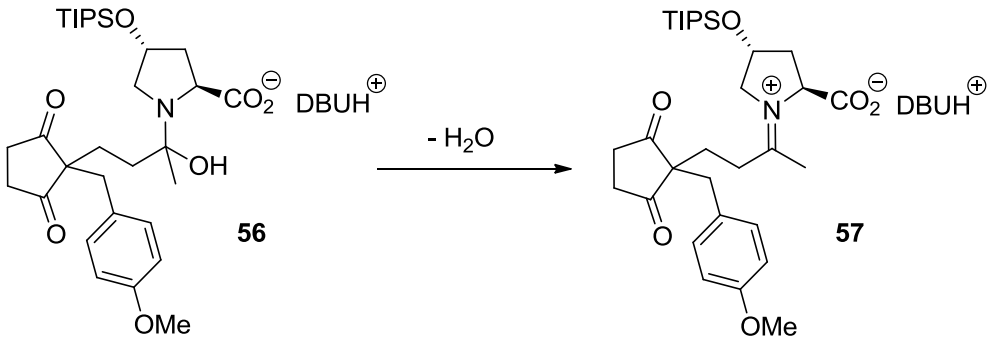


Figure 77: 55-catalysed HPESW reactions of triketone 46 using a solution of 55 in DMF with no additive (crosses), and 0.5 vol% DBU added (black circles); Yield determined by sampling/HPLC analysis with respect to PhCN (I. S.).

xvi) An alternative explanation for this reduced % *ee* in the presence of Et_3N is that C-C bond forming step could be reversible as in the prolinate-catalysed intermolecular aldol reaction.

A plausible cause of the lower yield would be loss of product due to DBU-mediated elimination to give enone **50**. However, peaks were not observed at the known retention time for this compound in the HPLC traces. If the rate-determining step precedes enamine formation, the most likely step that would be suppressed by a strong base such as DBU is the conversion of hemiaminal **56** to iminium **57** since this process requires a proton source to quench the nucleofuge (Scheme 72).



Scheme 72: Iminium formation step in the HPESW reaction; In the presence of a strong base, quenching of the nucleofuge to give water should be suppressed.

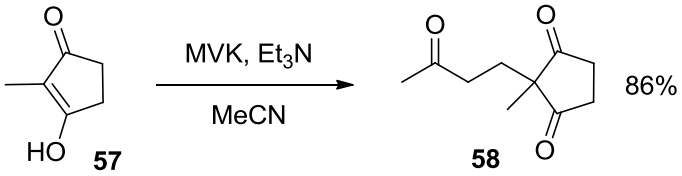
It should also be noted that in the presence of DBU, the catalyst will be deprotonated (as in the study of the amination reaction) and the catalyst may display different reactivity and correspondingly have a different rate-determining step compared with the proline-catalysed reaction.

If iminium formation is rate-determining, it is striking that protic additives do not increase the rate of reaction. Computational evidence suggests that the carboxylic acid of proline acts as an intramolecular acid for such processes[100] and it is a possibility that an additive acceleration cannot offer any further activation. Nevertheless, this would represent different reactivity compared with aldehydes for which enamine formation with proline is accelerated with acidic additives.[122]

Overall, the results with basic additives parallel the observations made for acidic additives, as basic additives are also incapable of increasing the rate of the process once solubility effects are eliminated.

6.7. NMR Experiments

It is also possible to monitor the HPESW reaction by ^{1}H NMR analysis. For the traditional substrate, the reaction can be monitored in the presence of an internal standard since the product peaks are clearly resolved. For the NMR spectroscopy experiments described below the standard methyl-substituted HPESW substrate **58** was synthesised by Michael reaction of cyclopentenone **57** with methyl vinyl ketone.



Scheme 73: Synthesis of triketone 58 by Michael reaction of cyclopentenone 57 with methyl vinyl ketone.

In the HPESW substrate there are four potential sites of enamine formation and it is possible that competition between these different sites affects the impact of additives. In the proline-catalysed reaction in DMSO or DMF only one product is observed, derived from the enamine at the terminal position. It is known, however, that with different enamine catalysts, alternative cyclisation products can be formed through enamine formation elsewhere.[85,174]

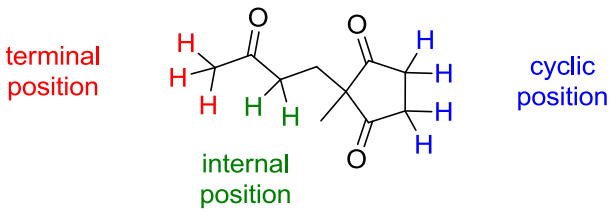
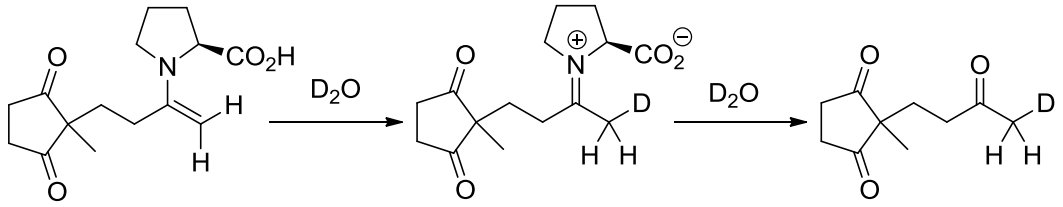


Figure 78: Sites for enamine formation in the standard HPESW substrate with enolisable protons highlighted.

Enamine formation at any of these positions could be detected through a deuterium labelling experiment. If the rate-determining step precedes C-C bond formation, any

enamine formation at the terminal position should be irreversible and result in product formation. Unproductive enamine formation in which the intermediate formed is converted back to the starting material would involve a protonation in the iminium-forming step and, in the presence of a deuteron source, deuteration would be expected.



Scheme 74: Mechanism for deuterium incorporation into unreacted enamine.

Following the previous observations that acidic additives have little effect on the proline-catalysed HPESW reaction, it was expected that it would be possible to carry out the reaction in the presence of D_2O which could act as the required deuteron source. To prove this, the reaction was monitored under these conditions by sampling and NMR analysis. As shown in Figure 79, the reaction proceeds efficiently under these conditions and is complete within 10 hours.

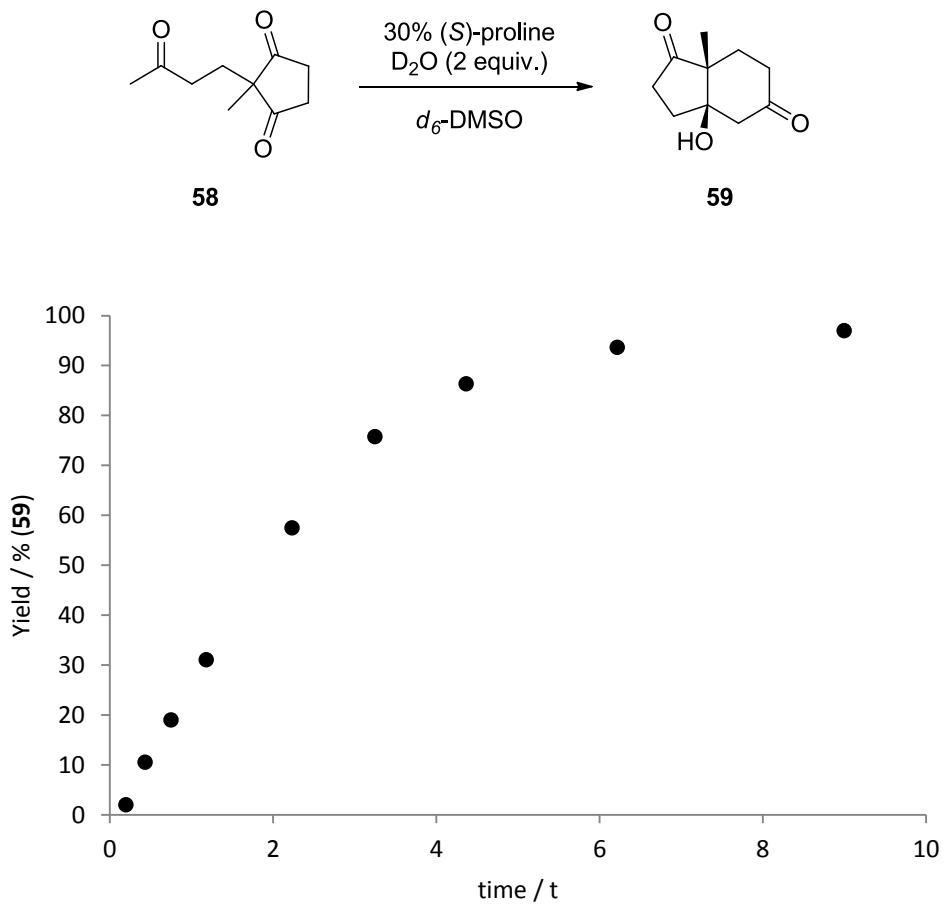


Figure 79: Proline-catalysed HPESW reaction of triketone 58, monitored by sampling / NMR analysis; Yield determined with respect to PhCN (I. S.).

Assessment of deuterium incorporation could not be directly made due to poor resolution of resonances associated with the starting material and product. Therefore in order to make this determination, the reaction was repeated and halted after 2.5 hours and the remaining starting material was recovered by chromatographic purification. According to the data shown in Figure 79, after this time around 50% conversion would have occurred. The level of deuterium incorporation in this recovered starting material was assessed by ^{1}H NMR using the resonance for the non-enolisable CH_3 group attached to the 5-ring as an internal standard. Surprisingly, it was found that deuterium is incorporated into the starting material at a level of 4.7% in the terminal position and 3.5% at the internal position.[xvii] This shows that unproductive

xvii) The ^{1}H NMR spectrum of the starting material that has not been subjected to these conditions shows no integration anomalies due to differences in spin relaxation.

enamine formation does indeed occur. A control experiment confirmed that this does not occur under these conditions in the absence of proline.

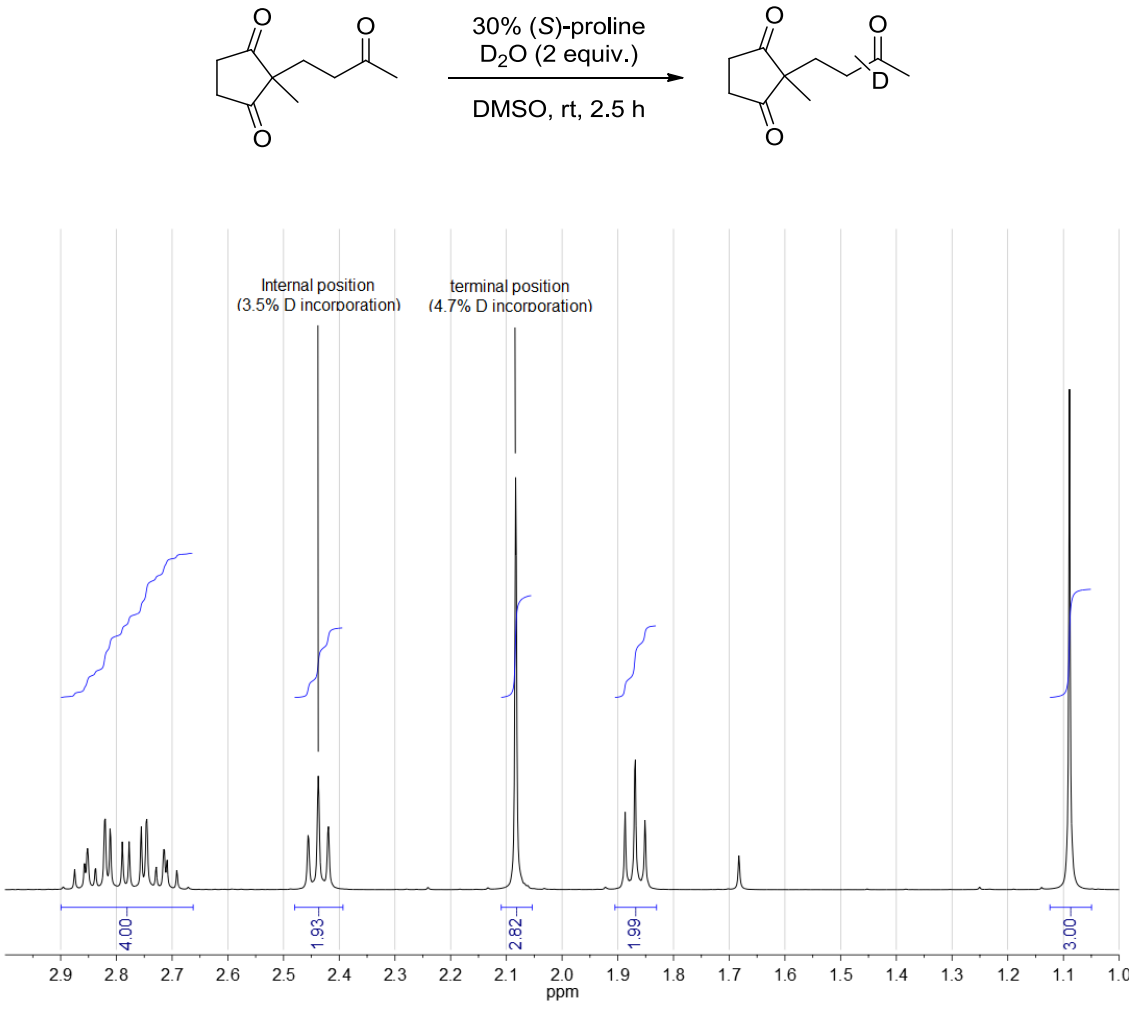


Figure 80: ^{1}H NMR spectrum of recovered starting material from a HPESW reaction performed in the presence of D_2O (2 equiv.).

In the proline-catalysed reaction, the only nucleophilic site in the HPESW substrate is the terminal position of the acyclic ketone group. This is the position that has shown to most readily undergo enamine formation, both productive and unproductive. An analogous compound to the nucleophilic fragment of triketone **58** is the linear ketone 2-pentanone. In 2-pentanone, all enamine formation in the presence of proline can be viewed as unproductive, since there is no internal electrophile as in substrates for the HPESW reaction. This compound therefore represents a control for the deuterium

incorporation experiment. The rate of deuterium incorporation at the terminal and internal positions of 2-pentanone was assessed by continuous ^{1}H NMR analysis (Figure 81).

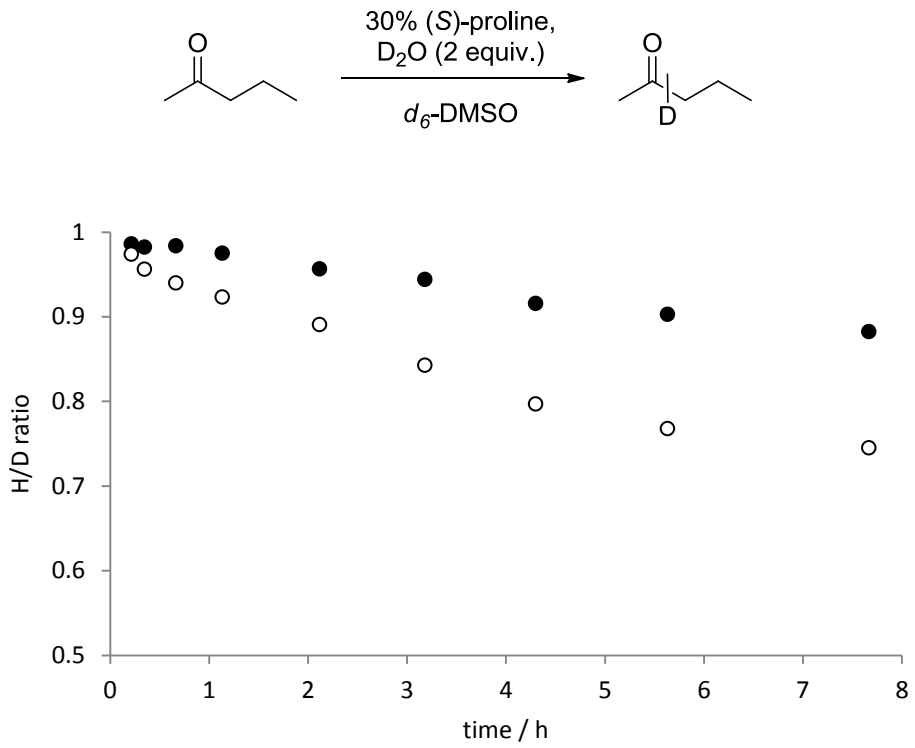


Figure 81: Proline-catalysed deuterium incorporation into 2-pentanone over time at the internal position (black circles) and terminal position (white circles); H/D ratio measured by ^{1}H NMR spectroscopy with respect to an internal standard (the non-enolisable CH_3 group).

Deuterium incorporation – and, hence, enamine formation – occurs more readily at the terminal position, whereas proline-catalysed transformations of ketones usually occur selectively at the internal position. This suggests that the internal enamine, while it is formed less readily, must generally be more reactive. Given this finding, it is surprising that the internal position is still favoured even with highly reactive electrophiles such as DEAD.[175]

The rate of deuterium incorporation into 2-pentanone matches the rate of the HPESW reaction reasonably well. After 8 hours, 26% deuterium incorporation into the terminal

position is observed. Deuterium incorporation of 33% would be synonymous with enamine formation having occurred on one equivalent of the ketone since there are three exchangeable protons. Therefore 26% deuterium incorporation is equivalent to 78% enamine formation. The yield in the HPESW reaction is slightly higher than this after 8 hours, but this can be attributed to inefficiencies of the deuteron quenching system.

Applying the same logic, the deuterium incorporation of 4.7% in the HPESW reaction corresponds to around 14% unproductive enamine formation. At this point in the HPESW reaction, around 50% conversion is expected, which can be described as productive enamine formation. The intramolecular aldol reaction is therefore faster than the reaction of the enamine with a deuteron from the reaction medium. The deuteration corresponds to the reverse of the enamine formation reaction that would occur upon protonation. Observation of even a small level of deuteration, however, shows that the rate-determining step is not rigidly defined in the reaction: if it was the case that rate was exclusively determined by a step prior to enamine formation it would be expected that no unproductive enamine formation would occur since the following aldolisation would occur too rapidly. If the rate-determining step was exclusively C-C bond formation, higher deuterium incorporation would be expected and the rate of the HPESW reaction would not be comparable to the deuteration rate for the analogue 2-pentanone.

6.8. Concluding Remarks

While additives can substantially change the rate of the HPESW reaction under heterogeneous conditions, these effects were found to be solely due to catalyst solubilisation. The findings of the NMR experiments, combined with the results of the study of additives effects, demonstrate that for the HPESW reaction the rate-determining step is not clearly defined. It remains to be determined whether additives are in fact capable of increasing the rate of the initial carbonyl functionalisation in enamine catalysis with ketone pronucleophiles.

Future investigations should be directed towards studying different transformations involving enamine catalysis with ketone pronucleophiles, to firstly identify the rate-determining step and then to apply additives as appropriate. The work presented in this chapter provides the methodology for deconvoluting solubilisation and intrinsic effects in such processes.

7. Summary of Novel Results

7.1. Amination Reaction

The reversal of enantioselectivity in the proline-catalysed amination with addition of DBU was confirmed and elaborated upon through investigation of the DBU to proline ratio.

The phenomenon was extended to a range of tertiary amines, phosphazenes, and alternative catalysts, and the dependence on additive basicity was confirmed by application of a range of isosteric guanidine bases. Through NMR titration experiments and kinetics studies, it was shown that the dependence on basicity arises due to the different degree to which basic additives can deprotonate proline.

It was found that group 1 prolinates catalyse the reaction in poor selectivity, however relatively high selectivity is observed on addition of the appropriate crown ether, which also massively increases the catalyst activity. Some examples of transition metal prolinates were also employed, which displayed proline-type selectivity.

Tetraalkyl ammonium and phosphonium counter cations were also found to give inverted enantioselectivity and it was found that while cation bulk influences the degree of selectivity, this could not be increased beyond a certain limit through structural changes.

A method for determining the steric influence of the substituents of a secondary amine organocatalyst was developed and demonstrated with a variety of prolinate catalysts.

7.2. Aldol Reaction

The DBU effect observed in the proline-catalysed amination reaction was extended to the intermolecular aldol reaction: again it was found that the additive switches the enantioselectivity of the reaction albeit with low absolute selectivity.

The combination of DBU and proline was also shown to racemise the formed aldol product. This occurs through a retroaldol process in which product enantiomers can reach equilibrium.

The product also suffers material loss, which is rationalised by the depletion of the aldehyde product of retroaldolisation known to occur in the presence of proline. Aldehyde depletion in turn leads to aldol product depletion because the two species are in equilibrium. It was shown that this can be suppressed with added water, and high yields can be obtained in the reaction under these wet conditions.

Following the observation of retroaldol reactivity, desymmetrising retroaldol of a tertiary keto alcohol was attempted with proline in the presence of DBU. While the catalyst was capable of effecting the transformation, no enantioenrichment was observed.

A proline analogue, dicarboxylic acid catalyst was synthesised and the reported base-induced rate enhancement was ascribed to catalyst solubilistion. It was found that the catalyst does not engage in prolinate-type catalysis.

7.3. HPESW Reaction

A model assay has been developed for monitoring the proline-catalysed HPESW reaction by sampling / HPLC analysis with a UV-active substrate. This allows simultaneous assessment of reaction kinetics and enantioselectivity.

Different methods were analysed for the formation of a catalytically active proline solution. Soluble proline analogues were assessed towards the same goal of achieving an active catalyst solution, and 4-siloxyproline structures were found to be effective. Through this work, it was possible to study the intrinsic role of additives in the HPESW reaction under homogeneous conditions with elimination of solubilisation effects.

It has been discovered that while acidic and basic additives can offer significant rate improvements in the HPESW reaction, this effect is due to increasing proline solubility rather than for an intrinsic mechanistic reason.

Through the results of this investigation, combined with a deuterium labelling study, it has been demonstrated that the rate determining-step of the HPESW reaction is not clearly defined.

8. Experimental

8.1. General Comments

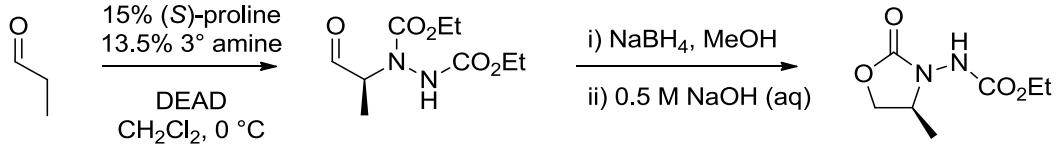
Reactions were performed with stirring, in oven-dried glassware, under argon unless otherwise stated. Dry solvents (CH_2Cl_2, toluene, MeOH, and THF) were obtained by filtration through activated drying columns. Anhydrous acetone, DMF, DMSO, MeCN were purchased and used without further purification. Bromine, 2-chlorobenzaldehyde, propanal, pyrrolidine, and triethylamine were freshly distilled prior to use. IR spectra were directly recorded on Perkin Elmer Spectrum 100 FT–IR spectrometer by means of a Universal ATR Sampling Accessory; selected peaks (ν_{max}) are reported (in units of cm^{-1}). ^1H NMR spectra were recorded at 400 MHz on Bruker AV400 instruments and chemical shifts (δ_H) are reported in ppm with respect to the residual solvent peak and assigned the qualifiers: s (singlet), d (doublet), t (triplet), q (quartet), m (multiplet), br (broad). Coupling constants (*J*) are reported in Hz to the nearest 0.1 Hz. ^{13}C NMR spectra were recorded at 100 MHz on Bruker AV400 instruments. Chemical shifts (δ_C) are reported in ppm referenced with respect to the residual solvent peak. Mass spectrometry was performed using ESI or CI on LCT Premier or AutospecQ instruments. GC analysis was performed using a VARIAN CP-3800 machine with FID detector and a Beta-Dextrin column (BETA DEXTM120, 60 M X 0.25 mm X 0.25 μm (SUPELCO)). HPLC analysis was either carried out on a HP Agilent 1100 Series or a modular JASCO instrument with 250 mm columns from the Daicel Chemical Industries Ltd. Reaction Calorimetry was performed using an Omnical Insight CPR220 reaction calorimeter with internal magnetic stirring. The system operates as a differential scanning calorimeter by comparing the heat released or consumed in a sample vessel compared with that from a reference compartment at intervals of 2–6 seconds over the course of the reaction. Melting points were obtained with a Reichert hot plate microscope and are uncorrected. Optical rotations were recorded on an Optical Activity polarimeter at 589 nm with a path length of 0.5 dm. Concentrations (c.) are quoted in units of g / 100 mL and specific rotations ($[\alpha]_D^{22}$) are quoted in units of 10^{-1} deg cm^2 g^{-1}.

8.2. Amination

8.2.1. Amination Reactions

In all cases a modified version of the method of Jørgensen and co-workers was used.[11]

Proline-Catalysed Reaction in the Presence of Tertiary Amines



12 13

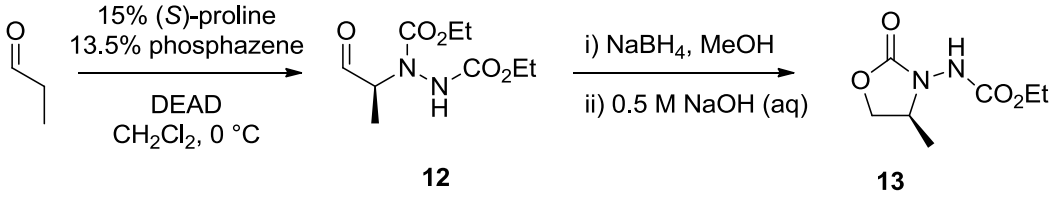
A mixture of (*S*)-Proline (32.9 mg, 0.286 mmol) and the required tertiary amine (0.257 mmol) was stirred in CH_2Cl_2 (5 mL) at 0 °C for 30 min. To this solution was added DEAD (300 µL, 1.91 mmol) then propanal (412 µL, 5.71 mmol) and the reaction mixture was stirred until the orange colouration due to the presence of DEAD no longer persisted (1-2 hours). Methanol (5 mL) was added, then $NaBH_4$ (289 mg, 7.64 mmol) was added portionwise, and the suspension was stirred. After 30 min, 0.5 M NaOH (aq) (7.5 mL) was added and the heterogeneous mixture was stirred vigorously for 15 hours. The organic and aqueous phases were separated, the aqueous phase was extracted with EtOAc (2×10 mL), and the combined organics were dried (Na_2SO_4), filtered, and evaporated under reduced pressure. The crude product was then purified by flash column chromatography (50% EtOAc in *n*-hexane) and enantiopurity was determined by chiral GC analysis. ν_{max} (ATR) 3558, 3289, 2984, 2938, 1770, 1715, 1513, 1220, 1051; δ_H 7.15 (1H, s, NH), 4.47 (1H, t, *J* = 8.3), 4.18 (2H, q, *J* = 7.1), 4.08 (1H, s), 3.88 (1H, t, *J* = 8.3), 1.27 (3H, d, *J* = 7.1), 1.25 (3H, t, *J* = 7.1). δc (100 MHz, $CDCl_3$) 157.6, 155.7, 68.7, 62.5, 52.9, 16.9, 14.3. These data are consistent with literature values.[11]

NMR yields of the non-isolated aldehyde product were determined by performing the reaction with a known amount of benzonitrile present (as an internal standard). After

consumption of DEAD and prior to derivatisation, a sample of the reaction mixture was taken (ca. 100 μL), dissolved in $CDCl_3$ (800 μL), and analysed by ^1H NMR spectroscopy; the yield was then determined by comparison of the aldehyde resonance of the product with the resonances corresponding to the internal standard.

GC Conditions (VARIAN CP-3800, FID detector, He flow rate = 3.0 mL/min, Column = BETA DEXTM120, 60 M X 0.25 mm X 0.25 μm (SUPELCO), Column temperature = 158 °C to 178 °C increasing rate = 0.3 °C/min, hold at 178 °C for 3 min, 178 to 210 increasing rate = 10 °C/min, Detector temperature = 50 °C, Injector temperature = 50 °C): t_R 61.0 (*R*-oxazolidinone product), 62.0 (*S*-oxazolidinone product).

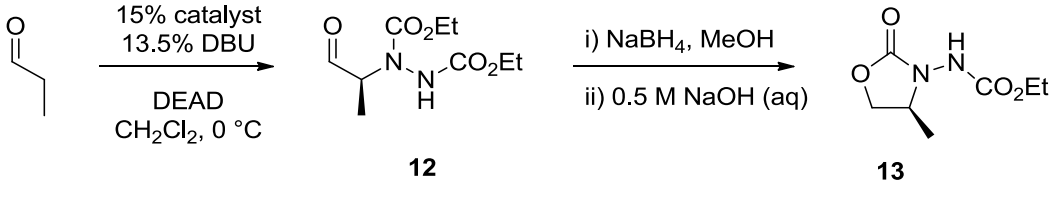
Proline-Catalysed Reaction in the Presence of Phosphazenes



12 **13**

The same procedure used for the reaction in the presence of tertiary amines was followed with the tertiary amine replaced by the appropriate phosphazene base.

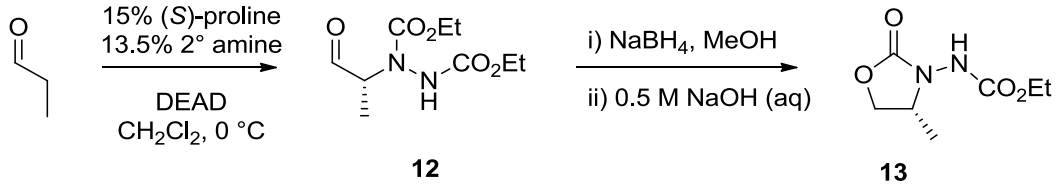
Reactions Catalysed by Proline Analogues in the Presence of DBU



12 **13**

The same procedure used for the proline-catalysed reaction in the presence of tertiary amines was followed with proline replaced by the required catalyst (0.286 mmol) and DBU (38.5 μL, 0.257 mmol) employed as the tertiary amine.

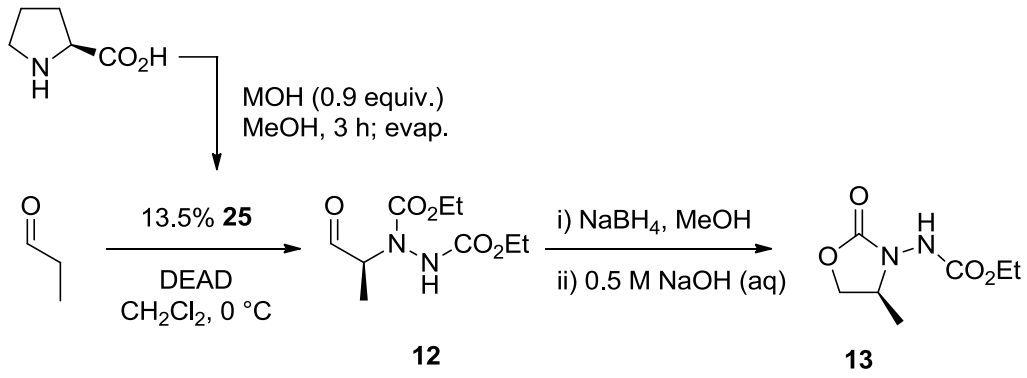
Proline-Catalysed Reaction in the Presence of Secondary Amines



12 **13**

The same procedure used for the reaction in the presence of tertiary amines was followed with the tertiary amine replaced by the required secondary amine (0.257 mmol).

Prolinate-Catalysed Reactions (Prolinates Generated from Hydroxide Salts)

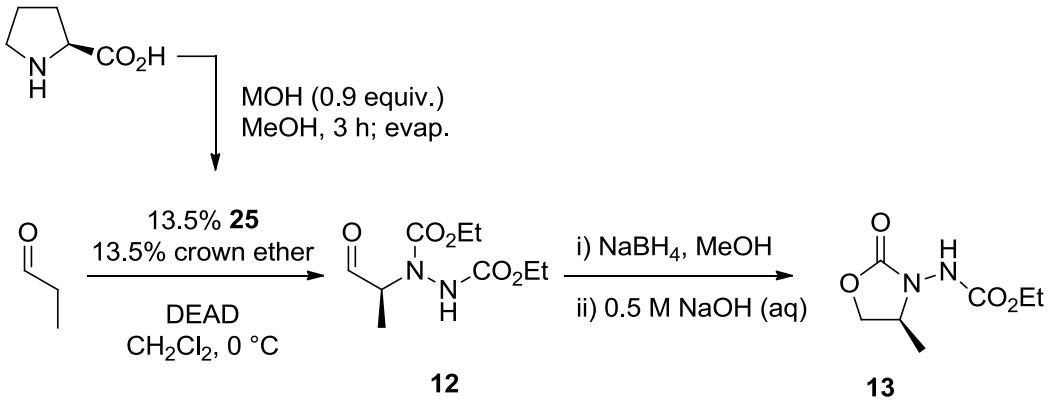


12 **13**

To a stirred solution of (*S*)-proline (32.9 mg, 0.286 mmol) in methanol (5 mL) at 0 °C was added the required metal hydroxide (0.257 mmol) portionwise. The mixture was stirred for 3 h and then evaporated under reduced pressure. Next, CH_2Cl_2 (5 mL) was added and the solution was cooled at 0 °C for 30 minutes. To this solution was added DEAD (300 µL, 1.91 mmol) then propanal (412 µL, 5.71 mmol) and the reaction mixture was stirred until the orange colouration due to the presence of DEAD no longer persisted (1-2 hours). Methanol (5 mL) was added, then $NaBH_4$ (289 mg, 7.64 mmol) was added portionwise, and the suspension was stirred. After 30 min, 0.5 M NaOH (aq) (7.5 mL) was added and the heterogeneous mixture was stirred vigorously for 15 hours. The organic and aqueous phases were separated, the aqueous phase was extracted with EtOAc (2×10 mL), and the combined organics were dried (Na_2SO_4),

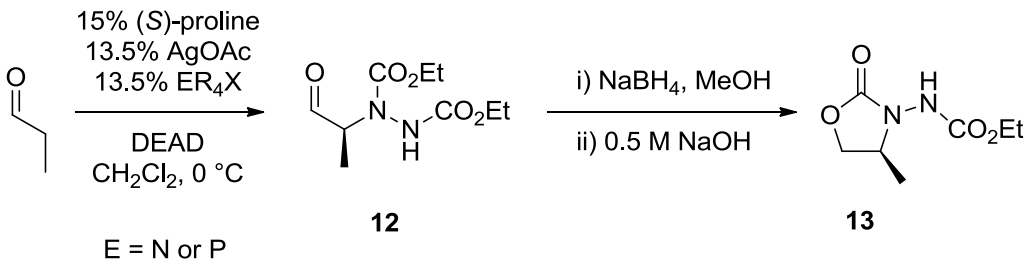
filtered, evaporated under reduced pressure. The crude product was then purified by flash column chromatography (50% EtOAc in *n*-hexane) and enantiopurity was determined by chiral GC analysis.

Prolinate-Catalysed Reactions in the Presence of Crown Ethers



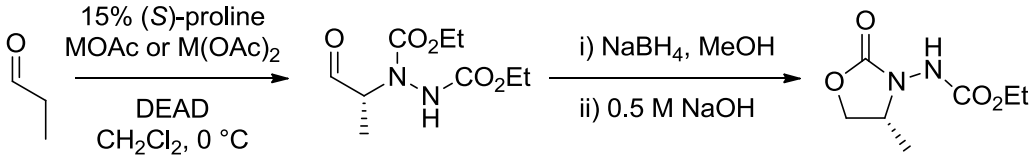
The same procedure used for the prolinate-catalysed reaction with prolinates generated from hydroxides salts was followed with the required crown ether (0.257 mmol) added along with the CH_2Cl_2 prior to the 30 minute cooling and equilibration period.

Prolinate-Catalysed Reactions (Prolinates Generated From AgOAc and Halide Salts)



The same procedure used for the reaction in the presence of tertiary amines was followed with the tertiary amine replaced by AgOAc (42.8 mg, 0.257 mmol) and the required halide salt (0.257 mmol).

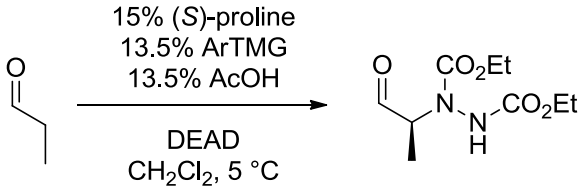
Prolinate-Catalysed Reactions (Prolinates Generated From Acetate Salts)



12 **13**

The same procedure used for the reaction in the presence of tertiary amines was followed with the tertiary amine replaced by the required acetate salt.

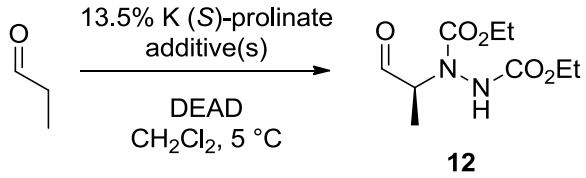
Guanidinium Prolinate-Catalysed Reactions Monitored by RC



12

Into a reaction calorimeter vial, a solution of (*S*)-proline (36.8 mg, 0.320 mmol), ArTMG (0.288 mmol), AcOH (16.5 μL, 0.288 mmol) was prepared in sufficient CH_2Cl_2 to make the total reaction volume 5.00 mL after addition of propanal and DEAD. The vial was placed in the RC adiabatic chamber, set at 5 °C, and allowed to stir. Two syringes were separately charged with DEAD (630 μL, 4.00 mmol) and propanal (397 μL, 5.50 mmol), then placed in the ports above the reaction vial and allowed to cool to 5 °C. Once a clear baseline had been obtained in the monitored heat flow, the DEAD and propanal was simultaneously added and the reaction heat flow data was collected (by the computer). Once the reaction had finished and a baseline had become re-established, the RC heat switch was engaged for 15 minutes to allow for the τ correction.

Potassium Prolinate-Catalysed Reactions Monitored by RC

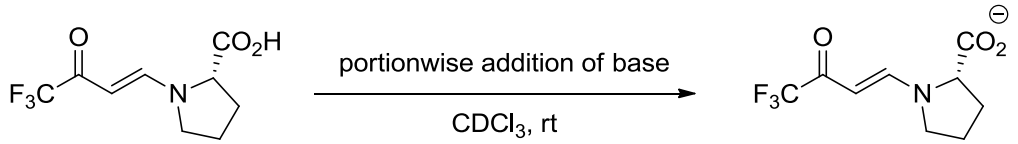


12

A solution of solution of (*S*)-proline (32.9 mg, 0.286 mmol) in methanol (5 mL) was prepared in a reaction calorimeter vial. To the mixture was added KOH (14.4 mg, 0.257 mmol) and after stirring for 3 hours, the solvent was evaporated under reduced pressure. 18-crown-6 (75.5 mg, 0.286 mmol) and / or AcOH (14.7 μL, 0.257 mmol) were added where required along with CH_2Cl_2 (5 mL) and the vial was placed in the RC adiabatic chamber, set at 5 °C, and allowed to stir. Two syringes were separately charged with DEAD (300 μL, 1.91 mmol) and propanal (412 μL, 5.71 mmol), then placed in the ports above the reaction vial and allowed to cool to 5 °C. Once a clear baseline had been obtained in the monitored heat flow, the DEAD and propanal was simultaneously added and the reaction heat flow data was collected (by the computer). Once the reaction had finished and a baseline had become re-established, the RC heat switch was engaged for 15 minutes to allow for the τ correction.

8.2.2. NMR Experiments

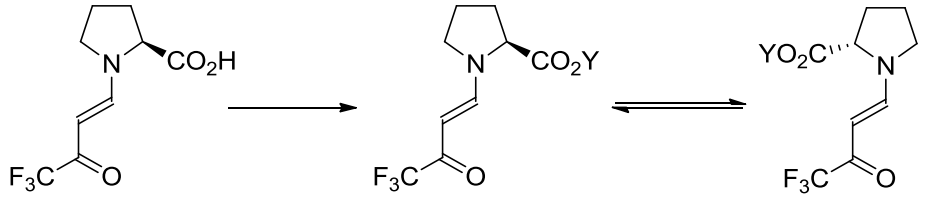
Titration Experiments Employing Enaminone 22[144]



Two solutions were prepared volumetrically, a 0.200 M solution of **22** in $CDCl_3$ and a 0.800 M solution of the required base in $CDCl_3$. Enaminone solution (800 μL, 0.160 mmol) was accurately transferred into an NMR tube and ^1H NMR analysis was

performed on the sample. After this, a sample of the base solution (40.0 μL, 0.0320 mmol) was added to the NMR tube, which was sealed and inverted and ^{1}H NMR analysis was once more performed. Samples of the base solution (40.0 μL, 0.0320 mmol) were then repeatedly added until no further change in ^{1}H NMR resonances was observed.

Use of Enaminone 22 as a Steric Probe for Counter Cation Bulk



22 *anti*-**30** *syn*-**30**

Y = DBUH, PhTMGH, TBA: To a stirred solution of enaminone **22** (37.9 mg, 0.160 mmol) in $CDCl_3$ (800 μL) was added the required amine (0.160 mmol). After stirring for 10 minutes, the mixture was transferred to an NMR tube for ^{1}H NMR analysis. The *anti*-**30** / *syn*-**30** ratio was determined by comparison of the corresponding protons geminal to the carboxylate group *anti*-**30** δ_H 4.19 (1H, dd, *J* = 7.4, 4.5) *syn*-**30** δ_H 4.01 (1H, dd, *J* = 8.3, 4.8).

Y = Bu_4N: Bu_4NOAc (48.2 mg, 0.160 mmol) was used in place of the amine.

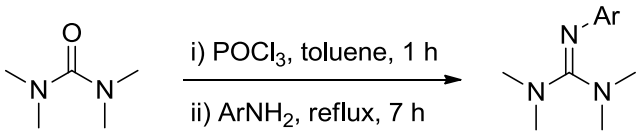
Y = Ph_4P: Ph_4PBr (67.1 mg, 0.160 mmol) and AgOAc (26.7 mg, 0.160 mmol) were used in place of the amine.

Y = Na + 15-c-5, K + 18-c-6, K + db-18-c-6: To a stirred solution of enaminone **22** (37.9 mg, 0.160 mmol) in methanol (1 mL) was added the required metal hydroxide (0.160 mmol). The mixture was stirred for 3 hours, then evaporated under reduced pressure. Next the required crown ether (0.160 mmol), and $CDCl_3$ (800 μL) was added. After

stirring for 10 minutes, the mixture was transferred to an NMR tube for ^{1}H NMR analysis as above.

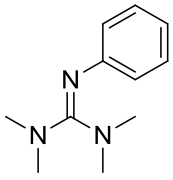
8.2.3. Synthesis of Required Materials

2-Aryl-1,1,3,3-tetramethylguanidines General Method



A modified version of previously reported methods was used:[136,137] To an ice bath-cooled solution of tetramethylurea (1.50 mL, 12.5 mmol) in toluene (100 mL) was added phosphorus oxychloride (1.75 mL, 18.8 mmol) dropwise and the mixture was stirred for 1 hour at room temperature, over which time a suspension of a wispy white solid formed. The required aniline (18.8 mmol) was then added and the mixture was heated at reflux for 7 hours. After cooling, the oily lower layer was separated and added to H_2O (50 mL), the pH was adjusted to 8 with 2M NaOH (aq), and the mixture was washed with toluene (3 × 50 mL). The pH of the aqueous partition was adjusted to 14 with 2M NaOH (aq) and then extracted with toluene (3 × 75 mL). This final organic partition was dried (Na_2SO_4), filtered, and evaporated under reduced pressure to give the appropriate ArTMG in high purity.

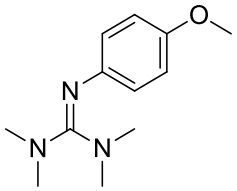
2-Phenyl-1,1,3,3-tetramethylguanidine (19a)[137]



Pale brown oil (1.16 g, 49%); ν_{max} (ATR) 2930, 2884, 1605, 1562, 1505, 1483, 1375; δ_H (400 MHz, $CDCl_3$) 7.19 (2H, t, *J* = 7.5, Ar*H*), 6.83 (1H, t, *J* = 7.5), 6.70 (2H, d, *J* = 7.5, Ar*H*),

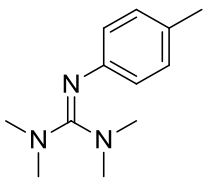
2.69 (12H, s, N(C*H*$_3$)$_2$); δ_C (100 MHz, $CDCl_3$) 159.7, 151.5, 128.4, 121.4, 119.6, 39.3; HRMS (ESI) $[M+H]^+$ Calc. for $C_{11}H_{18}N_3^+$: 192.1495, Found: 192.1492. These data are consistent with literature values.[137]

2-(4-Methoxyphenyl)-1,1,3,3-tetramethylguanidine (19b)[136]



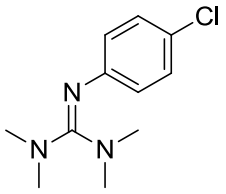
Red, viscous oil (2.05 g, 74%); ν_{max} (ATR) 2930, 2894, 1584, 1566, 1494, 1463, 1374; δ_H (400 MHz, $CDCl_3$) 6.78 (2H, d, *J* = 8.8, Ar*H*), 6.64 (2H, d, *J* = 8.8, Ar*H*), 3.76 (3H, s, OC*H*$_3$), 2.69 (12H, s, N(C*H*$_3$)$_2$); δ_C (100 MHz, $CDCl_3$) 153.5, 145.4, 122.3, 114.1, 55.5, 39.5; HRMS (ESI) $[M+H]^+$ Calc. for $C_{12}H_{20}N_3O^+$: 222.1601, Found: 222.1601. These data are consistent with literature values.[136]

2-(4-Methylphenyl)-1,1,3,3-tetramethylguanidine (19c)[136]



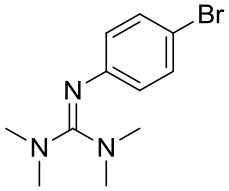
Pale purple, viscous oil (1.56 g, 61%); ν_{max} (ATR) 2927, 2873, 1579, 1562, 1495, 1452, 1373; δ_H (400 MHz, $CDCl_3$) 7.00 (2H, d, *J* = 7.9, Ar*H*), 6.80 (2H, d, *J* = 7.9, Ar*H*), 2.69 (12H, s, N(C*H*$_3$)$_2$), 2.26 (3H, s, ArC*H*$_3$); δ_C (100 MHz, $CDCl_3$) 159.7, 149.2, 129.3, 128.8, 121.5, 39.5, 20.7; HRMS (ESI) $[M+H]^+$ Calc. for $C_{12}H_{20}N_3^+$: 206.1652, Found: 206.1657. These data are consistent with literature values.[136]

2-(4-Chlorophenyl)-1,1,3,3-tetramethylguanidine (19d)[136]



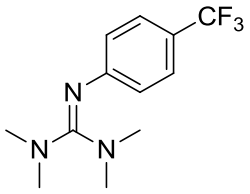
2.51 mmol scale; Colourless crystals (hexagonal prisms, 246 mg, 38%); m.p. 56–57 °C (toluene) (lit. 55–56 °C)[136]; ν_{max} (ATR) 2894, 2994, 1598, 1558, 1509, 1483, 1426, 1382, 740; δ_H (400 MHz, $CDCl_3$) 7.09 (2H, d, *J* = 8.7, Ar*H*), 6.58 (2H, d, *J* = 8.7, Ar*H*), 2.69 (12H, s, N(CH_3)$_2$); δ_C (100 MHz, $CDCl_3$) 160.3, 150.7, 128.7, 124.6, 122.8, 39.6; HRMS (ESI) $[M+H]^+$ Calc. for $C_{11}H_{17}ClN_3^+$: 226.1106, Found: 226.1105. These data are consistent with literature values.[136]

2-(4-Bromophenyl)-1,1,3,3-tetramethylguanidine (19e)[136]



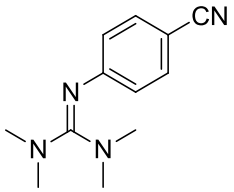
Colourless crystals (hexagonal prisms, 3.10 g, 92%); m.p 54–55 °C (toluene) (lit. 53–54 °C)[136]; ν_{max} (ATR) 2919, 2881, 1547, 1520, 1469, 1446, 1418, 1388; δ_H (400 MHz, $CDCl_3$) 7.27 (2H, d, *J* = 8.5, Ar*H*), 6.56 (2H, d, *J* = 8.5, Ar*H*), 2.69 (12H, s, N(CH_3)$_2$); δ_C (100 MHz, $CDCl_3$) 160.2, 151.2, 131.6, 123.4, 122.1, 39.7; HRMS (ESI) $[M+H]^+$ Calc. for $C_{11}H_{17}BrN_3^+$: 270.0600, Found: 270.0594. These data are consistent with literature values.[136]

2-(4-(Trifluoromethyl)phenyl)-1,1,3,3-tetramethylguanidine (19f)[130]



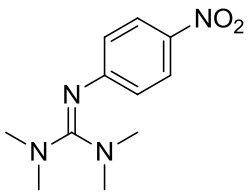
Colourless oil (990 mg, 31%); ν_{max} (ATR) 2941, 2886, 1558, 1503, 1385, 1320, 1148; δ_H (400 MHz, $CDCl_3$) 7.42 (2H, d, *J* = 8.4, Ar*H*), 6.72 (2H, d, *J* = 8.4, Ar*H*), 2.72 (12H, s, N(C*H*$_3$)$_2$); δ_F (377 MHz, $CDCl_3$) -61.2; HRMS (ESI) $[M+H]^+$ Calc. for $C_{12}H_{17}F_3N_3^+$: 260.1369, Found: 260.1371. These data are consistent with literature values.[130]

2-(4-Cyanophenyl)-1,1,3,3-tetramethylguanidine (19g)[136]



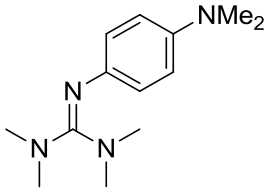
Pale yellow crystals (needles, 1.86 g, 69%); m.p. 57–59 °C (toluene); ν_{max} (ATR) 2937, 2891, 2216, 1540, 1494, 1429, 1384; δ_H (400 MHz, $CDCl_3$) 7.44 (2H, d, *J* = 8.5, Ar*H*), 6.66 (2H, d, *J* = 8.5, Ar*H*), 2.72 (12H, s, N(C*H*$_3$)$_2$); δ_C (100 MHz, $CDCl_3$) 160.8, 156.7, 132.8, 121.6, 120.2, 101.0, 39.5; HRMS (ESI) $[M+H]^+$ Calc. for $C_{12}H_{17}N_4^+$: 217.1448, Found: 217.1449.

2-(4-Nitrophenyl)-1,1,3,3-tetramethylguanidine (19g)[136]



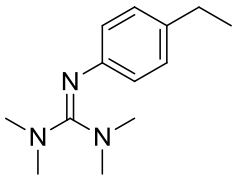
Bright yellow crystals (needles, 1.93 g, 65%; m.p. 80–81 °C (toluene) (lit. 80–82 °C)[136]; ν_{max} (ATR) 2937, 2891, 1526, 1488, 1424, 1389, 1302; δ_H (400 MHz, $CDCl_3$) 8.03 (2H, d, *J* = 9.2, Ar*H*), 6.60 (2H, d, *J* = 9.2, Ar*H*), 2.72 (12H, s, N(C*H*$_3$)$_2$); δ_C (100 MHz, $CDCl_3$) 161.5, 159.5, 139.9, 125.4, 120.8, 39.8; HRMS (ESI) $[M+H]^+$ Calc. for $C_{11}H_{17}N_4O_2^+$: 237.1346, Found: 237.1340. These data are consistent with literature values.[136]

2-(4-(Dimethylamino)phenyl)-1,1,3,3-tetramethylguanidine (19i)



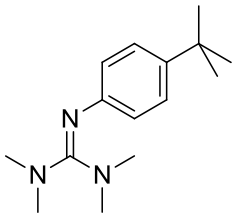
2.51 mmol scale; Dark brown, viscous oil (424 mg, 72%); ν_{max} (ATR) 2880, 2794, 1583, 1495, 1443, 1373, 1332; δ_H (400 MHz, $CDCl_3$) 6.70 (4H, s, Ar*H*), 2.87 (ArNC*H*$_3$), 2.69 (N=CN(C*H*$_3$)$_2$); δ_C (100 MHz, $CDCl_3$) 159.4, 145.2, 142.8, 122.1, 114.5, 41.7, 39.4; HRMS (ESI) $[M+H]^+$ Calc. for $C_{13}H_{23}N_4^+$: 235.1917, Found: 235.1910.[136]

2-(4-Ethylphenyl)-1,1,3,3-tetramethylguanidine (19j)



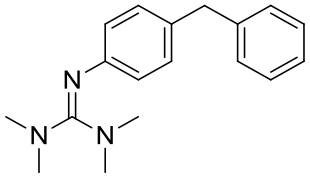
2.51 mmol scale; Pale brown, viscous oil (356 mg, 65%); ν_{max} (ATR) 2930, 2862, 1581, 1500, 1454, 1376; δ_H (400 MHz, $CDCl_3$) 7.03 (2H, d, *J* = 7.4, Ar*H*), 6.66 (2H, d, *J* = 7.4, Ar*H*), 2.71 (12H, s, N(C*H*$_3$)$_2$), (2H, q, *J* = 7.5, C*H*$_2$CH$_3$), (3H, t, *J* = 7.5, CH$_2$C*H*$_3$); δ_C (100 MHz, $CDCl_3$) 159.9, 149.5, 135.8, 128.2, 121.7, 39.7, 28.3, 16.0; HRMS (ESI) $[M+H]^+$ Calc. for $C_{13}H_{22}N_3^+$: 220.1808, Found: 220.1811.

2-(4-*tert*-Butyl)-1,1,3,3-tetramethylguanidine (19k)



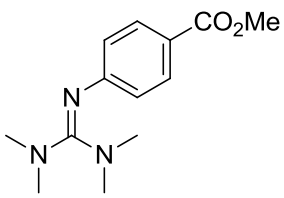
2.51 mmol scale; Pale brown, viscous oil (308 mg, 50%); ν_{max} (ATR) 2959, 2873, 1580, 1500, 1462, 1376; δ_H (400 MHz, $CDCl_3$) 7.24–7.19 (2H, m, Ar*H*), 6.75–6.65 (2H, m, Ar*H*), 2.73 (12H, s, N(C*H*$_3$)$_2$), 1.28 (9H, s, C(C*H*$_3$)$_3$); δ_C (100 MHz, $CDCl_3$) 159.9, 149.1, 142.6, 125.6, 121.2, 39.7, 34.1, 31.7; HRMS (ESI) $[M+H]^+$ Calc. for $C_{15}H_{26}N_3^+$: 248.2121, Found: 248.2117.

2-(4-Benzylphenyl)-1,1,3,3-tetramethylguanidine (19l)



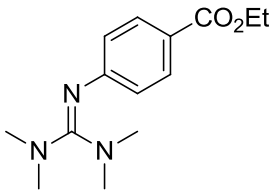
Brown, viscous oil, yield (433 mg, 61%); ν_{max} (ATR) 3024, 3005, 2927, 1580, 1495, 1454, 1377 ; δ_H (400 MHz, $CDCl_3$) 7.33–7.11 (5H, m, Ar*H*), 7.07–6.95 (2H, m, Ar*H*), 6.71–6.56 (2H, m, Ar*H*), 3.91 (2H, s, ArC*H*$_2$), 2.69 (12H, s, N(C*H*$_3$)$_2$); δ_C (100 MHz, $CDCl_3$) 160.0, 150.0, 142.3, 132.4, 129.5, 129.0, 128.4, 125.9, 121.8, 41.4, 39.8; HRMS (ESI) $[M+H]^+$ Calc. for $C_{18}H_{24}N_3^+$: 282.1965, Found: 282.1961.

2-(4-Methoxycarbonylphenyl)-1,1,3,3-tetramethylguanidine (19m)



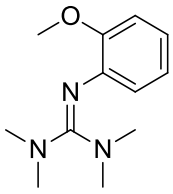
Pale yellow oil (286 mg, 46%); ν_{max} (ATR) 2945, 2891, 1707, 1545, 1436; δ_H (400 MHz, $CDCl_3$) 7.90 (2H, d, *J* = 8.6, Ar*H*), 6.72 (2H, d, *J* = 8.6, Ar*H*), 3.87 (3H, s, CO_2CH_3), 2.75 (12H, s, $N(CH_3)_2$); δ_C (100 MHz, $CDCl_3$) 167.5, 160.8, 157.0, 130.8, 121.1, 120.8, 51.6, 39.7; HRMS (ESI) $[M+H]^+$ Calc. for $C_{13}H_{20}N_3O_2^+$: 250.1550, Found: 250.1549.

2-(4-Ethoxycarbonylphenyl)-1,1,3,3-tetramethylguanidine (19n)



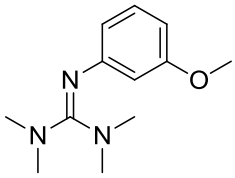
Pale yellow oil (344 mg, 52%); ν_{max} (ATR) 2934, 1704, 1547, 1473, 1424, 1386; δ_H (400 MHz, $CDCl_3$) 7.84 (2H, d, *J* = 8.4, Ar*H*), 6.63 (2H, d, *J* = 8.4, Ar*H*), 4.27 (3H, q, *J* = 7.1, CH_2CH_3), 2.66 (12H, s, $N(CH_3)_2$), 1.31 (3H, t, *J* = 7.1, CH_2CH_3); δ_C (100 MHz, $CDCl_3$) 167.0, 160.7, 156.8, 130.7, 121.1, 121.0, 60.2, 39.6, 14.4; HRMS (ESI) $[M+H]^+$ Calc. for $C_{14}H_{22}N_3O_2^+$: 264.1707, Found: 264.1707.

2-(2-Methoxyphenyl)-1,1,3,3-tetramethylguanidine (20a)[136]



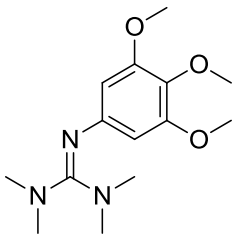
Red-brown viscous oil (356 mg, 64%); ν_{max} (ATR) 2937, 2889, 1602, 1563, 1493, 1383; δ_H (400 MHz, $CDCl_3$) 6.87–6.78 (3H, m, Ar*H*), 6.68–6.61 (1H, m, Ar*H*), 3.89 (3H, s, OCH_3), 2.70 (12H, s, $N(CH_3)_2$); δ_C (100 MHz, $CDCl_3$) 160.7, 151.3, 141.1, 122.4, 120.7, 120.3, 110.4, 55.4, 39.2; HRMS (ESI) $[M+H]^+$ Calc. for $C_{12}H_{20}N_3O^+$: 222.1601, Found: 222.1599. These data are consistent with literature values.[136]

2-(3-Methoxyphenyl)-1,1,3,3-tetramethylguanidine (20b)[136]



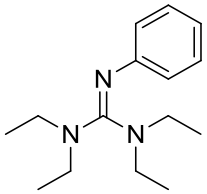
Red-brown, viscous oil (389 mg, 70%); ν_{max} (ATR) 2932, 1562, 1509, 1482, 1382; δ_H (400 MHz, $CDCl_3$) 7.10 (1H, t, *J* = 7.9, Ar*H*), 6.44 (1H, d, *J* = 7.9, Ar*H*), 6.36 (1H, s, Ar*H*), 6.30 (1H, d, *J* = 7.9, Ar*H*), 3.77 (3H, s, OCH_3), 2.73 (12H, s, N(CH_3)$_2$); δ_C (100 MHz, $CDCl_3$) 160.3, 160.1, 153.0, 129.2, 114.3, 107.1, 105.8, 55.0, 39.6; HRMS (ESI) $[M+H]^+$ Calc. for $C_{12}H_{20}N_3O^+$: 222.1601, Found: 222.1598. These data are consistent with literature values.[136]

2-(3',4',5'-Trimethoxyphenyl)-1,1,3,3-tetramethylguanidine (20c)



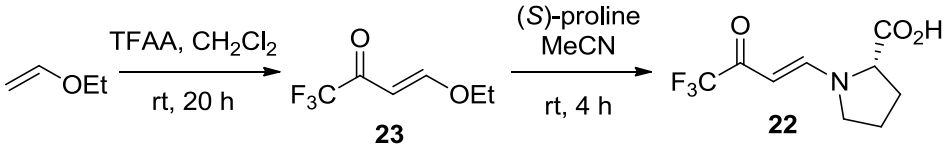
Red, viscous oil (318 mg, 45%); ν_{max} (ATR) 2934, 2248, 1566, 1495, 1451, 1380; δ_H (400 MHz, $CDCl_3$) 5.99 (2H, s, Ar*H*), 3.81 (6H, s, *m*-OCH_3), 3.79 (3H, s, *p*-OCH_3), 2.74 (12H, s, N(CH_3)$_2$); δ_C (100 MHz, $CDCl_3$) 160.0, 153.3, 148.0, 131.8, 98.7, 61.0, 55.8, 39.6; HRMS (ESI) $[M+H]^+$ Calc. for $C_{14}H_{24}N_3O_3^+$: 282.1812, Found: 282.1809.

2-Phenyl-1,1,3,3-tetraethylguanidine (21)



Tetraethyl urea (476 μL, 2.51 mmol) used in place of tetramethyl urea; 2.51 mmol scale; Pale brown, viscous oil, (312 mg, 50%); ν_{max} (ATR) 2970, 2934, 1574, 1481, 1417, 1378; δ_H (400 MHz, $CDCl_3$) 7.19 (2H, t, *J* = 7.5, Ar*H*), 6.84 (1H, t, *J* = 7.5, Ar*H*), 6.78 (2H, d, *J* = 7.5, Ar*H*) 3.28–2.82 (8H, m, $N(CH_2CH_3)_2$), 1.18–0.94 (12H, m, $N(CH_2CH_3)_2$); δ_C (100 MHz, $CDCl_3$) 158.0, 128.8, 121.4, 120.1, 42.8, 13.1; HRMS (ESI) $[M+H]^+$ Calc. for $C_{15}H_{26}N_3^+$: 248.2121, Found: 248.2126.

(2*S*)-1-[(*E*)-4,4,4-Trifluoro-3-oxo-1-butenyl]tetrahydro-1*H*-2-pyrrolecarboxylic acid (22)[144]

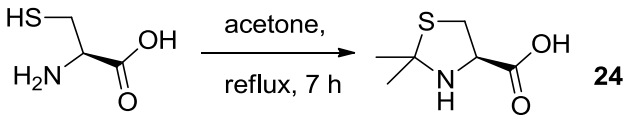


According to the method of Andrew and Mellor:[144] To an ice bath-cooled solution of TFAA (17 mL, 120 mmol) and pyridine (1.08 mL, 13.3 mmol) in CH_2Cl_2 (25 mL) was added ethyl vinyl ether (3.83 mL, 40.0 mmol) over 10 minutes; the mixture was then stirred at room temperature for 20 hours. After this time, the solvent and excess reagents were evaporated to yield **23** as a red-brown oil, used in the next step without further purification. δ_H (400 MHz, $CDCl_3$) 7.90 (1H, d, *J* = 12.5, C=C*H*(CO_2CF_3)), 5.86 (1H, d, *J* = 12.5, C=C*H*(OEt)), 4.10 (2H, q, *J* = 7.0, CH_2CH_3), 1.41 (3H, t, *J* = 7.0, CH_2CH_3).

To a stirred solution of **23** in acetonitrile (50 mL) was added (*S*)-proline (5.99 g, 52.0 mmol) and the suspension was stirred for 4 hours. The crude product was then

evaporated, purified by flash column chromatography (20% MeOH/EtOAc), and recrystallised (Et_2O/hexane) to yield **22** as pale tan crystals (7.08 g, 75% yield). m. p. 107–108 °C (Et_2O/hexane) (lit. = 109–110 °C)[144]; ν_{max} (ATR) 2953, 2884, 1728, 1641, 1531; δ_H (400 MHz, $CDCl_3$) *maj. rot.* (83%) 8.23 (1H, d, *J* = 12.5, C=C*H*(CO_2CF_3)), 7.98 (1H, br s, CO_2*H*), 5.42 (1H, d, *J* = 12.5, C=C*H*(NR_2)), 4.48 (1H, t, *J* = 6.0, C*H*CO_2H), 3.60–3.51 (1H, m, NC*H*H), 3.47–3.36 (1H, m, NCH*H*), 2.39–2.07 (4H, m, CH_2CH_2); *min. rot.* (17%) 8.18-8.10 (1H, m, C=C*H*(CO_2CF_3)), 5.24 (1H, d, *J* = 12.5, C=C*H*(NR_2), 4.30–4.21 (1H, m, C*H*CO_2H), 3.79–3.80 (1H, m, NC*H*H), 3.74–3.65 (1H, m, NCH*H*), 2.49–1.95 (4H, m, CH_2CH_2); δ_C (100 MHz, $CDCl_3$) *maj. rot.* 178.0 (q, J_{CF} = 32.9), 172.9, 117.9 (q, J_{CF} = 289.4), 155.5, 90.3, 65.0, 48.7, 29.6, 23.6; *min. rot.* 153.7, 60.5, 53.9, 30.7, 23.8; δ_F (377 MHz) -76.8. These data are consistent with literature values.[144]

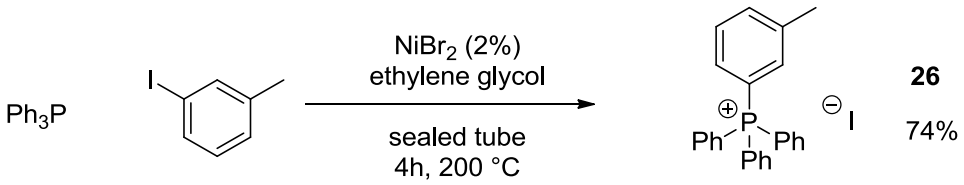
2,2-Dimethylthiazolidine-(4*R*)-carboxylic acid (24)[176]



24

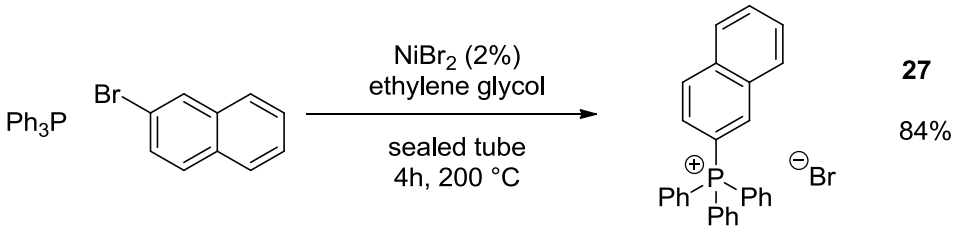
According to a modified version of the method of Howard-Lock *et al*:[176] A mixture of (*R*)-cysteine (1.21 g, 10.0 mmol), $MgSO_4$ (1 g) and anhydrous acetone (200 mL) was heated at reflux for 7 hours after which time the solvent was evaporated under reduced pressure. The resulting cream solid was recrystallised (acetone) to yield **24** (829 mg, 51%) as white crystals (needles); m.p. 149–151 °C (decomp.) (acetone); ν_{max} (ATR) 3070 br (OH), 1718 (C=O), 1632, 1513, 1383; δ_H (400 MHz, CD_3OD) 4.33 (1H, t, *J* = 8.0, C*H*CO_2H), 3.54 (1H, dd, *J* = 11.5, 8.0, C*H*H), 3.33 (1H, dd, *J* = 11.5, 8.0, CH*H*), 1.75 (3H, s, CH_3), 1.68 (3H,s, CH_3); δ_C (100 MHz, CD_3OD) 172.8, 74.8, 66.0, 36.5, 30.0, 29.0; HRMS (ESI) $[M+H]^+$ Calc. for $C_6H_{12}NO_2S^+$: 162.0589, Found: 162.0594. These data are consistent with those previously reported.[176]

3-Tolyltriphenylphosphonium iodide (26)[177]



According to the method of Charette and co-workers:[157] A reaction vial was charged with a suspension of 3-iodotoluene (385 μL, 3.00 mmol), triphenylphosphine (826 mg, 3.15 mmol), and $NiBr_2$ (13.1 mg, 0.060 mmol, 2%) in ethylene glycol (1 mL) and then sealed. The mixture was heated at around 180 °C. After 30 minutes the cloudy green suspension had turned into a clear dark brown solution. After 4 hours of heating, the mixture was allowed to cool to rt, then diluted with CH_2Cl_2 (40 mL), washed with H_2O (3×30 mL), then sat. aq NaCl (30 mL), and then concentrated under reduced pressure to give a pink solid. This crude material was then purified by recrystallisation (CH_2Cl_2/Et_2O) to furnish **26** as a light brown solid (1.06 g, 74%); m. p. 199–200 (lit. 201–203)[177]; ν_{max} (ATR) 3047, 3020, 1484, 1435, 1107; δ_H (400 MHz, $CDCl_3$) 7.95–7.88 (3H, m, C_6H_5), 7.84–7.76 (6H, m, C_6H_5), 7.71–7.59 (8H, m, C_6H_5 + $C_6H_4CH_3$), 7.42 (1H, dd, J = 13.2, 6.7, $C_6H_4CH_3$), 7.35 (1H, d, J = 13.2, $C_6H_4CH_3$), 2.46 (3H, s, CH_3); δ_C (100 MHz, $CDCl_3$) 141.0 (d, J_{CP} = 12.8), 136.6 (d, J_{CP} = 2.9), 135.7 (3C, d, J_{CP} = 2.9), 134.2 (6C, d, J_{CP} = 10.4), 134.1 (d), 131.6 (d, J_{CP} = 10.3), 130.8 (6C, d, J_{CP} = 12.8), 130.6 (d), 117.3 (3C, d, J_{CP} = 89.5), 117.0 (d, J_{CP} = 89.2), 21.7; δ_P (162 MHz, $CDCl_3$) 23.0. These data are consistent with those previously reported.[177]

2-Naphthyltriphenylphosphonium bromide (27)

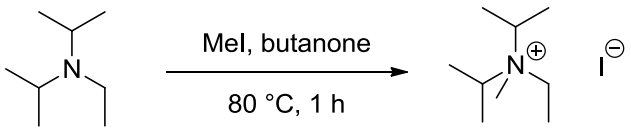


27

84%

According to the method of Charette and co-workers:[157] A reaction vial was charged with a suspension of 2-bromonaphthalene (621 μL, 3.00 mmol), triphenylphosphine (826 mg, 3.15 mmol), and $NiBr_2$ (13.1 mg, 0.060 mmol, 2%) in ethylene glycol (1 mL) and then sealed. The mixture was heated at around 180 °C. After 30 minutes, the cloudy mixture had turned into a deep green solution. After 4 hours of heating, the mixture was allowed to cool to rt, then diluted with CH_2Cl_2 (40 mL), washed with H_2O (3×30 mL), then sat. aq NaCl (30 mL), dried (Na_2SO_4), filtered through a plug of Celite®, and then concentrated under reduced pressure. This crude residue was then purified by trituration (Et_2O) to furnish **27** as a white crystalline solid (flakes, 1.19 g, 84%); m. p. 223–224 °C (Et_2O); ν_{max} (ATR) 3460, 3376, 3059, 1622, 1585, 1437, 1103; δ_H (400 MHz, $CDCl_3$) 8.26 (1H, dd, *J* = 8.7, 3.3, $C_{10}H_7$), 8.12 (1H, d, *J* = 15.4, $C_{10}H_7$), 8.05 (1H, d, *J* = 8.2, $C_{10}H_7$), 8.00–7.89 (4H, m, $C_{10}H_7$ + C_6H_5), 7.86–7.75 (7H, m, $C_{10}H_7$ + C_6H_5), 7.73–7.63 (7H, m, $C_{10}H_7$ + C_6H_5), 7.58 (1H, t, *J* = 9.8); δ_C (100 MHz, $CDCl_3$) 133.1, 132.2, 132.1, 132.00, 131.97, 128.6, 128.5; δ_P (162 MHz, $CDCl_3$) 29.1.

Ethyldiisopropylmethylammonium iodide (28)[178]



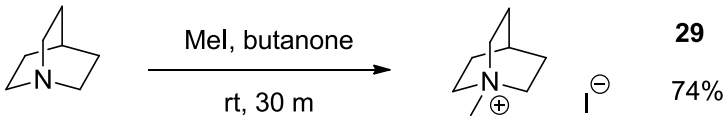
28

71%

A reaction tube was charged with a solution of methyl iodide (124 μL, 2.00 mmol) in butanone (4 mL). To this was added DIPEA (281 μL, 2.00 mmol), the tube was sealed and the mixture was heated at 80 °C. After an hour, a large amount of white

precipitate had formed and the reaction mixture was allowed to cool to rt. The precipitate was collected by filtration under vacuum to give **28** as a white, crystalline solid (cubes, 364.9 mg, 71%); m. p. 248–250 °C (butanone) (lit. = 256–257 °C);[179] ν_{max} (ATR) 2986, 1482, 1449, 1407, 1198, 1141; δ_H (400 MHz, D_2O) 3.89 (2H, septet, *J* = 6.7, 2×C*H*(CH_3)$_2$), 3.33 (2H, q, *J* = 7.3, C*H*$_2$$CH_3$), 2.80 (3H, s, NCH_3), 1.38 (12H, d, *J* = 6.7, 2×CH(C*H*$_3$)$_2$), 1.31 (3H, t, *J* = 7.3, CH_2C*H*$_3$); δ_C (100 MHz, D_2O) 62.8, 52.2, 42.6, 16.4, 9.3. These data are consistent with literature data.[178]

N-Methylquinuclidinium iodide (29)[180]



29

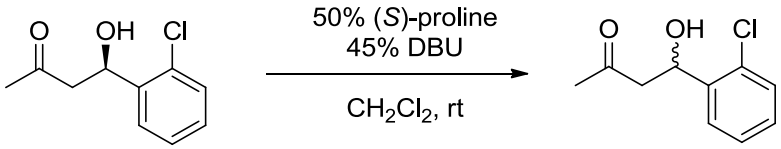
74%

A reaction tube was charged with a solution of freshly sublimated quinuclidine (222 mg, 2.00 mmol) in butanone (20 mL). To the stirred mixture was added methyl iodide (124 μL, 2.00 mmol) dropwise and spontaneous precipitation of a white solid occurred. The precipitate was collected by filtration under vacuum to give **29** as a white amorphous solid (376.4 mg, 74%). m. p. >300 °C (butanone) (lit. >300 °C);[180] ν_{max} (ATR) 3604, 2948, 2879, 1462, 1428, 1330; δ_H (400 MHz, D_2O) 3.42–3.34 (6H, m, 3×NCH_2), 2.89 (3H, s, CH_3), 2.16 (1H, septet, *J* = 3.3, CH_2C*H*), 2.00–1.91 (6H, m, 3×C*H*$_2$CH); δ_C (100 MHz, D_2O) 56.9, 51.8, 23.4, 18.6. These data are consistent with literature values.[180]

8.3. Aldol

8.3.1. Aldol Reactions

Aldol Product Racemisation Studies



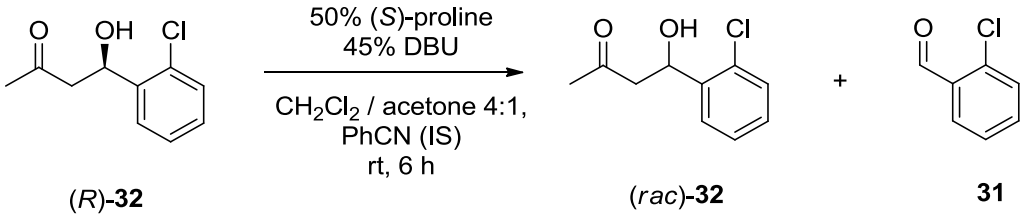
(*R*)-**31** (*rac*)-**31**

A suspension of (*S*)-proline (15.7 mg, 0.136 mmol, 50%) and DBU (18.3 μL, 0.123 mmol) was stirred in CH_2Cl_2 (0.5 mL) for 20 minutes to allow equilibration. After this time, aldol product (*R*)-**31** (54.1 mg, 0.272 mmol) in CH_2Cl_2 (0.5 mL) was added (t=0) and racemisation was monitored by periodic sampling: A 50 μL aliquot is added to 1 mL sat. aq NH_4Cl, extracted with EtOAc (2 mL), dried ($MgSO_4$), filtered, and analysed by HPLC.

HPLC Conditions: AS-H column; Flow rate = 1 mL min^{-1}; Solvent System = 80:20 (hexane/IPA); λ = 220 nm; 2-chlorobenzaldehyde t_r = 4.90 m, scaling factor = 0.329; PhCN t_r = 5.85 m, scaling factor = 1.00; (*R*)-**31** t_r = 11.82, scaling factor = 0.671; (*S*)-**31** t_r = 13.40, scaling factor = 0.671.

For the control experiments the same method was followed with (*S*)-proline or DBU omitted as required or with the enantioenriched aldol product replaced with racemic material.

Retroaldol Reaction

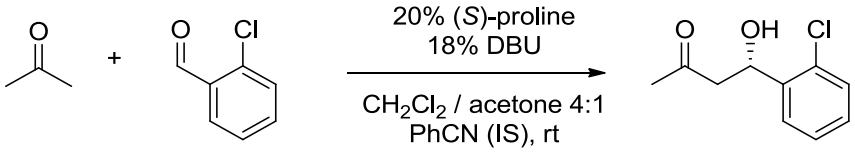


(*R*)-**32** (*rac*)-**32** **31**

A solution of (*S*)-proline (28.3 mg, 0.246 mmol, 50%) and DBU (33.0 μL, 0.221 mmol, 45%) was stirred in CH_2Cl_2 (1.1 mL) and acetone (0.4 mL) for 20 minutes to allow equilibration. After this time, aldol product (*R*)-**31** (97.6 mg, 0.491 mmol) and a known amount of benzonitrile (as an internal standard) in CH_2Cl_2 (0.5 mL) was added. After 6 hours, the composition was determined by HPLC: A 50 μL aliquot was added to 1 mL sat. aq NH_4Cl, extracted with EtOAc (2 mL), dried ($MgSO_4$), filtered, and analysed by HPLC.

For the experiment carried out in the presence of H_2O, the same procedure was carried out with H_2O (18.9 μL, 1.05 mmol) added to the initial solution of proline and DBU in CH_2Cl_2 and acetone.

Proline/DBU-Catalysed Aldol Reactions Monitored by HPLC



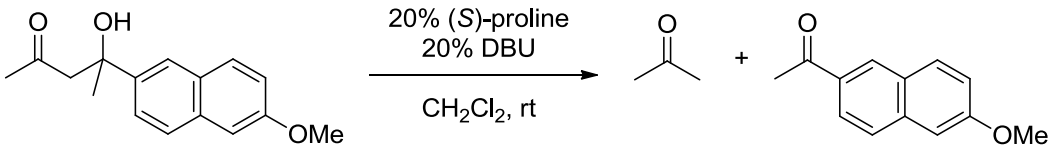
31 (*S*)-**32**

A solution of (*S*)-proline (61.3 mg, 0.533 mmol, 20%), DBU (33.0 μL, 0.221 mmol, 18%), and a known amount of benzonitrile (as an internal standard) was stirred in CH_2Cl_2 (8 mL) and acetone (0.4 mL) for 20 minutes to allow equilibration. After this time, 2-chlorobenzaldehyde (300 μL, 2.66 mmol) was added to initiate the reaction (t=0) and the reaction was monitored by periodic sampling: A 50 μL aliquot is added to sat. aq

NH_4Cl (1 mL), extracted with EtOAc (2 mL), dried ($MgSO_4$), filtered, and analysed by HPLC.

For experiments carried out in the presence of H_2O, the same procedure was carried out with the required amount of H_2O added to the initial solution of proline and DBU in CH_2Cl_2 and acetone.

Retroaldol Reaction of (*rac*)-33 Monitored by HPLC



(*rac*)-**33** **34**

A solution of (S)-proline (5.7 mg, 0.0499 mmol) and DBU (6.7 μL, 0.0499 mmol) in CH_2Cl_2 (500 μL) was stirred for 20 minutes. After this time, a solution of hydroxyketone (*rac*)-**33** (25.8 mg, 0.0999 mmol) and a known amount of PhCN (as an internal standard) in CH_2Cl_2 (500 μL) was added to initiate the reaction (t=0) and the reaction was then monitored by periodic sampling: A 50 μL aliquot is added to sat. aq NH_4Cl (1 mL), extracted with EtOAc (2 mL), dried ($MgSO_4$), filtered, and analysed by HPLC.

HPLC Conditions: AS-H column; Flow rate = 1 mL min^{-1}; Solvent System = 95:05 (hexane/IPA); λ = 210 nm; PhCN t_r = 5.41 m, scaling factor = 1.00; 6-methoxy-2-acetophenone t_r = 7.76 m, scaling factor = 0.338; **33** t_r = 14.00, 16.97 m, scaling factor = 0.289.

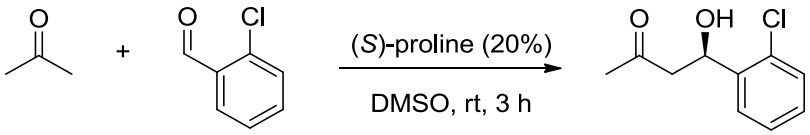
For the attempted reaction with (*S*)-proline alone, the same conditions were used with the omission of DBU.

Control aldol reaction: A solution of (*S*)-proline (61.3 mg, 0.533 mmol), DBU (71.6 μL, 0.479 mmol) and a known amount of PhCN as an internal standard in CH_2Cl_2 (7 mL) and

acetone (2 mL) was stirred for 20 minutes. After this time, a solution of 6-methoxyacetonaphthone (533 mg, 2.66 mmol) in CH_2Cl_2 (1 mL) was added to initiate the reaction (t=0) and the reaction was then monitored by periodic sampling: A 50 μL aliquot is added to sat. aq NH_4Cl (1 mL), extracted with EtOAc (2 mL), dried ($MgSO_4$), filtered, and analysed by HPLC.

8.3.2. Synthesis of Required Materials

(*R*)-4-(2-Chlorophenyl)-4-hydroxybutanone ((*R*)-32)[181]

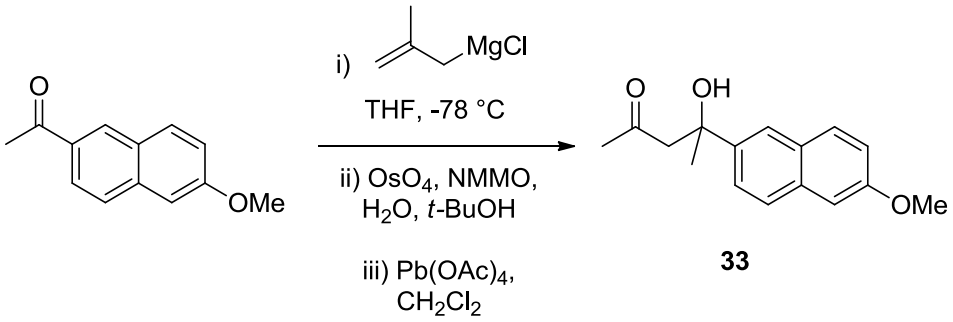


32

According to the procedure of List, Lerner, and Barbas:[6] To a stirred suspension of proline (204 mg, 1.78 mmol, 20%) in DMSO (40 mL) and acetone (10 mL) was added 2-chlorobenzaldehyde (1.00 mL, 8.88 mmol). After 3 hours the reaction was diluted with H_2O (100 mL), extracted with EtOAc (3×50 mL), dried ($MgSO_4$), filtered, and evaporated under reduced pressure. The crude product was then purified by flash column chromatography (25% EtOAc in *n*-hexane) to give (*R*)-**32** as a yellow oil (1.36 g, 77%). ν_{max} (ATR) 3425 br s (OH), 3069, 2916, 1706 s (C=O), 147, 1440, 1362; δ_H (400 MHz, $CDCl_3$) 7.62 (1H, d, *J* = 7.7, C_6H_4Cl), 7.35–7.28 (2H, m, C_6H_4Cl), 7.22 (1H, t, *J* = 7.7, C_6H_4Cl), 5.54–5.48 (1H, m, C*H*OH), 3.51 (1H, d, *J* = 3.3, OH), 3.00 (1H, dd, *J* = 17.8, 2.3, CH_aH_bCOH), 2.68 (1H, dd, 17.8, 9.7, CH_aH_bCOH), 2.22 (3H, s, CH_3); δ_C (100 MHz, $CDCl_3$) 209.3, 140.2, 131.2, 129.4, 128.7, 127.3, 127.1, 66.6, 50.1, 30.7. These data are consistent with literature values.[181]

Additional material was isolated from sampling reactions after purification.

4-Hydroxy-4-methyl-4-(6'-methoxy-2'-naphthyl)butanone ((rac)-33)[161]



33

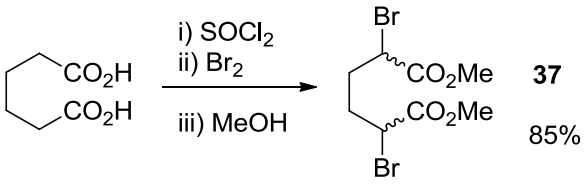
According to the method of List, Lerner, and Barbas:[161] To a stirred solution of 6-methoxy-2-acetonaphthone (1.20 g, 6.00 mmol) in THF (15 mL) at −78 °C was added 0.5 M 2-methylallylmagnesium chloride solution in THF (15 mL, 7.50 mmol). After 5 minutes, the reaction mixture was warmed to −30 °C and quenched by addition of sat. aq NH_4Cl solution (1.2 mL). Next Et_2O (20 mL) was and the mixture was warmed to room temperature, dried ($MgSO_4$), filtered and evaporated under reduced pressure to yield a colourless product which was used without purification in the next step.

To a stirred solution of the product of the first step (1.40 g) in acetone (20 mL) was added 60% wt solution NMMO in H_2O (3.09 mL, 15.8 mmol), followed by 2.5% OsO_4 solution in *t*BuOH (1.8 mL, 0.18 mmol). On addition of the OsO_4 solution, the reaction mixture turned from colourless to orange. After stirring for 1 hour the reaction was adjudged to be complete by TLC. The mixture was cooled in an ice bath and to it was added saturated aq $Na_2S_2O_5$/$NaHSO_3$ solution (20 mL). After stirring for 20 minutes, the mixture was diluted by adding water (100 mL), separated and extracted with Et_2O (5 × 50 mL). The combined organics were then dried ($MgSO_4$), filtered and evaporated under reduced pressure to yield a white solid, which was used without purification in the next step.

To a stirred solution of the product of the second step (1.60 g) in CH_2Cl_2 (90 mL) was added $Pb(OAc)_4$ (2.79 g, 6.30 mmol) portionwise. After 10 minutes, solid Na_2CO_3 was added and the mixture was stirred for 30 minutes. Filtration, evaporation and flash

column chromatography yielded (*rac*)-**33** as a white solid (117.9 mg, 7.6%). ν_{max} (ATR) 3425 br (OH), 2975, 2940, 1692 (C=O), 1609, 1268, 1198, 1135; δ_H (400 MHz, $CDCl_3$) 7.83 (1H, s), 7.76–7.68 (2H, m), 7.48 (1H, dd, *J* = 8.5, 2.0) 7.18–7.09 (2H, m), 4.67 (1H, s, O*H*), 3.91 (3H, s, ArOC*H*$_3$), 3.26 (1H, d, *J* = 17.0, $CH_3COCH_aH_b$), 2.90 (1H, d, *J* = 17.0, $CH_3COCH_aH_b$, 2.07 (3H, s, COC*H*$_3$), 1.60 (3H, s, C(OH)(C*H*$_3$)); δ_C (100 MHz, $CDCl_3$) 210.9, 157.8, 142.5, 133.5, 129.8, 128.8 127.0, 123.6, 122.9, 119.1, 105.6, 73.5, 55.4, 54.0, 32.1, 30.1. These data are consistent with literature values.[161]

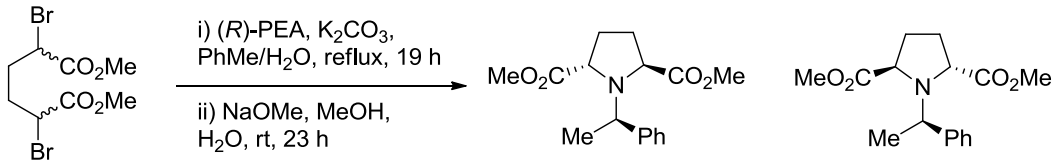
Dimethyl 2,5-dibromoadipate (37)[182]



To adipic acid (15.0 g, 103 mmol) was added thionyl chloride (19 mL, 260 mmol) dropwise through a reflux condenser. The condenser was fitted with a trap containing 5 N NaOH (aq) to quench the gaseous by-products evolved and the mixture was then heated at reflux. After 2 hours, excess thionyl chloride was removed by evaporation under reduced pressure to yield adipoyl chloride as a colourless oil. To this (18.8 g, 103 mmol) was added freshly distilled bromine (12.1 mL, 236 mmol) and the mixture was heated at reflux for 6.5 hours. The mixture was cooled to 0 °C and methanol (40 mL) was added portionwise after which the mixture was allowed to reach rt over 1 hour and then water (40 mL) was added. The aqueous phase was separated and extracted with diethyl ether (40 mL). The combined organics were washed sequentially with 0.5 M aq $Na_2S_2O_3$ solution (2×20 mL), sat. aq $NaHSO_3$ solution (2×20 mL), and H_2O (3×20 mL), dried ($MgSO_4$), filtered, and evaporated under reduced pressure to yield crude diester **37** (28.8 g, 85 %) as a pale yellow oil. Composition: 69% *meso*-isomer, 31% *rac*-isomer by ^{1}H NMR. δ_H ($CDCl_3$, 400 MHz) 4.30–4.23 (2H, m, *rac* + *meso*, C*H*Br), 3.79 (6H, s, *meso*, CO_2CH_3), 3.78 (6H, s, *rac*, CO_2CH_3), 2.25–2.12 (2H, m, *meso*, CH*H*CH*H*), 2.12–2.02 (2H, m, *meso*, C*H*HC*H*H), 1.89–1.77 (2H, m, *rac*, CH*H*CH*H*), 1.75–1.63 (2H, m, *rac*, C*H*HC*H*H). These data are consistent with literature values.[182]

N-((*R*)-1-Phenylethyl)-(2*S*,5*S*)-pyrrolidine-2,5-dicarboxylic dimethyl ester ((*S*,*S*)-39)[163]

N-((*R*)-1-Phenylethyl)-(2*R*,5*R*)-pyrrolidine-2,5-dicarboxylic dimethyl ester ((*R*,*R*)-39)[163]



37 (*S*,*S*)-**39** (*R*,*R*)-**39**

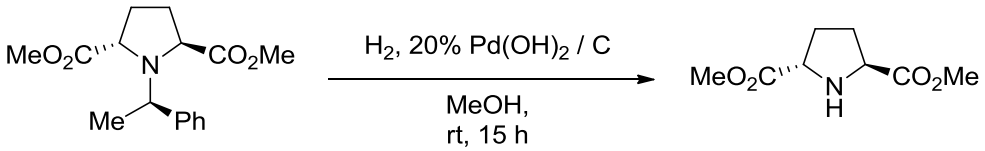
To a mixture of dimethyl-2,5-dibromoadipate (**37**) (28.1 g, 84.6 mmol), K_2CO_3 (14.0, 102 mmol), toluene (60 mL) and water (30 mL) was added (*R*)-1-phenylethylamine. The vigorously stirred biphasic mixture was heated at reflux for 19 hours and then partitioned. The aqueous phase was extracted with hexane (2×40 mL) and the combined organics were washed with brine (2×40 mL), dried ($MgSO_4$), filtered and evaporated under reduced pressure to yield *N*-((*R*)-1-phenylethyl)pyrrolidine-2,5-dicarboxylic dimethyl ester as a diastereomeric mixture. To this was added 1.41 M NaOMe solution (in methanol) (60 mL, 84.6 mmol) dropwise and then water (610 µL, 33.8 mmol). The reaction mixture was stirred for 22 hours after which time, H_2SO_4 (1.95 mL) was added dropwise with external cooling. The mixture was evaporated under reduced pressure, and partitioned into water (30 mL) and toluene (30 mL). The aqueous phase was then extracted with toluene (2×30 mL) and the combined organics were washed with brine (50 mL), dried ($MgSO_4$), filtered and evaporated under reduced pressure to yield a crude brown oil (14.5 g) which was purified by gravity column chromatography (10 % EtOAc in petroleum) gave (*S*,*S*)-**39** (1.51 g, 6 %) and (*R*,*R*)-**39** (3.79 g, 15 %) as white solids:

(*S*,*S*)-**39** $[\alpha]_D^{22}$: −24 (*c* = 1.0, $CHCl_3$); ν_{max} (ATR) 2956 (sp^3 C-H), 1722 (C=O), 1436, 1272, 1146; δ_H ($CDCl_3$, 400 MHz) 7.36–7.18 (5H, m, C_6H_5), 4.05–3.95 (3H, m), 3.46 (6H, s,

CO_2CH_3), 2.45–2.30 (2H, m), 1.89–1.76 (2H , m), 1.39 (3H, d, *J* = 6.5, $CHCH_3$); δ_C ($CDCl_3$, 100 MHz) 175.8, 144.6, 128.3, 127.3, 127.2, 62.9, 59.9, 51.5, 29.2, 23.4; MS (ESI+) $[M+H]^+$ 292. These data are consistent with literature values.[163]

(*R*,*R*)-**39** $[\alpha]_D^{22}$: +98 (*c* = 1.0, $CHCl_3$); ν_{max} (ATR) 2954 (sp^3 C-H), 1735 (C=O), 1434, 1197, 1155; δ_H ($CDCl_3$, 400 MHz) 7.18-7.36 (5H, m, C_6H_5)), 4.00 (1H, q, *J* = 6.7, $CHCH_3$), 3.74-3.81 (2H, m), 3.67 (6H, s, CO_2CH_3), 2.26-2.40 (2H, m), 1.76-1.88 (2H, m), 1.28 (3H, d, *J* = 6.7, $CHCH_3$); δ_C ($CDCl_3$, 100 MHz) 175.8, 144.6, 128.3, 127.3, 127.2, 62.9, 59.9, 51.5, 29.2, 23.4; MS (ESI+) $[M+H]^+$ 292. These data are consistent with literature values.[163]

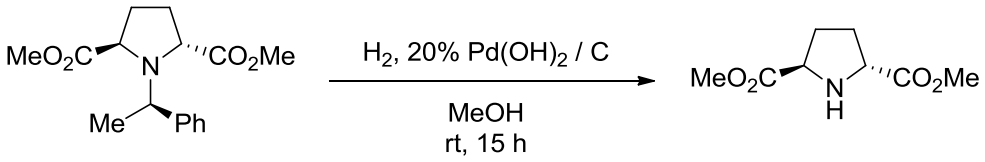
Dimethyl (2*S*,5*S*)-pyrrolidine-2,5-dicarboxylic ester ((*S*,*S*)-41)[163]



(*S*,*S*)-**39** (*S*,*S*)-**41**

A flask containing (*S*,*S*)-**39** (1.27 g, .35 mmol) and 20% $Pd(OH)_2/C$ (531 mg, 0.870 mmol) was thrice evacuated and filled with an atmosphere of argon before being evacuated and filled with an atmosphere of hydrogen. Degassed methanol was added and the suspension was stirred at rt for 15 hours. The reaction mixture was filtered through Celite® under a flow of argon and the cake was washed with methanol. The filtrate was evaporated under reduced pressure to yield (*S*,*S*)-**41** (779 mg, 96 %) as a colourless oil. $[\alpha]_D^{22}$: −42 (*c* = 1.0, $CHCl_3$); ν_{max} (ATR) 3350 (NH br), 2957 (sp^3 C-H), 1733 (C=O), 1437, 1206, 1155; δ_H ($CDCl_3$, 400 MHz) 4.05–3.97 (2H, m), 3.73 (6H, s, CH_3), 2.70 (1H, s br, N*H*), 2.54–2.11 (2H, m), 2.03–1.89 (2H, m); δ_C ($CDCl_3$, 100 MHz) 174.9, 59.6, 52.2, 29.2; MS (ESI+) $[M+H]^+$ 188. These data are consistent with literature values.[163]

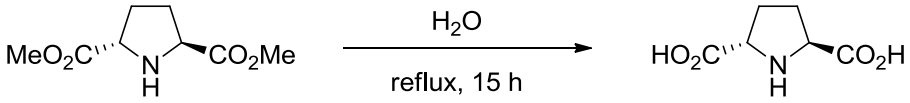
Dimethyl (2*R*,5*R*)-pyrrolidine-2,5-dicarboxylic ester ((*R*,*R*)-41)[163]



(*R*,*R*)-**39** (*R*,*R*)-**41**

A flask containing (*R*,*R*)-**39** (1.61 g, 5.54 mmol) and 20% Pd(OH)2/C (778 mg, 1.11 mmol) was charged with argon, then evacuated and refilled with hydrogen three times. Degassed methanol was added and the suspension was stirred at 22 °C for 15 hours. The reaction mixture was filtered through Celite® under a flow of argon and the cake was washed with methanol. The filtrate was evaporated under reduced pressure to yield (*R*,*R*)-**41** (989 mg, 95 %) as a colourless oil. $[\alpha]_D^{22}$: +42 (*c* = 1.0, $CHCl_3$); ν_{max} (ATR) 3350 (NH br), 2957 (sp^3 C-H), 1733 (C=O), 1437, 1206, 1155; δ_H ($CDCl_3$, 400 MHz) 4.05–3.97 (2H, m), 3.73 (6H, s, CH_3), 2.70 (1H, s br, N*H*), 2.54–2.11 (2H, m), 2.03–1.89 (2H, m); δ_C ($CDCl_3$, 100 MHz) 174.9, 59.6, 52.2, 29.2; MS (ESI+) $[M+H]^+$ 188. These data are consistent with literature values.[163]

(2*S*,5*S*)-Pyrrolidine-2,5-dicarboxylic acid ((*S*,*S*)-42)[163]

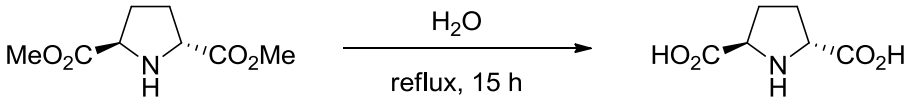


(*S*,*S*)-**41** (*S*,*S*)-**42**

A solution of (*S*,*S*)-**41** (725 mg, 3.87 mmol) in water (20 mL) was heated at reflux for 15 hours. The reaction mixture was then evaporated under reduced pressure, giving a solid which was isolated by suction and washed with methanol to yield (*S*,*S*)-**42** (103 mg, 14 %) as a white, crystalline solid (prisms). m. p. 214–216 °C (MeOH); $[\alpha]_D^{22}$: −96 (*c* = 1.0, H_2O); ν_{max} (ATR) 3350 (NH br), 2957 (sp^3 C-H), 1733 (C=O), 1437, 1206, 1155; δ_H (2% NaOD in D_2O, DSS, 400 MHz) 3.73–3.65 (2H, m), 3.33 (1H, s, NH), 2.19–2.06 (2H,

m), 1.81–1.68 (2H, m); δ_C (2% NaOD in D_2O, DSS, 100 MHz) 178.0, 64.4, 31.7; These data are consistent with literature values.[163]

(2*R*,5*R*)-Pyrrolidine-2,5-dicarboxylic acid ((*R*,*R*)-42)[163]



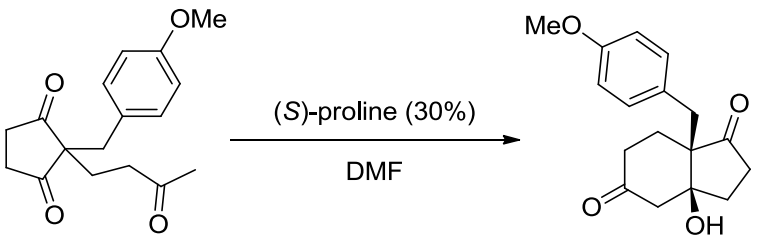
(*R*,*R*)-**41** (*R*,*R*)-**42**

A solution of (*R*,*R*)-**41** (900 mg, 4.81 mmol) in water (25 mL) was heated at reflux for 15 hours. The reaction mixture was then evaporated under reduced pressure, giving a solid which was isolated by suction and washed with methanol to yield (*R*,*R*)-**42** (580 mg, 64 %) as a white, crystalline solid (prisms). m. p. 214–216 °C (MeOH); $[\alpha]_D^{22}$: +96 (*c* = 1.0, H_2O); ν_{max} (ATR) 3350 (NH br), 2957 (sp^3 C-H), 1733 (C=O), 1437, 1206, 1155; δ_H (2% NaOD in D_2O, DSS, 400 MHz) 3.73–3.65 (2H, m) 3.33 (1H, s, N*H*), 2.19–2.06 (2H, m), 1.81–1.68 (2H, m); δ_C (2% NaOD in D_2O, DSS, 100 MHz) 178.0, 64.4, 31.7; These data are consistent with literature values.[163]

8.4. HPESW

8.4.1. HPESW Reactions

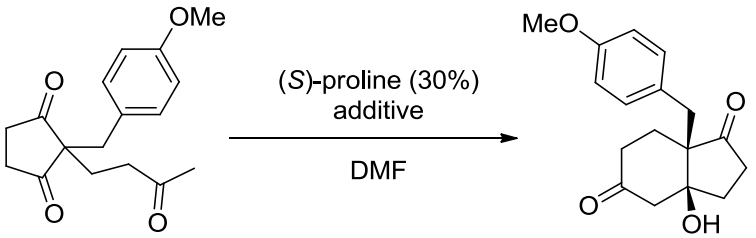
Reactions Using Proline Suspensions Monitored by HPLC



46 **49**

To a stirred solution of triketone **46** (288.3 mg, 1.00 mmol) and a known amount of PhCN (ca. 50 mg, I. S.) in DMF (5 mL) was added (*S*)-proline (34.5 mg, 0.30 mmol) in one portion to initiate the reaction (t=0). The reaction was then monitored by periodic sampling: A 100 µL aliquot is added to NH_4Cl (aq, 1 mL), extracted with EtOAc (2 mL), dried ($MgSO_4$), filtered and analysed by HPLC.

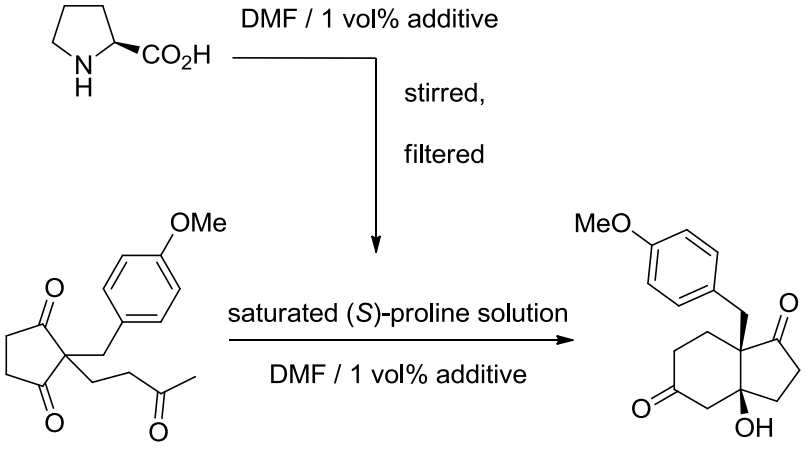
HPLC Conditions: OD-H column; Flow rate = 1 mL min^{-1}; Solvent System = 98:02 (hexane/IPA) hold 16 m, 98:02–90:10 over 75 m, 90:10 hold 65 m; λ = 230 nm; PhCN t_r = 12.1 m, scaling factor = 1.00; **46** t_r = 43.3, scaling factor = 0.89; **49** (minor) t_r = 49.8, scaling factor = 0.92; **49** (major) t_r = 57.0, scaling factor = 0.92.



46 **49**

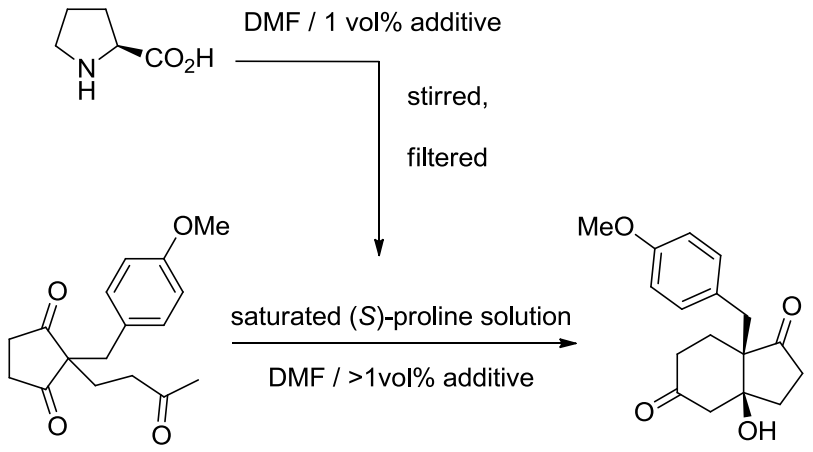
Where additives were employed, the required amount was added to the initial stirred solution in DMF.

Reactions Using Proline Solutions Monitored by HPLC



46 **49**

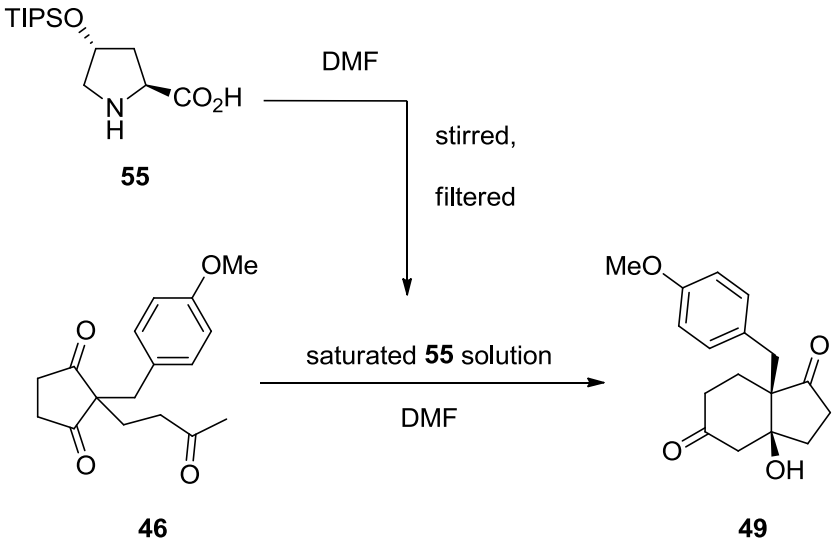
To prepare a proline solution an excess of (*S*)-proline was stirred in DMF for 20 minutes and the suspension was then passed through a 45 μm pore filter. To initiate the HPESW reaction: 5 mL of the proline solution was added to a mixture of triketone **46** (288.3 mg, 1.00 mmol) and a known amount of PhCN (ca. 50 mg, I. S.). The reaction was then monitored by periodic sampling: A 100 μL aliquot is added to NH_4Cl (aq, 1 mL), extracted with EtOAc (2 mL), dried ($MgSO_4$), filtered and analysed by HPLC.



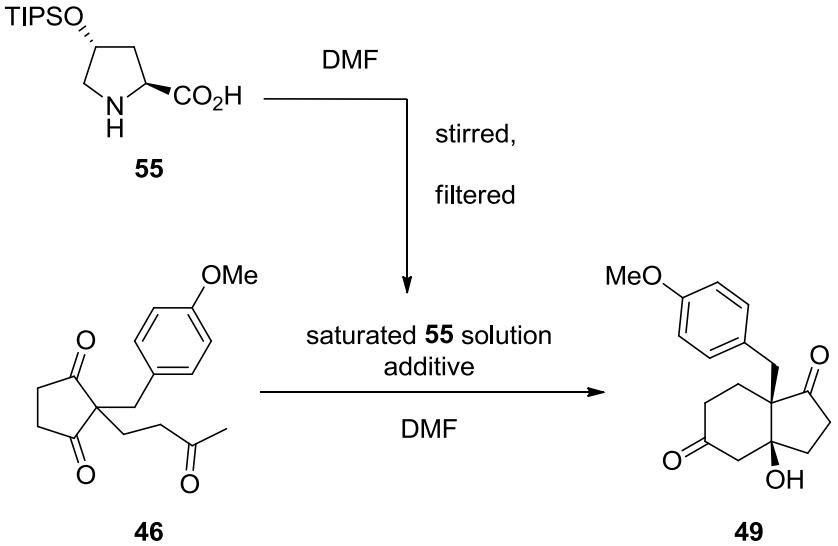
46 **49**

For reactions with total loading of additive in excess of 1 vol%, the required additional amount of additive was added to the mixture of **46** and PhCN prior to addition of the catalyst solution.

Reactions Using Solutions of 55 Monitored by HPLC



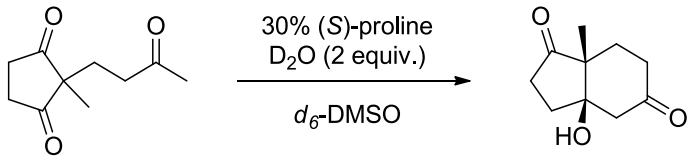
To prepare a solution of **55** an excess of **55** was stirred in DMF for 20 minutes and the suspension was then passed through a 45 μm pore filter. To initiate the HPESW reaction 5 mL of the **55** solution was added to a mixture of triketone **46** (288.3 mg, 1.00 mmol) and a known amount of PhCN (ca. 50 mg, I. S.). The reaction was then monitored by periodic sampling: A 100 μL aliquot is added to NH_4Cl (aq, 1 mL), extracted with EtOAc (2 mL), dried ($MgSO_4$), filtered and analysed by HPLC.



Where additives were employed, the required amount was added to the mixture of **46** and PhCN prior to addition of the catalyst solution.

8.4.2. Deuterium Labelling Experiments

Reaction in the Presence of D_2O Monitored by ^1H NMR Spectroscopy

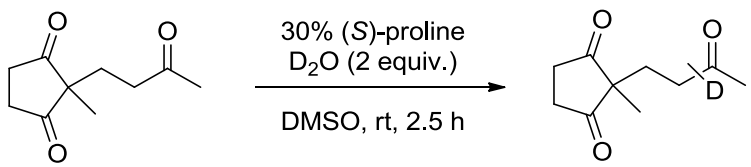


58 **59**

To a stirred solution of triketone **58** (364 mg, 2.00 mmol), PhCN (50 μL), and D_2O (72.4 μL, 4.00 mmol) in d_6-DMSO (10 mL) was added (*S*)-proline (69.1 mg, 0.600 mmol, 30%) in one portion to initiate the reaction (t=0). The reaction was then monitored by periodic sampling: A 1 mL aliquot is transferred to a standard NMR tube, particulates are allowed to settle, and the sample is analysed by ^1H NMR spectroscopy.

For the control experiment carried out to determine the effect of D_2O alone, the same protocol was carried out without proline.

Reaction in the Presence of D_2O – Recovery of Unreacted Triketone 58

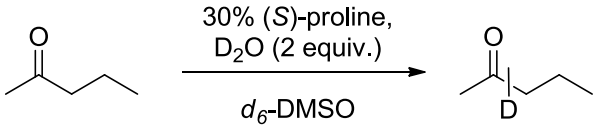


To a stirred solution of triketone **58** (182 mg, 1.00 mmol) and D_2O (36.2 μL, 2.00 mmol) in DMSO (10 mL) was added (*S*)-proline (69.1 mg, 0.300 mmol, 15%) in one portion. After 2.5 hours, a 2.5 mL sample was taken, quenched by addition to H_2O (2.5 mL), extracted with EtOAc (3 mL), dried (Na_2SO_4), filtered, evaporated under reduced

pressure, and purified by flash column chromatography. Unreacted triketone **58** (35.2 mg) was recovered and analysed by ^{1}H NMR spectroscopy to determine the degree of deuterium incorporation.

Quenching control experiment: From the same reaction mixture after 2.5 hours, an additional 2.5 mL sample was taken and quenched by addition to D_2O (2.5 mL) and after subsequent manipulation (as above) unreacted triketone **58** (34.1 mg) was recovered which showed the same degree of deuterium incorporation.

Deuteration of 2-Pentanone by Proline in the Presence of D_2O

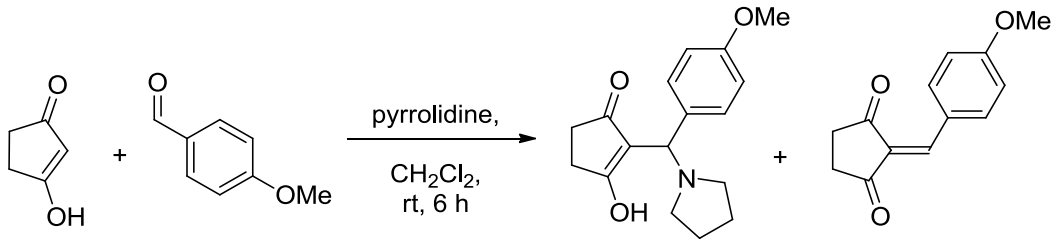


To a stirred solution of 2-pentanone (213 μL, 2.00 mmol), PhCN (50 μL), and D_2O (72.4 μL, 4.00 mmol) in d_6-DMSO (10 mL) was added (*S*)-proline (69.1 mg, 0.600 mmol, 30%) in one portion to initiate the reaction (t=0). The reaction was then monitored by periodic sampling: A 1 mL aliquot is transferred to a standard NMR tube, particulates are allowed to settle, and the sample is analysed by ^{1}H NMR spectroscopy.

For the control experiment carried out to determine the effect of D_2O alone, the same protocol was carried out without proline and no deuterium incorporation was observed.

8.4.3. Synthesis of Required Materials

3-Hydroxy-2-((4'-methoxyphenyl)-pyrrolidyl)methyl-2-cyclopentenone (44)[168]

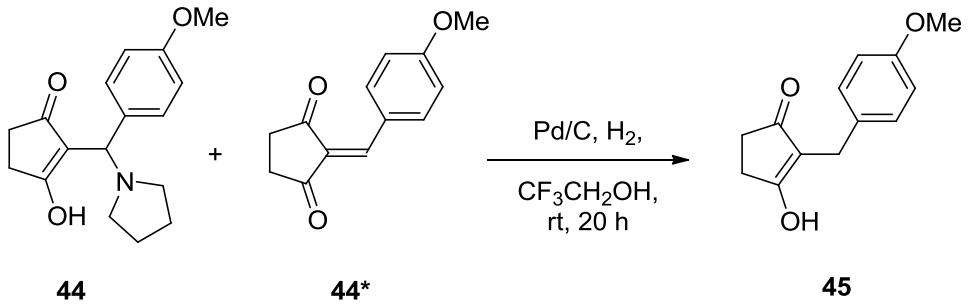


44 **44***

According to the method of Brittain and co-workers:[168] To a stirred solution of 4-methoxybenzaldehyde (2.28 mL, 18.8 mmol) and pyrrolidine (1.07 mL, 12.8 mmol) in CH_2Cl_2 (35 mL) was added a solution of 3-hydroxy-2-cyclopentenone (1.14 g, 12.5 mmol) and pyrrolidine (0.5 mL, 6.0 mmol) in CH_2Cl_2 (35 mL). Over 30 minutes the colour of the mixture changed from yellow to orange. After stirring for 6 hours, the solvent was evaporated under reduced pressure. On addition of EtOAc (20 mL), a light orange precipitate formed which was collected by filtration and washed with EtOAc. ^{1}H NMR analysis showed that the precipitate (1.80 g) consisted of **44** (44%) and **44*** (7%) in an 84:16 ratio. ν_{max} (ATR) 3403, 3043, 2960, 2922, 2835, 1535, 1512, 1444, 1357, 1251; δ_H (400 MHz, CD_3OD) 7.56 (2H, d, *J* = 9.0, Ar*H*), 6.90 (2H, d, *J* = 9.0, Ar*H*), 4.72 (1H, s, C*H*N), 3.78 (3H, s, OC*H*$_3$, 3.24–3.05 (4H, m), 2.33 (4H, s); δ_C (100 MHz, CD_3OD) 203.3, 131.1, 130.8, 115.2, 110.6, 68.3, 55.8, 54.7, 33.2, 25.0, 24.3; MS (ESI) **44*** $[M+H]^+$ 217.1, **44** $[M+H]^+$ 288.2. These data are consistent with literature values.[168]

3-Hydroxy-2-(4'-methoxyphenylmethyl)-2-cyclopentenone (45)[168]

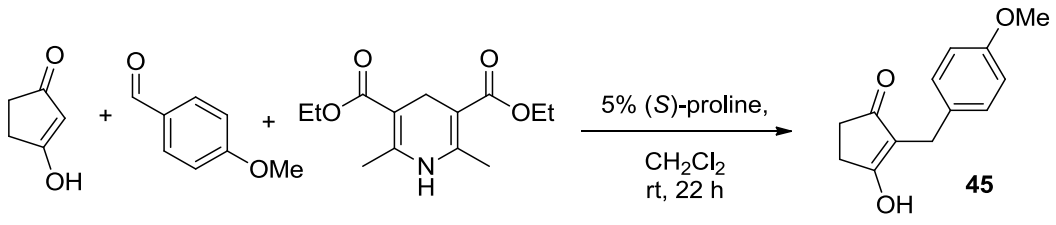
Method 1



44 **44*** **45**

According to the method of Brittain and co-workers:[168] A suspension of 86:14 **44** / **44*** (1.67 g, 6.02 mmol) and 10% wt Pd/C (275 mg, 0.259 mmol Pd) in CF_3CH_2OH (50 mL) was stirred under a balloon of hydrogen. After 20 hours, the reaction vessel was purged with argon and the mixture was filtered through Celite®. The cake was washed with MeOH (20 mL) and the combined filtrate and washings were concentrated under reduced pressure. On addition of 1N HCl (aq, 10 mL), a cream precipitate formed from the orange residue and was collected by filtration, washed with 1N HCl (aq, 5 mL) and dried under high vacuum to yield **45** as a pale yellow solid (1.08 g, 82%).

Method 2

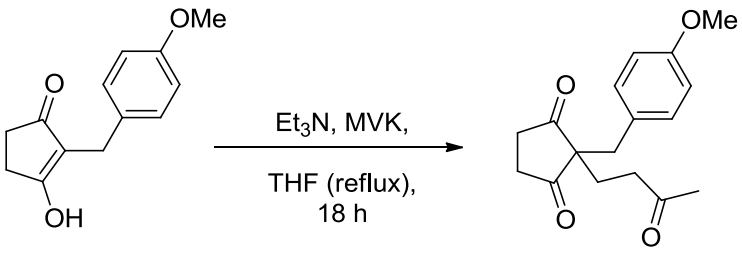


According to the method of Ramachary and Kishor:[169] To a stirred suspension of 3-hydroxy-2-cyclopentenone (2.45 g, 25.0 mmol), 4-methoxybenzaldehyde (9.13 mL, 90.0 mmol) and diethyl-1,4-dihydro-2,6-dimethyl-3,5-pyridine dicarboxylate (6.33 g, 25.0 mmol) in CH_2Cl_2 (83 mL) was added (*S*)-proline (144 mg, 1.25 mmol). After 22

hours, the mixture was filtered and the isolated material washed with CH_2Cl_2 (10 mL) and 1N HCl (aq, 5 mL) to yield **45** as a pale yellow solid (3.38 g, 62%).

m.p. 182–184 °C; ν_{max} (ATR) 3412, 3014, 2969, 2939, 2913, 2834, 1585, 1508; δ_H (400 MHz, CD_3OD) 7.13 (2H, d, *J* = 9.0, Ar*H*), 6.78 (2H, d, *J* = 9.0, Ar*H*), 3.76 (3H, s, OC*H*$_3$), 3.38 (2H, s, ArC*H*$_2$), 2.53 (4H, s, C*H*$_2$C*H*$_2$); δ_C (100 MHz, CD_3OD) 186.0, 159.3, 135.6, 130.3, 118.5, 114.5, 55.6, 31.3, 26.7; HRMS (ESI) $[M+H]^+$ Calc. for $C_{13}H_{15}O_3$: 219.1021, Found: 219.1016. These data are consistent with literature values.[168]

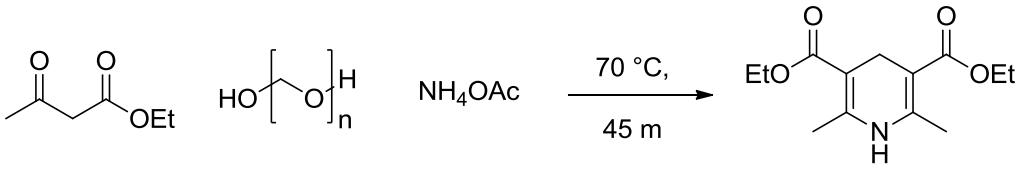
2-(4-methoxybenzyl)-2-(3'-oxobutyl)-1,3-cyclopentanedione (46)[168]



45 **46**

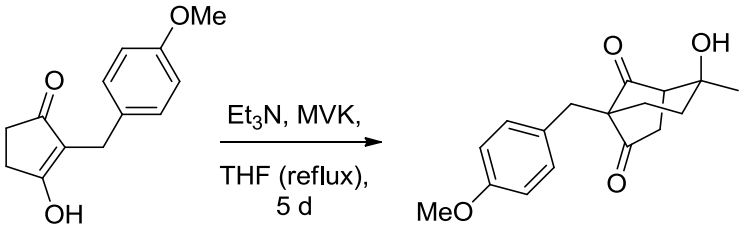
According to the method of Brittain and co-workers:[168] To a stirred solution of **45** (3.38 g, 15.5 mmol) in THF (200 mL) was added triethylamine (10.3 mL, 74.3 mmol) and methyl vinyl ketone (2.99 mL, 30.9 mmol) sequentially. The solution was heated at reflux for 18 hours after which time, the solvent was evaporated under reduced pressure. The crude product was then purified by flash column chromatography (25% EtOAc in *n*-hexane) to yield triketone **46** as a crystalline white solid (2.72 g, 61%). m. p. (EtOAc/*n*-hexane); ν_{max} (ATR) 3023, 2969, 2935, 2845, 1711 s (C=O), 1615, 1516; δ_H (400 MHz, $CDCl_3$) 6.94 (2H, d, *J* = 9.0, Ar*H*), 6.75 (2H, d, *J* = 9.0, Ar*H*), 3.75 (3H, s, OC*H*$_3$) 2.88 (2H, s, ArC*H*$_2$), 2.56 (1H, d, *J* = 7.0, CH_3COC*H*H), 2.51 (1H, d, *J* = 7.0, CH_3COCH*H*), 2.43 (2H, t, *J* = 7.0, $COCH_2$C*H*$_2$), 2.10 (3H, s, COC*H*$_3$), 2.04–1.95 (4H, m, -C*H*$_2$C*H*$_2$C(OH)); δ_C (100 MHz, $CDCl_3$) 217.5, 207.7, 158.8, 130.8, 127.0, 114.1, 61.4, 55.4, 42.5, 38.0, 36.5, 30.1, 28.4; HRMS (NH_3 CI) $[M+NH_4]^+$ Calc. for $C_{17}H_{24}NO_4$: 306.1705 Found: 306.1708. These data are consistent with the literature values.[168]

Diethyl-1,4-dihydro-2,6-dimethyl-3,5-pyridine dicarboxylate (47)[170]



According to the method of Charette and co-workers:[170] A stirred mixture of ethyl acetoacetate (39.0 g, 300 mmol), paraformaldehyde (4.50 g, 150 mmol) and ammonium acetate (17.3 g, 225 mmol) in a 600 mL beaker was heated to 70 °C in a water bath. After 15 minutes, the initial suspension of white solid in colourless liquid had transformed into a pale yellow paste, which thickened and turned orange after a further 30 minutes at which point the mixture was cooled to room temperature. Water (200 mL) was added and the resulting suspension was stirred for 20 minutes and filtered and washed with water (5 × 10 mL). To the filtered material was added ethanol (200 mL) and the suspension was heated at reflux for 5 minutes, then cooled to room temperature, filtered, washed with ethanol (5 × 10 mL) and dried to yield **47** as a bright yellow solid (20.4 g, 54%); m.p. 178–180 °C (EtOH) (lit. 182–183 °C)[183]; ν_{max} (ATR) 3351, 3112, 2990, 1695 s, 1654 s, 1506; δ_H (400 MHz, $CDCl_3$) 5.24 (1H, s, N*H*), 4.16 (4H, q, *J* = 7.0, C*H2*CH3), 3.26 (2H, s, CH_2C=), 2.18 (6H, s, =CCH_3), 1.27 (6H, t, *J* = 7.0, CH_2CH_3); δ_C (100 MHz, $CDCl_3$) 168.1, 144.8, 99.5, 59.7, 24.8, 19.2, 14.5; HRMS (ESI) $[M+H]^+$ Calc. for $C_{13}H_{20}NO_4$: 254.1292, Found: 254.1386. These data are consistent with literature values.[183,184]

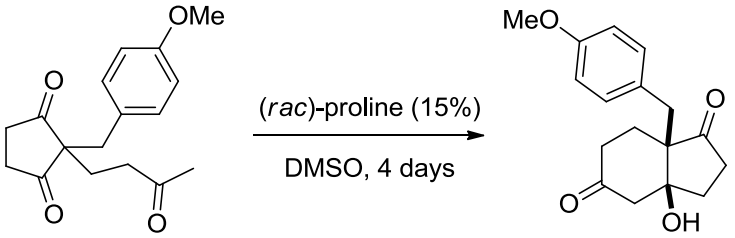
(1,4,5)-4-Hydroxy-1-(4'-methoxyphenyl)methyl-4-methyl-bicyclo[3.2.1]octane-7,8-dione (48)



45 **48**

Exposure of **45** (30.8 mmol) to the reaction conditions described above over 5 days rather than 18 hours resulted in the isolation (after purification) of the expected triketone product **46** (5.14 g, 58%) as well as hydroxy ketone **48** (2.38 g, 27%); m. p. 124–127 °C (EtOAc/*n*-hexane); ν_{max} (ATR) 3432, 2968, 2933, 2853, 1769, 1717, 1612, 1515; δ_H (400 MHz, $CDCl_3$) 7.22 (2H, d, *J* = 8.5, Ar*H*), 6.75 (2H, d, *J* = 8.5, Ar*H*), 3.75 (3H, s, OC*H*$_3$), 2.97–2.84 (2H, m), 2.68 (1H, d, *J* = 7.0), 2.56–2.40 (2H, m), 2.16–2.03 (1H, m), 1.95 (1H, s, O*H*), 1.89–1.79 (1H, m), 1.73–1.65 (2H, m), 1.36 (3H, s, C-C*H*$_3$); δ_C (100 MHz, $CDCl_3$) 213.8, 211.1, 158.0, 131.7, 128.9, 113.3, 80.6, 63.0, 57.3, 55.1, 43.1, 37.6, 32.4, 31.9, 28.2; HRMS (NH_4 CI) $[M+NH_4]^+$ Calc. for $C_{17}H_{21}O_4$: 289.1434 Found: 289.1450. Relative stereochemistry is tentatively assigned by analogy to the known configuration of 4-hydroxy-1-methyl-4-methyl-bicyclo[3.2.1]octane-7,8-dione formed in which the same conditions were applied but under high pressure,[171] which has been determined by X-ray crystallography.[174]

(1*RS*,6*RS*)-1-Hydroxy-6-(4'-methoxyphenyl)methylbicyclo[4.3.0]nonan-3,7-dione (49)[168]

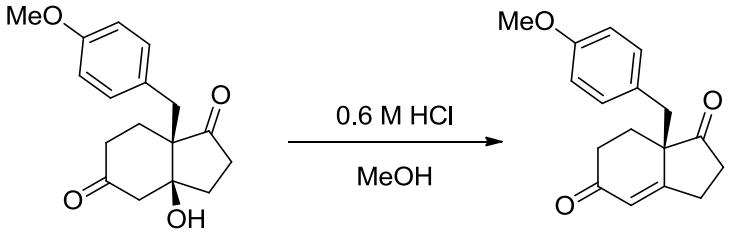


46 **49**

To a solution of **46** (77.6 mg, 0.269 mmol) in DMSO (3 mL) was added (*rac*)-proline (9.3 mg, 0.0807 mmol). After stirring for 4 days, the reaction mixture was added to water (50 mL), extracted (5 × 10 mL CH_2Cl_2), dried ($MgSO_4$), filtered and evaporated under reduced pressure. The crude material was purified by flash column chromatography (30% EtOAc in *n*-hexane) to yield **49** as a white solid (19.1 mg, 25%); m. p. 253–255 °C (EtOAc/*n*-hexane); ν_{max} (ATR) 3019, 2845, 1711 s (C=O), 1613, 1513, 1256; δ_H (400 MHz, $CDCl_3$) 7.15 (2H, d, *J* = 7.0, Ar*H*), 6.81 (2H, d, *J* = 7.0, Ar*H*), 3.78 (3H, s, OCH_3), 3.05 (1H, d, *J* = 14.0), 2.99 (1H, d, *J* = 14.0), 2.63–2.34 (4H, m), 2.28 (1H, s), 2.24–2.11 (2H, m) 2.08–1.88 (2H, m), 1.83 (1H, d, *J* = 7.0), 1.81 (1H, d, *J* = 7.0); δ_C (100 MHz, $CDCl_3$) 217.1, 208.9, 158.8, 131.6, 128.7, 114.0, 82.3, 56.6, 55.4, 51.5, 37.2, 36.1, 34.5, 33.7, 27.8. These data are consistent with literature values.[168]

Additional material was isolated from sampling reactions after purification.

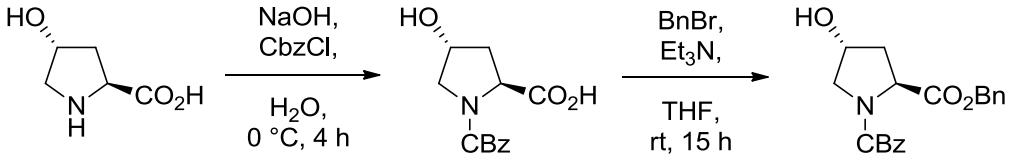
(*R*)-7a-(4-Methoxyphenyl)methyl-2,3,7,7a-tetrahydro-6*H*-indene-1,5-dione (50)[168]



49 **50**

To **49** (24.0 mg, 0.0832 mmol) was added 0.6 M HCl solution in methanol (500 µL) and the solution was stirred for 24 hours after which time the solvents were evaporated and the residue was triturated (EtOH) to yield enone **50** as a white solid (19.8 mg, 88%). m. p. 114–116 °C (EtOH); ν_{max} (ATR) 2962, 2937, 1737, 1664, 1612, 1511; δ_H (400 MHz, $CDCl_3$) 6.99 (2H, d, *J* = 8.5, Ar*H*), 6.80 (2H, d, *J* = 8.5, Ar*H*), 6.05 (1H, s, C(O)C*H*=C), 3.78 (3H, s, OC*H*$_3$), 3.06–2.95 (2H, m), 2.62–2.35 (3H, m), 2.34–2.17 (3H, m), 2.16–2.03 (1H, m), 1.87–1.75 (1H, m); δ_C (100 MHz, $CDCl_3$) 217.9, 198.3, 169.7, 159.1, 130.7, 127.5, 125.1, 114.1, 55.3, 53.4, 41.7, 37.1, 33.0, 29.2, 28.2; HRMS $[M+H]^+$ (ESI) Calc. for $C_{17}H_{19}O_3$: 271.1334, Found: 271.1337. These data are consistent with literature values.[168]

(2*S*, 4*R*)-*N*-Benzyloxycarbonyl-4-hydroxyprolinate benzyl ester (58)[185]



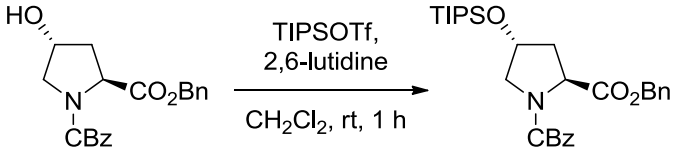
57 **58**

According to the method of Hruby and co-workers:[185] To a stirred solution of (2*S*,4*R*)-4-hydroxyproline (25.6 g, 195 mmol) in H_2O (200 mL) at 0 °C was added NaOH (15.6 g, 390 mmol). After the NaOH had fully dissolved, CBzCl (95%, 31.8 mL, 215 mmol) was

added and the mixture was allowed to stir for 4 hours. The reaction was then quenched with 1N HCl to a pH of 2, extracted with EtOAc (3×200 mL), washed with sat. aq NaCl (200 mL), dried (Na_2SO_4), filtered, and evaporated under reduced pressure to give **57** as a colourless foam (50.5 g) which was used in the next step without further purification; δ_H (400 MHz, $CDCl_3$) 7.42–7.19 (5H, m, ArH), 6.43 (2H, br s, CO_2H + OH) 5.21–5.03 (2H, m, C*H*$_2$Ph), 4.54–4.38 (2H, m), 3.64–3.50 (2H, m), 2.40–2.03 (2H, m).

To a stirred solution of **57** (50.5 g, 190 mmol) and BnBr (25 mL, 209 mmol) in THF (200 mL) at 0 °C was added Et_3N (29 mL, 209 mmol). The mixture was allowed to warm to rt and stirred for 15 hours. After this time, the reaction was evaporated under reduced pressure, redissolved in CH_2Cl_2 (200 mL), sequentially washed with 1N HCl (200 mL), H_2O (200 mL), sat. aq $NaHCO_3$ (200 mL), and H_2O (200 mL), dried (Na_2SO_4), filtered, and evaporated under reduced pressure. The crude product was then purified by elution with 5% MeOH in $CHCl_3$ through a plug of silica to give **58** as a colourless oil (61.1 g, 88% over 2 steps); ν_{max} (ATR) 3441 br (OH), 2955, 2886, 1747, 1685, 1421, 1358, 1192, 1171; δ_H (400 MHz, $CDCl_3$) 7.41–7.15 (10H, m, ArH), 5.26–4.96 (4H, m, 2×C*H*$_2$Ph), 4.62–4.47 (2H, m), 3.74–3.52 (2H, m), 2.37–2.24 (1H, m), 2.15–2.05 (1H, m), 1.74 (1H, br s, OH); δ_C (100 MHz, $CDCl_3$, mixture of *cis* and *trans* conformers) 172.6, 172.4, 155.1, 154.6, 136.5, 136.3, 135.6, 135.4, 128.63, 128.55, 128.5, 128.44, 128.35, 128.21, 128.17, 128.08, 127.96, 127.9, 70.2, 69.4, 67.3, 67.0, 66.9, 58.1, 57.9, 55.3, 54.7, 39.2, 38.4. These data are consistent with literature values.[185]

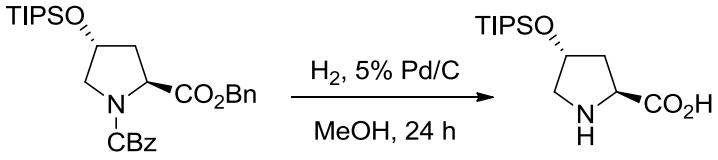
(2*S*, 4*R*)-*N*-Benzyloxycarbonyl-4-triisopropylsiloxyprolinate benzyl ester (59)[173]



58 **59**

To a stirred solution of **58** (4.98 g, 14.0 mmol) in CH_2Cl_2 at 0 °C was added 2,6-lutidine (2.1 mL, 18.2 mmol), then TIPSOTf (4.9 mL, 18.2 mmol). The mixture was allowed to warm to rt and stirred for 1 hour. After this time the reaction was quenched by addition of pH 7 phosphate buffer (20 mL). The layers were separated and the aqueous partition was extracted with EtOAc (3×20 mL), dried (Na_2SO_4), filtered, and evaporated under reduced pressure. The crude product was then purified by flash column chromatography (20% EtOAc in *n*-hexane) to give **59** as a colourless oil (7.11 g, 99%); δ_H (400 MHz, $CDCl_3$) 7.40–7.19 (10H, m, ArH), 5.26–4.92 (4H, m, 2×C*H*$_2$Ph), 4.62–4.46 (2H, m), 3.76–3.63 (2H, m), 3.58–3.44 (2H, m), 1.10–0.93 (21H, m, 3×CH(CH_3)$_2$); δ_C (100 MHz, $CDCl_3$, mixture of *cis* and *trans* conformers) 172.7, 172.5, 155.1, 154.4, 136.7, 136.5, 135.7, 135.5, 128.6, 128.5, 128.42, 128.37, 128.3, 128.23, 128.17, 128.0, 127.9, 127.8, 70.6, 69.9, 67.1, 66.9, 66.8, 58.3, 58.1, 55.3, 54.9, 40.1, 39.1, 17.9, 12.0; HRMS (ESI) Calc. for $C_{29}H_{42}NO_5Si^+$: 512.2827, Found: 512.2804. These data are consistent with literature values.[173]

(2*S*, 4*R*)-Triisopropylsiloxyproline (55)[173]

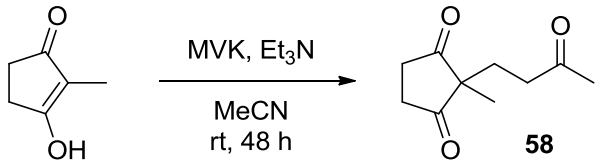


59 **55**

According to the method of Hayashi and co-workers: To a stirred suspension of 10 wt% Pd/C (733 mg, 0.689 mmol, 5%) in MeOH (5 mL) was added **59** (7.05 g, 13.8 mmol) in MeOH (9 mL). The reaction vessel was thrice evacuated and filled with an atmosphere of argon before being evacuated and filled with an atmosphere of hydrogen. The mixture was then stirred for 24 hours after which time it was filtered through a plug of Celite® under a flow of argon and washed with MeOH (ca. 10 mL). The filtrate was then evaporated under reduced pressure to give **55** as a light tan solid which required no further purification (3.39 g, 85%). $[\alpha]_D^{22}$: −15.6 (*c* = 1.0, $CDCl_3$); m. p. 128–130 °C (MeOH); ν_{max} (ATR) 3442, 2940, 1621, 1415, 1120; δ_H (400 MHz, $CDCl_3$) 10.2 (1H, br s,

CO_2H), 8.6 (1H, br, s, NH), 4.72–4.63 (1H, m), 4.58–4.46 (1H, m), 3.83–3.71 (1H, m), 3.40–3.26 (1H, m), 2.41–2.21 (2H, m), 1.17–0.94 (21H, m); δ_C (100 MHz, $CDCl_3$) 171.7, 70.9, 59.2, 54.2, 38.6, 18.0, 12.0. These data are consistent with literature values.[173]

2-Methyl-2-(3'-oxobutyl)cyclopentane-1,3-dione (58)[186]



According to the method of Vincent, Landais, and co-workers: To a stirred suspension of 3-hydroxy-2-methyl-2-cyclopentenone (1.00 g, 8.91 mmol) in MeCN (13 mL) was added Et_3N (4.35 mL, 31.2 mmol). The mixture was stirred for 15 minutes before addition of MVK (891 μL, 10.7 mmol). After 48 hours, the reaction mixture was evaporated under reduced pressure and the crude product was purified by flash column chromatography (50% EtOAc in *n*-hexane) to give **58** as a pale yellow oil (1.39 g, 86%); ν_{max} (ATR) 2982, 2933, 1764, 1713 (C=O), 1420, 1367; δ_H (400 MHz, $CDCl_3$) 2.91–2.68 (4H, m, $COCH_2CH_2CO$), 2.45 (2H, t, *J* = 7.1, CH_3COCH_2), 2.09 (3H, s, $COCH_3$), 1.88 (2H, *t*, J = 7.0, $CH_3COCH_2CH_2$), 1.10 (3H, s, CR_3CH_3); δ_C (100 MHz, $CDCl_3$) 215.8, 207.8, 55.0, 37.3, 34.6, 29.9, 27.7, 18.8. These data are consistent with literature values.[186]

9. References

(1) Movassaghi, M.; Jacobsen, E. N. *Science* **2002**, *298*, 1904.

(2) For a recent historical perspective see: List, B. *Angew. Chem., Int. Ed.* **2010**, *49*, 1730.

(3) Denmark, S. E.; Beutner, G. L. *Angew. Chem., Int. Ed.* **2008**, *47*, 1560.

(4) Murugan, R.; Scriven, E. F. V. *Aldrichimica Acta* **2003**, *36*, 21.

(5) Melchiorre, P.; Marigo, M.; Carlone, A.; Bartoli, G. *Angew. Chem., Int. Ed.* **2008**, *47*, 6138.

(6) List, B.; Lerner, R. A.; Barbas, C. F. *J. Am. Chem. Soc.* **2000**, *122*, 2395.

(7) Ahrendt, K. A.; Borths, C. J.; MacMillan, D. W. C. *J. Am. Chem. Soc.* **2000**, *122*, 4243.

(8) List, B. *J. Am. Chem. Soc.* **2000**, *122*, 9336

(9) Pojarliev, P.; Biller, W. T.; Martin, H. J. *J. Am. Chem. Soc.* **2002**, *124*, 827.

(10) Notz, W.; Sakthivel, K.; Bui, T.; Zhong, G. F.; Barbas, C. F. *Tetrahedron Lett.* **2001**, *42*, 199.

(11) Bøgevig, A.; Juhl, K.; Kumaragurubaran, N.; Zhuang, W.; Jørgensen, K. A. *Angew. Chem., Int. Ed.* **2002**, *41*, 1790.

(12) List, B. *J. Am. Chem. Soc.* **2002**, *124*, 5656.

(13) Brown, S. P.; Brochu, M. P.; Sinz, C. J.; MacMillan, D. W. C. *J. Am. Chem. Soc.* **2003**, *125*, 10808.

(14) Hayashi, Y.; Yamaguchi, J.; Hibino, K.; Shoji, M. *Tetrahedron Lett.* **2003**, *44*, 8293.

(15) Zhong, G. F. *Angew. Chem., Int. Ed.* **2003**, *42*, 4247.

(16) Kano, T.; Ueda, M.; Takai, J.; Maruoka, K. *J. Am. Chem. Soc.* **2006**, *128*, 6046.

(17) Cordova, A.; Sunden, H.; Engqvist, M.; Ibrahem, I.; Casas, J. *J. Am. Chem. Soc.* **2004**, *126*, 8914.

(18) Enders, D.; Huttl, M. R. M. *Synlett* **2005**, 991.

(19) Steiner, D. D.; Mase, N.; Barbas, C. F. *Angew. Chem., Int. Ed.* **2005**, *44*, 3706.

(20) Beeson, T. D.; MacMillan, D. W. C. *J. Am. Chem. Soc.* **2005**, *127*, 8826.

(21) Marigo, M.; Fielenbach, D. I.; Braunton, A.; Kjærsgaard, A.; Jørgensen, K. A. *Angew. Chem., Int. Ed.* **2005**, *44*, 3703.

(22) Brochu, M. P.; Brown, S. P.; MacMillan, D. W. C. *J. Am. Chem. Soc.* **2004**, *126*, 4108.

(23) Halland, N.; Braunton, A.; Bachmann, S.; Marigo, M.; Jørgensen, K. A. *J. Am. Chem. Soc.* **2004**, *126*, 4790.

(24) Marigo, M.; Wabnitz, T. C.; Fielenbach, D.; Jørgensen, K. A. *Angew. Chem., Int. Ed.* **2005**, *44*, 794.

(25) Tiecco, M.; Carlone, A.; Sternativo, S.; Marini, F.; Bartoli, G.; Melchiorre, P. *Angew. Chem., Int. Ed.* **2007**, *46*, 6882.

(26) Notz, W.; List, B. *J. Am. Chem. Soc.* **2000**, *122*, 7386.

(27) Sakthivel, K.; Notz, W.; Bui, T.; Barbas, C. F. *J. Am. Chem. Soc.* **2001**, *123*, 5260.

(28) Cordova, A.; Notz, W.; Barbas, C. F. *J. Org. Chem.* **2002**, *67*, 301.

(29) Northrup, A. B.; MacMillan, D. W. C. *J. Am. Chem. Soc.* **2002**, *124*, 6798.

(30) Pidathala, C.; Hoang, L.; Vignola, N.; List, B. *Angew. Chem., Int. Ed.* **2003**, *42*, 2785.

(31) Northrup, A. B.; Mangion, I. K.; Hettche, F.; MacMillan, D. W. C. *Angew. Chem., Int. Ed.* **2004**, *43*, 2152.

(32) Northrup, A. B.; MacMillan, D. W. C. *Science* **2004**, *305*, 1752.

(33) Kano, T.; Sugimoto, H.; Maruoka, K. *J. Am. Chem. Soc.* **2011**, *133*, 18130.

(34) Urushima, T.; Yasui, Y.; Ishikawa, H.; Hayashi, Y. *Org. Lett.* **2010**, *12*, 2966.

(35) Kano, T.; Noishiki, A.; Sakamoto, R.; Maruoka, K. *Chem. Commun.* **2011**, *47*, 10626.

(36) Cordova, A.; Watanabe, S.; Tanaka, F.; Notz, W.; Barbas, C. F. *J. Am. Chem. Soc.* **2002**, *124*, 1866.

(37) Cordova, A.; Notz, W.; Zhong, G. F.; Betancort, J. M.; Barbas, C. F. *J. Am. Chem. Soc.* **2002**, *124*, 1842.

(38) Dambruoso, P.; Massi, A.; Dondoni, A. *Org. Lett.* **2005**, *7*, 4657.

(39) Tokuda, O.; Kano, T.; Gao, W. G.; Ikemoto, T.; Maruoka, K. *Org. Lett.* **2005**, *7*, 5103.

(40) Samanta, S.; Zhao, C. G. *J. Am. Chem. Soc.* **2006**, *128*, 7442.

(41) Qiu, L. H.; Shen, Z. X.; Shi, C. Q.; Liu, Y. H.; Zhang, Y. W. *Chin. J. Chem.* **2005**, *23*, 584.

(42) Zhang, D.; Yuan, C. *Tetrahedron* **2008**, *64*, 2480.

(43) Hara, N.; Tamura, R.; Funahashi, Y.; Nakamura, S. *Org. Lett.* **2011**, *13*, 1662.

(44) Duangdee, N.; Harnying, W.; Rulli, G.; Neudoerfl, J.-M.; Groeger, H.; Berkessel, A. *J. Am. Chem. Soc.* **2012**, *134*, 11196.

(45) Almasi, D.; Alonso, D. A.; Najera, C. *Tetrahedron: Asymmetry* **2007**, *18*, 299.

(46) Vignola, N.; List, B. *J. Am. Chem. Soc.* **2004**, *126*, 450.

(47) Beeson, T. D.; Mastracchio, A.; Hong, J.-B.; Ashton, K.; MacMillan, D. W. C. *Science* **2007**, *316*, 582.

(48) Shih, H.-W.; Vander Wal, M. N.; Grange, R. L.; MacMillan, D. W. C. *J. Am. Chem. Soc.* **2010**, *132*, 13600.

(49) Jang, H.-Y.; Hong, J.-B.; MacMillan, D. W. C. *J. Am. Chem. Soc.* **2007**, *129*, 7004.

(50) Nagib, D. A.; Scott, M. E.; MacMillan, D. W. C. *J. Am. Chem. Soc.* **2009**, *131*, 10875.

(51) Afewerki, S.; Ibrahem, I.; Rydfjord, J.; Breistein, P.; Cordova, A. *Chem. Eur. J.* **2012**, *18*, 2972.

(52) Cozzi, P. G.; Benfatti, F.; Zoli, L. *Angew. Chem., Int. Ed.* **2009**, *48*, 1313.

(53) Benfatti, F.; Benedetto, E.; Cozzi, P. G. *Chem. Asian J.* **2010**, *5*, 2047.

(54) Allen, A. E.; MacMillan, D. W. C. *J. Am. Chem. Soc.* **2010**, *132*, 4986.

(55) Allen, A. E.; MacMillan, D. W. C. *J. Am. Chem. Soc.* **2011**, *133*, 4260.

(56) Skucas, E.; MacMillan, D. W. C. *J. Am. Chem. Soc.* **2012**, *134*, 9090.

(57) Erkkila, A.; Majander, I.; Pihko, P. M. *Chem. Rev.* **2007**, *107*, 5416.

(58) Yang, J. W.; Fonseca, M. T. H.; Vignola, N.; List, B. *Angew. Chem., Int. Ed.* **2005**, *44*, 108.

(59) Ouellet, S. G.; Tuttle, J. B.; MacMillan, D. W. C. *J. Am. Chem. Soc.* **2005**, *127*, 32.

(60) Marigo, M.; Franzén, J.; Poulsen, T. B.; Zhuang, W.; Jørgensen, K. A. *J. Am. Chem. Soc.* **2005**, *127*, 6964.

(61) Vesely, J.; Ibrahem, I.; Zhao, G.-L.; Rios, R.; Cordova, A. *Angew. Chem., Int. Ed.* **2007**, *46*, 778.

(62) Hashimoto, T.; Maruoka, K. The Basic Principle of Phase-Transfer Catalysis and Some Mechanistic Aspects. In *Asymmetric Phase Transfer Catalysis*; Maruoka, K. Ed.; Wiley-VCH, **2008**.

(63) Ooi, T.; Maruoka, K. *Angew. Chem., Int. Ed.* **2007**, *46*, 4222.

(64) Enders, D.; Thanh Vinh, N. *Org. Biomol. Chem.* **2012**, *10*, 5327.

(65) Corey, E. J.; Xu, F.; Noe, M. C. *J. Am. Chem. Soc.* **1997**, *119*, 12414.

(66) Jew, S. S.; Yoo, M. S.; Jeong, B. S.; Park, I. Y.; Park, H. G. *Org. Lett.* **2002**, *4*, 4245.

(67) Ooi, T.; Kameda, M.; Maruoka, K. *J. Am. Chem. Soc.* **2003**, *125*, 5139.

(68) Kitamura, M.; Shirakawa, S.; Maruoka, K. *Angew. Chem., Int. Ed.* **2005**, *44*, 1549.

(69) Akiyama, T.; Itoh, J.; Yokota, K.; Fuchibe, K. *Angew. Chem., Int. Ed.* **2004**, *43*, 1566.

(70) Uraguchi, D.; Terada, M. *J. Am. Chem. Soc.* **2004**, *126*, 5356.

(71) Rueping, M.; Antonchick, A. R.; Theissmann, T. *Angew. Chem., Int. Ed.* **2006**, *45*, 3683.

(72) Rueping, M.; Nachtsheim, B. J.; Ieawsuwan, W.; Atodiresei, I. *Angew. Chem., Int. Ed.* **2011**, *50*, 6706.

(73) Rueping, M.; Kuenkel, A.; Atodiresei, I. *Chem. Soc. Rev.* **2011**, *40*, 4539.

(74) Sigman, M. S.; Jacobsen, E. N. *J. Am. Chem. Soc.* **1998**, *120*, 4901.

(75) Okino, T.; Hoashi, Y.; Takemoto, Y. *J. Am. Chem. Soc.* **2003**, *125*, 12672.

(76) Doyle, A. G.; Jacobsen, E. N. *Chem. Rev.* **2007**, *107*, 5713.

(77) Marcelli, T.; Hiemstra, H. *Synthesis* **2010**, 1229.

(78) Noyori, R. *Angew. Chem., Int. Ed.* **2002**, *41*, 2008.

(79) Knowles, W. S. *Angew. Chem., Int. Ed.* **2002**, *41*, 1999.

(80) Sharpless, K. B. *Angew. Chem., Int. Ed.* **2002**, *41*, 2024.

(81) Ishikawa, H.; Suzuki, T.; Hayashi, Y. *Angew. Chem., Int. Ed.* **2009**, *48*, 1304.

(82) Michrowska, A.; List, B. *Nat. Chem.* **2009**, *1*, 225.

(83) Grondal, C.; Jeanty, M.; Enders, D. *Nat. Chem.* **2010**, *2*, 167.

(84) Eder, U.; Sauer, G.; Weichert, R. *Angew. Chem., Int. Ed.* **1971**, *10*, 496.

(85) Hajos, Z. G.; Parrish, D. R. *J. Org. Chem.* **1974**, *39*, 1615.

(86) Cobb, A. J. A.; Shaw, D. M.; Ley, S. V. *Synlett* **2004**, 558.

(87) Torii, H.; Nakadai, M.; Ishihara, K.; Saito, S.; Yamamoto, H. *Angew. Chem., Int. Ed.* **2004**, *43*, 1983.

(88) Hartikka, A.; Arvidsson, P. I. *Eur. J. Org. Chem.* **2005**, 4287.

(89) Dahlin, N.; Bøgevig, A.; Adolfsson, H. *Adv. Synth. Catal.* **2004**, *346*, 1101.

(90) Saito, S.; Nakadai, M.; Yamamoto, H. *Synlett* **2001**, 1245.

(91) Alexakis, A.; Andrey, O. *Org. Lett.* **2002**, *4*, 3611.

(92) Tang, Z.; Yang, Z. H.; Chen, X. H.; Cun, L. F.; Mi, A. Q.; Jiang, Y. Z.; Gong, L. Z. *J. Am. Chem. Soc.* **2005**, *127*, 9285.

(93) Franzén, J.; Marigo, M.; Fielenbach, D.; Wabnitz, T. C.; Kjærsgaard, A.; Jørgensen, K. A. *J. Am. Chem. Soc.* **2005**, *127*, 18296.

(94) Hayashi, Y.; Gotoh, H.; Hayashi, T.; Shoji, M. *Angew. Chem., Int. Ed.* **2005**, *44*, 4212.

(95) Jung, M. E. *Tetrahedron* **1976**, *32*, 3.

(96) Puchot, C.; Samuel, O.; Dunach, E.; Zhao, S.; Agami, C.; Kagan, H. B. *J. Am. Chem. Soc.* **1986**, *108*, 2353.

(97) Hoang, L.; Bahmanyar, S.; Houk, K. N.; List, B. *J. Am. Chem. Soc.* **2003**, *125*, 16.

(98) Klussmann, M.; Iwamura, H.; Mathew, S. P.; Wells, D. H.; Pandya, U.; Armstrong, A.; Blackmond, D. G. *Nature* **2006**, *441*, 621.

(99) List, B.; Hoang, L.; Martin, H. J. *Proc. Natl. Acad. Sci. U. S. A.* **2004**, *101*, 5839.

(100) Clemente, F. R.; Houk, K. N. *Angew. Chem., Int. Ed.* **2004**, *43*, 5766.

(101) Bahmanyar, S.; Houk, K. N. *J. Am. Chem. Soc.* **2001**, *123*, 12911.

(102) Bahmanyar, S.; Houk, K. N. *J. Am. Chem. Soc.* **2001**, *123*, 11273.

(103) Bahmanyar, S.; Houk, K. N.; Martin, H. J.; List, B. *J. Am. Chem. Soc.* **2003**, *125*, 2475.

(104) Cheong, P. H. Y.; Houk, K. N. *Synthesis* **2005**, 1533.

(105) Armstrong, A.; Bhonoah, Y.; White, A. J. P. *J. Org. Chem.* **2009**, *74*, 5041.

(106) Seebach, D.; Beck, A. K.; Badine, D. M.; Limbach, M.; Eschenmoser, A.; Treasurywala, A. M.; Hobi, R.; Prikoszovich, W.; Linder, B. *Helv. Chim. Acta* **2007**, *90*, 425.

(107) Schmid, M. B.; Zeitler, K.; Gschwind, R. M. *Angew. Chem., Int. Ed.* **2010**, *49*, 4997.

(108) Hein, J. E.; Bures, J.; Lam, Y.-h.; Hughes, M.; Houk, K. N.; Armstrong, A.; Blackmond, D. G. *Org. Lett.* **2011**, *13*, 5644.

(109) Schmid, M. B.; Zeitler, K.; Gschwind, R. M. *Chem. Eur. J.* **2012**, *18*, 3362.

(110) Schmid, M. B.; Zeitler, K.; Gschwind, R. M. *J. Am. Chem. Soc.* **2011**, *133*, 7065.

(111) Schmid, M. B.; Zeitler, K.; Gschwind, R. M. *Chem. Sci.* **2011**, *2*, 1793.

(112) Bock, D. A.; Lehmann, C. W.; List, B. *Proc. Natl. Acad. Sci. U. S. A.* **2010**, *107*, 20636.

(113) Blackmond, D. G. *Angew. Chem., Int. Ed.* **2005**, *44*, 4302.

(114) Gruttadauria, M.; Giacalone, F.; Noto, R. *Adv. Synth. Catal.* **2009**, *351*, 33.

(115) Pihko, P. M.; Laurikainen, K. M.; Usano, A.; Nyberg, A. I.; Kaavi, J. A. *Tetrahedron* **2006**, *62*, 317.

(116) Nyberg, A. I.; Usano, A.; Pihko, P. M. *Synlett* **2004**, 1891.

(117) Zotova, N.; Franzke, A.; Armstrong, A.; Blackmond, D. G. *J. Am. Chem. Soc.* **2007**, *129*, 15100.

(118) Zotova, N.; Broadbelt, L. J.; Armstrong, A.; Blackmond, D. G. *Bioorg. Med. Chem. Lett.* **2009**, *19*, 3934.

(119) Mathew, S. P.; Iwamura, H.; Blackmond, D. G., *Angew. Chem., Int. Ed.* **2004**, *43*, 3317.

(120) Iwamura, H.; Mathew, S. P.; Blackmond, D. G. *J. Am. Chem. Soc.* **2004**, *126*, 11770.

(121) Mathew, S. P.; Klussmann, M.; Iwamura, H.; Wells, D. H.; Armstrong, A.; Blackmond, D. G. *Chem. Commun.* **2006**, 4291.

(122) Zotova, N.; Moran, A.; Armstrong, A.; Blackmond, D. G. *Adv. Synth. Catal.* **2009**, *351*, 2765.

(123) Jencks, W. P. *Acc. Chem. Res.* **1976**, *9*, 425.

(124) Dinér, P.; Kjærsgaard, A.; Lie, M. A.; Jørgensen, K. A. *Chem. Eur. J.* **2008**, *14*, 122.

(125) Sharma, A. K.; Sunoj, R. B. *Chem. Commun.* **2011**, *47*, 5759.

(126) Kubota, Y.; Takeuchi, K.; Hanaoka, T. A.; Sugi, Y. *Catal. Today* **1996**, *31*, 27.

(127) Fuji, T.; Nishida, H.; Abiru, Y.; Yamamoto, M.; Kise, M. *Chem. Pharm. Bull.* **1995**, *43*, 1872.

(128) Castro, E. A.; Campodonico, P. R.; Contreras, R.; Fuentealba, P.; Santos, J. G.; Leis, J. R.; Garcia-Rio, L.; Saez, J. A.; Domingo, L. R. *Tetrahedron* **2006**, *62*, 2555.

(129) Castro, E. A.; Aliaga, M.; Santos, J. G. *J. Org. Chem.* **2004**, *69*, 6711.

(130) Leffek, K. T.; Pruszynski, P.; Thanapaalasingham, K. *Can. J. Chem.* **1989**, *67*, 590.

(131) Schwesinger, R.; Schlemper, H.; Hasenfratz, C.; Willaredt, J.; Dambacher, T.; Breuer, T.; Ottaway, C.; Fletschinger, M.; Boele, J.; Fritz, H.; Putzas, D.; Rotter, H. W.; Bordwell, F. G.; Satish, A. V.; Ji, G. Z.; Peters, E. M.; Peters, K.; von Schnering, H. G.; Walz, L. *Liebigs Ann. Chem.* **1996**, 1055.

(132) Fouque, E.; Rousseau, G. *Synthesis* **1989**, 661.

(133) Fickling, M. M.; Fischer, A.; Mann, B. R.; Packer, J.; Vaughan, J. *J. Am. Chem. Soc.* **1959**, *81*, 4226.

(134) Chrystiuk, E.; Williams, A. *J. Am. Chem. Soc.* **1987**, *109*, 3040.

(135) Oszczapowicz, J.; Raczynska, E. *J. Chem. Soc., Perkin Trans. 2* **1984**, 1643.

(136) Pruszynski, P. *Can. J. Chem.* **1987**, *65*, 626.

(137) Cunningham, I. D.; Woolfall, M. *J. Org. Chem.* **2005**, *70*, 9248.

(138) Im, G. Y. J.; Bronner, S. M.; Goetz, A. E.; Paton, R. S.; Cheong, P. H. Y.; Houk, K. N.; Garg, N. K. *J. Am. Chem. Soc.* **2010**, *132*, 17933.

(139) Velcicky, J.; Soicke, A.; Steiner, R.; Schmalz, H.-G. *J. Am. Chem. Soc.* **2011**, *133*, 6948.

(140) Anzini, M.; Chelini, A.; Mancini, A.; Cappelli, A.; Frosini, M.; Ricci, L.; Valoti, M.; Magistretti, J.; Castelli, L.; Giordani, A.; Makovec, F.; Vomero, S. *J. Med. Chem.* **2010**, *53*, 734.

(141) Okujima, T.; Tomimori, Y.; Nakamura, J.; Yamada, H.; Uno, H.; Ono, N. *Tetrahedron* **2010**, *66*, 6895.

(142) Dippy, J.F.J.; Hughes, S.R.C.; Rozanski, A. *J. Chem. Soc.* **1959**, 2492.

(143) Bartnicka, H.; Bojanowska, I.; Kalinowski, M. K. *Aust. J. Chem.* **1991**, *44*, 1077.

(144) Andrew, R. J.; Mellor, J. M. *Tetrahedron* **2000**, *56*, 7267.

(145) Tong, S.-T.; Brimble, M. A.; Barker, D. *Tetrahedron* **2009**, *65*, 4801.

(146) Bella, M.; Schietroma, D. M. S.; Cusella, P. P.; Gasperi, T.; Visca, V. *Chem. Commun.* **2009**, 597.

(147) Xu, L.-W.; Luo, J.; Lu, Y. *Chem. Commun.* **2009**, 1807.

(148) Khan, M. N. J. Chem. Soc., Perkin Trans. 2 **1989**, 199.

(149) Yamaguchi, M.; Shiraishi, T.; Igarashi, Y.; Hirama, M. *Tetrahedron Lett.* **1994**, *35*, 8233.

(150) Yamaguchi, M.; Shiraishi, T.; Hirama, M. *J. Org. Chem.* **1996**, *61*, 3520.

(151) Fernandez-Lopez, R.; Kofoed, J.; Machuqueiro, M.; Darbre, T. *Eur. J. Org. Chem.* **2005**, 5268.

(152) Marcoux, D.; Charette, A. B. *Adv. Synth. Catal.* **2008**, *350*, 2967.

(153) Shao, Z.; Zhang, H. *Chem. Soc. Rev.* **2009**, *38*, 2745.

(154) Loh, C. C. J.; Enders, D. *Chem. Eur. J.* **2012**, *18*, 10212.

(155) Hein, J. E.; Armstrong, A.; Blackmond, D. G. *Org. Lett.* **2011**, *13*, 4300.

(156) Blackmond, D. G.; Moran, A.; Hughes, M.; Armstrong, A. *J. Am. Chem. Soc.* **2010**, *132*, 7598.

(157) Kanzian, T.; Lakhdar, S.; Mayr, H. *Angew. Chem., Int. Ed.* **2010**, *49*, 9526.

(158) http://www.cup.uni-muenchen.de/oc/mayr/DBintro.html

(159) Wang, J.; Feringa, B. L. *Science* **2011**, *331*, 1429.

(160) Luo, S.; Zhou, P.; Li, J.; Cheng, J.-P. *Chem. Eur. J.* **2010**, *16*, 4457.

(161) List, B.; Barbas, C. F.; Lerner, R. A. *Proc. Natl. Acad. Sci. U. S. A.* **1998**, *95*, 15351.

(162) Gu, Q.; Wang, X. F.; Wang, L.; Wu, X. Y.; Zhou, Q. L. *Tetrahedron: Asymmetry* **2006**, *17*, 1537.

(163) Yamamoto, Y.; Hoshino, J.; Fujimoto, Y.; Ohmoto, J.; Sawada, S. *Synthesis* **1993**, 298.

(164) Kemp, D. S.; Curran, T. P. *J. Org. Chem.* **1988**, *53*, 5729.

(165) For a comprehensive review on applications of the Wieland Miescher ketone: Bradshaw, B.; Bonjoch, J. *Synlett* **2012**, 337.

(166) Zhu, H.; Clemente, F. R.; Houk, K. N.; Meyer, M. P. *J. Am. Chem. Soc.* **2009**, *131*, 1632.

(167) Patil, M. P.; Sunoj, R. B. *J. Org. Chem.* **2007**, *72*, 8202.

(168) Kennedy, J. W. J.; Vietrich, S.; Weinmann, H.; Brittain, D. E. A. *J. Org. Chem.* **2008**, *73*, 5151.

(169) Ramachary, D. B.; Kishor, M. *Org. Biomol. Chem.* **2008**, *6*, 4176.

(170) Barbe, G.; Charette, A. B *J. Am. Chem. Soc.***2008**, 130, 18.

(171) Dauben, W. G.; Bunce, R. A. *J. Org. Chem.* **1983**, *48*, 4642.

(172) Hayashi, Y.; Sumiya, T.; Takahashi, J.; Gotoh, H.; Urushima, T.; Shoji, M. *Angew. Chem., Int. Ed.* **2006**, *45*, 958.

(173) Hayashi, Y.; Yamaguchi, J.; Hibino, K.; Sumiya, T.; Urushima, T.; Shoji, M.; Hashizume, D.; Koshino, H. *Adv. Synth. Catal.* **2004**, *346*, 1435.

(174) Davies, S. G.; Russell, A. J.; Sheppard, R. L.; Smith, A. D.; Thomson, J. E. *Org. Biomol. Chem.* **2007**, *5*, 3190.

(175) Kumaragurubaran, N.; Juhl, K.; Zhuang, W.; Bøgevig, A.; Jørgensen, K. A. *J. Am. Chem. Soc.* **2002**, *124*, 6254.

(176) Howard-Lock, H. E.; Lock, C. J. L.; Martins, M. L.; Smalley, P. S.; Bell, R. A. *Can. J. Chem.* **1986**, *64*, 1215.

(177) Marcoux, D.; Charette, A. B. *J. Org. Chem.* **2008**, *73*, 590.

(178) Wempe, M. F. *J. Mol. Struct.* **2001**, *562*, 63.

(179) Patroni, J. J.; Skelton, B. W.; Stick, R. V.; White, A. H. *Aust. J. Chem.* **1980**, *33*, 987.

(180) Wyman, I. W.; Macartney, D. H. *J. Org. Chem.* **2009**, *74*, 8031.

(181) Bellis, E.; Kokotos, G. *Tetrahedron* **2005**, *61*, 8669.

(182) Watson Jr., H. A.; O'Neill, B.T., *J. Org. Chem.*, **1990**, 55 (9), 2950

(183) Eynden, J. J. V.; Delfosse, F.; Mayence, A.; Haverbeke, Y. V. *Tetrahedron* **1995**, *51*, 6511.

(184) Torchy, S.; Cordonnier, G.; Barbry, D.; Vanden Eynde, J. J. *Molecules* **2002**, *7*, 528.

(185) Tamaki, M.; Han, G. X.; Hruby, V. J. *J. Org. Chem.* **2001**, *66*, 1038.

(186) Lacoste, E.; Vaique, E.; Berlande, M.; Pianet, I.; Vincent, J.-M.; Landais, Y. *Eur. J. Org. Chem.* **2007**, 167.